Modelling and Simulation of a fully Electrified Urban Private Transport – a Future Scenario for Berlin

vorgelegt von
M. Sc.
Florian Straub
ORCID: 0000-0002-3883-7741

an der Fakultät V – Verkehrs- und Maschinensysteme
der Technischen Universität Berlin
zur Erlangung des akademischen Grades

Doktor der Ingenieurwissenschaften
- Dr.-Ing. -

genehmigte Dissertation

Promotionsausschuss:

Vorsitzender: Prof. Dr. rer. nat. Kai Nagel
Gutachter: Prof. Dr.-Ing. Dietmar Göhlich
Gutachter: Prof. Dr.-Ing. Christian Rehtanz

Tag der wissenschaftlichen Aussprache: 20. April 2023

Berlin 2023

Florian Straub

Modelling and Simulation of a fully Electrified Urban Private Transport – a Future Scenario for Berlin

Technische Universität Berlin – Faculty of Mechanical Engineering and Transport Systems
Chair of Methods for Product Development and Mechatronics

April 2023

Abstract

Global climate change and air pollution in urban areas are leading to the introduction of agreements, regulations, and laws worldwide to reduce emissions. The best known is the 2015 Paris Climate Agreement, with its goal of limiting worldwide global warming to below 2°C. One important driver of emission reduction is the decarbonization of the transport sector. In Europe, road transport accounted for 72% of total CO_2-equivalent emissions from the transport sector in 2019, with passenger cars accounting for 60.7% of road transport emissions. Germany shows similar numbers: in 2019, passenger cars accounted for 61% of CO_2-equivalent emissions from road transport. As a result, passenger cars with internal combustion engines have to be replaced by passenger cars with decarbonized drive systems. In this context, a clear trend toward battery electric vehicles (BEVs) can be observed.
However, the growing number of BEVs and the resulting increase in demand for electrical energy can lead to bottlenecks in energy generation and power supply. A reinforced electric grid infrastructure may be necessary in many cases for increased power demand. In order to enable electric grid operators to identify congestions in the grid, accurate models are needed to predict the charging energy demand resulting from the electrification of private combustion engine vehicles. Such models require high spatial resolution to assess energy demand peaks even for small areas and high time resolution to identify peak loads throughout the course of the day.
Especially in urban areas, spatial variance in charging demand can be expected, as areas with completely different types of uses are located close to each other. For example, it is possible that one district consists of single-family homes, while an industrial area is located in the directly adjacent district. Due to the different activities performed in these areas, the demand for charging energy differs significantly.

Existing approaches for determining the BEV charging demand in urban regions have significant limitations. Some methods only determine the temporal distribution of BEV charging energy demand, while other methods only determine the spatial distribution. Methods that determine both usually determine the spatial distribution of BEV charging demand with limited accuracy and have very limited applicability to other regions. To overcome these limitations, this cumulative dissertation develops a method that allows forecasting the spatial and temporal distribution of charging energy and power demand resulting from the electrification of private internal combustion engine vehicles (ICEVs) in an urban area. This method consists of three main parts:
Firstly, the urban area is divided into districts and the current conventional vehicle fleet in the districts is replaced by electric reference vehicles. For each vehicle, a mobility profile is created, consisting of a sequence of activities and trips between activities. However, the generated mobility profiles have one major limitation. Due to insufficient data, the geographic location where the vehicle is parked while the BEV user is performing an activity is unknown. Therefore, charging demand can only be determined by assuming that BEVs are exclusively charged at, or near the residences of BEV owners.

To overcome this limitation, the locations of activities need to be determined. An important input variable in this determination is the car-access attractiveness of the districts which is developed in the second part of the method. The car-access attractiveness is a measure of how attractive districts are to drive to by car for a particular activity.
Thirdly, the unknown geographical locations of the activities are determined. For this purpose, a route assignment approach is developed that assigns a destination district to each vehicle trip. By determining the destinations of BEV trips, a complete mobility profile is available for each BEV. This allows determining the spatial and temporal distribution of BEV charging demand in the urban area by applying charging scenarios. The application of the methodology is demonstrated for the urban area of Berlin, Germany. Full electrification of Berlin's private transport is assumed and the spatial and temporal distribution of BEV charging demand is determined for four charging scenarios.

The results show that between 5468 MWh and 6093 MWh of charging energy is required on an average working day in Berlin, depending on the charging scenario. At least 61.8% of this energy is charged at the residences.
Charging energy demand at residences ranges from 0 kWh per day in uninhabited districts to 40.7 MWh per day in districts with high population and motorization levels.
The temporal distribution of the charging power demand in Berlin is highly dependent on the charging scenario as well. The peak power demand ranges from 328 MW to 412 MW.

Based on the complete mobility profiles of BEVs and the charging demand of BEVs determined for Berlin, further research is conducted. In this second part of the dissertation, (i) the load shifting potential through controlled charging of BEVs is investigated, (ii) the Vehicle to grid (V2G) potential of BEVs is studied, and (iii) the future charging station demand in Berlin is determined. The results show that it is possible to reduce peak power demand by up to 31.7% through load shifting compared to uncontrolled charging. By applying V2G, the entire electricity demand of households and BEVs in Berlin can be covered by renewable energies.

The developed model is an important building block for the estimation of the energy demand due to the massive electrification of conventional vehicles expected in the next years. Possible further developments include transferring the developed model to other vehicle types (e.g. commercial vehicles) and extending it to larger areas (e.g. Germany).

Florian Straub
Modellbildung und Simulation eines vollständig elektrifizierten urbanen Individualverkehrs – ein Zukunftsszenario für Berlin
Technische Universität Berlin – Fakultät für Verkehrs- und Maschinensysteme
Fachgebiet Methoden der Produktentwicklung und Mechatronik
April 2023

Kurzfassung

Der globale Klimawandel und die Luftverschmutzung in städtischen Gebieten führen dazu, dass weltweit Abkommen, Verordnungen und Gesetze zur Reduzierung von Emissionen verabschiedet werden. Das Bekannteste ist das Pariser Klimaabkommen von 2015 mit dem Ziel, die weltweite Erderwärmung auf unter 2°C zu begrenzen. Ein wichtiger Hebel für die Emissionsreduzierung ist die Dekarbonisierung des Verkehrssektors. In Europa entfielen im Jahr 2019 72% der gesamten CO_2-äquivalenten Emissionen des Verkehrssektors auf den Straßenverkehr, wobei 60,7% der Emissionen des Straßenverkehrs durch Personenkraftwagen verursacht wurden. In Deutschland sind die Zahlen ähnlich: 2019 entfielen 61% der CO_2-äquivalenten Emissionen des Straßenverkehrs auf Personenkraftwagen. Das bedeutet, dass Personenkraftwagen mit Verbrennungsmotoren durch Personenkraftwagen mit nachhaltigeren Antrieben ersetzt werden müssen. Hierbei ist ein deutlicher Trend hin zu batterieelektrischen Fahrzeugen (BEVs) zu beobachten.
Die wachsende Zahl von BEVs und die damit verbundene steigende Nachfrage nach elektrischer Energie kann jedoch zu Engpässen bei der Energieerzeugung und Stromversorgung führen. Ein Ausbau der Stromnetzinfrastruktur kann in vielen Fällen notwendig sein, um den erhöhten Strombedarf zu decken. Damit die Betreiber von Stromnetzen Engpässe im Netz erkennen können, sind genaue Modelle zur Vorhersage des Ladeenergiebedarfs erforderlich. Solche Modelle erfordern eine hohe räumliche Auflösung, um Energiebedarfsspitzen auch für kleine Gebiete zu ermitteln und eine hohe zeitliche Auflösung um Spitzenlasten im Tagesverlauf zu identifizieren.
Vor allem in städtischen Gebieten sind räumliche Unterschiede im Bedarf nach Ladeenergie zu erwarten, da Gebiete mit völlig unterschiedlichen Nutzungsarten nahe beieinander liegen. So ist es möglich, dass ein Stadtteil aus Einfamilienhäusern besteht, während sich im direkt angrenzenden Stadtteil ein Industriegebiet befindet. Aufgrund der unterschiedlichen Aktivitäten, die in diesen Gebieten ausgeübt werden, ist der der Bedarf an Ladeenergie sehr unterschiedlich.

Bestehende Ansätze zur Ermittlung des BEV-Ladeenergiebedarfs in städtischen Regionen weisen erhebliche Einschränkungen auf. Einige Methoden bestimmen lediglich die zeitliche Verteilung des Ladeenergiebedarfs, während andere Methoden nur die räumliche Verteilung bestimmen. Methoden, die beides ermitteln, ermitteln die räumliche Verteilung des Ladebedarfs in der Regel nur mit begrenzter Genauigkeit und sind nur sehr eingeschränkt auf andere Regionen übertragbar. Um diese Einschränkungen zu überwinden, wird in dieser kumulativen Dissertation eine Methode entwickelt, die es ermöglicht, die räumliche und zeitliche Verteilung des Ladebedarfs zu prognostizieren, die sich aus der Elektrifizierung von privaten Fahrzeugen mit Verbrennungsmotor in einem städtischen Gebiet ergibt. Diese Methode besteht aus drei Hauptteilen: Im ersten Teil wird das Stadtgebiet in Bezirke unterteilt und die aktuellen konventionellen Fahrzeuge in den Bezirken durch elektrische Referenzfahrzeuge ersetzt. Für jedes Fahrzeug wird ein Mobilitätsprofil erstellt, das aus einer Abfolge von Aktivitäten und Fahrten zwischen den Aktivitäten besteht.

Die erstellten Mobilitätsprofile weisen jedoch eine wesentliche Einschränkung auf. Aufgrund unzureichender Daten ist der Ort, an dem das Fahrzeug geparkt ist, während der BEV-Nutzer eine Aktivität ausführt, unbekannt. Der Ladebedarf kann daher im ersten Schritt lediglich unter der Annahme bestimmt werden, dass die BEVs ausschließlich an den Wohnorten ihrer Besitzer geladen werden.
Um diese Einschränkung zu überwinden, müssen die Orte der Aktivitäten bestimmt werden. Eine wichtige Eingangsgröße für diese Bestimmung ist die Pkw-Zugangsattraktivität der Bezirke, die im zweiten Teil der Methode entwickelt wird. Diese ist ein Maß dafür, wie attraktiv ein Bezirk ist, um für eine bestimmte Tätigkeit dorthin zu fahren.
Im dritten Teil der Methode werden die Orte der Aktivitäten bestimmt. Hierfür wird ein Routenzuweisungsverfahren entwickelt, das jeder Fahrzeugfahrt einen Zielbezirk zuweist. Die Kenntnis über die Zielorte der Fahrten ermöglicht die Bestimmung der räumlichen und zeitlichen Verteilung des BEV-Ladebedarfs durch Anwendung von Ladeszenarien.
Die Methodik wird für Berlin, Deutschland, angewandt. Es wird eine vollständige Elektrifizierung des Berliner Individualverkehrs simuliert und die räumliche und zeitliche Verteilung des Ladebedarfs für vier Ladeszenarien ermittelt.

Die Ergebnisse zeigen, dass an einem durchschnittlichen Werktag in Berlin, je nach Ladeszenario, zwischen 5468 MWh und 6093 MWh an Ladeenergie benötigt werden. Mindestens 61,8% dieser Energie wird an den Wohnorten geladen.
Der Ladeenergiebedarf an Wohnorten reicht von 0 kWh pro Tag in unbewohnten Bezirken bis zu 40,7 MWh pro Tag in Bezirken mit hoher Bevölkerungszahl und hohem Motorisierungsgrad. Auch die zeitliche Verteilung des Ladeenergiebedarfs in Berlin ist stark vom Ladeszenario abhängig. Der Spitzenleistungsbedarf reicht von 328 MW bis 412 MW.

Basierend auf den vollständigen Mobilitätsprofilen der BEVs und dem für Berlin ermittelten Ladebedarf der BEVs werden weitere Untersuchungen durchgeführt. In diesem zweiten Teil der Dissertation wird (i) das Lastverschiebungspotenzial durch gesteuertes Laden von BEVs untersucht, (ii) das Vehicle-to-Grid (V2G) Potenzial von BEVs untersucht und (iii) der zukünftige Ladestationsbedarf in Berlin ermittelt. Die Ergebnisse zeigen, dass es möglich ist, den Spitzenstrombedarf durch Lastverschiebung im Vergleich zu ungesteuertem Laden um bis zu 31,7% zu reduzieren. Durch den Einsatz von V2G kann der gesamte Strombedarf von Haushalten und BEVs in Berlin durch erneuerbare Energien gedeckt werden.

Das entwickelte Modell ist ein wichtiger Beitrag zur Abschätzung des Energiebedarfs, der durch die in den nächsten Jahren zu erwartende massive Elektrifizierung konventioneller Fahrzeuge entsteht. Mögliche Weiterentwicklungen sind die Übertragung des entwickelten Modells auf andere Fahrzeugtypen (z.B. Nutzfahrzeuge) und die Ausweitung auf größere Gebiete (z.B. Deutschland).

Acknowledgments

This cumulative dissertation was written while I was working as a research associate at the Chair of Methods for Product Development and Mechatronics (MPM) at the Technische Universität Berlin. I would like to thank those who contributed to the success of my work.

First I like to thank Prof. Dr.-Ing. Dietmar Göhlich for supervising this work, for the trust he has placed in me, and for the freedom he has given me in implementing my ideas. His help, feedback, and questions have been instrumental in improving this dissertation and exploring new topics.

I would also like to thank Prof. Dr.-Ing. Christian Rehtanz for his willingness to be the second supervisor of this dissertation and to Prof. Dr. rer. nat. Kai Nagel for chairing the examination. I appreciate your time, interest and effort.

Furthermore, I would like to thank my colleagues at MPM for the cooperation in a great atmosphere and the mutual support.

I would also like to thank Mr. Simon Streppel, Mr. Kilian Ebmeyer, and Mr. Mostafa Hamied as well as all other students who contributed to the success of this work with their bachelor and master theses. I would like to make special mention of Mr. Otto Maier, who contributed significantly to the success of this work through his master thesis and his work as a student assistant.

A special thanks to Dr. techn. Francesco Cigarini for the hours he spent proofreading this dissertation.

I would like to thank my parents for enabling my educational path and for their support.

Finally, Maren, thank you for always standing by me unconditionally!

Berlin, April 2023 Florian Straub

Contents

List of Abbreviations and Symbols

Abbreviations

BEV	Battery electric vehicle
CCCV	Constant-current constant-voltage
FCEV	Fuel cell electric vehicle
GHTS	German household travel survey
ICEV	Internal combustion engine vehicle
LOR	“Lebensweltlich orientierter Raum” (neighbourhood oriented district)
MSCC	Multi-stage constant-current
O-D	Origin-destination
OSM	OpenStreetMap
POI	Point of interest
RE	Renewable energy
SOC	State of charge
V2G	Vehicle to grid
WLTP	Worldwide harmonized light vehicles test procedure

Symbols

Symbol	Meaning	Unit
E	Electrical energy	Wh
t	Time	s
$P(t)$	Time-dependent charging power	W
η	Charging efficiency	
K_1	Ratio of net internal area to gross floor area, for residential and commercial buildings	
K_2	Ratio of sales area to net internal area for buildings	
K_3	Ratio of sales area to gross floor area for buildings	
O_t	Total operating area of a building. The total operating area of a building equals the buildings' gross floor area multiplied by its number of floors	m^2
O_i	Operating area of the company i in a building	m^2
c_a	Average operating area per type of business	m^2
E_o	Employees per m^2 of operating area	
E_b	Total number of employees in a building	
E_t	Total number of employees in a LOR	
C_t	Capacity of a parking space (number of parking spots)	
C_i	Number of a parking space's spots assigned to the building i	
S_b	Total sales area in a building	m^2
S_t	Total sales area in a LOR	m^2
x_s	Attraction-factor of a building with sales area for shopping trips	
y_{1s}	Criterion 1 for the evaluation of x_s. Parking spots per m^2 sales area of the building	
y_{2s}	Criterion 2 for the evaluation of x_s. The distance of a parking space to the building with sales area	m
y_{3s}	Criterion 3 for the evaluation of x_s. Parking fees of the parking space assigned to the building with sales area	yes/ no
α_{1s}, α_{2s}, α_{3s}	Global rating-coefficients of the criteria y_{1s}, y_{2s}, y_{3s} for determining x_s, using a weighted sum model	
β_{2s}, β_{3s}	Rating-coefficients of a parking space for determining α_{2s}, α_{3s}	
w_{1s}, w_{2s}, w_{3s}	Weighting-coefficients of of the criteria y_{1s}, y_{2s}, y_{3s} for determining x_s, using a weighted sum model	
A_s	Car-access attractiveness of a LOR for shopping trips	

Symbol	**Meaning**	**Unit**
x_w	Attraction-factor of a building with employees for working trips	
y_{1w}	Criterion 1 for the evaluation of x_w. Parking spots per employees of the building	
y_{2w}	Criterion 2 for the evaluation of x_w. The distance of a parking space to the building with employees	m
y_{3w}	Criterion 3 for the evaluation of x_w. The distance of the building with employees to the nearest public transportation stop	m
α_{1w}, α_{2w}, α_{3w}	Global rating-coefficients of the criteria y_{1w}, y_{2w}, y_{3w} for determining x_w, using a weighted sum model	
β_{2w}	Rating-coefficients of a parking space for determining α_{2w}	
w_{1w}, w_{2w}, w_{3w}	Weighting-coefficients of of the criteria y_{1w}, y_{2w}, y_{3w} for determining x_w, using a weighted sum model	
A_w	Car-access attractiveness of a LOR for working trips	
k_d	Rating value of the travel distance criterion	
k_s	Rating value of the travel speed criterion	
k_a	Rating value of the criterion "Car-access attractiveness"	
k_c	Rating value of the criterion "Availability of parking spots"	
R_{LOR}	Rating of a destination LOR	
w_d, w_s, w_a, w_c	Weighting-coefficients of of the criteria k_d, k_s, k_a, k_c for determining R_{LOR}, using a weighted sum model	
PDI	Peak power demand increase	
BLI	Battery load increase	
E_c	Amount of energy charged by the vehicles which participate in V2G	kWh
E_d	Amount of energy consumed by the vehicles which participate in V2G during their trips	kWh

List of Figures

List of Tables

1 Introduction

This chapter motivates this dissertation, defines its objective, and shows its structure.

1.1 Motivation

To reduce the adverse effects of global climate change, reduce air pollution, and limit global temperature increase, emissions of greenhouse gases and air pollutants must be reduced and avoided in all sectors. The signing parties of the 2015 Paris Climate Agreement have therefore committed themselves to reduce their greenhouse gas emissions to such an extent that the human-induced temperature increase is limited to below 2°C [1]. The European Union has agreed on the European Green Deal, which includes net-zero greenhouse gas emissions by 2050 and a zero-pollutant target [2]. To achieve these targets, Germany developed and implemented the Climate Protection Plan 2050 [3], the Federal Climate Protection Act [4] and the National Clean Air Program [5]. This has resulted in a 40% reduction in greenhouse gas emissions since 1990, as shown in Figure 1.1. The most significant progress has been made in the energy sector, through the reform of European emissions trading, the expansion of renewable energies (RE), and the shutdown of coal-fired power plants [6]. However, the transport sector is stagnating at 1990 levels and is responsible for about 20% of total greenhouse gas emissions in 2020. This is mostly due to the increased traffic volume worldwide which compensates for the technical improvements to the vehicles.
Emissions of air pollutants have also declined since 1990. However in 2020, the transportation sector was still responsible for a significant share of the emission generation, especially for nitrogen oxides (~36%), carbon monoxide (~32%), and particulate matter (PM 2.5: ~20%, PM 10: ~14%) [7].

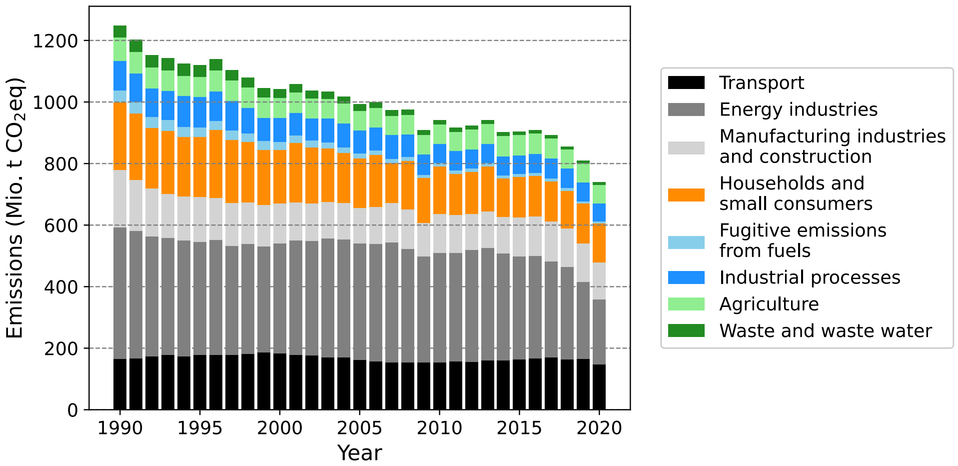

Figure 1.1: Development of greenhouse gas emissions in Germany since 1990 [8].

To reduce greenhouse gas and air pollutant emissions in the transport sector, various measures are being taken, such as traffic avoidance, efficiency improvements, the use of more environmentally friendly means of transport, and the electrification of vehicles [3].

In particular, the electrification of private motorized transport is seen as central to achieve the reduction targets in the transport sector. In Europe, road transport accounted for 72% of total CO_2-equivalent emissions from the transport sector in 2019, with passenger cars accounting for 60.7% of road transport emissions [9]. Germany shows similar numbers: in 2019, passenger cars accounted for 61% of CO_2-equivalent emissions from road transport [10]. The European Union has therefore agreed on an emission limit of 95 $g\, CO_2/km$ for passenger cars registered by 2021 [11].
As a result, passenger cars with internal combustion engines have to be replaced by passenger cars with decarbonized drive systems. In this context, there is a clear trend towards battery-electric passenger cars instead of fuel-cell-powered passenger cars. In the following, passenger cars with internal combustion engines are referred to as ICEVs, battery electric passenger cars are referred to as battery electric vehicles (BEVs). Fuel-cell-powered passenger cars are referred to as fuel cell electric vehicles (FCEVs).

The development of annual BEV registrations in Germany from 2010 to 2021 is shown in Figure 1.2. While 11,410 BEVs were registered in 2016, 355,961 BEVs were registered in 2021, corresponding to an increase of over 3000% in the last 5 years. The trend towards increasing sales of BEVs can be observed worldwide [12].
For FCEVs a similar trend cannot be observed. In Germany, for example, only 464 FCEVs were registered in 2021 [13]. The low registration numbers of FCEVs are mainly due to the high acquisition costs, the lack of infrastructure and the lack of a stable, long-term policy framework [14]. Therefore, only BEVs are considered in this dissertation. However, if the barriers described can be overcome, a significant increase in FCEV numbers can be expected in the future [15].
At this point, it should be noted that 41.1% of electricity in Germany was generated from renewable sources in 2021 (45.2% in 2020) [16]. Worldwide, 28.1% of electricity was generated from renewable sources in 2021 [17] (27% in 2020 [18]). Therefore, BEVs do not currently operate with a net zero carbon footprint. BEVs will achieve their full greenhouse gas abatement effect when the charged electricity originates entirely from renewable sources.

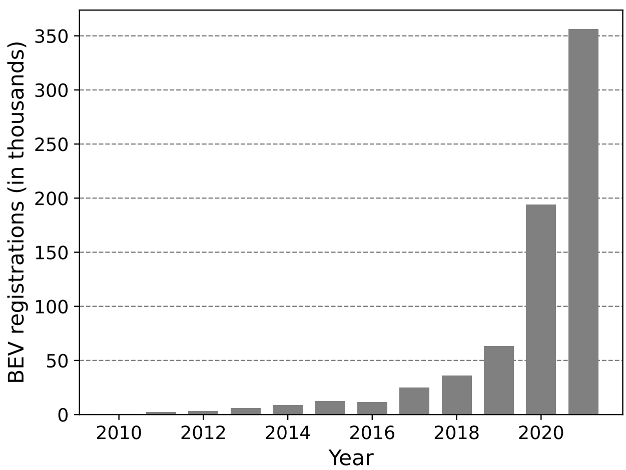

Figure 1.2: Number of annual BEV registrations in Germany from 2010 to 2021 [19].

The rapid growth in BEV numbers and the resulting increase in demand for electrical energy and power can lead to bottlenecks in energy generation and power supply. A reinforced electric grid infrastructure may be necessary in many cases for increased power demand [20]–[23]. Various studies have shown that the demand for electrical energy and power for charging BEVs varies depending on the time of day (due to different activities) and the type of day (weekday or weekend day) [20]–[22]. In addition, spatial variance in energy demand can be expected. An industrial area, for example, has a different charging energy demand compared to a residential area [24], [25]. As a result, the electric network needs to be reinforced to different extents depending on the specific requirements of the considered area. To support such targeted grid expansion, precise models are required to identify the distribution of the energy demand and evaluate potential power system overload due to ICEV electrification. Such models require high spatial resolution to assess energy demand peaks even for small regions and areas and high time resolution to identify peak loads throughout the course of the day.

1.2 Objective and Structure of this Dissertation

Especially in urban areas, spatial variance in charging demand can be expected, as areas with completely different types of uses are located close to each other. For example, it is possible that a district consists mainly of single-family houses, while the directly adjacent districts contain an industrial area or commercial areas. However, as shown in the literature review in Chapter 2, existing approaches for determining the spatial and temporal distribution of BEV charging energy demand in urban regions have significant limitations. Therefore, the objective of this dissertation is to overcome these limitations and develop a method that allows for determining the spatial and temporal distribution of charging energy and power demand resulting from the electrification of private internal combustion engine passenger cars in urban areas. The method is demonstrated using the urban area of Berlin, Germany as example. Due to the limited available data for commercially used vehicles (such as e.g. cabs and rental cars), in this dissertation, the determination of charging energy demand is restricted to private cars. In Berlin, the share of private cars in the total car population in 2020 was 86.3%, in Germany 89.0% [26].

This cumulative dissertation consists of 4 published papers and one additional topic. A summary of these 5 topics can be found in Chapter 3.
The topics can be divided into two main parts. In the first part (Chapter 4), the development of the model for determining the spatial and temporal distribution of BEV charging energy demand is discussed. In the second part (Chapter 5), it is shown how the results can be used for determining Vehicle to grid (V2G) potential, and estimating charging infrastructure demand. In Chapter 6, the developed method and the results are discussed and placed in the context of existing research. The dissertation concludes with a summary and outlook in Chapter 7.

1.3 List of Publications

This cumulative dissertation contains the accepted manuscripts of the following publications:

- Publication I – [27] – F. Straub, S. Streppel, D. Göhlich: "Methodology for Estimating the Spatial and Temporal Power Demand of Private Electric Vehicles for an Entire Urban Region Using Open Data". *Energies*, 2021
- Publication II – [28] – F. Straub, O. Maier, D. Göhlich: "Car-Access Attractiveness of Urban Districts Regarding Shopping and Working Trips for Usage in E-Mobility Traffic Simulations". *Sustainability*, 2021
- Publication III – [29] – F. Straub, O. Maier, D. Göhlich, Y. Zou: "Forecasting the Spatial and Temporal Charging Demand of Fully Electrified Urban Private Car Transportation based on Large-Scale Traffic Simulation". *Green Energy and Intelligent Transportation*, 2023
- Publication IV – [30] – F. Straub, O. Maier, D. Göhlich, K. Strunz: "Sector Coupling through Vehicle to Grid: A Case Study for Electric Vehicles and Households in Berlin, Germany". *World Electric Vehicle Journal*, 2023

2 State of the Art and Research Needs

This cumulative dissertation consists of thematically self-contained published papers. Each publication individually discusses the fundamentals and state of the art necessary for understanding the publication. Therefore, this chapter only covers necessary fundamentals, which are not included in the publications. These fundamentals include a discussion of available charging interfaces for BEVs and battery charging protocols (Section 2.1), as well as transport models to predict travel behavior and determine travel demand in the area under consideration (Section 2.2).
The second part of this chapter evaluates related scientific work on determining the spatial and temporal distribution of BEV charging energy demand (Section 2.3). From the limitations of this state of the art, the research objectives of the dissertation are derived (Section 2.4).

2.1 Electric Vehicle Charging

The electrical energy E that can be absorbed by the BEV's battery during charging can be determined according to Equation 2.1:

$$E = \eta \int_{t_0}^{t_1} P(t)dt \tag{2.1}$$

where P is the charging power provided at the charging station, t is the time and η the efficiency of the system between charging station and BEV battery. Usually, charging losses of about 10% occur [31]–[33]. However, experimental measurements have shown that charging losses can reach up to 20% for individual vehicles [34].

The time-dependent charging power and thus the charging time is limited by two main factors. The first factor is the charging interface at the charging station, which only allows a certain maximum charging power. Common charging interfaces for BEVs are discussed in Section 2.1.1.
The second factor is the vehicle itself. This vehicle dependence is discussed in Section 2.1.2.

2.1.1 Charging Interfaces

The most common conductive charging interfaces for battery electric vehicles are shown in Table 2.1. The available charging power varies from 2.3 kW for the household socket up to 400 kW for CHAdeMO chargers. The latest developments allow up to 900 kW. In principle, it is possible to use inductive charging systems or battery swapping stations instead of the conductive systems listed. However, although there is much research on inductive systems [35]–[42] and battery swapping stations [43]–[48], these systems have not been able to establish themselves on a large scale yet.
The predominant charging plugs in Europe and Germany are the Type 2 plug for alternating current (AC) charging and the CCS Combo 2 plug (Combined Charging System with the Type 2 plug), which enables both AC and direct current (DC) charging [49].

Table 2.1: Common charging interfaces for battery electric vehicles [50]–[56].

Type	Electric current	Region	Max. charging power (kW)
Schuko plug	AC	Europe	3.68/2.3[a]
Type 1 plug	AC	North America and Japan	9.2
Type 2 plug	AC	Europe and China	43/22[b]
CCS Combo 1	AC/DC	North America	350 (DC)
CCS Combo 2	AC/DC	Europe	350 (DC)
CHAdeMO	DC	Europe and Asia	200/50[b]
CHAdeMO 2.0	DC	Asia	400
CHAdeMO 3.0, ChaoJi[c]	DC	Asia	900
Tesla Supercharger	DC	Worldwide	250
GB/T	DC	China	237.5

[a] Schuko plugs are not designed for continuous operation at maximum power. Continuous output is usually 2.3 kW.

[b] Usual max. charging power at charging stations

[c] ChaoJi standard is still under development

2.1.2 Battery Charging Protocols and Charging Curves

In addition to the charging interface, the maximum charging power that can be used by a BEV depends on its battery management system [57]. The battery management system specifies the charging protocol with which the vehicle is charged. The charging protocol is the control of electric current and voltage when charging the battery. The protocols aim to fully charge the battery within its operating limits while keeping battery aging to a minimum [58].

In the electromobility sector, the lithium-ion battery has become the standard in recent years due to its high volumetric and gravimetric energy density [59]. An overview of the most common lithium-ion battery types for battery electric vehicles can be found in [60]. For charging lithium-ion batteries there are a variety of charging protocols, such as the constant-current constant-voltage (CCCV) protocol, the multi-stage constant-current (MSCC) protocol, and the pulse charging protocol. Among these, the CCCV charging protocol is currently the most widely used protocol due to its simplicity and its easy implementation [58], [61].

The CCCV charging cycle is shown in Figure 2.1 and consists of a constant-current (CC) and a constant-voltage (CV) phase. In the constant-current phase, the charging current is kept constant until the increasing cell voltage reaches a defined maximum threshold. In this phase, the charging power is nearly constant. The battery state of charge (SOC)[1] increases almost linearly with time, as can be seen in Figure 2.1. Once the voltage has reached its threshold value i.e. the point of transition (PT), the voltage of the cell is kept constant.

[1] The SOC indicates the available capacity of a battery relative to its nominal capacity. SOC values are expressed as a percentage, with 0% SOC corresponding to an empty battery and 100% SOC corresponding to a full battery.

The charging current is exponentially reduced to a predefined minimum threshold value. In this constant-voltage phase, the available charging power is also progressively reduced [62]–[64].
In contrast to the CCCV process, the MSCC process has several constant-current phases. The charging current of phase n+1 is lower than the charging current of phase n [63].

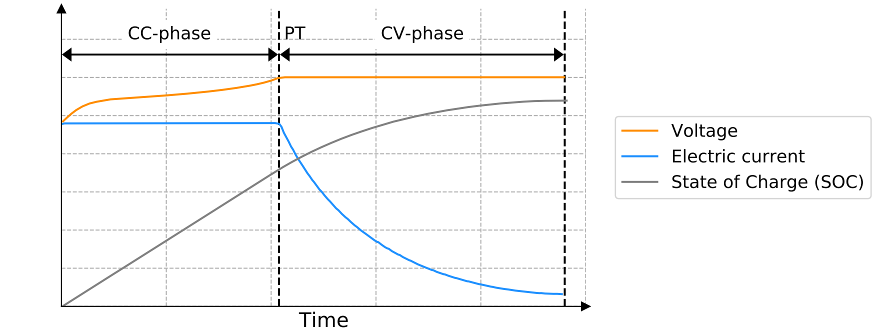

Figure 2.1: CCCV charge cycle according to [62], [64].

In addition to the discussed representation as a correlation between SOC and time, the charging behavior of BEVs is often given in the literature as a correlation between charging power (y-axis) and SOC (x-axis). The resulting curves are referred to as charging curves. In Figure 2.2, the charging curves of nine BEVs are shown, which were determined by experimental measurements [65]. It can be seen that most vehicles use the CCCV charging protocol. The KIA e-Niro and the Hyundai Kona are charged using the MSCC charging protocol.
Furthermore, it can be seen that the transition point (after which the cell voltage is kept constant) varies greatly from vehicle to vehicle. However, there is a tendency for higher maximal charging powers to be associated with charging transition points at lower SOC values. The reason for this is the increased internal resistance of the battery at higher charging powers due to thermal effects [59].

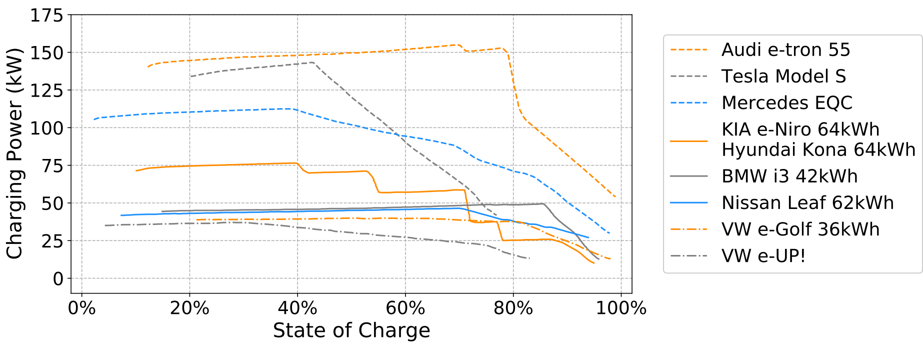

Figure 2.2: Charging curves of BEVs [65].

2.2 Transport Models

Transport models are used to predict travel patterns and travel demand in a study area. The standard model used is the four-step transport model which is described in Section 2.2.1. To overcome the limitations of four-step models, activity-based models were developed which are described in Section 2.2.2.

2.2.1 Four-Step Transport Model

The general form of the four-step transport model is schematically depicted in Figure 2.3. The basis of the model is the division of the considered area into traffic cells, which are connected by traffic lines. Traffic cells and lines together form the network system. This is used together with a database containing data for all traffic zones regarding the population, the degree of motorization, as well as data on employment, sales areas, educational and recreational facilities.
This data is then used in the "*Trip generation*" step to determine the total number of trips generated and attracted by each traffic zone. Based on the trip generation, the distribution of trips to destination traffic zones is unknown.
Therefore, in the "*Trip distribution*" step, trip origins and destinations are linked, which means that the traffic flow between the traffic cells is determined. The gravity model is often used for this purpose. It is based on the assumption that a traffic cell behaves like a gravitational point, i.e. the more mass a cell has (e.g. number of employees or sales area), the higher its gravitational pull. As the distance between two cells increases, the cell's gravitational pull decreases.
Then, in the "*Mode choice*" step, the mode of transportation for each trip is determined. Usually, this is based on the "modal share" of the considered area, which indicates the share of a type of transportation in the total traffic volume.
Finally, the "*Route assignment*" step determines which route the generated traffic chooses to get from the origin to the destination. Typically, a distinction is made between a private and a public transportation network [66], [67].

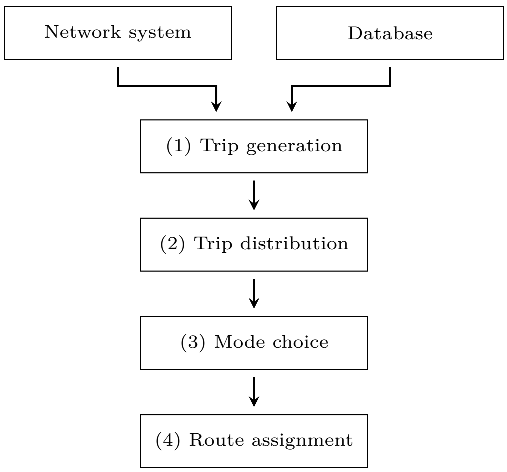

Figure 2.3: Four-step transport model according to [66].

2.2.2 Activity-Based Transport Model

The main limitation of the four-step transport model is that the trips generated are considered independent variables and therefore the trips cannot be linked to individual persons. Thus, only the aggregate travel behavior of all persons in the area under consideration can be modeled, but not the travel behavior of individual persons. In contrast, activity-based models operate at a disaggregated person level and are based on the concept that travel demand results from the activity patterns of the persons in the considered area. The activity pattern of a person depends on the individual characteristics of the person (e.g. the place of residence, income, age, household, and other social characteristics). In contrast to the zone-based description in traditional transportation models, activity-based models typically identify full-day travel schedules for each person in the considered area. The travel schedules which are also referred to as mobility profiles[2] describe the relationship between activities, trips, mode of transportation, and the location where the activities are performed [66], [68]. Travel schedules are typically derived from travel surveys which are obtained by interviewing households in the considered area about their activities and trips on reference days.
In Figure 2.4 an example of a mobility profile of a person is depicted. The person goes shopping in the morning and uses the bicycle to do so. The person then returns home and drives to work from there. The person arrives back home at 17:15.

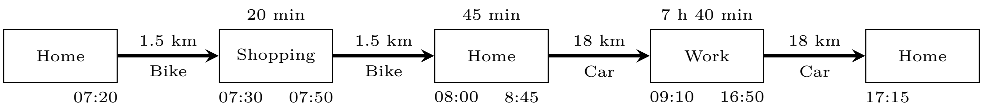

Figure 2.4: Example of a mobility profile.

2.3 Related Scientific Publications

This chapter reviews related scientific publications on determining the spatial and temporal distribution of BEV charging energy demand and summarizes their methodological approach. From the limitations of this state of the art, the research objectives of the dissertation are derived in Section 2.4.

The authors of [24] develop a method for estimating the spatial and temporal distribution of BEV charging demand in urban areas. First, they divide the area into several different functional areas (e.g residential, working, shopping entertainment areas). However, the methodology for dividing the city into these areas is not discussed.
After the division, the BEVs are distributed to the functional areas in the city (hereinafter referred to as the "home" area). The methodology used for this distribution is also not discussed. Then, each vehicle is assigned a mobility profile that contains information on the distances traveled, activities, and parking times of the BEVs. The database is a travel survey. Subsequently, the destination functional area of the first trip is determined. The basis of this determination is the known "home" area and the travel distance of the first trip. From all destinations that can be reached from the "home" area with the given travel distance, one is randomly selected. This destination area is then the origin area of the second trip. The destination area of the second trip is again randomly selected from all areas that can

[2] In the following, the terms full-day travel schedules and mobility profiles are used interchangeably.

be reached with the given travel distance of the second trip. The destination areas of the remaining trips are determined analogously to the first and second trip. Knowledge of the geographic location of activities then allows (along with mobility profiles) the determination of the spatial and temporal distribution of BEV charging demand.
However, the spatial distribution determined has limited accuracy due to the random selection of destinations. Each functional area differs from the others (e.g., number of employees or number of available parking spaces) and therefore has a different probability of attracting trips which is not considered.

The authors of [69] develop a methodology to determine the temporal distribution of BEV charging energy demand for urban areas and demonstrate their approach for the city of Auckland, New Zealand. In their method, the current fleet of vehicles with combustion engines (e.g., cars, trucks, buses, commercial vehicles) is first replaced by electric reference vehicles. Then, the daily distance of each vehicle is determined based on probability distributions. A distribution is available for each vehicle class individually and is derived from a travel survey. By multiplying the daily distance by the average consumption of the individual vehicles, their daily energy demand is calculated. Finally, the start time of charging is determined for each vehicle from the travel survey. Using the charging demand and the start time of charging, the charging time is obtained. This allows for determining the temporal distribution of charging power demand. Since the geographic locations where the vehicles charge are not determined, the methodology cannot be used to determine the spatial distribution of charging energy demand.

In [25], the authors develop a method to determine the spatial distribution of BEV charging demand and identify the most suitable locations for public and semi-public charging stations. The method is demonstrated for 8 counties in Bavaria, Germany. In order to obtain the spatial distribution of charging demand they first determine the points of interest (POIs) and their geographic locations in the considered area using OpenStreetMap (OSM) geodata analysis. The POIs are divided into 4 POI classes where different activities can be performed. These are “living”, “working”, “shopping”, and “recreation”. For each POI class, the total annual charging energy demand is then determined by multiplying the annual mileage of the vehicles by their average consumption. The total demand per POI class is then distributed evenly among all POIs in the class. As a result, the charging demand at each POI is known, and thus the spatial distribution of charging demand.
Due to the even distribution, the energy demand is high at locations with many POIs and low at locations with few POIs. It is neglected that different POIs attract different numbers of people, e.g., because of their different size or their different accessibility. Therefore the determined spatial distribution is limited.
Since only the annual energy demand is determined, the temporal distribution of the charging demand cannot be determined with the method.

In [70], the authors address the question of what charging infrastructure is required for a fully electrified private transport. They demonstrate their method for the city of Rome, Italy. A dataset representing 6% of traffic flow in Rome is used as the base dataset. The data is collected by the authors using GPS modules in cars. For the trips made by vehicles with internal combustion engines, it is assumed that electric vehicles are used. The energy demand per trip is determined by the acceleration profile of the individual trip and a look-up matrix that links the vehicle’s acceleration and current speed with energy demand. To determine the spatial distribution of charging demand it is assumed that the energy demand of each trip is fully recharged at the trip's destination. Since no activities are assigned to the trips and the single trips are not linked to each other, the method does not allow to determine the temporal distribution of power demand.

The authors of [71] develop a model to determine the spatial distribution of BEV charging demand in urban areas. The method is demonstrated for the city of Porto, Portugal. In the first step, they divide the urban area into several cells and determine for each of them the number of BEVs located in it. The basis of this determination is the number of residents in the cells and their BEV adoption rate. For each vehicle, a daily energy demand of 4.2 kWh is assumed. Assuming that this energy demand is charged exclusively at the residences, the spatial distribution of charging demand is determined. Since only the daily energy demand of the BEVs is determined, the method does not allow to determine the temporal distribution of charging power demand.

In [72] the authors simulate the spatial and temporal distribution of charging energy demand for an artificial city consisting of a city center, suburban areas, and connecting highways. All simulated persons and their vehicles undertake a round trip, which starts in a suburban area and then goes to a randomly selected location within the city center and back. Different activities in the city center are not considered. The arrival and departure times of the vehicles in the city center are drawn from probability distributions, which are derived from a publicly available travel survey. At each stop, the persons decide whether to charge their car, depending on the current SOC. Using the charging demand of the vehicles at the different locations and the start time of charging, the charging times are obtained, which allows for determining the spatial and temporal distribution of charging demand.
However, due to the assumption that all vehicles undertake two trips per day and travel to a random location in the city, both the spatial and temporal distribution of charging demand have limited accuracy. The study does not discuss how to transfer the approach to a real city. Therefore, the presented methodology can only be used for the specific artificial city.

For 11 districts in the city of Reykjavík, Iceland, the authors of [73] determine the spatial and temporal distribution of BEV energy demand considering 4 BEV market ramp-up scenarios to 2050. In order to determine the energy demand per district, the daily distances of the vehicles and the arrival times of the vehicles at the places of residence are first extracted from an extensive travel survey which is not publicly available. Based on the population in the districts and assuming that a reference BEV with 60 kWh battery capacity and an average energy consumption of 0.2 kWh/km is used for all trips, the energy demand for each district is determined. For the charging demand computation, it is assumed that all vehicles are charged at home at the end of the day, as this charging scenario is considered to have the greatest impact on the power grid. Since only arrival times at residences and the geographic locations of the residences are determined, the method can only determine the spatial and temporal distribution of charging demand, assuming that charging occurs exclusively at the residences. This does not reflect reality. Therefore the results are limited.

In a study commissioned by the Berlin government [74], the authors determine the demand for private, semi-public, and public charging infrastructure in Berlin, Germany. For their investigations, they divide the city of Berlin into 448 sub-districts and consider 7 charging use-cases (e.g. charging at the places of residence, at work or at customer parking spaces, public charging). Mobility profiles are generated for 5 different user groups (residents, commuters, day visitors, overnight visitors, and commercial traffic), providing information on the distances traveled, activities, and parking times of individuals, but not on the locations of the activities. Using the information from the mobility profiles as well as assumptions about the average consumption of the BEVs, the temporal distribution of the charging power demand can be determined. Since the geographic locations where activities are performed are not known, the spatial distribution of charging energy demand can not be directly determined. To determine the spatial distribution, the total charging energy demand per day for each charging use case is calculated first. The total demand is then distributed among the 448 districts using distribution keys. These distribution keys are based on oversimplified assumptions. For the charging use case "work charging", for example, it is assumed that the more employees in the district, the higher the charging demand (for further information see Section 6.1.2). However, there are other relevant factors that determine how many trips a district attracts. For example, the number of available parking spots. If there are no parking possibilities in a district, employees cannot come by car but have to choose other means of transport. Since such factors are not considered, the calculated spatial distribution of charging demand has limited accuracy.

In [75], the authors develop a method to estimate the number of public charging stations in an urban area needed for future BEV drivers to maintain their current ICEV driving patterns. The approach is demonstrated for Beijing, China. To determine this demand, a mobility profile is first created for each vehicle, including information on activities (home and other), trip distances, parking times, and geographic locations of activities. The data basis for this determination is a detailed travel survey which is not publicly available. Since the data set is based on conventional vehicles, a reference BEV with an average consumption of 0.15 kWh/km is used to replace the combustion engine vehicles. Using the BEV consumption as well as the BEVs' arrival and departure times and the travel distances from the mobility profiles, the temporal distribution of charging demand can be determined. Since the geographic locations where activities are performed are known, the spatial distribution of charging demand can be determined. However, since only one reference vehicle is used, the determined spatial distribution is limited. In general, larger and heavier vehicles tend to have a higher energy consumption compared to smaller and lighter vehicles. If vehicle size is not taken into account, the charging demand is underestimated in districts with a high number of large vehicles and overestimated in districts with many small vehicles.

For the Seattle metropolitan area, the USA, the authors of [76] also investigate how to electrify the current ICEV travel patterns of the population. The current driving behavior of the population is derived from extensive GPS measurements taken in conventional vehicles. The measurements were carried out by the authors themselves. For each vehicle in the considered area, this data is used to create a mobility profile that includes information about activities (home and other), trip distances, parking times, and geographic locations of activities. The conventional vehicles are then replaced by a reference BEV with an average consumption of 0.186 kWh/km and a range of 161 km (100 miles). Using the BEV consumption and the mobility profiles, the temporal and spatial distribution of charging demand can be determined. Since only one reference vehicle is used, the determined spatial distribution is limited. The reasons for this have been discussed in the previous paragraph (see study [75]).

The authors of [77] develop a methodology to determine the spatial and temporal charging power demand on the country level in high resolution. They demonstrated their approach for the Flemish region of Belgium. The basis of the determination is the number of vehicles in each district in the considered region, which are then replaced by electric reference vehicles of three different vehicle-size classes. For each vehicle, a mobility profile is generated, which includes information on activities (home, work, and other), trip distances, parking times, and geographic locations of activities. The mobility profiles are determined from a very detailed travel survey that the authors conducted themselves and which is not publicly available. Based on the average consumption of the reference BEVs and the arrival and departure times and travel distances of the BEVs, the temporal distribution of charging demand is determined. Since the geographical locations where the activities are performed are known, the spatial distribution of charging demand in the districts can be determined. However, this spatial distribution has limited accuracy because it is assumed that the shares of the three vehicle size classes are the same in all districts. In general, larger and heavier vehicles tend to have a higher energy consumption compared to smaller and lighter vehicles. Thus, if the individual distribution of vehicle size classes in the districts is not taken into account, the charging demand is underestimated in districts with a high number of large vehicles and overestimated in districts with many small vehicles.

The authors of [78] determine the spatial and temporal BEV charging demand in urban areas. Their approach is demonstrated for Singapore. They first determine the number of current internal combustion engine cars in each district, based on several unspecified statistics. These are subsequently replaced by electric reference vehicles. The number of different reference vehicles is not specified. For each vehicle, a mobility profile is generated, which includes information on activities, trip distances, parking times, and geographic locations of activities. The mobility profiles are determined from a very detailed travel survey that was provided to the authors by the Singapore authorities and is not publicly available. These mobility profiles and a vehicle dynamics model are used to determine the temporal and spatial distribution of BEV charging demand in Singapore and its districts. Analogous to the method developed in [77], it is assumed that the shares of vehicle size classes are the same in all districts. Therefore, the spatial distribution of charging demand has limited accuracy, as previously justified.

A summary of the discussed studies is shown in Table 2.2.

Table 2.2: Overview and limitations of related scientific publications. Legend: ● yes, ○ no, ◐ limited result.

Reference	Charging demand is determined with high spatial resolution	Charging demand is determined with high temporal resolution	Consideration of different activities	Mobility profile for the individual vehicle is generated	Method transferable to other urban areas
[24]	○	●	●	●	○
[69]	○	●	○	○	○
[25]	◐	○	●	○	●
[70]	●	○	○	○	○
[71]	●	○	○	○	●
[72]	◐	◐	○	●	●
[73]	◐	◐	○	○	○
[74]	◐	●	●	●	●
[75][a]	◐	●	○	●	○
[76][a]	◐	●	○	●	○
[77][a]	◐	●	●	●	○
[78][a]	◐	●	●	●	○

[a] Activity-based method

2.4 Evaluation of Existing Literature and Identification of Research Needs

The following section analyzes the limitations of the methods used in the literature to estimate BEV charging demand. The research objectives of the dissertation are then derived from the limitations of these methods.

In order to identify possible congestions in the electric grid resulting from the electrification of private ICEVs in urban regions, both the spatial and temporal distribution of BEV charging demand must be determined. Charging demand data with high temporal resolution enables the identification of critical peak loads generated by BEVs during the course of the day, while high spatial resolution allows such peak loads to be located for small neighborhoods and districts, enabling grid planners to target grid expansion and reinforcement.
However, the methods described in [24], [69] can only be used to determine the temporal distribution of BEV charging energy demand, while the methods developed in [25], [70], [71] only allow determining the spatial distribution.

The determination of charging demand resulting from the electrification of private ICEVs is the prediction of a future scenario. This future spatial and temporal distribution of charging demand is directly dependent on the future charging behavior of BEV users, which is unknown. Therefore, a methodology for estimating the spatial and temporal distribution of BEV charging demand must allow for the investigation of different charging scenarios. In order to achieve high accuracy and variability, it should be possible to simulate not only the charging behavior of the entire fleet but also the dependency between the charging events of an individual vehicle (e.g. if the vehicle has already been charged a certain amount at work, it will not be recharged afterward when shopping). For this purpose, it is necessary to track the status of all BEVs in the considered area as a function of time. The status of a BEV includes the activity of the BEV user and the geographic location where the activity is performed as well as the SOC of the BEV.
In addition to the influence of the charging scenario on the spatio-temporal distribution of charging demand, status tracking also enables the study of the influence of different charging scenarios on the number and location of charging stations required to meet the charging demand as well as the type of charging infrastructure needed (e.g. charging stations at workplaces, at shopping locations or at public spaces).
Tracking of the vehicles additionally allows for investigation of how an electrified private transport can be used as intermediate electricity storage for renewable energies thus contributing to the efficient use of renewable energies and the integration of renewable energies into the electricity mix[3]. The methods developed by [72], [73] do not allow full tracking of BEV status because they do not capture the activities of BEV users. Since the method developed by [74] does not capture the geographic locations where activities are performed, full status tracking is also not possible.

Tracking the status of BEVs is possible by using activity-based transport models that create individual full-day travel schedules for each BEV in the considered area (see Section 2.2.2). An activity-based approach for the determination of the spatial and temporal distribution

[3] Vehicles can be charged whenever renewable energy generation exceeds power demand. If the power demand exceeds renewable power generation, the energy from the vehicle's batteries can be fed back into the electric grid. This strategy of feeding electricity back into the electric grid is called Vehicle to grid (V2G).

of charging energy demand is used by [75]–[78]. Common to all of these studies is that insufficient assumptions were made for the spatial distribution of vehicle size classes in the considered area. As explained in Section 2.3, this leads to the fact that the computed spatial distribution of the BEV charging demand has limited accuracy.
Another major limitation of studies [75]–[78] is, that they rely on detailed travel surveys to determine the traffic flow in the considered area. Such surveys are typically unavailable or difficult to obtain for most locations in the world, which severely limits the transferability of the methods.

From the analysis of the limitations of the existing studies, the research objectives of this dissertation emerge. A method needs to be developed which allows for the determination of the BEV charging demand resulting from the electrification of private internal combustion engine vehicles in urban areas. The method should satisfy the following requirements:

- The BEV charging demand needs to be determined with high spatial and temporal resolution, thus enabling the determination of the additional spatio-temporal grid load in the considered area.
- For each vehicle in the considered area, its SOC, the activity of the BEV user, and the geographic location of the activity need to be tracked as a function of time. This enables to study:
  - the effect of different charging scenarios on the spatial and temporal distribution of BEV charging demand.
  - the effect of different charging scenarios on the charging station demand.
  - the contribution of the electrified private transport to the efficient use of renewable energies and the integration of renewable energies into the electricity mix.
- The method should be transferable to other urban areas.

3 Summary and Overall Context of the Publications

This cumulative dissertation consists of two main parts. In the first part, the method is developed which allows forecasting the spatial and temporal distribution of BEV charging energy demand in an urban area resulting from the electrification of private internal combustion engine passenger cars. This first part consists of three published papers:

- Publication I [27]
- Publication II [28]
- Publication III [29]

In the second part of the dissertation, further research is conducted based on the results from part one. This second part consists of one published paper and one additional unpublished topic:

- Publication IV [30]
- Unpublished topic "Charging infrastructure demand in Berlin"

In Section 3.1, the three topics of the first part are briefly summarized. In Section 3.2, the topics of the second part are summarized.
Figure 3.1 shows an overview graphic that schematically illustrates how these five topics are connected.

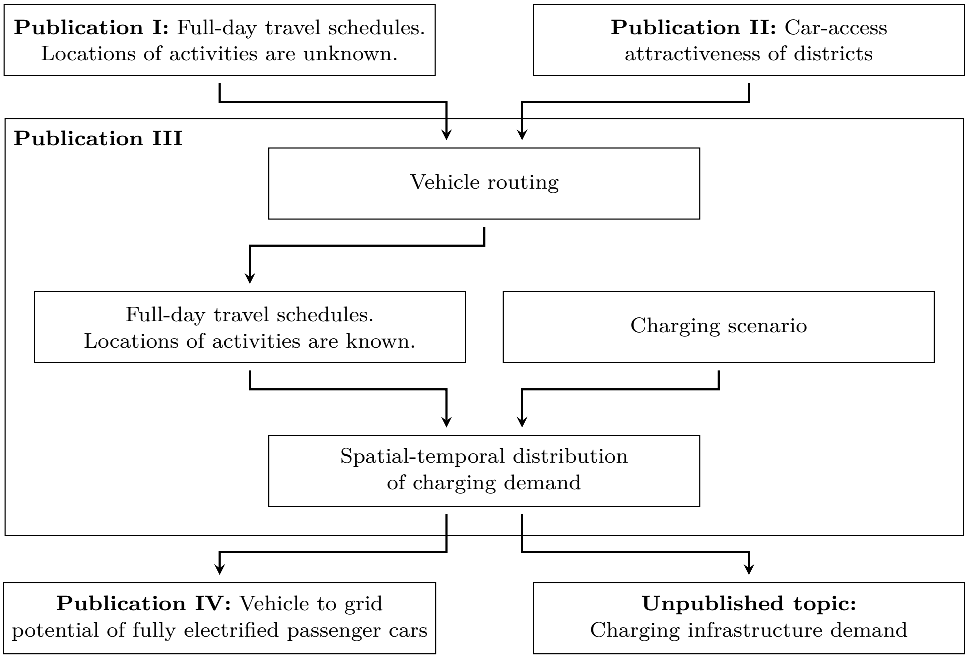

Figure 3.1: Schematic overview of this cumulative dissertation.

3.1 Estimating the Spatial and Temporal Distribution of BEV Charging Demand in Urban Areas - Method and Implementation

In the first part, the method is developed which allows forecasting the spatial and temporal distribution of BEV charging energy demand in an urban area resulting from the electrification of private internal combustion engine passenger cars. The method is demonstrated for the urban area of Berlin and its 448 sub-districts, assuming full electrification of Berlin's private transport. The development of the method is described in Chapter 4.

3.1.1 Publication I

In the publication "Methodology for Estimating the Spatial and Temporal Power Demand of Private Electric Vehicles for an Entire Urban Region Using Open Data" [27] Berlin is divided into 448 districts and then, assuming full electrification, the conventional private passenger vehicles in the districts are replaced by electric reference vehicles. By using an activity-based approach full day travel schedules are generated for each private car. Since the underlying dataset is limited, the schedules generated do not include information about the geographic location where a vehicle is parked while the BEV user is performing an activity. Accordingly, the spatial and temporal distribution of charging demand can only be determined by assuming that charging occurs exclusively at the residences of BEV owners. The original publication can be found in Section 4.1.

3.1.2 Publication II

To overcome this limitation, the geographic location where the vehicle is parked while the BEV user is performing an activity needs to be determined. An important input variable in this determination is the car-access attractiveness of the districts. The car-access attractiveness is a measure of how attractive districts are to drive to by car for a particular activity. A high attractiveness indicates that a location is highly likely to be accessed by car, while a low attractiveness means that the location is more likely to be accessed by another mode of transportation. The method to determine the car-access attractiveness of locations is developed in the publication "Car-Access Attractiveness of Urban Districts Regarding Shopping and Working Trips for Usage in E-Mobility Traffic Simulations" [28].
The original publication can be found in Section 4.2.

3.1.3 Publication III

In the publication "Forecasting the Spatial and Temporal Charging Demand of Fully Electrified Urban Private Car Transportation based on Large-Scale Traffic Simulation" [29], the unknown geographical locations of the activities are determined. For this purpose, a route assignment approach is developed that assigns a destination district to each vehicle trip based on a destination choice model. In addition to the car-access attractiveness determined in the second part of the method, the distance and travel speed between districts, as well as the availability of parking spots in the districts are considered for destination choice. By determining the destinations of BEV trips, a complete travel schedule is available for each BEV. This allows determining the spatial and temporal distribution of BEV charging demand in the urban area by applying charging scenarios.
The original publication can be found in Section 4.3.

3.2 Further Research

In the second part of this dissertation, further research is conducted based on the results of the first part. This second part can be found in Chapter 5.

3.2.1 Publication IV

The publication "Sector Coupling through Vehicle to Grid: A Case Study for Electric Vehicles and Households in Berlin, Germany" [30] examines the Vehicle to grid (V2G) potential of fully electrified passenger cars in Berlin. The method developed for this purpose allows to determine for each Berlin sub-district, the percentage of residential and BEV energy demand that can be met by renewables if V2G is deployed, and answer the question of whether a full renewable supply is possible. In addition, the increase in peak load in the districts and the increase in battery load due to V2G are determined.
The original publication can be found in Section 5.1.

3.2.2 Charging Infrastructure Demand in Berlin

Based on the determined BEV charging demand in Berlin, the number and spatial distribution of the charging stations required to meet the charging demand are determined. The required number of charging stations is determined for different parking space types and utilization levels.
This unpublished topic can be found in Section 5.2.

4 Estimating the Spatial and Temporal Distribution of BEV Charging Demand in Urban Areas - Method and Implementation

In this chapter, the method is developed that allows forecasting the spatial and temporal distribution of BEV charging energy demand in an urban area resulting from the complete electrification of private internal combustion engine passenger cars. The method is developed in three publications. These original publications can be found in Sections 4.1, 4.2 and 4.3.

4.1 Publication I

Methodology for Estimating the Spatial and Temporal Power Demand of Private Electric Vehicles for an Entire Urban Region using Open Data

Florian Straub[1], Simon Streppel[1], Dietmar Göhlich[1]

[1]Chair of Methods for Product Development and Mechatronics, Technische Universität Berlin, Strasse des 17.Juni 135, 10623 Berlin, Germany

(This article has been published on 08 April 2021 by MDPI in the "Energies" Special Issue: Integrated Energy Systems and Transportation Electrification, available online: https://doi.org/10.3390/en14082081)

Abstract: With continuous proliferation of private battery electric vehicles (BEVs) in urban regions, the demand for electrical energy and power is constantly increasing. Electrical grid infrastructure operators are facing the question of where and to what extent they need to expand their infrastructure in order to meet the additional demand. Therefore, the aim of this paper is to develop an activity-based mobility model that supports electrical grid operators in detecting and evaluating possible overloads within the electrical grid, deriving from the aforementioned electrification. We apply our model, which fully relies on open data, to the urban area of Berlin. In addition to a household travel survey, statistics on the population density, the degree of motorisation, and the household income in fine spatial resolution are key data sources for generation of the model. The results show that the spatial distribution of the BEV charging energy demand is highly heterogeneous. The demand per capita is higher in peripheral areas of the city, while the demand per m^2 area is higher in the inner city. For reference areas, we analysed the temporal distribution of the BEV charging power demand, by assuming that the vehicles are solely charged at their residential district. We show that the households' power demand peak in the evening coincide with the BEV power demand peak while the total power demand can increase up to 77.9%.

Keywords: electric vehicle; activity-based simulation; transportation electrification; charging power demand; spatial temporal distribution; open data

4.1.1 Introduction

Poor air quality in cities and continuously rising greenhouse gas emissions worldwide have led to a steady tightening of emission limits in recent years. The European Union has committed itself to reducing greenhouse gas emissions by 2050 by 80–95% of the level of 1990 [79]. In Germany, greenhouse gas emissions are planned to be reduced by 50% by 2030 compared to 1990 [80]. One key driver of this reduction is the substitution of internal combustion engine vehicles (ICEVs) with vehicles with alternative drive systems, primarily battery electric vehicles (BEVs). However, an increasing number of BEVs and the resulting large demand of electrical energy and power can lead to bottlenecks in the power supply if the necessary electrical grid infrastructure is not established or reinforced [20]–[23]. The investigations in this paper are restricted to the electrification of private internal combustion engine cars. The electrification of other urban vehicles such as buses or urban freight transport vehicles was investigated, for example, by the authors of [81]–[83]. The additional demand of private battery electric cars for electrical energy and power varies greatly depending on spatial and temporal factors. In general, areas with high population density and a high vehicle per capita rate have a higher demand for electrical energy compared to sparsely populated areas with few vehicles per inhabitant [22], [77], [78]. The authors of [20]–[22], [24] show that the electrical energy and power demand for charging BEVs differs depending on the time of the day and the type of the day (working day or weekend day). This large degree in variability creates difficulties concerning the planning of the expansion and optimisation of the electric grid, which is necessary to meet the additional charging energy and power demand. To overcome this limitation, data-based models with high spatial resolution are required in order to make realistic statements about the spatial and temporal energy and power requirements arising from the electrification of motorised individual traffic.

The authors of [71] developed a model based on diffusion theory that determines the spatial power requirements in the city of Porto, considering different charging capacities and five battery electric vehicle penetration rates from 10% to 100%. However, the study does not include a differentiated temporal determination of the power demand. By generating commuting travel chains for their investigation, the authors of [24] estimate the spatial and temporal distribution of the charging power demand of BEVs in urban areas. Result-relevant values such as the start time of the first trip or the covered trip distance are random and independent of the activity drawn from a normal distribution and a lognormal distribution, respectively. The distributions are adjusted to average values derived from a travel survey. The authors of [72] simulate the spatial and temporal distribution of the charging energy demand for an artificial city consisting of a city center, suburban areas, and connecting highways. All simulated persons and their vehicles undertake a round trip, which starts in a suburban area then goes to a random point within the city center and back. Within the city center, the persons decide whether to charge their car, depending on the depth of discharge. The arrival and departure times of the vehicles in the city center are drawn from a gamma distribution and are imprinted on the vehicles. The distribution is fitted to the results of a travel survey, which was conducted in Chicago.
Another approach to modelling the spatial and temporal energy and power demand deriving from electrification of the traffic is offered by activity-based models [77], [78], [84]. In activity-based models, the individual properties of individual persons within the research space are used to create full-day travel schedules for those persons. The resulting daily patterns for individual persons consist of a consecutive sequence of activities and trips.

According to [84], activity-based models are particularly suitable for simulating the energy and power demand of BEVs. They capture the relationship between activity and mobility patterns, which can be used to determine the dwell times of the persons and their vehicles at different locations. The energy and power demand can then be determined by imposing charging strategies.
An example for an activity-based mobility model is the framework FEATHERS [85], which the authors of [77] used to simulate spatial and temporal charging power demand in the Flemish region in Belgium. Therefore, they divided the region into several districts. As there were no empirical data such as a travel survey available in the region, the authors used self-acquired data including "activity-travel diaries", information on "activity (re)scheduling decisions of individuals" and "data on household multi-day activity scheduling". The vehicle class category distribution, which has a significant impact on the energy and power demand (larger and heavier vehicles tend to have a higher energy consumption compared to smaller and lighter vehicles), matches the numbers for the entire region and not the individual districts. This results in a non-precise estimate of the spatial distribution of the energy and power demands. Furthermore, the authors do not verify their results by comparing them with the empirical data from the underlying survey. The authors of [78] used a household interview travel survey to create a activity-based mobility model for the Singapore urban area. After the division of Singapore into several districts, they used their model to estimate the spatial and temporal distributions of the charging energy demand for a working day and a weekend day, considering different electrification rates for private vehicles. Similar to [77], the vehicle class categories were drawn from a distribution that matches the overall vehicle class category distribution in Singapore. Additionally, the mobility model was not verified by comparison with the underlying survey results.
In their research on decarbonisation of the urban traffic, the authors of [86] used the activity-based simulation framework MATSim [87], [88] to analyse the effects of complete replacement of the current population of ICEVs with BEVs in urban regions. The authors focused on electrification of the entire transport system including private vehicles, the public transportation sector, and commercial and municipal traffic. Since the authors studied the impact of ICEV electrification for the entire urban area of Berlin and not its districts, they did not focus on the spatial resolution of the occurring charging energy and power demand. The vehicle class categories were drawn from a distribution that matches the overall vehicle class category distribution in Berlin and not the distribution in the Berlin districts. Between the MATSim data basis, namely census data, and the resulting trips in the simulation, there are several process steps leading to a risk of inaccuracies in spatial resolution. For this reason, we decided to infer the activity pattern and the energy and power demand in the individual districts directly from the census data and other data sources.

The aim of this paper is to develop a model that supports electrical grid operators to detect and evaluate possible overloads within the electrical grid, deriving from the electrification of private ICEVs in urban regions. Therefore, we develop a methodology, the novelty of which lies in the generation of an activity-based mobility model through the direct combination of a survey on travel behaviour [89]–[91], with data sets containing information about the population density [92], the degree of motorisation (which indicates the amount of vehicles per 1000 inhabitants) [93], and the household income in fine spatial resolution [94], [95]. Through this direct combination, our model provides data-based results with high spatial and temporal resolution. Furthermore, the fine resolution of the household income enables

us to determine the vehicle class category distribution in fine spatial resolution, which has, as we discussed in the previous paragraphs, a significant impact on the energy and power demand and is neglected by other researchers. In contrast to most other scientific works, we do not use a person-based but a vehicle-based approach. This allows us to realistically depict the use of the same vehicle by several persons (for example, in family groups). Since all used data sets are openly available and therefore relatively easy to acquire in most places of the world, our methodology is transferable to other urban areas. We apply our methodology to the urban area of Berlin and assume a scenario where 100% of the current private car population is electrified. We consider a working day and a Saturday in our simulation. We exclude Sundays from our simulation as 69% of the vehicles remain parked on Sundays, compared to 56% on Saturdays. In addition, the average distance of all vehicles is 23.9 km on Sundays, which is below the 26.1 km on Saturdays [90]. A higher energy and power demand on Sundays compared to Saturdays is therefore not to be expected. By applying the charging strategy "home-charging", we calculate the spatial and temporal energy and power demand distribution resulting from charging the BEVs.
In the city of Berlin, 40% of the population has access to private car parking spaces [90] while the remaining cars are parked in public spaces. Therefore, in this paper "home-charging" does not mean that all cars are charged in private parking lots at the owner's place of residence but that they are charged within the district where the owner of the vehicle lives. We assume that sufficient public charging infrastructure is available. We chose the strategy "home-charging" since, according to [96], 65% of the German population prefers home charging to charging at public charging stations (15%) or at work (7.5%). Reference [96] is a study on the acceptance of e-mobility in Germany. It was conducted in 2019 by interviewing 1200 German households.

This paper is structured as followed: In Section 4.1.2, our methodology is described and the implemented scenario is presented. The results are shown and analysed in Section 4.1.3. Finally, the main conclusions of this paper are derived in Section 4.1.4.

4.1.2 Methodology

The methodology used for our mobility model consists of three main parts. As a first step, we divide the city of Berlin into districts and determine for each the number of electric vehicles and the vehicle class categories within it. To do so, we use data sets containing information about the population density [92], the degree of motorisation [93], and the household income within the districts [94], [95]. In the second step, we generate individual daily patterns for the vehicles based on a household travel survey [89]–[91]. Finally, we use these daily patterns to determine the energy and power demand generated by charging the BEVs for a working day and a Saturday. These results are compared to the base power demand of the households within the districts.

4.1.2.1 District Classification and Vehicle Population

Most activity-based mobility models share one disadvantage. When the daily patterns of the persons are created and the means of transport is chosen, they assign each person their own vehicle. Therefore, multiple use of one vehicle is not considered. Since the dwell times of the vehicles are then determined incorrectly, the determination of the temporal distribution of the charging power demand is inaccurate. To overcome this problem, in our mobility model, we do not consider the individual persons but the vehicles within the system boundaries.

We assume a scenario where 100% of the current private car population is electrified having the same share regarding vehicle class category as the current car population. Due to the lack of open data, commercially used vehicles such as delivery vehicles or taxis are not considered in our study. According to the “Kraftfahrtbundesamt”, which is the German Federal Motor Transport Authority, 1.203 million cars were registered in Berlin in 2018, of which 1.045 million of them were private cars [97]. In order to distribute this number of vehicles spatially correctly, we make use of the official classification of the Berlin administration [98], which divides the twelve Berlin districts into 448 subdistricts, called “Lebensweltlich orientierte Räume” (neighbourhood oriented districts) (LORs). The LOR classification was firstly introduced in 2006. Within each LOR, the structure of the contained buildings and the socioeconomical status of the inhabitants are similar. The LORs are usually separated from each other by major roads, rivers, or rails.
We derive the number of inhabitants for each LOR from [92], which is a freely available statistic provided by the Berlin authorities. The statistic is created by counting all registered residents within the LORs in 2018. The LOR classification, the population density, and the number of inhabitants within the LORs are depicted in Figure 4.1.

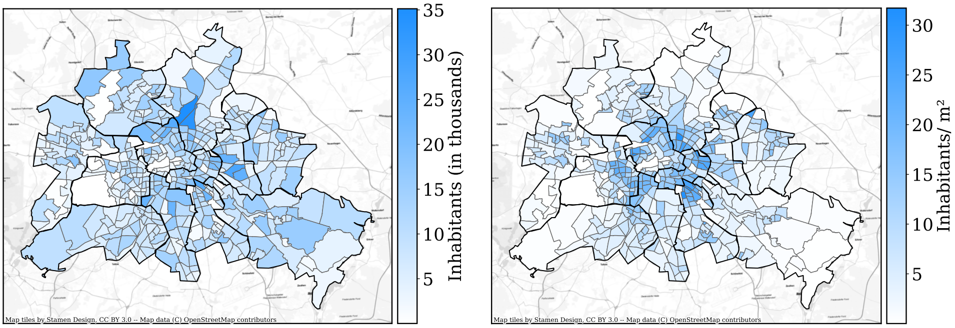

(a) Inhabitants in the Berlin LORs

(b) Population density in the Berlin LOR

Figure 4.1: Distribution of the population in the Berlin subdistricts, “Lebensweltlich orientierte Räume” (LORs).

To estimate the number of vehicles in each LOR, we use freely available data about the degree of motorisation (amount of vehicles per 1000 inhabitants) in each LOR [93]. The degree of motorisation for the Berlin LORs is depicted in Figure 4.2. It can be seen that the degree of motorisation is higher in LORs that are located in the peripheral areas of the city compared to the city center. By multiplying the amount of vehicles per person with the total amount of persons within the LORs, we calculate the number of vehicles for each LOR separately.

Since the BEVs’ energy consumption is highly dependent on the vehicle class category (larger and heavier vehicles tend to have a higher energy consumption compared to smaller and lighter vehicles), the vehicle class category distribution for all vehicles within the LORs has to be determined. To do so, we make use of the 2017 German household travel survey (GHTS) [89]–[91]. The survey contains information on 316,361 persons from 156,420 households in Germany and on almost one million trips. For the study, the members of a household were asked about their activities and trips during reference days. This allowed for conclusions on daily travel patterns. Furthermore, as a classical household travel survey, the study contains sociodemographic information such as gender and age, or the income of the household. It contains further information, such as the amount of vehicles in the household and information on the vehicle class category. The data set can be obtained freely, either as raw data [90] or already pre-evaluated [91]. As the data set contains information on the travel behaviour in all of Germany, we initially limited the data set to households and persons within the city of Berlin. Furthermore, we excluded all trips that were not undertaken by car.

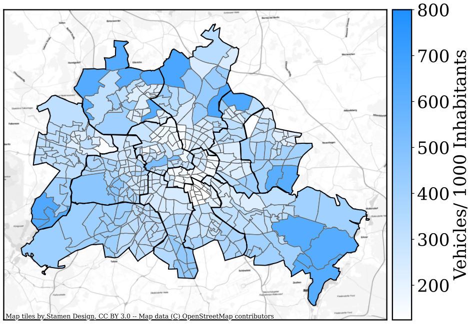

Figure 4.2: Degree of motorisation in the Berlin LORs.

According to the GHTS data set, the amount of cars per household in Berlin correlates with the income of the household. In general, households with higher income own more vehicles compared to households with lower income. Furthermore, the GHTS indicates that the vehicle class category distribution in Berlin also depends on the income of the household. Households with high income tend to own larger vehicles. The distributions are depicted in Table 4.1. In the GHTS data set, the household's income is divided into five income categories. For a one-person household, the average net income for the income category "very low" lies below €900, between €900 and €1500 for the category "low", between €1500 and €2800 for the category "medium", between €2800 and €4000 for the category "high", and above €4000 for the category "very high".

Table 4.1: Correlation between household income and vehicles in Berlin.

Household Income	Average Amount of Cars per Household	Relative Frequency Vehicle Class Category			
		Mini Compact	Compact	Medium	Large
very low	0.3	0.31	0.37	0.27	0.054
low	0.5	0.35	0.35	0.25	0.052
medium	0.7	0.27	0.39	0.26	0.074
high	1.0	0.24	0.34	0.32	0.11
very high	1.3	0.18	0.30	0.34	0.19

In their research on the socio-structural situation in Berlin, the authors of [99] show that the residential area quality strongly correlates with the household income. This means that households with higher income tend to live in areas with higher quality. High-quality residential areas are mostly located close to the city center and are usually characterised

by rather high greening. In comparison, low-quality residential areas mostly have high building density, which may be intermixed with or adjacent to commerce and industry. In addition, simple residential areas usually have little greenery [95]. According to [99], we estimate the shares of household income in the LORs by analysing the residential area quality [95]. To verify our results, we check whether our results match the distributions of the household income in the twelve Berlin districts. We derived those distributions from the 2018 census data [94]. The census is conducted on a yearly basis in Germany by interviewing 1% of the population. It is freely available and provides information on the economic and social situation of the population in Germany, such as information on household and family structures, employment, or income situation. The resulting distribution of the household income for the Berlin LORs is depicted in Figure 4.3.
By combining the aforementioned information, we obtain the amount of vehicles for each vehicle class category within the LORs.

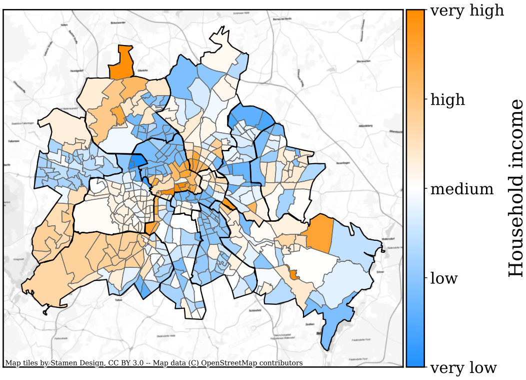

Figure 4.3: Household income distribution in the Berlin LORs.

4.1.2.2 Mobility Profiles

As a basis for the mobility profiles of the vehicles, we analysed the data set from the 2017 German household travel survey (GHTS) [89]–[91]. A mobility profile is a sequence of activities and trips between those activities. For our study, we assumed that BEV drivers show the same mobility behaviour as ICEV users. In Figure 4.4, a general mobility profile of a vehicle is shown. The vehicle starts at "Home" in the morning before spending 7 h and 50 min at the activity "Working" and 30 min at the activity "Shopping". It arrives back "Home" at 17:00. In order to create mobility profiles, we extracted the relevant information on trips (activity, departure and arrival times, and trip distance) from the GHTS data. The data set distinguishes more than 25 activities. Similar to [78], [88], we divide those activities into five superordinate activities for simplification reasons: "Working", "Shopping", "Education", "Home", and "Else".

The GHTS data set is evaluated for an average working day (Monday–Thursday) and Saturdays. We exclude Fridays from our analysis, as the average distance of all vehicles is 15.1 km on Fridays, which is less than half of the 32.6 km average distance on the other working days. On Fridays, 62% of the vehicles remain parked, compared to 45% on the other working days. Sundays are excluded from our analysis, as 69% of the vehicles remain parked compared to 56% on Saturdays. In addition, the average distance of all vehicles is 23.9 km on Sundays, which is below the 26.1 km on Saturdays. A higher energy and power requirement on Sundays compared to Saturdays and on Fridays compared to the other working days is therefore not to be expected.

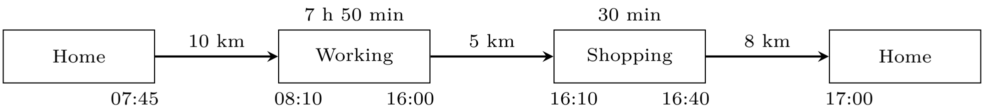

Figure 4.4: Example of a general mobility profile.

The creation of the mobility profiles is performed successively for each individual vehicle within the individual LOR. The basis for this process is the distribution of the vehicle class categories we derive in Section 4.1.2.1. For each of the four vehicle class categories, we considered three reference vehicles, making in total a sum of twelve considered reference vehicles, which are depicted in Table 4.2. For each reference vehicle, the energy demand per 100 km and the vehicles' battery capacity can be obtained from Table 4.2. The average consumption is divided into inner-city trips, which are characterised by distances of less than 20 km and outer-city trips. The values of the energy consumption and the battery capacity are based on test drives of the "Allgemeine Deutsche Automobil Club" (ADAC), a German motoring association, and already include charging losses [100].

Table 4.2: Reference Vehicles.

Class	Model	Battery Capacity (kWh)	Consumption (kWh/100km)	
			Inner City	Outer City
Mini compact	Mitsubishi i-MiEV [101]	15.9	11.3	16.9
	Renault Zoe [102]	64.3	14.5	19.0
	VW e-Up! [103]	18.6	14.0	17.7
Compact	BMW i3 [104]	48.8	13.0	17.9
	Hyundai Kona E [105]	73.9	14.0	19.5
	VW e-Golf [106]	34.9	12.7	18.2
Medium	Kia e-Niro [107]	72.3	12.5	18.1
	Nissan Leaf [108]	68.4	17.2	22.7
	Tesla Model 3 [109]	60.0	17.4	19.3
Large	Audi e-tron [110]	94.3	23.5	25.8
	Mercedes EQC [111]	93.1	23.0	27.6
	Tesla Model S [112]	100.4	21.2	24.2

The general process for creating the mobility profile for one vehicle consists of six main steps (1)–(6). The process is depicted in Figure 4.5 and is described below. Taking the vehicle class category of the vehicle as input, one of the three reference vehicles is drawn from Table 4.2 with equal distribution (1).

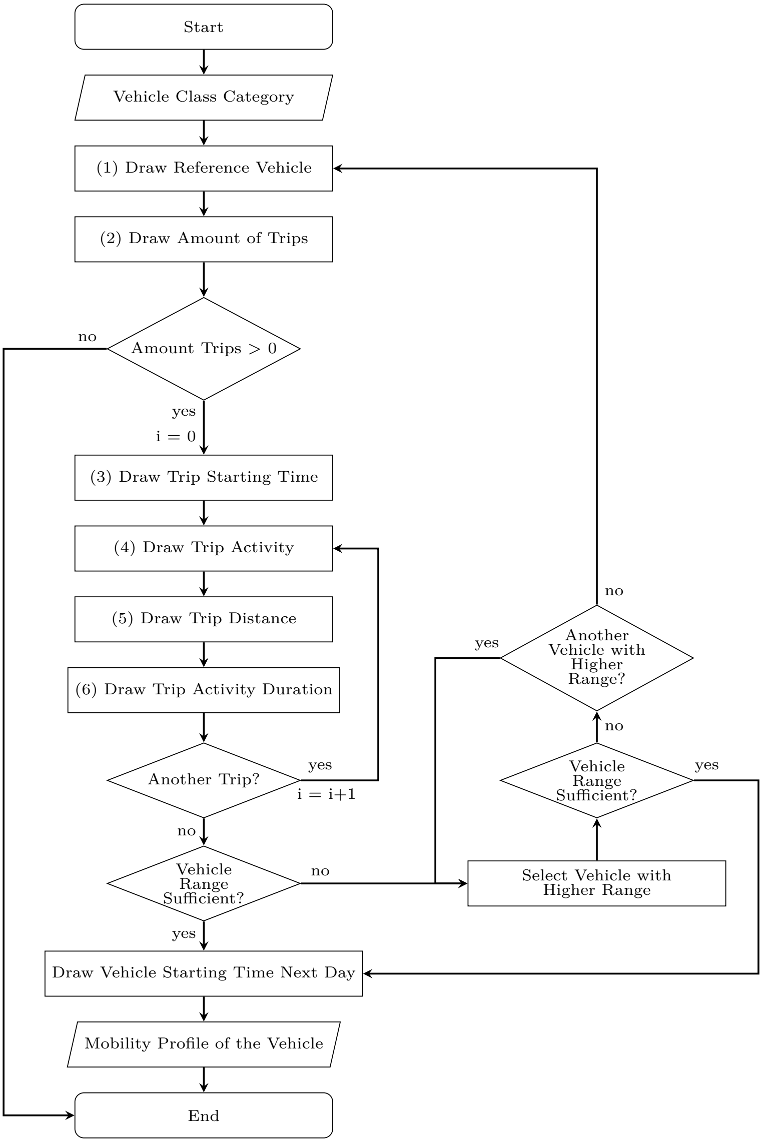

Figure 4.5: General process for creating the mobility profile for one vehicle.

In (2), the number of trips per day for the vehicle is drawn. We derive the underlying discrete probability distribution by analysing the GHTS data set. A separate probability function is evaluated for each vehicle class category. If the number of trips is zero, no mobility profile is created for the vehicle and the process starts with the next vehicle. If the number of trips is greater than zero, the starting time of the first trip is drawn from a probability distribution we generated for a 24 h interval by analysing the GHTS data set (3). The probability distributions we use in (3) are depicted in Figure 4.6 for a working day (Monday–Thursday) and a Saturday. On a working day, one sharp peak can be seen at around 08:00 in the morning. This is due to the fact that many vehicles are used early in the morning on the way to work. In comparison, two less sharp peaks can be seen on Saturdays. Vehicles tend to be used on weekends for shopping or leisure activities, which start either in the late morning or afternoon.

Depending on the trip's starting time, the trip's activity is drawn afterwards (4). For this purpose, we use discrete distribution functions on an hourly basis, which provide information about the probability that a certain activity will occur. In (5), the distance of the trip is drawn depending on the trip's activity. For the activities "Working", "Shopping", and "Home", the underlying probability distributions are depicted in blue in Figure 4.7a–c for a working day and in Figure 4.7d–f for a Saturday. It can be seen that "Working" trips on working days usually cover higher distances compared to "Shopping" and "Home" trips. The trip distance for 80% of the "Shopping" trips is below 11 km, while it is below 16 km for "Home" trips and 29 km for "Working" trips. On Saturdays, the trip distance for 80% of the "Shopping", "Working", and "Home" trips is about 19 km. The distributions in (4) and (5) are generated by analysing the GHTS data set.

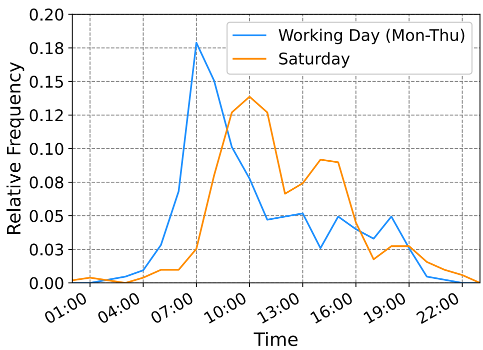

Figure 4.6: Starting time of the first trip on a working day (Monday–Thursday) and a Saturday.

To determine the respective travel times for the trips, we use speed assumptions. We use [113] to estimate the activity duration in (6). Reference [113] is a survey from German authorities on the time usage behaviour of German citizens. The statistic provides information on how much time is spent on different activities such as working, shopping, education, or leisure activities. The survey was conducted in 2012, the third time after 1992 and 2002. For the survey, a total of 11,000 persons in approximately 5000 households in Germany were interviewed. If the vehicle undertakes further trips, the loop is repeated with (4). The starting time of the next trip is the ending time of the last trip. If the last trip is for the activity "Home", the loop is repeated with (3) and a new starting time is drawn. Finally we check whether the total driven distance between two consecutive charging events is covered by the range of the reference vehicle. As we only consider "home-charging", a charging event can only occur if the activity is "Home". If the vehicle's range is not sufficient, a vehicle with a higher range within the same vehicle class category is drawn. If the vehicle's range is still too small to cover the driven distance, a vehicle with a sufficient range is searched for in the other vehicle class categories. If the total driven distance between two consecutive charging events exceeds the maximum range of all reference vehicles, the vehicle is re-simulated starting with (1). If the total driven distance can be covered by the reference vehicle, steps (2) and (3) are repeated to determine whether and when the vehicle drives off again the next day.

4.1.2.3 Assumptions to Calculate the Spatial and Temporal Power Demand

Based on the created mobility profiles for all privately owned vehicles in Berlin, we simulated 24 h of a working day (Monday–Thursday) and a Saturday to derive the spatial and temporal distribution of the BEV charging energy and power demand. Vehicles that started within this period are allowed to return later than 24:00. The results are then projected onto a 24 h interval. We made the following assumptions for the simulation in this paper:

- The vehicle's state of charge (SOC) at the start of the day is 100%.
- Charging exclusively at the home LOR. Sufficient public charging infrastructure is available.
- Charging starts immediately upon arrival at home and does not end until the vehicle is fully charged or drives off again.
- Constant charging power, which is independent of the SOC. To show the effects of different charging powers on the spatial and temporal distribution of the charging power demand, we run our simulation for charging powers of 3.7 kW and 11 kW, respectively.
- Power demand can be fully covered by the electrical grid at any time.

4.1.3 Results and Discussion

The first part of this section compares the simulation results with the GHTS data set. The comparison results are shown and discussed for the vehicles' trip distance distribution, the vehicles' average daily distances, and the amount of moving vehicles in Section 4.1.3.1; for the vehicle class category distribution in Section 4.1.3.2; and for the vehicles' trip starting time distribution in Section 4.1.3.3

In the second part of this section, we show and discuss in Section 4.1.3.4 the simulated result of the spatial distribution of the charging energy demand. In Section 4.1.3.5, the results of the temporal distribution of the charging power demand are presented and discussed.

4.1.3.1 Trip Distance and Moving Vehicles–Simulation and GHTS Data Comparison

In Figure 4.7, a comparison of the cumulative distribution function of the trip distance of the simulation (blue) and the GHTS data set (orange) is shown. Figure 4.7a–c show the results for a working day (Monday–Thursday), Figure 4.7d–f show the results for Saturday. The figures are depicted for the activities "Working", "Shopping", and "Home". The steps in the GHTS data graphs result from the self-reported travel times in the survey. Participants tend to report rounded numbers rather than give exact values. As it can be seen, the general distribution shape matches for all activities and days. In Figure 4.8, the modelling errors of the results in Figure 4.7 are depicted as a boxplot. The blue square indicates the mean error. The boxplot's whiskers are modeled in such way that they represent the 2.5% quantile and the 97.5% quantile, respectively; 95% of all errors are thus within the whisker limits.

The mean error is between −6.1% and 2.6% for a working day and between −2.0% and 3.3% on a Saturday. This indicates that the simulation represents the GHTS data with high accuracy.

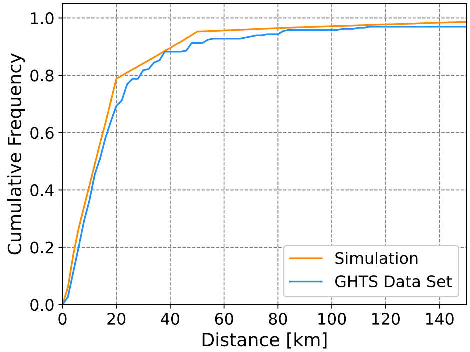

(a) Trip distance for working (Monday–Thursday)

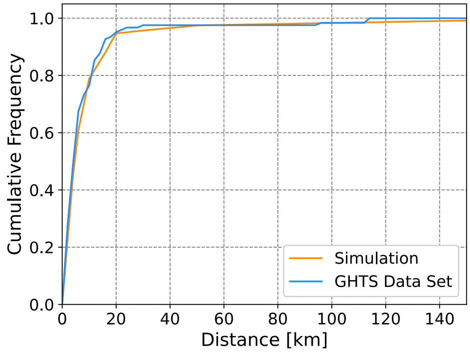

(b) Trip distance for shopping (Monday–Thursday)

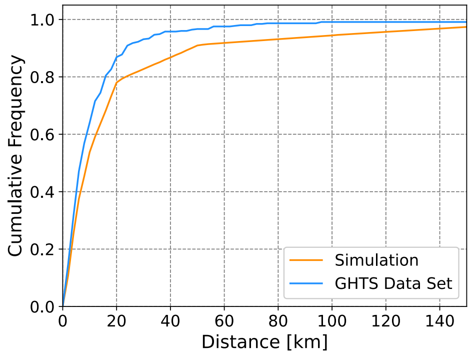

(c) Trip distance for home (Monday–Thursday)

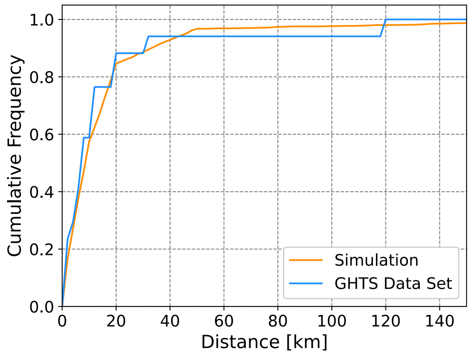

(d) Trip distance for working (Saturday)

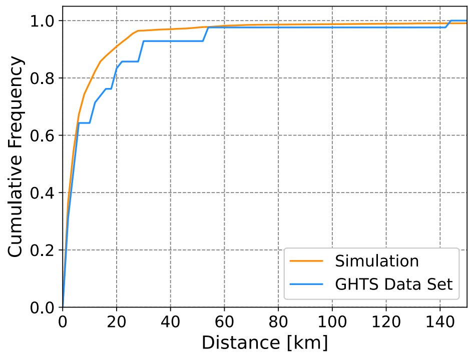

(e) Trip distance for shopping (Saturday)

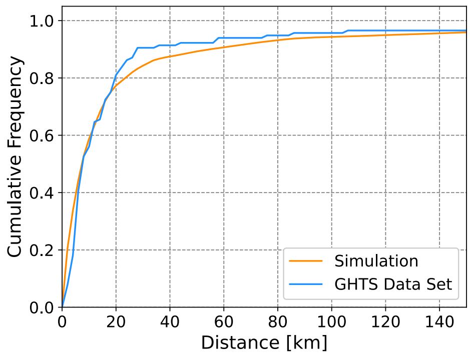

(f) Trip distance for home (Saturday)

Figure 4.7: Cumulative distribution function for trip distance–simulation and German household travel survey (GHTS) data set comparison.

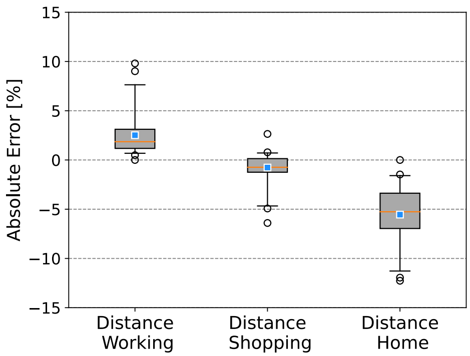

(a) Working day (Monday–Thursday)

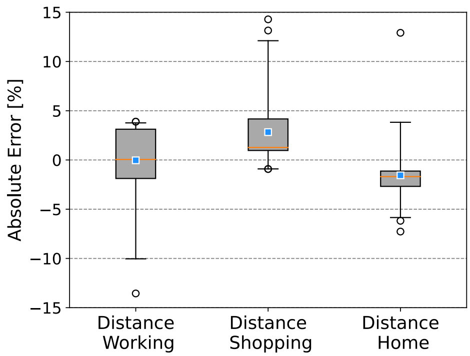

(b) Saturday

Figure 4.8: Modelling error distance distributions. The blue square depicts the mean error.

Table 4.3 compares the average daily distance driven by the simulated vehicles with the GHTS data set. The relative error is −10.4% for working days (Monday–Thursday) and −5.7% on Saturdays. This error can be easily explained. As we show in Section 4.1.2.2, the daily distances of the simulated vehicles are limited. Vehicles that cover large daily distances are not represented in our simulation. For working days (Monday–Thursday) trips with high distances are mostly "Working" trips, as can be seen in Figure 4.7a. The GHTS data set indicates that 95% of all "Working" trips are below 85 km, whereas the remaining 5% can reach values up to 750 km. On Saturdays, trips with high distances are mostly "Home" trips, as can be seen in Figure 4.7f. The GHTS data set shows that 95% of all "Home" trips on Saturdays are below 80 km whereas the remaining 5% can reach values up to 320 km. "Home" trips on Saturdays are higher compared to working days, as persons tend to travel higher distances for their leisure activities on Saturdays, which results in accordingly higher home distances.

Table 4.3: Comparison of the simulation and the GHTS data set–average daily distance and moving vehicles.

	Type of Day	GHTS Data Set	Simulation	Relative Error
Average Daily Distance	Working Day	32.6 km	29.2 km	−10.4%
	Saturday	26.1 km	24.6 km	−5.7%
Percentage Moving Vehicles	Working Day	54.8%	54.9%	0.18%
	Saturday	43.3%	43.8%	1.15%

This small share of trips with high distances in the GHTS data set lead to a higher average daily distance compared to our simulation. As time-consuming, inter-trip charging is necessary to cover high-distance trips, we assume that those trips are not undertaken with a private BEV but with other vehicles (e.g., shared vehicles) with alternative drives (e.g., hydrogen) in the future. Therefore, the reliability of the model is not affected by this error.
In Table 4.3, the proportion of moving vehicles for the simulation and the GHTS data set is shown. The relative error is 0.18% on a working day and 1.15% on a Saturday, which indicates that the simulation represents the GHTS data set with high accuracy.

4.1.3.2 Vehicle Class Category Distribution–Simulation and GHTS Data Comparison

In Table 4.4, the simulated vehicle class category distribution is compared to the GHTS data set. The relative error is 5.9% for the mini compact class, −1.7% for the compact class, −1.0% for the medium class, and −6.3% for the large class; hence, our simulation represents the data set well.

Table 4.4: Comparison of the simulation and the GHTS data set–vehicle class category distribution.

Vehicle Class Category	GHTS Data Set	Simulation	Relative Error
Mini Compact	25.5%	27.0%	5.9%
Compact	36.2%	35.6%	−1.7%
Medium	28.7%	28.4%	−1.0%
Large	9.6%	9.0%	−6.3%

4.1.3.3 Trip Starting Time–Simulation and GHTS Data Comparison

In Figure 4.9, a comparison of the simulated cumulative distribution function of the trip's starting time (blue) and the cumulative distribution function derived from the GHTS data set (orange) is shown. Figure 4.9a–c show the results for a working day (Monday–Thursday), Figure 4.9d–f show the results for Saturday. The figures are depicted for the activities "Working", "Shopping", and "Home". While the general distribution shape for the activity "Home" matches well, errors exist for the activities "Working" and "Shopping". Further improving the fit of those distributions would be a valuable future improvement. In Figure 4.10, the modelling errors of the results in Figure 4.9 are depicted as a boxplot. The mean error is between −4.3% and 2.6% for a working day (Monday–Thursday) and between −5.3% and 3.1% on a Saturday.

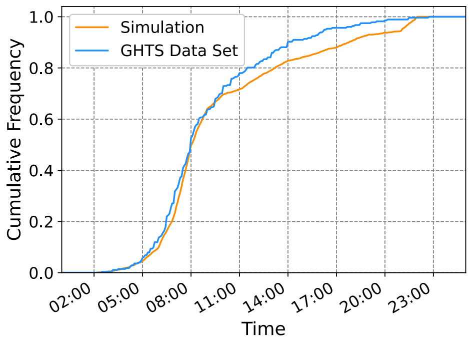

(a) Trip starting time for working (Monday–Thursday)

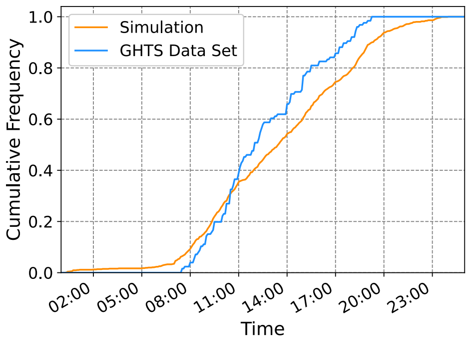

(b) Trip starting time for shopping (Monday–Thursday)

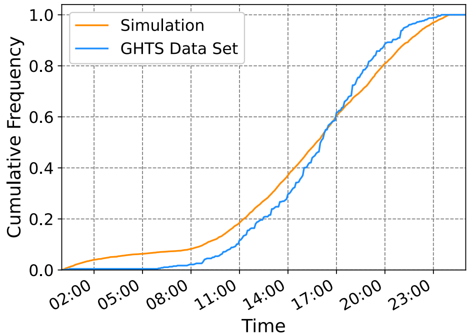

(c) Trip starting time for home (Monday–Thursday)

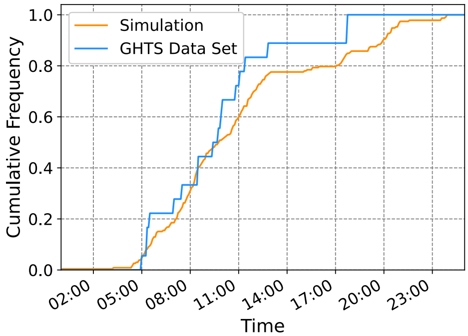

(d) Trip starting time for working (Saturday)

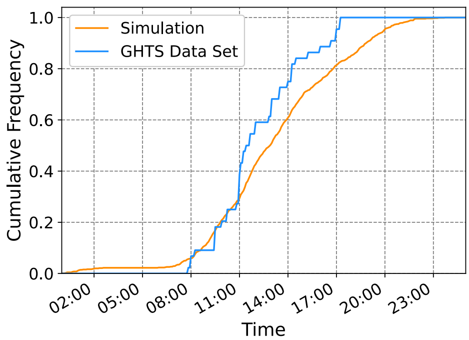

(e) Trip starting time for shopping (Saturday)

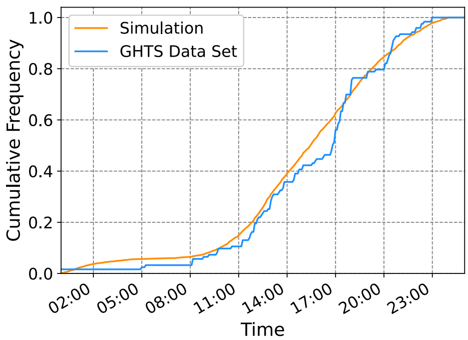

(f) Trip starting time for home (Saturday)

Figure 4.9: Cumulative distribution function for trip starting time–simulation and GHTS data set comparison.

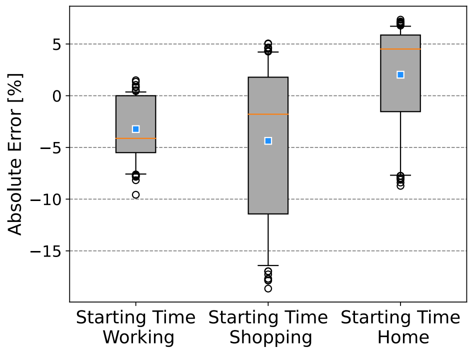

(a) Working day (Monday–Thursday)

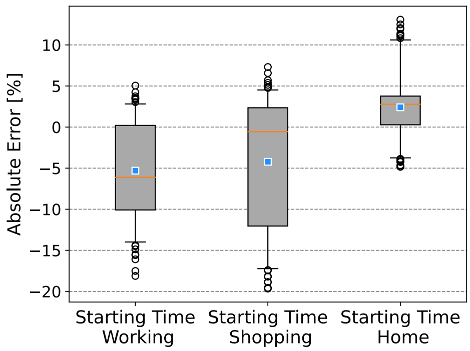

(b) Saturday

Figure 4.10: Modelling error starting time distributions.

4.1.3.4 Spatial Distribution of the Charging Energy Demand

By using the mobility model explained in Section 4.1.2.2 and the assumptions made in Section 4.1.2.3, we calculate the spatial distribution of the charging energy demand in Berlin. Figure 4.11 shows the resulting spatial distribution of the charging energy demand in the Berlin LORs for a working day (Monday–Thursday). As we consider "home-charging" only, the spatial demand of energy is equally distributed over Berlin on Saturdays compared to working days. The total charging energy demand in Berlin of 4730 MWh on Saturdays is around 14.9% less compared to a working day with 5435 MWh.

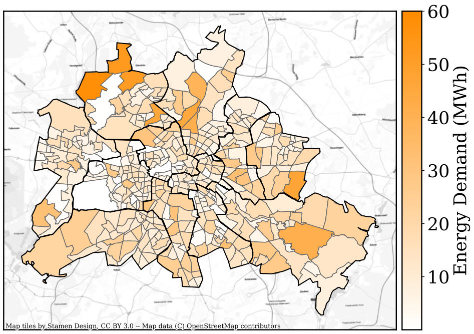

Figure 4.11: Spatial distribution of the battery electric vehicle (BEV) charging energy demand in the Berlin LORs for a working day (Monday–Thursday).

This can be explained as follows. The average distance of all vehicles is 18.7% higher on working days than on Saturdays. The proportion of moving vehicles is 25.3% higher on working days compared to Saturdays (see Table 4.3). This leads to the fact that the daily distances of moving vehicles are greater on Saturdays compared to working days. According to Section 4.1.2.3, a higher energy consumption is assumed for higher distances. Therefore, the energy consumption on Saturdays is 14.9% lower compared to working days and not, as may expected 18.7% lower. As it can be seen in Figure 4.11, the energy demand in LORs located in the peripheral areas of the city are higher compared to the ones located in the city center. This is due to a higher degree of motorisation and a higher household income in the peripheral areas. LORs with near zero charging energy demand are pure forest, lake, or industrial areas without inhabitants. It can be seen that LORs with a high energy demand coincide with LORs of high populations, high degrees of motorisation, and high household incomes.

The influence of the factors "degree of motorisation", "population size", and "household income" on the LOR's energy demand is illustrated for five LORs in Table 4.5. The energy demand is depicted for a working day (Monday–Thursday). The comparison of the LOR "Stülerstrasse" with the LOR "Huttenkiez" shows the influence of the household income distribution on the energy demand within a LOR. Although more cars are registered in the LOR "Huttenkiez", the LOR "Stülerstrasse" has a higher energy demand (5275 kWh compared to 4441 kWh). This is due to the fact that there are more high-income households in the "Stülerstrasse" LOR, which tend to own larger cars, which require more energy. The influence of the motorisation degree can be studied, for example, by comparing the LOR "Griessingerstrasse" with the LOR "Lübarser Strasse". Both LORs have a similar distribution of household income, with slightly higher income in "Griessingerstrasse". The lower degree of motorisation in "Lübarser Strasse" leads to the lower daily energy consumption of 3423 kWh compared to "Griessingerstrasse", with 6151 kWh.
In Figure 4.12, the spatial distribution of the BEVs' charging energy demand is depicted per m^2 and per inhabitant for the Berlin LORs. It can be seen that the charging energy demand per m^2 is higher in the inner city LORs compared to the peripheral areas. The higher population densities within the inner city LORs compensates the lower degree of motorisation and lower household income. The charging energy demand per inhabitant is higher in the peripheral areas of the city, as the degree of motorisation and the household income are higher in the peripheral LORs.

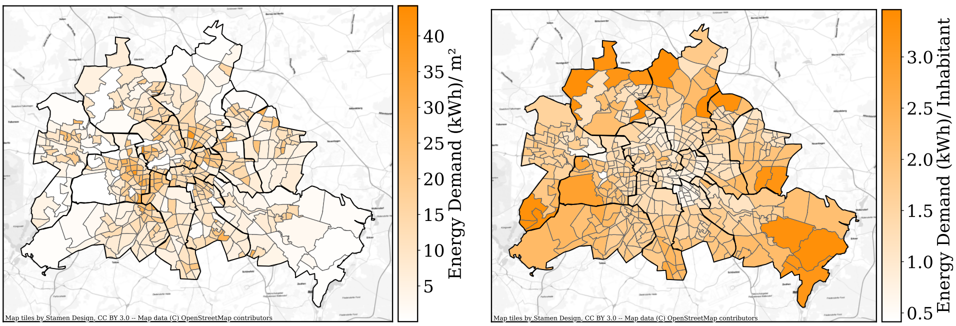

(a) Energy demand per m^2 **(b)** Energy demand per inhabitant

Figure 4.12: Spatial distribution of the BEV charging energy demand for a working day (Monday–Thursday) normalised to the size and the inhabitants in the Berlin LORs.

Table 4.5: Influence of the household income distribution, the amount of inhabitants, and the amount of vehicles in the LORs on the BEV charging energy demand on a working day (Monday–Thursday).

LOR	Inhabitants	Vehicles Per 1000 Inhabitants	Household Income Distribution					Energy Demand (kWh)
			Very Low	Low	Medium	High	Very High	
Stülerstrasse	3258	288	0.084	0.134	0.265	0.382	0.135	5275
Huttenkiez	3424	288	0.270	0.330	0.40	0.0	0.0	4441
Griesingerstr	3473	322	0.247	0.279	0.350	0.122	0.002	6151
Alt-Biesdorf	3367	397	0.110	0.220	0.360	0.220	0.09	7177
Lübarser Strasse	3214	228	0.309	0.313	0.285	0.088	0.005	3423

Table 4.6: Amount of households in the LORs “Heiligensee” and “Invalidenstrasse” and their yearly energy demand.

Household Size	Amount of Households in the LOR “Heiligensee”	Amount of Households in the LOR “Invalidenstrasse”	Yearly Energy Demand Per Household (kWh)
One Person	4318	6894	2110
Two Persons	3046	2401	3640
Three Persons	947	771	4600
Four or more Persons	1088	911	4850

4.1.3.5 Temporal Distribution of the Charging Power Demand

For charging powers of 3.7 kW and 11 kW, respectively, we evaluate the temporal distribution of the charging power demand for the LOR "Heiligensee". "Heiligensee" is located in the district "Reinickendorf" in the northwest of Berlin. This LOR was chosen for evaluation as it has the highest energy demand of all LORs for the simulated working day. The result is compared to the cumulative power demand of the households within this district. The cumulative power demand of the households is calculated by scaling the standard load profile for Berlin households, which we received from [114]. Standard load profiles are forecasts of the electrical energy consumption at quarter-hourly intervals, provided by the energy supplier. In Germany, they are usually normalised to 1000 kWh per year, which makes scaling necessary [115]. This scaling at the LOR level requires knowledge concerning the distribution of different household sizes as well as annual household electricity consumption. The relevant data is shown in Table 4.6. We derive the yearly energy demand per household size from [116]. The authors specify the yearly energy demand of different German household sizes as a normal distribution. For our calculations, we use the mean values. The cumulative LOR household power demand is calculated for a working day and a Saturday in May 2018.

In Figure 4.13a,b, temporal distribution of the charging power demand for a working day (Monday–Thursday) is depicted in blue for 11 kW charging power and 3.7 kW charging power, respectively. In orange, the temporal distribution of the cumulative household power demand within the LOR can be seen. In grey, the superposition with the simulated charging power demand of the BEVs is shown. The results for a Saturday are depicted in Figure 4.13c for 11 kW charging power and in Figure 4.13d for 3.7 kW charging power. As it can be seen, the cumulative household power demand between 06:00 and 23:00 is higher on Saturdays, since persons are more likely to be at home, as they do not have to work.
As depicted in Figure 4.13, the charging power demand curves of the BEVs for 11 kW charging power show a more pronounced valley and peak compared to their corresponding curves for 3.7 kW charging power. Due to the uncontrolled charging strategy, the vehicles start charging immediately upon arrival at home, which is mainly in the evening hours. The resulting simultaneity of the charging events leads to a peak in the evening hours (maximum around 20:00), which is higher for an 11 kW charging power compared to a 3.7 kW charging power. Since vehicles that are charged with 11 kW charging power need less charging time to fully recharge, the valley of the BEV charging power demand curve is lower for 11 kW charging power compared to 3.7 kW charging power. As illustrated, the households' power demand peak in the evening coincides with the BEVs' power demand peak for Saturdays and working days. The maximum total power demand of the LOR "Heiligensee" is increased by 77.9% for 11 kW charging power and 59.1% for 3.7 kW on working days with additional BEV load. It is increased by 64.2% for 11 kW charging power and 50.4% for 3.7 kW on Saturdays.

In Figure 4.14, the temporal distribution of the BEV charging power demand is compared to the cumulative power demand of the households for the LOR "Invalidenstrasse", which is located in the district "Mitte" in the center of Berlin. The results are shown for a working day and charging powers of 3.7 kW and 11 kW. The cumulative household power demand curve is calculated by scaling the standard load profile for Berlin households, as described in the previous paragraph. The distribution of the different household sizes needed for scaling can be found in Table 4.6.

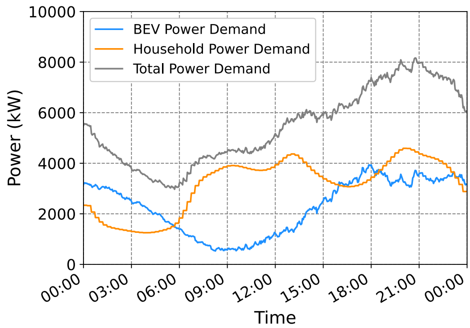

(a) Working day (Monday–Thursday), 11 kW

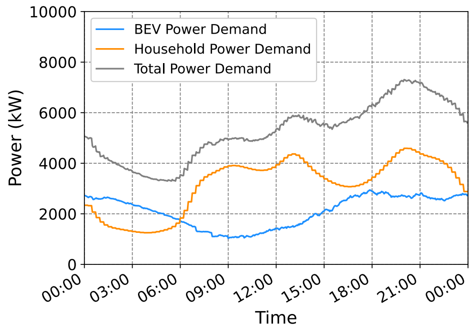

(b) Working day (Monday–Thursday), 3.7 kW

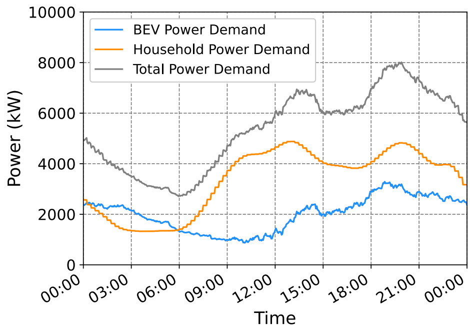

(c) Saturday, 11 kW

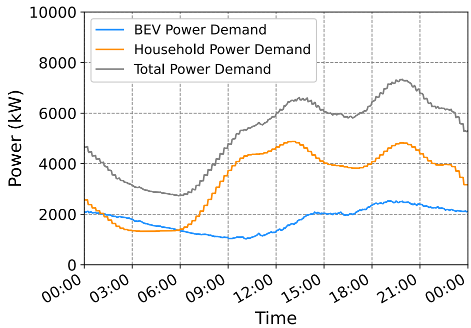

(d) Saturday, 3.7 kW

Figure 4.13: Temporal distribution of the BEV charging power demand for the LOR "Heiligensee".

Since more single-person households are located in the LOR "Invalidenstrasse" compared to "Heiligensee", the cumulative household power demand is higher. In comparision to "Heiligensee" the maximum total power demand of the LOR "Invalidenstrasse" is only increased by 19.0% for 11 kW charging power and by 15.7% for 3.7 kW with the additional BEV load. Both LORs have a similar population (18,070 in "Heiligensee" and 17,950 in "Invalidenstrasse") and similar household incomes. Since the degree of motorisation in "Heiligensee" (638 vehicles/1000 inhabitants) is almost four times higher compared to the LOR "Invalidenstrasse" (173 vehicles/1000 inhabitants), the BEV charging power demand is accordingly higher. The temporal distribution of the charging power demand on Saturdays is not depicted for the LOR "Invalidenstrasse", since it shows the same behaviour compared to a working day as already shown for the LOR "Heiligensee".

The computed results of the temporal distribution of the BEV charging power demand can be compared to other studies. The authors of [20] investigated the impact of uncoordinated BEV charging on a medium voltage distribution network. They assumed 1.5 vehicles per household and a 10% electric vehicle penetration rate, resulting in a total of 1270 electric vehicles in the network area. The charging power of the vehicles is between 1.5 kW and 6 kW. They showed that the peak charging power demand can reach values up to 2500 kW in the evening hours. This number is 2.7 times higher than the peak demand of 900 kW that we determined for the LOR "Invalidenstraße" (3126 BEVs) and 3.7 kW charging power on a working day. The difference arises since the authors assume that all vehicles are used during the simulated day and then are charged almost simultaneously in the evening hours. In contrast to our results, this simultaneity of the charging events reduces the charging power demand in the study to near zero in the early morning.

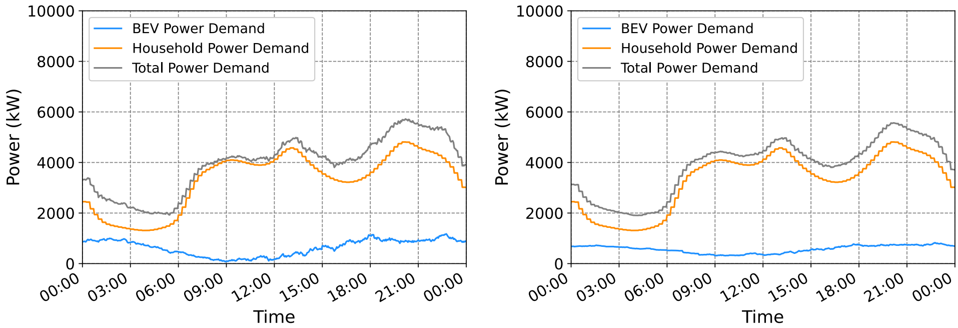

(a) Working day (Monday–Thursday), 11 kW

(b) Working day (Monday–Thursday), 3.7 kW

Figure 4.14: Temporal distribution of the BEV charging power demand for the LOR "Invalidenstrasse".

The author of [117] investigated the impact of uncoordinated BEV charging on the residential power demand of 200 households in the midwest region of the USA. Similar to our work, the author showed an increased demand in the evening hours. For a motorisation degree of 347 vehicles per 1000 inhabitants, the author showed that the maximum total power demand can increase by 44% for 6.6 kW charging power and 31% for 1.92 kW on working days with the additional BEV load. These findings are comparable to our results. We showed for a charging power of 3.7 kW that the total power demand can increase by 59.1% for a motorisation degree of 638 vehicles per 1000 inhabitants and by 15.7% for a motorisation degree of 173 vehicles per 1000 inhabitants. In contrast to our work, the author showed a similar power demand on Saturdays and on working days, which is mainly due to the different driving behaviours in Berlin and the USA.

4.1.4 Conclusions and Outlook

In this paper, a methodology was presented to estimate the spatial and temporal distribution of the charging energy and power demand that derives if urban, privately owned cars are fully electrified. The results support the electrical grid operators in detecting and evaluating possible overloads within the electrical grid. The novelty of our approach lies in the development of an activity-based mobility model by directly combining the 2017 German household travel survey (GHTS) with statistics on the population density, the degree of motorisation, and the household income in fine spatial resolution. Through this direct combination, our model provides data-based results with high spatial and temporal resolution. In contrast to other researchers, we take the vehicle class category distribution, which has an significant impact on the energy and power demand, in fine spatial resolution into account. Additionally, unlike most other scientific works, our model is vehicle-based and not person-based. The multiple use of the same vehicle by several persons is therefore better portrayed. We applied our methodology to the urban area of Berlin in Germany. Since the data sets we used to create our mobility model are available in a similar or identical form to many rural and urban regions in Germany, an upscaling of our model is feasible. Due to our open-data approach, it is relatively easy to obtain similar data sets in most places of the world. Therefore, our methodology is transferable to non-German regions.

The results of our developed mobility model match well with the underlying key data sources. The mean simulation error is between −5.3% and 3.1% for the trip starting time of the vehicles and the activities “Home”, “Working”, and “Shopping”. For those activities and the trip distance, the mean simulation error is between −6.1% and 3.3%. The application of our model showed that the spatial distribution of the charging energy demand in Berlin is highly heterogeneous. In the peripheral areas of the city, the total energy demand and the energy demand per capita is higher compared to the city center, mainly because the residents own more cars per capita. Since their household income is higher, the residents in peripheral areas own larger cars that consume more energy. The energy demand per m^2 area is higher in the inner city LORs compared to the peripheral areas, since the higher population densities compensate the lower degree of motorisation within the inner city LORs. We additionally showed that the total daily charging demand in Berlin is about 14.9% less on Saturdays compared to working days, which is mainly due to the fact that fewer cars travel on Saturdays.

Regarding the temporal distribution of charging power demand, we compared the cumulative household power demand with the additional BEV charging demand for two LORs. We showed the variability of the BEV charging power demand in the LORs. While the total power demand is only increased by 19.0% in the LOR “Invalidenstraße” on a working day and a charging power of 11 kW, it is increased by up to 77.9% in the LOR “Heiligensee”. For a charging power of 3.7 kW, the increase is 59.1% in the LOR “Heiligensee”. These results shows the necessity for and are the basis for intelligent load shifting methods. Those methods can be used to reduce the charging power demand peaks and to flatten the load curve, as shown by other studies [21], [81], [118]–[120].

In further research, we will investigate load-shifting potentials by combining our model with a smart charging algorithm. We will investigate if the BEVs’ charging power demand peaks can be reduced without limiting the vehicle’s range. Furthermore, as we currently solely consider “home-charging” in our model, we will use geodata to analyse the building structure in each LOR. The results can be used to evaluate the attractiveness for vehicles to enter the LORs for specific activities. By using a routing algorithm and the attractiveness information, the daily routes for all vehicles can be determined. The resulting knowledge about the location and the duration of stay for the different activities will be used for the investigation of combined charging strategies.

4.1.5 Author Contributions

Florian Straub: Conceptualization, Supervision, Validation, Visualisation, Writing - Original Draft.
Florian Straub, Simon Streppel: Methodology, Investigation.
Florian Straub, Dietmar Göhlich: Writing - Review & Editing.
Dietmar Göhlich: Project administration, Funding acquisition.

4.2 Publication II

Car-access Attractiveness of Urban Districts Regarding Shopping and Working Trips for Usage in E-Mobility Traffic Simulations

Florian Straub[1], Otto Maier[1], Dietmar Göhlich[1]

[1]Chair of Methods for Product Development and Mechatronics, Technische Universität Berlin, Strasse des 17.Juni 135, 10623 Berlin, Germany

(This article has been published on 14 October 2021 by MDPI in the "Sustainability" Special Issue: Transportation Planning and Public Transport, available online: https://doi.org/10.3390/su132011345)

Abstract: With the continuous proliferation of private battery electric vehicles, the demand for electrical energy and power is constantly increasing. As a result, the electrical grid may need to be expanded. To plan for such expansion, information about the spatial distribution of the energy demand is necessary. This can be determined from e-mobility traffic simulations, where travel schedules of individuals are combined with an attractiveness rating of locations to estimate traffic flows. Typically, attractiveness is determined from the "size" of locations (e.g., number of employees or sales area), which is applicable when all modes of transportation are considered. This approach leads to inaccuracies for the estimation of car traffic flows, since the parking situation is neglected. To overcome these inaccuracies and fill this research gap, we have developed a method to determine the car-access attractiveness of districts for shopping and working trips. Our method consists of two steps. First, we determine the car-access attractiveness of buildings within a district based on the parking situation of each individual building and then aggregate the results at the district level. The approach is demonstrated for the city of Berlin. The results confirm that conventional models cannot be used to determine the car-access attractiveness of districts. According to these models, attractive districts are predominantly located in the city centre due to the large amount of sales areas or the large number of employees. However, due to the high density of buildings, only limited space is available for parking. Attractive districts rated according to our new approach are mainly located in the outer areas of the city and thus match the parking situation.

Keywords: electric vehicle; traffic simulation; traffic assignment; location attractiveness; transportation electrification; open geodata

4.2.1 Introduction

This introduction consists of three subsections. In Section 4.2.1.1, we discuss how the conversion from private internal combustion engine vehicles (ICEVs) to battery electric vehicles (BEVs) contributes to a reduction in greenhouse gas emission. Furthermore, we discuss how e-mobility traffic simulations are used to estimate the spatial and temporal distribution of the charging demand of BEVs and why these simulations are necessary. Since the currently used models rely on data that is not always available, we have developed a novel research approach to estimate the charging demand of BEVs. This is presented in Section 4.2.1.2. This paper is one of three main parts that together form the research approach. Therefore, this subsection also discusses which part of the overall research approach is addressed in this paper. In Section 4.2.1.3, a literature review about the car-access attractiveness of locations is conducted, and the research gap filled by this paper is identified.

4.2.1.1 Global Warming and E-Mobility Traffic Simulations to Estimate the Charging Demand of BEVs

In recent years, emission limits have been steadily tightened due to continuously rising greenhouse gas emissions and poor air quality. Germany, for example, is planning to reduce greenhouse gas emissions by 50% by 2030 compared to 1990 [80]. The European Commission agreed on the “European Green Deal”, with the intention to achieve net zero greenhouse gases emissions by 2050. To achieve this goal, “a 90% reduction in transport emissions is needed by 2050” [2]. This reduction leads to a substitution of private internal combustion engine vehicles with vehicles with alternative drive systems, primarily battery electric vehicles. As a result, the increasing demand for electrical energy and power can lead to bottlenecks in the power supply if the electrical grid infrastructure is not reinforced [20], [21]. In order to support the electrical grid operators to detect and evaluate possible overloads within the electrical grid, accurate models are needed to predict the spatial and temporal energy and power requirements arising from the electrification of private internal combustion engine vehicles.

E-mobility traffic simulations, mostly in the form of activity-based models, are commonly used for this purpose [27], [77], [78], [86]. In activity-based models, individual full-day travel schedules are generated for all persons or vehicles within the considered geographical area. These travel schedules, also referred to as mobility profiles, consist of a consecutive sequence of activities at different locations and trips between those activities. An example of a mobility profile is shown in Figure 4.15, where the individual starts at ”Home” in the morning before spending 8 h and 30 min at the activity “Working” and 40 min at the activity “Shopping”. The person arrives back “Home” at 18:00.

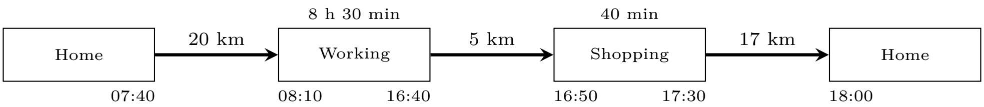

Figure 4.15: Example of a general mobility profile.

Since the mobility profiles capture the relationship between activity and mobility patterns and mode of transportation, they can be used to determine the idle times of the vehicles at different activities. If the geographic locations of the activities are known, the spatial and temporal distribution of the charging energy and power demand for a geographic area can be calculated from the mobility profiles by applying charging strategies.

In activity-based models, the standard approach to determine mobility profiles containing information about the activity locations is to combine a travel survey with an origin-destination (O-D) matrix [77], [78]. The travel surveys are obtained by questioning households within a geographical area about their activities and trips during reference days, which allows for determining the daily travel patterns of the population in the investigated area. An O-D matrix is then used to derive the locations of the activities. In O-D matrices, each cell represents the probability of a trip from an origin location (row) to a destination location (column) within a geographical area. As the starting location of the first trip (usually the "Home" location) is known through, e.g., statistics on population density or the degree of motorisation, O-D matrices are used to assign the destination locations for different activities. In some cases, travel surveys contain sufficient data to directly derive an O-D matrix [77], [78]. If the data availability is insufficient, O-D matrices have to be generated by other approaches, usually by using traffic count data [121]–[124] or mobile phone data [125]–[127].

4.2.1.2 Novel Research Approach for Estimating the Charging Demand of BEVs

In the case where an O-D matrix neither exists nor can be determined, we have developed a new approach which can be used to determine mobility profiles containing information about the activity locations for the considered geographical area. This approach is depicted in Figure 4.16. As a first step (depicted in the blue box), a travel survey is used to create mobility profiles that do not contain information about the activity locations. The mobility profiles are vehicle-based and not person-based. This means that individual travel schedules are created for BEVs in the geographic area and not for persons. In this way, the multiple use of the same vehicle by several people can be realistically represented. Population density statistics as well as data on the degree of motorisation are used to determine the residence of the individuals and thus the spatial distribution of the vehicles in the investigated area.

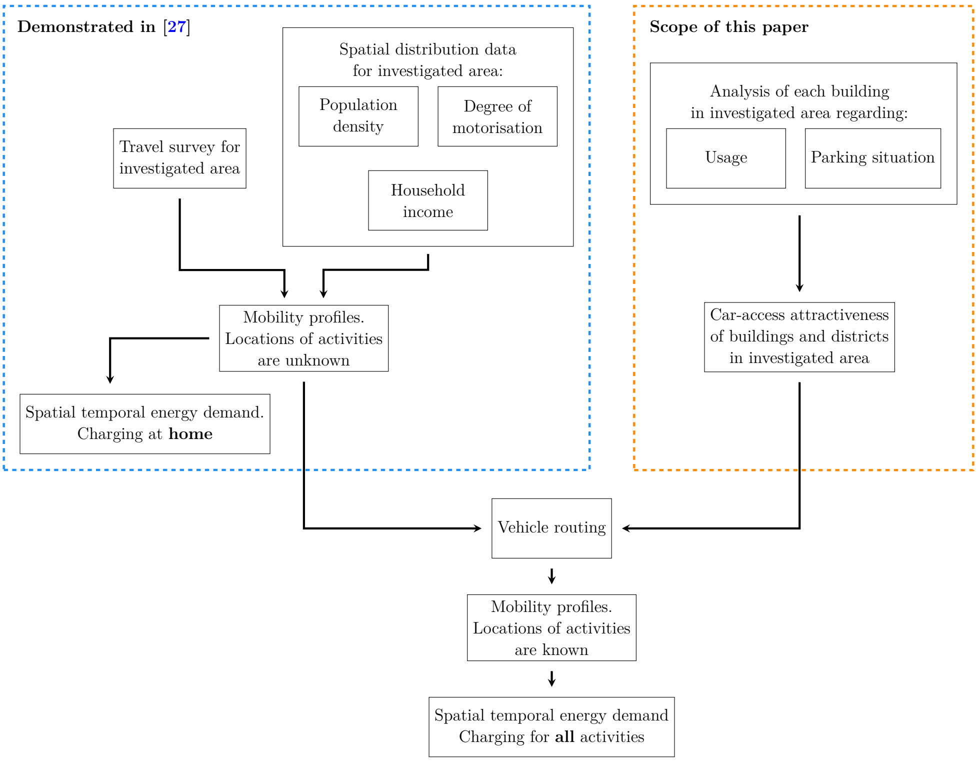

Figure 4.16: Method for estimating the spatial and temporal energy and power demand from the electrification of private ICEVs.

From the spatial distribution of household incomes, vehicle size classes and therefore vehicle consumption can be determined. Based on these partial results, it is possible to estimate the spatial distribution of the charging energy and power demand that arises when the individuals solely charge their BEVs at home. This approach has been demonstrated in [27] for the urban area of Berlin, Germany, and its 448 sub-districts. However, these results need further refinement as they neglect the fact that vehicles do not always charge at home but can also charge at, e.g., work and shopping locations.

Therefore, as second step we determine the car-access attractiveness of locations, as depicted in the orange box of Figure 4.16. Car-access attractiveness is a measure of how attractive locations are to drive to by car for a certain activity. A high attractiveness means that a location is highly likely to be accessed by car, while a low attractiveness indicates that a location is more likely to be accessed by another mode of transportation. In order to determine the car-access attractiveness of a location for a certain activity, the performed activities at each location need to be known. Therefore, the usage of each building in the investigated area is first determined and then the car-access attractiveness of each building is computed based on its usage and parking situation. The results for the buildings are subsequently aggregated at the district level. In the last step, the attractiveness information and the mobility profiles without information about the activity locations are combined with a suitable routing method. The routing of the vehicles allows for determining the locations of the activities based on the location attractiveness. This enables the estimation of the spatial distribution of the charging energy and power demand, considering charging at all activities. Whereas the routing method will be part of future work, this paper deals with the evaluation of the car-access attractiveness of buildings and districts.

4.2.1.3 Literature Review and Research Gap Filled by This Paper

Typically, attractiveness is represented by the “size” of locations, assuming that larger places attract more persons than smaller ones [66]. Horni et al. [128] as well as Kubis and Hartmann [129] proposed an attractiveness factor depending on store size to model the location choice of individuals for shopping trips. They assume that larger stores attract more persons than smaller ones. In order to relate retailing attractiveness of an urban district with its resulting freight and shopping trip attraction rates, Gonzalez-Feliu and Peris-Pla [130] assume that districts with a high number of employees attract more trips as their attractiveness increases. Caceres et al. [131] assume that districts with high population attract more trips and propose a relative attractiveness factor to estimate traffic flow profiles. Drezner and Drezner [132] propose that the annual sales of a retail facility indicate its attractiveness.
The described models can only be applied when all modes of transport are considered. They cannot be applied when cars are the only mode of transport under consideration. This is mostly because these models do not consider the availability of parking spaces. An example is that of large department stores, which are usually located in the city centres. Since they offer a large amount of sales area, they are characterized by very high car-access attractiveness if evaluated with conventional attractiveness models. However, within the city centres, usually limited or no space is available for parking.

Since the evaluation of the car-access attractiveness of locations has not been addressed so far in the literature, this research gap is filled by this paper. The car-access attractiveness is evaluated separately for shopping and working trips and is based on the consideration

of the available parking space in relation to the sales area per district and the number of employees per district, respectively. To refine our attractiveness rating, we also consider the distance of the parking spaces from the shops and working locations, the distance of the working location to the nearest public transportation stop and information about the parking fees. We apply our method to the urban area of Berlin, Germany, and its 448 sub-districts. The car-access attractiveness rating is based on open geodata and freely available data sets, making the approach traceable and reproducible.
Since the car-access attractiveness of the districts is determined solely for shopping and work trips, vehicle routing can only determine the locations for shopping and work activities. However, in addition to the places of residence, these are the locations with the highest charging potential, as they have the highest average car idle times in Berlin (places of residence: 20.9 h per day, workplaces: 1.7 h and shopping locations: 0.1 h) [27].

This paper is structured as follows: in Section 4.2.2, the method for the attractiveness-based district rating is introduced. The results are presented and analysed in Section 4.2.3, which is divided into two main parts. In Section 4.2.3.1, the results of the attractiveness-based district rating are shown for shopping trips. The results are shown for working trips in Section 4.2.3.2. The conclusions are presented in Section 4.2.4.

4.2.2 Methodology

The methodology used to rate districts regarding their car-access attractiveness consists of four main parts, which are depicted in Figure 4.17. As a first step, we divide the city of Berlin into districts and analyse the usage of each building inside the districts. The building usage describes how the building is used, e.g., as a commercial or residential building. For the division we make use of the official classification of the Berlin administration, which divides the twelve Berlin districts into 448 sub-districts called “Lebensweltlich orientierte Räume” (neighbourhood oriented districts) (LORs). Within each LOR, the structure of the contained buildings and the socio-economic status of the inhabitants are similar. The LORs are usually separated from each other by major roads, rivers or rails [98], [133]. The analysis of the buildings’ usage is based on geodata, which is information about geographic positions in a computer-processable format.

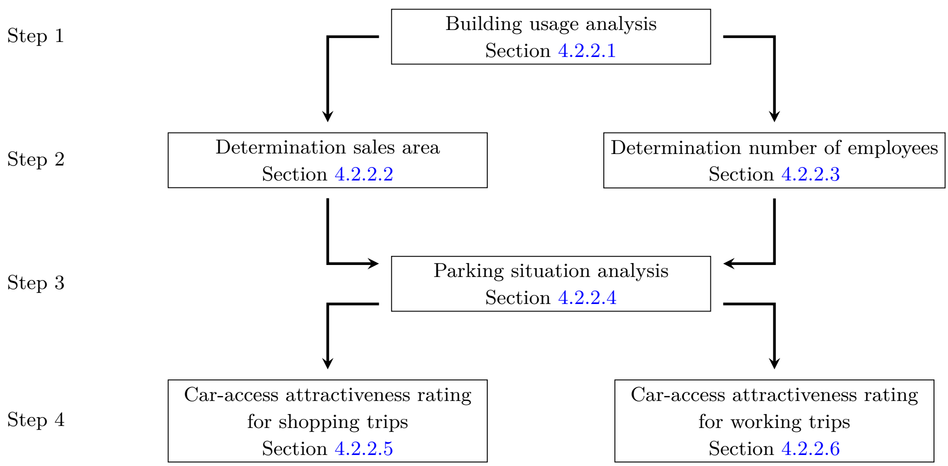

Figure 4.17: Method for the attractiveness-based district rating for shopping and working trips.

For the analysis of the buildings' usage within the LORs, we use OpenStreetMap (OSM) geodata [134], derived from the Geofabrik GmbH Karlsruhe [135]. We chose OSM geodata because it is freely available under an open database license 1.0 [136] for the whole earth. The car-access attractiveness of a district is based on the available parking space in relation to the sales area per district and the number of employees per district, respectively. Therefore, in the second step we use the results of the building usage analysis to derive the sales area and the number of employees for all buildings in the Berlin LORs. We analyse the parking space availability in the Berlin LORs in step three. As a last step, we combine the obtained results and introduce the methodology for the attractiveness-based district rating.

4.2.2.1 Building Usage Analysis in the Berlin LORs

In this section, we derive the building's usage for every building inside the Berlin LORs. Additionally, we determine the number of floors for each building, which is necessary to compute the sales area and the number of employees per building. For the building usage analysis we solely rely on OSM raw data, which is xml-formatted. The OSM raw data structure is composed of the three elements—"nodes", "ways" and "relations"—as well as "tags" associated with the elements [137].

- "Nodes" are points defined by their latitude and longitude and therefore correspond to locations on the surface of the earth.
- "Ways" are ordered lists of nodes. Up to 2000 nodes define a polyline, which can be used to define linear features (e.g., rivers or roads) or boundaries of areas in the form of a polygon (e.g., buildings or parking spaces).
- "Relations" are used to model logical or geographical relationships between elements.
- "Tags" describe the element they are attached to. A tag consists of a key and a value. For example, a supermarket would be assigned the key = "shop" and the value = "supermarket".

For each building, three main pieces of information can be obtained from the OSM data set: firstly, the predominant land use of the area the building lies in (e.g., residential, industrial or retail land use); secondly, the building type such as an office, church or residential building; and thirdly the points of interest (POIs) within the building. While the land use and the building type are mainly given as polygons, POIs are usually given as nodes and give deeper insights into the building's usage.

The Berlin OSM geodata set includes 19 different land uses, 191 different building types and 852 different POIs. Conditions are defined to categorize the Berlin buildings into their corresponding building usage class, taking the buildings land use, type and POIs within it into account. For example, if no POI is given and the building's land use and the building's type are "residential", the building is considered as a residential building. The POI "supermarket" within a building of the land use and building type "residential" would reveal that a supermarket is located inside the building, and the building would be considered as a residential building with additional retail usage.

For the categorization, we consider 10 different building usage classes in total:

- Residential buildings;
- Residential buildings with additional commercial usage, such as small offices or doctor's practices;
- Residential buildings with additional retail usage, such as small supermarkets or bakeries;
- Residential buildings with additional commercial and retail usage;
- Commercial buildings, such as an office building;
- Retail buildings, such as supermarkets or furniture stores;
- Commercial buildings with additional retail usage;
- Industrial buildings, such as factories;
- Department stores;
- Others, such as churches, monuments or stadiums.

The number of floors can be directly derived from the OSM geodata set for most Berlin buildings. However, since the data set is not complete, the floor numbers for the buildings without information need to be determined. The Berlin LORs are defined in such a way that the building structure within each LOR is similar [98], [133]; hence, the number of floors of the buildings is similar. Therefore, we estimate the number of floors for buildings without information by calculating the average number of floors for each building usage class in the LOR and assign the results to buildings without information.

4.2.2.2 Determination of the Sales Area of the Buildings in the Berlin LORs

In order to calculate the sales area of a building, two major pieces of information need to be known: namely, the sales area per floor and the number of floors within the building containing sales areas. To derive the relevant information for a building, we make use of its usage class and its number of floors, derived in Section 4.2.2.1. We calculate sales areas for the following building usage classes:

- Residential buildings with additional retail usage;
- Residential buildings with additional commercial and retail usage;
- Retail buildings;
- Commercial buildings with additional retail usage;
- Department stores.

As the OSM data set reveals no information concerning the number of floors per building that contain sales area, we assume that for a residential and a commercial building with additional retail usage, only one floor contains sales area. For retail buildings and department stores, we assume that each floor contains sales area. We further assume that each floor contains the same amount of sales area. To avoid overestimating the sales areas of department stores with additional commercial usage such as offices or a hotel, we limit the number of floors containing sales area to two floors for those.

Two steps are then necessary to derive the sales area per floor from the gross floor area of a building. First, the net internal area needs to be calculated. The net internal area equals the gross floor area minus the area used for, e.g., stairs and elevators, electrical services or walls and columns. As second step, the sales area needs to be determined from the net internal area. The sales area only contains the shelf areas and the paths running between them, as well as counters and the checkout area. The sales area does not include storage areas or administration offices. For Germany, Tillman et al. [138] have published guideline factors to derive the net internal area from the gross floor area for residential and commercial buildings. For both building types, this factor K_1 can be computed as

$$K_1 = \frac{\text{Net Internal Area}}{\text{Gross Floor Area}} = 0.8 \tag{4.1}$$

The authors additionally provided a guideline factor of $K_2 = 0.8$ for the estimation of the sales area from the net internal area, resulting in a total factor of $K_3 = 0.64$ for the estimation of the sales area from the gross floor area.

$$K_2 = \frac{\text{Sales Area}}{\text{Net Internal Area}} = 0.8 \tag{4.2}$$

$$K_3 = K_1 \cdot K_2 = \frac{\text{Sales Area}}{\text{Gross Floor Area}} = 0.64 \tag{4.3}$$

While the factor K_2 is also applicable for the usage classes “retail building” and “department store”, no values are available to estimate the net internal area from the gross floor area for these two usage classes. We therefore assume $K_1 = 0.8$ as well for these building usage classes. To check this assumption, we compare the calculated sales areas of retail buildings and department stores with reference values in the following. As Berlin is highly populated and construction land is rare, pure retail buildings are uncommon. The few that exist are mostly supermarkets. Accordingly, we take Aldi Nord and Kaufland supermarkets into account for the comparison. Aldi Nord supermarkets are chosen for the verification, since they offer an “average” product assortment on an average sales area size of 850 m^2 and hence can be considered as an “average” Berlin supermarket [139]. Kaufland supermarkets are chosen, since they offer a wide product assortment on large sales areas of 4340 m^2 on average [140] and therefore differ in means of building structure compared to Aldi Nord supermarkets. Thus, they provide a useful second comparison value. The results of the comparison are depicted in Table 4.13. Since the relative error between the computed average sales area and its reference value is −2.8% for Aldi Nord supermarkets and −1.1% for Kaufland supermarkets, we consider a factor of $K_3 = 0.64$ as applicable to derive the sales area from the gross floor area for retail buildings. For department stores, we verify the assumption by comparing the calculated sales areas with known numbers for 15 department stores in Berlin. As the calculated mean relative error is 4.2%, we assume an applicability of the factor $K_3 = 0.64$ to derive the sales area from the gross floor area for department stores as well. The results of the comparison are depicted for three departments stores in Table 4.13.

The computed total sales areas for the Berlin buildings needs to be verified. Therefore, we compare our computed results with a study on Berlin retail structures and sales areas, commissioned by Berlin authorities in 2014 [141]. The study provides information on the sales area per inhabitant in the 12 Berlin districts in the year 2016. In order to calculate the sales area per district, we use census data, which provides the number of inhabitants for the Berlin districts in 2016 [142]. The number of inhabitants in Berlin has grown by 1.9% from 3,537,100 in 2016 [142] to 3,604,100 in 2019 [143]. Accordingly, we assume that the total sales area increased by 1.9% from 2016 to 2019. The results of the comparison can be found in Table 4.14. The maximum relative error is 5.8% for all districts, except for the district Tempelhof-Schöneberg, indicating high accuracy of the computation. The high error of −9.7% in the district Tempelhof-Schöneberg is most likely due to the incomplete data set available for this district.

Figure 4.18 shows the computed sales area of each building in the LORs “Emdener Straße” and “Karl-August-Platz”. The usage distribution of the buildings in the LOR “Emdener Straße” can be considered as rather typical for Berlin. The LOR contains mostly residential buildings, intermixed with some commercial buildings and a main street (in the south of the LOR), where most of the buildings are used for retail or commercial purposes. The total sales area is 16,287 m^2. In comparison, the buildings in the LOR “Karl-August-Platz” are mainly used for retail and commercial purposes. In addition, this LOR contains a shopping street with department stores. The total sales area is 66,555 m^2.

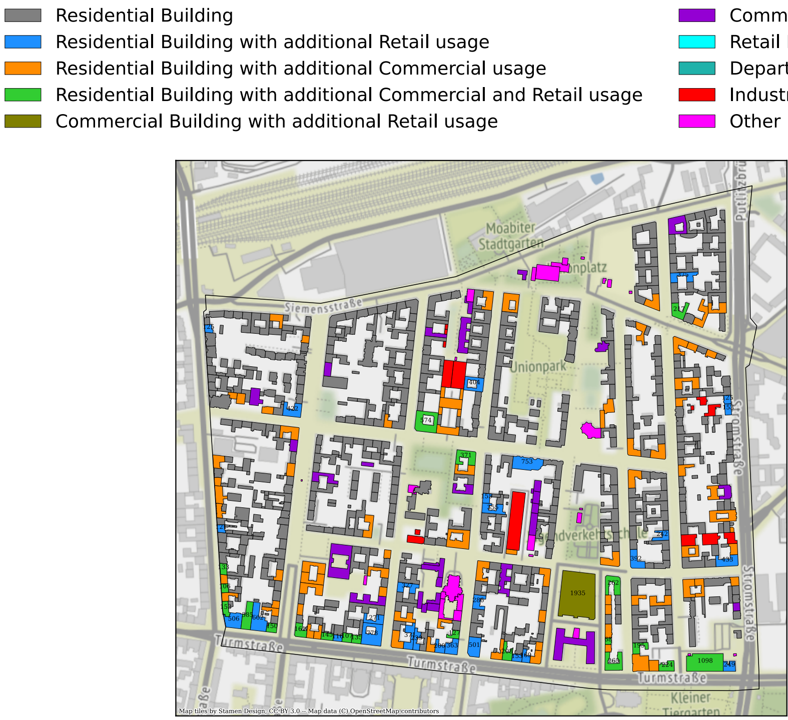

(a) “Emdener Straße” LOR.

(b) “Karl-August-Platz” LOR.

Figure 4.18: Computed sales area per building for two Berlin LORs.

4.2.2.3 Determination of the Number of Employees of the Buildings in the Berlin LORs

The calculation of the employees per building is carried out for each usage class introduced in Section 4.2.2.1, except for “residential buildings” and “other” usage classes, as they only have few or no employees. For the calculation, three major pieces of information need to be known: first, the number of companies per building, which we derived by analysing the POIs for each building; second, the number of employees per m^2 of operating area for each company; and third, the share of the buildings operating area used by the individual companies. The total operating area of a building equals the gross floor area multiplied by the number of floors.

The number of employees per m^2 of operating area E_o can be directly derived for more than 30 types of businesses from [144]. Reference [144] is a study on the energy consumption of different economic sectors in Germany and also gives the average operating area c_a of the business types. Exemplary values for five types of businesses can be found in Table 4.7.

Table 4.7: Number of employees per m^2 of operating area and average operating area for different types of businesses.

Type of Business	Employees per m^2 Operating Area E_o	Average Operating Area c_a
Restaurants	0.023	260 m^2
Retail non-food	0.011	530 m^2
Insurances	0.036	477 m^2
Small offices (e.g., law firm)	0.039	210 m^2
Public institutions	0.019	2890 m^2

According to the determination of the sales area per building, we limit the number of floors used by the companies to one for residential buildings with additional retail and/or commercial usage. If the building’s usage class is a retail building, a department store or an industrial building, we consider all floors of the building for commercial activities. We limit the number of floors of department stores with additional commercial usage to two. The remaining floors are treated as a commercial building. If several companies are located in the same building, the total operating area is distributed among the companies according to their weighted average operating area, as expressed in Equation (4.4).

$$O_i = O_t \cdot \frac{c_{ai}}{\sum_{j=1}^{n} c_{aj}} \tag{4.4}$$

where O_t is the building’s total operating area, O_i the operating area of the company i located in the building and c_{ai} is the average operating area of the company i, while n equals the total number of companies in the building and their corresponding average operating area c_{aj}.

Based on the values determined, the number of employees for all buildings in Berlin can be determined. For each building, its total number of employees E_b can be calculated as

$$E_b = \sum_{i=1}^{n} O_i \cdot E_{oi} \tag{4.5}$$

where O_i is the operating area of the company i located in the building, and E_{oi} is the number of employees per m^2 of operating area of the company i, while n equals the total number of companies in the building.

In order to evaluate the generated results, we compare them to the 2019 Berlin census data [143]. The census data specify the total number of employees in Berlin and their distribution among three major commercial sectors: the manufacturing sector (e.g., automotive industry or chemical industry); the trade, hospitality and transport sector; and third, other commercial services sector (e.g., doctors or lawyers). The generated numbers from the OSM data, the numbers from the census and the relative error between them are depicted in Table 4.8. The numbers of employees as derived from the census data are scaled to take commuters into account [145], [146]. The computed total number of employees deviates by −41.8% compared to the census data. While the relative error is only 0.185% for the manufacturing sector, it is −58.7% for the trade, hospitality and transport sector and −43.6% for the other commercial services sector. Since OpenStreetMap is a community project, geographic data are collected on a voluntary basis by project members using their GPS devices [135]. Therefore, the large error for the trade, hospitality and transport sector and other commercial services sector is most likely due to the incompleteness of the OSM data set. The comparison of the OSM data with local knowledge confirms this assumption. Many small offices (e.g., architects, lawyers, consultancies), small doctor's practices, restaurants or the offices of self-employed persons are not included in the data set, while large companies and factories of the manufacturing sector are fully included. In order to fit the calculated results to the census data, we linearly scale the computed results for each building with employees by economic sector.

Table 4.8: Number of employees in Berlin in 2019 by summarized economic sector. Comparison of census data and computed results.

Economic Sector	Census Data	Computed Results	Relative Error (%)
Manufacturing Sector	284,319	284,844	0.185
Trade, Hospitality and Transport	580,933	239,903	−58.7
Other Commercial Services	1,201,074	677,209	−43.6
Total Number	2,066,326	1,201,956	−41.8

The results of the determination of the number of employees are shown in Figure 4.19 for the LORs "Emdener Straße" and "Germaniagarten". For each building, the calculated total number of employees is given. The usage of the buildings in the LOR "Emdener Straße" has been discussed in Section 4.2.2.2. The calculated total number of employees is 4901. Although the LOR "Germaniagarten" contains two industrial areas in the south and west as well as a commercial area in the centre, the number of employees in the LOR "Germaniagarten" is 3078 and thus is lower than in the LOR "Emdener Straße". This is due to the fact that most of the industrial and commercial buildings in the LOR "Germaniagarten" have only one floor, while most buildings in the LOR "Emdener Straße" have more than two floors. Furthermore, industrial buildings have fewer employees per square metre operating area compared to buildings with solely or partly commercial usage which are common in the LOR "Emdener Straße".

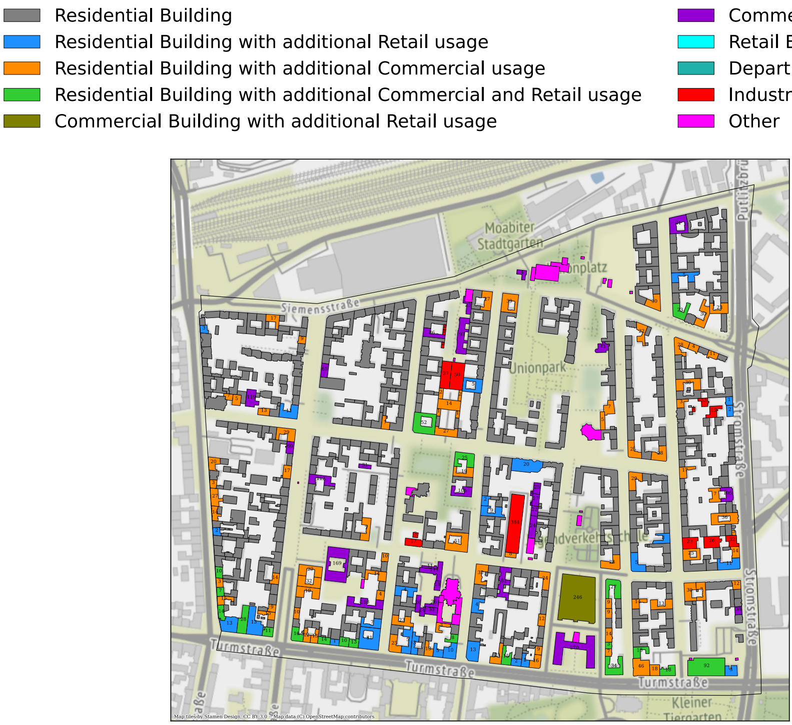

(a) "Emdener Straße" LOR.

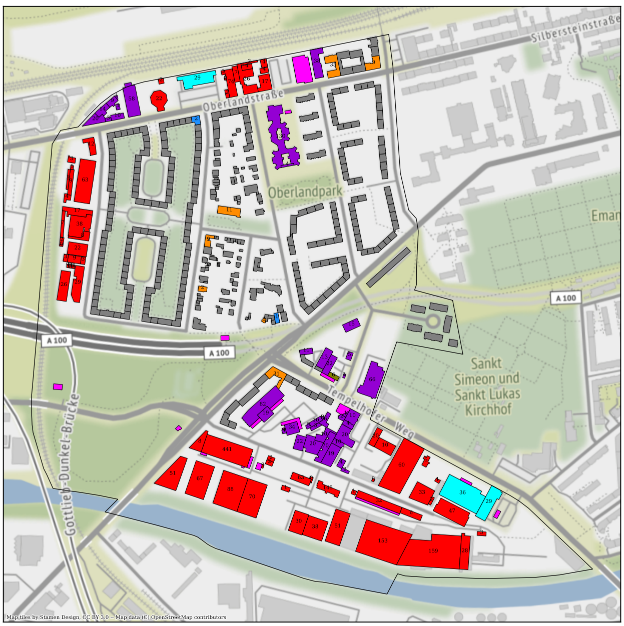

(b) "Germaniagarten" LOR.

Figure 4.19: Computed number of employees per building for two Berlin LORs.

4.2.2.4 Parking Situation Analysis in the Berlin LORs

The goal of the parking situation analysis is to determine the number of parking spaces and their individual capacity within each LOR. The capacity of a parking space equals its number of parking spots. In addition, the intended use of the parking spaces is determined by the assignment of the parking spaces to one or more buildings. Since we aim to determine the attractiveness of the Berlin LORs for access by car for the activities working and shopping, this step is necessary to differentiate between employee, customer and other parking spaces.

For the analysis, we make use of the OSM data set which distinguishes between three different parking space classes that are suitable for cars.

- Surface parking spaces, which are single-level on the surface. Their gross parking area is equal to the surface area they cover, which can be directly derived from the OSM data set. The gross parking area includes areas for parking spots as well as areas that are part of the parking space but cannot be used for parking (e.g., columns or roads between parking spots).

- Multi-storey parking spaces such as parking garages. Their gross parking area equals the gross parking area per floor multiplied with the number of parking floors. The gross parking area per floor can be directly derived from the OSM data set, whereas the determination of the amount of parking floors is described in Section 4.2.2.1.

- Underground parking spaces, which are usually located beneath a building. Their gross parking area is calculated identically to that of multi-storey parking spaces. However, the OSM data set does not specify the gross parking area per floor as a percentage of the gross floor area of the building nor does it indicate the number of parking floors. Due to the high building density in Berlin and the resulting necessity for efficient use of construction space, we assume that the total gross floor area of the building is used for underground parking.

For each parking space class, there are parking spaces in the OSM data set for which their capacity is specified. In total, the capacity is known for 12.3% of the parking spaces. This allows easy back-calculation to parking spots per m^2 of gross parking area. This correlation is shown in Figure 4.20, where each data point equals the given capacity information. By using linear regression, linear curves can be fitted to the data tuples. This relation can be used to determine the number of parking spots for parking spaces without capacity information. In order to confirm the applicability of this approach, we compared the number of parking spots estimated using the curves in Figure 4.20 with the correct number which was determined by manual counting for several parking spaces in all three parking space classes. The comparison showed reasonable deviations. In Figure 4.20, it can be seen that the curve for multi-storey parking spaces is steeper compared to the curve of surface parking spaces, which is due to the more efficient use of space. Since no information is provided on the number of parking floors for underground parking spaces, their capacities are normalized to one floor. This results in an underestimation of gross parking area. The curve is therefore steeper compared to surface and multi-storey parking spaces since parking floors are implicitly included.

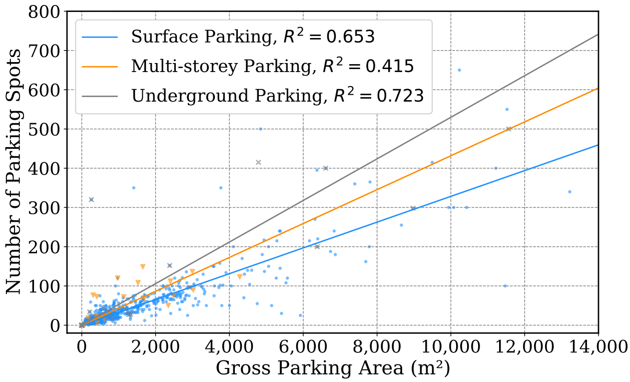

Figure 4.20: Linear approximation of the amount of parking spots per m^2 gross parking area from OSM data.

Since the number of parking spots of each parking space is known from the previous step, the usage class for each parking space needs to be determined through the assignment of the parking spaces to one or more buildings. The general assignment process is depicted in Figure 4.21 and is described below.

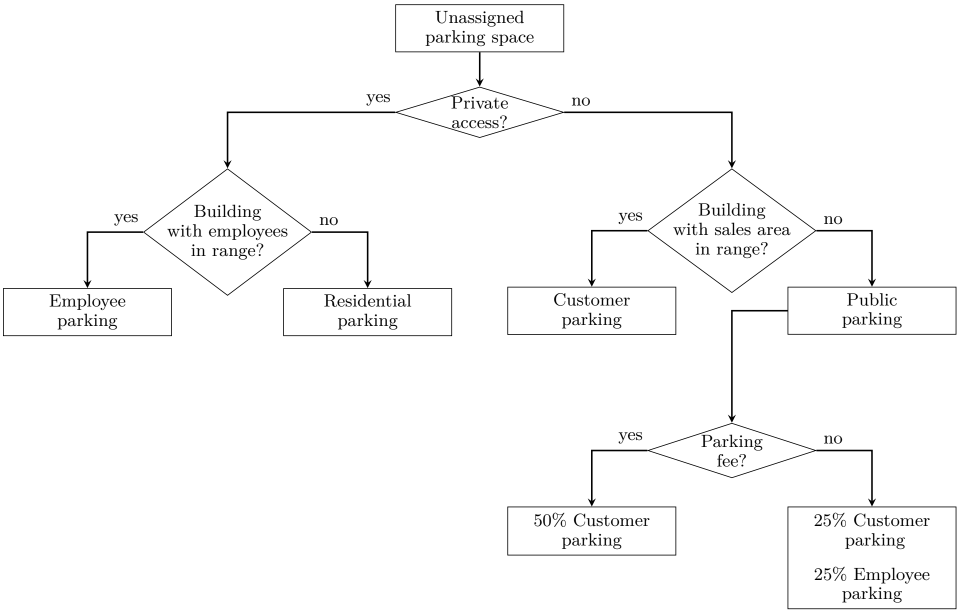

Figure 4.21: General process for the utilization assignment of parking spaces.

The access type for each parking space is given in the OSM data set. This information can be used to differentiate the parking spaces into four different usage classes: customer parking spaces (only accessible for shopping trips), private parking spaces for employee parking (accessible only for working trips), private parking spaces for residential parking (not accessible) and public parking spaces, which are accessible for shopping and working trips.

Parking spaces with private access need to be distinguished as parking spaces for employees or residential parking spaces. For this purpose, we consider all buildings that have a minimum distance of less than 50 m from the parking space (the influence of different distances on the result is investigated in Sections 4.2.3.1 and 4.2.3.2) as potentially assignable to the parking space. If none of the potential buildings contains employees, the parking space is considered as a residential parking space. If one of the potential buildings contains employees, the parking space is assigned to this building and is considered as an employee parking space. If the parking space can be assigned to several buildings containing employees, the parking space is shared among those buildings according to their weighted number of employees, as expressed in Equation (4.6).

$$C_i = C_t \cdot \frac{E_{bi}}{\sum_{j=1}^{m} E_{bj}} \tag{4.6}$$

where C_t is the number of parking spots of the parking space, C_i the number of the parking space's spots assigned to the building i and E_{bi} is the number of employees in building i, while m is the total number of buildings which are assigned to the parking space and their corresponding number of employees E_{bj}. If the access to the parking space is non-private, we check whether buildings exist that contain sales area and have a minimum distance of less than 10 m from the parking space. If one building meets these requirements, the parking space is assigned to this building as a customer parking space. If several buildings meet the requirements, the parking space is shared among those buildings according to their weighted sales area, as expressed in Equation (4.7).

$$C_i = C_t \cdot \frac{S_{bi}}{\sum_{j=1}^{k} S_{bj}} \tag{4.7}$$

where C_t is the capacity of the parking space, C_i the amount of the parking space's spots assigned to the building i and S_{bi} is the sales area in building i, while k equals the total number of buildings which are assigned to the parking space and their corresponding sales area S_{bj}.

If no building meets the aforementioned requirements, the parking space is considered as a public parking space. The usage of public parking spaces varies greatly. Depending on their location and size, a different share of the parking space capacity is used for different activities. Therefore, it is difficult to make a general statement about their usage. We therefore assume that 50% of their capacity is used for activities which are not considered in this paper, such as leisure activities or doctor visits. For public charged parking, the remaining 50% of the parking space's capacity is assigned to the buildings with sales area that have a minimum distance of less than 100 m from the parking space. The information on parking fees can be obtained directly from the OSM data set. The parking space's spots are distributed among those buildings according to their weighted sales area (see Equation (4.7)). For free public parking spaces, we assign 25% of their capacity to buildings with sales areas and 25% to buildings with employees, according to their weighted sales area and number of employees. For this assignment we only consider buildings with sales area which have a minimum distance of less than 100 m from the parking space and buildings with employees which have a minimum distance of less than 200 m from the parking space (the influence of different distances on the result is investigated in Sections 4.2.3.1 and 4.2.3.2).

4.2.2.5 Attractiveness-Based District Rating for Shopping Trips

In order to compute the attractiveness of districts to drive to by car for shopping trips, we use a two-step approach. In the first step, we determine the car-access attractiveness of the individual buildings in the LOR. In the second step, we aggregate the results at the LOR level to derive an overall rating for the district. In the literature, the attractiveness of shopping locations is typically represented by their amount of sales area [128], [129]. The parking situation, which is crucial for the car-access attractiveness of shopping locations, is not considered. To overcome this limitation, in this paper, we determine the attractiveness of each building in the LORs by considering both the sales area and the overall availability of parking spots. To achieve this, we combine the following three criteria:

- Criterion y_{1s}: the amount of parking spots per m^2 sales area.
- Van der Waerden et al. [147] as well as Zhang et al. [148] showed that persons prefer low walking distances between a parking facility and their final destination. Thus, as a second criterion, y_{2s}, we consider the distance of the parking space to the building.
- Hymel [149] and van der Waerden et al. [150] showed that when a shopping location charges for parking, the number of shopping trips there decreases. Therefore, the third criterion for car-access attractiveness evaluation y_{3s} is whether parking fees have to be paid for the use of the parking space.

To determine the car-access attractiveness of a building from the three criteria, we apply the weighted sum model, which is typically used for multicriteria decision analysis [151]. The fundamental concept behind this technique is the additive utility assumption. If each criterion is measurable and has the same unit, then the best alternative is the one with the largest cumulative value [151], [152]. The value R of each alternative j can be computed as

$$R_j = \sum_{i=1}^{n} a_i \cdot w_i \quad \text{for } j = 1, 2, \ldots, m \tag{4.8}$$

where n is the number of criteria, a_i is the value of the criterion i and w_i is the individual weighting-coefficient of the criterion i. In principle, the higher the weighting, the more important the criterion. Normally, the weighting-coefficients are normalized so that they sum to one [151]. For the application of the weighted sum model, all criteria must have the same unit. For this purpose, we use the rating-coefficients β_{1s}, β_{2s} and β_{3s} that assign a discrete value between 1 (very unattractive) and 5 (very attractive) to value ranges of the criteria y_{1s}, y_{2s} and y_{3s}. In Table 4.9, the value ranges of the criteria and their corresponding rating-coefficients are given. Since there is no parking space ordinance in Berlin that prescribes the number of parking spots for buildings with retail usage, the value ranges for y_{1s} are derived in this paper by manually calculating the number of parking spots per m^2 of sales area for fifteen “Aldi” supermarkets. “Aldi” supermarkets are chosen, as they can be regarded as “average” Berlin supermarkets (see Section 4.2.2.2). The computed average value of 0.1 parking spots per m^2 sales area is considered as very attractive. Linear division is used to specify the remaining value ranges. As we described in Section 4.2.2.4, parking spaces can only be assigned to buildings with sales area to which they have a minimal distance of less than 100 m. Accordingly the value ranges of y_{2s} are divided linearly. For the criterion parking fee y_{3s}, we do not consider ranges. We differentiate between free parking spaces which are very attractive and parking spaces with fees which are very unattractive. In Section 4.2.3.1, the influence of modified value ranges of the factors y_{1s}, y_{2s} and y_{3s} on the result is investigated.

For each building with sales area and assigned parking spaces, its car-access attractiveness, hereinafter called attraction-factor x_s, is computed as the weighted sum of the three aforementioned criteria according to Equation (4.9). It is possible that several parking spaces can be assigned to a building, each with a different distance to the building and different parking fees. Therefore, in order to receive a global rating-coefficient α_{2s} and α_{3s} for each building, the rating-coefficients of the parking spaces are weighted according to their number of parking spots assigned to the building.

$$\begin{aligned} x_s &= a_{1s} \cdot w_{1s} + a_{2s} \cdot w_{2s} + a_{3s} \cdot w_{3s} \quad \text{with} \quad \sum_{i=1}^{3} w_{is} = 1 \\ a_{1s} &= \beta_{1s} \\ a_{2s} &= \frac{1}{C_{tb}} \sum_{i=1}^{n} C_{ib} \cdot \beta_{i2s} \\ a_{3s} &= \frac{1}{C_{tb}} \sum_{i=1}^{n} C_{ib} \cdot \beta_{i3s} \end{aligned} \tag{4.9}$$

In Equation (4.9), C_{tb} is the total number of parking spots assigned to the building, n is the total number of parking spaces assigned to the building and C_{ib} is the number of parking spots of the parking space i. w_{1s}, w_{2s} and w_{3s} are the weighting-coefficients of the criteria. Their values can range from 0 to 1, and their sum equals 1. Hence, the attraction-factor x_s of the building can take continuous values between 1 and 5. Buildings with sales area that have not been assigned a parking space receive an attraction-factor x_s of 0.

Since the attraction-factor x_s of each building is known, the total LOR attractiveness A_s for shopping trips by car can be calculated by weighting each building by its sales area according to Equation (4.10).

$$A_s = \frac{1}{S_t} \sum_{i=1}^{m} S_{bi} \cdot x_{is} \tag{4.10}$$

In Equation (4.10), S_t is the total number of sales areas in the LOR, m is the total number of buildings with sales area in the LOR and S_{bi} is the sales area of the building i. Since the attraction-factor x_s can take values between 0 and 5, the attractiveness A_s of the LOR can take continuous values between 0 and 5 as well. A high car-access attractiveness A_s means that an LOR is highly likely to be accessed by car for a shopping activity, while low attractiveness means that people who shop at the LOR are more likely to choose another mode of transportation to travel there.

Table 4.9: Value ranges of the parking spots per m^2 sales area y_{1s}, the building's distance to the parking space y_{2s}, parking fees y_{3s} and their corresponding rating.

Rating-Coefficient	**Parking Spots per m^2 Sales Area** y_{1s}	**Distance to Parking Space** y_{2s}	**Parking Fees** y_{3s}
1 (very unattractive)	$y_{1s} \leq 0.025$	$80\ m < y_{2s} \leq 100\ m$	yes
2 (unattractive)	$0.025 < y_{1s} \leq 0.05$	$60\ m < y_{2s} \leq 80\ m$	-
3 (medium)	$0.05 < y_{1s} \leq 0.075$	$40\ m < y_{2s} \leq 60\ m$	-
4 (attractive)	$0.075 < y_{1s} \leq 0.1$	$20\ m < y_{2s} \leq 40\ m$	-
5 (very attractive)	$y_{1s} > 0.1$	$y_{2s} \leq 20\ m$	no

Table 4.10: Value ranges of the parking spots per employee y_{1w}, the building's distance to the parking space y_{2w} and public transport stop y_{3w} and their corresponding rating.

Rating-Coefficient	**Parking Spots per Employee** y_{1w}	**Distance to Parking Space** y_{2w}	**Distance to Public Transport Stop** y_{3w}
1 (very unattractive)	$y_{1w} \leq 0.01\overline{6}$	$160\ m < y_{2w} \leq 200\ m$	$y_{3w} < 200\ m$
2 (unattractive)	$0.0\overline{3} < y_{1w} \leq 0.01\overline{6}$	$120\ m < y_{2w} \leq 160\ m$	$200\ m \leq y_{3w} < 400\ m$
3 (medium)	$0.05 < y_{1w} \leq 0.0\overline{3}$	$80\ m < y_{2w} \leq 120\ m$	$400\ m \leq y_{3w} < 600\ m$
4 (attractive)	$0.0\overline{6} < y_{1w} \leq 0.05$	$40\ m < y_{2w} \leq 80\ m$	$600\ m \leq y_{3w} < 800\ m$
5 (very attractive)	$y_{1w} > 0.0\overline{6}$	$y_{2w} \leq 40\ m$	$y_{3w} \geq 800\ m$

4.2.2.6 Attractiveness-Based District Rating for Working Trips

In order to compute the attractiveness of districts to drive to by car for working trips, we use the same two-step approach as for the attractiveness-based district rating for shopping trips. In the literature, the attractiveness of working locations is typically represented by its number of employees [130]. We describe the car-access attractiveness of the buildings with employees by combining three criteria related to the parking situation.

- Criterion y_{1w}: the parking spots per employee.
- Criterion y_{2w}: the distance of the parking space to the building [147], [148].
- Boulange et al. [153] and Limtanakool et al. [154] showed that short distances to public transportation services encourage public transport use. Therefore, the third criterion y_{3w} is the average distance of the building to the nearest public transportation stop.

To apply the weighted sum model, all criteria must have the same unit. Therefore, we use the rating-coefficients β_{1w}, β_{2w} and β_{3w} that assign a discrete value between 1 and 5 to the value ranges of the criteria y_{1w}, y_{2w} and y_{3w}. This relationship is shown in Table 4.10.

In the city of Berlin, there is no parking space ordinance that prescribes the number of parking spots for buildings with commercial usage. Therefore, the value ranges of y_{1w} are derived by manually calculating the number of parking spots per employee for 15 companies with 250+ employees. The computed average value of $0.0\overline{6}$ parking spots per employees is considered as very attractive. Linear division is used to specify the remaining value ranges. As we described in Section 4.2.2.4, parking spaces can only be assigned to buildings to which they have a minimal distance of less than 200 m. Accordingly, the value ranges for the criterion y_{2w} are divided linearly.

According to Wibowo and Olszewski [155], a distance of 400 to 800 m can be considered as acceptable walking distance to the nearest public transportation stop. In the state of Zürich in Switzerland, a distance of 400 to 750 m is considered as acceptable walking distance according to Schäffeler [156]. For the city of London, [157] considered 960 m as the maximum acceptable walking distance for rail, underground and light rail services. For Sydney, Daniels and Mulley [158] showed that people walk on average 573 m to a public transportation stop. In accordance with these findings, the value ranges of the criterion y_{3w} are divided linearly. A walking distance of less than 200 m is considered as very unattractive, and a walking distance greater than 800 m is considered as very attractive to undertake the trip by car. Since the computation time to compute the average air distance between a building and its nearest public transportation stop is much faster compared to the computation of a walking distance, we introduce a general conversion factor of $1.494 \approx 1.5$, which means that 100 m of air distance equals 150 m of walking distance in the city of Berlin. This factor is determined by using the OpenRouteService Distance Matrix API [159] to compute the walking distance between two coordinates. For a data set containing 50,000 randomly distributed coordinates on Berlin roads (motorways, forests and parks are excluded), the conversion factor for all coordinate pairs with a walking distance of less than one kilometre is computed. The average result is used as a general conversion factor. In Figure 4.22, the average walking distance of the district buildings to the nearest public transportation is depicted for the district “Mitte”, which is located in the centre of Berlin, and the peripheral district “Spandau” in the west of

Berlin. As expected, the comparison shows a high density of public transportation stops in the centre district "Mitte" and a low density in the peripheral district "Spandau".

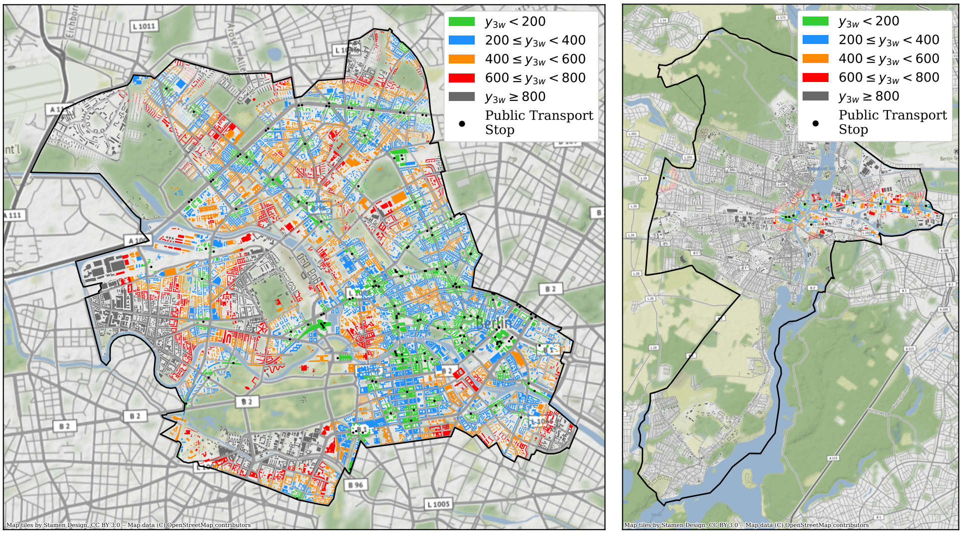

(a) District "Mitte". **(b)** District "Spandau".

Figure 4.22: Average distance to the nearest public transportation stop y_{3w} in the districts "Mitte" and "Spandau".

For each building with employees that also has assigned parking spaces, its attraction-factor x_w is computed as the weighted sum of the three aforementioned criteria according to Equation (4.11). Since several parking spaces can be assigned to a building, each with a different distance to the building, the rating-coefficients β_{2w} of the parking spaces are weighted.

$$\begin{aligned} x_w &= a_{1w} \cdot w_{1w} + a_{2w} \cdot w_{2w} + a_{3w} \cdot w_{3w} \quad \text{with} \quad \sum_{i=1}^{3} w_{iw} = 1 \\ a_{1w} &= \beta_{1w} \\ a_{2w} &= \frac{1}{C_{tb}} \sum_{i=1}^{n} C_{ib} \cdot \beta_{i2w} \\ a_{3w} &= \beta_{3w} \end{aligned} \tag{4.11}$$

In Equation (4.11), C_{tb} is the total number of parking spots assigned to the building, n is the total number of parking spaces assigned to the building and C_{ib} is the number of parking spots of the parking space i. w_{1w}, w_{2w} and w_{3w} are the weighting-coefficients of the criteria. Buildings with employees that have not been assigned a parking space receive an attraction-factor x_w of 0.

Since the attraction-factor x_w of each building is known, the total LOR attractiveness A_w for working trips by car can be calculated by weighting each building by its number of employees.

$$A_w = \frac{1}{E_t} \sum_{i=1}^{m} E_{bi} \cdot x_{iw} \tag{4.12}$$

In Equation (4.12), E_t is the total number of employees in the LOR, m is the total number of buildings with employees in the LOR and E_{bi} is the number of employees of the building i. As shown for shopping trips in Section 4.2.2.5, the attractiveness A_w of the LOR can take continuous values between 0 and 5. While a high car-access attractiveness indicates that a LOR is highly likely to be accessed by car for a working activity, a low attractiveness A_w means that people who work at the LOR are more likely to choose another mode of transportation to travel there.

4.2.3 Results and Discussion

This section is organized as follows: the results of the attractiveness-based district rating are presented for shopping trips in Section 4.2.3.1 and for working trips in Section 4.2.3.2. In Section 4.2.3.3, the limits of the developed model are discussed, as well as possible future steps to improve the accuracy.

4.2.3.1 Attractiveness-Based District Rating for Shopping Trips

This section is divided into two parts. First, the results of the district rating are presented and discussed for the entire city of Berlin. Subsequently, the results for the buildings in two LORs are analysed.

4.2.3.1.1 Results on Berlin Level for Shopping Trips

As we described in Section 4.2.2.5, the car-access attractiveness of the districts is computed by applying the weighted sum model. Depending on the choice of parameters, different results are obtained. Therefore, in this section, we conduct a sensitivity analysis based on 15 parameter combinations (hereafter referred to as cases) to assess the impact of different combinations on the car-access attractiveness of the LORs (see Table 4.11). In the first step, the influence of the search range (i.e., the maximum distance between a parking space and the building it is assigned to) is analysed. In a further comparison, the influence of different value ranges of the criteria and different weighting-coefficients on the results is investigated.

In order to investigate the sensitivity of LOR attractiveness to search ranges, the cumulative distribution function of the car-access attractiveness A_s of the LORs is depicted in Figure 4.23a for three different combinations of search ranges. For each combination, we also investigate the sensitivity of the LOR attractiveness to the criteria y_{1s}, y_{2s} and y_{3s} by successively setting the corresponding weighting-coefficient to 1 (as shown in Table 4.11). First, it can be seen that for each case investigated, the cumulative frequency is non-zero for $A_s = 0$. This is due to the fact that there are LORs in which no parking space has been assigned to a building with sales area. In addition, there are LORs which do not contain buildings with sales areas, as in the case of forest, lake or industrial areas. As a result, those LORs receive an attractiveness A_s of 0. It can be observed that the smaller the search ranges, the greater the number of LORs with a car-access attractiveness A_s of 0, as simply fewer parking spaces are assigned to buildings.

Table 4.11: Investigated cases and selected parameters to compute the attractiveness of the Berlin LORs to drive to by car for shopping trips.

Cases	Weighting-Factors			Search Range Parking Space (m)			Parking Spots per m^2 Sales Area y_{1s}		Distance to Parking Space y_{2s}		Parking Fees y_{3s}	
	w_{1s}	w_{2s}	w_{3s}	Employee	Public	Customer	Very Attractive	Very Unattractive	Very Attractive	Very Unattractive	No Fee	Fee
Case S1	1.0	0.0	0.0									
Case S2	0.0	1.0	0.0				$y_{1s} > 0.1$	$y_{1s} \leq 0.025$			very attractive	very unattractive
Case S3	0.0	0.0	1.0									
Case S4	1.0	0.0	0.0				$y_{1s} > 0.2$	$y_{1s} \leq 0.05$				
Case S5	0.0	0.0	1.0		100.0	10.0			$y_{2s} \leq 20.0\ m$	$y_{2s} > 80.0\ m$	very attractive	medium
Case S6	0.8	0.1	0.1									
Case S7	0.6	0.3	0.1									
Case S8	0.6	0.1	0.3	50.0								
Case S9	$0.\overline{3}$	$0.\overline{3}$	$0.\overline{3}$									
Case S10	1.0	0.0	0.0				$y_{1s} > 0.1$	$y_{1s} \leq 0.025$			very attractive	very unattractive
Case S11	0.0	1.0	0.0		50.0				$y_{2s} \leq 10.0\ m$	$y_{2s} > 40.0\ m$		
Case S12	0.0	0.0	1.0			5.0						
Case S13	1.0	0.0	0.0									
Case S14	0.0	1.0	0.0		300.0				$y_{2s} \leq 60.0\ m$	$y_{2s} > 240.0\ m$		
Case S15	0.0	0.0	1.0									

The highest attractiveness ratings are obtained by the cases S3, S12 and S15 (grey), where only the criterion parking fee is considered, since the weighting-coefficient w_{3s} is set to 1. The high rating is due to the fact that buildings that have been assigned one or more parking spaces without parking fees automatically receive an attraction factor x_s of 5 (very attractive). However, this neglects the fact that only a very small number of parking spots may be assigned to the building or that the assigned parking spaces might be far away, since the weighting-coefficients w_{1s} and w_{2s} are set to 0. Good results are also obtained by cases S2, S11 and S14 (orange), where only the distance of the buildings from the parking spaces is considered to determine the attractiveness of the LORs. This is also mainly due to the fact that the number of parking spots is neglected. The lowest scores are achieved by cases S1, S10 and S13 (blue), where only the number of parking spots per m^2 sales area is considered.

In order to investigate the sensitivity of LOR attractiveness to different value ranges of the criteria and different weighting-coefficients, the cumulative distribution function of car-access attractiveness A_s is depicted in Figure 4.23b for a fixed search range. The comparison of case S1 and case S4 shows that when the threshold values of the criterion y_{1s} (i.e., customer parking spots per sales area) are doubled, a significant decrease in LOR attractiveness A_s is observed. This shows that the attractiveness rating is very sensitive to criterion y_{1s}. The car-access attractiveness rating is significantly less sensitive to a change in the parking fee criterion y_{3s}. This is shown by comparing cases S3 and S5, where it can be observed that the car-access attractiveness of the LORs increases only slightly when the threshold values of y_{3s} are increased.

By comparing cases S6, S7, S8 and S9, the influence of different combinations of the weighting-coefficients on the results can be investigated. In accordance with the previous results, it can be seen that an increased weighting of the criterion y_{1s} leads to a decreasing attractiveness of the LORs. Furthermore, the comparison of case S7 and case S8 shows that the influence of criteria y_{2s} and y_{3s} on the attractiveness of LORs is similar if the car-access attractiveness is determined using all three criteria.

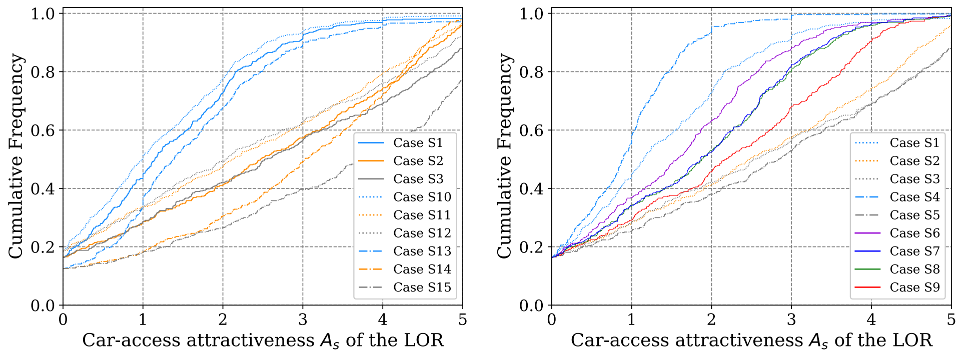

(a) Variable search range for parking spaces. **(b)** Constant search range for parking spaces.

Figure 4.23: Attractiveness-based district rating for shopping trips in the Berlin LORs. Cumulative distribution function.

In Figure 4.24, the spatial distribution of the car-access attractiveness A_s of the Berlin LORs is shown for case S6 and is compared to the amount of sales area in the LORs. The parameter combination of case S6 is chosen because it results in medium attractiveness values for the entire city of Berlin (as shown in Figure 4.23b). The comparison of Figure 4.24a and Figure 4.24b shows that LORs with a high amount of sales area are mostly located in the city centre and do not match LORs with a high number of customer parking spaces per m^2 of sales area, which are mostly located in the outer areas of the city. This is mainly due to the fact that the building density in the outer districts is low and therefore more space is available for parking. These results show that an attractiveness rating based only on total sales area is not an appropriate evaluation parameter to estimate the probability that a person will drive to a district for shopping by car, as the parking situation is neglected.

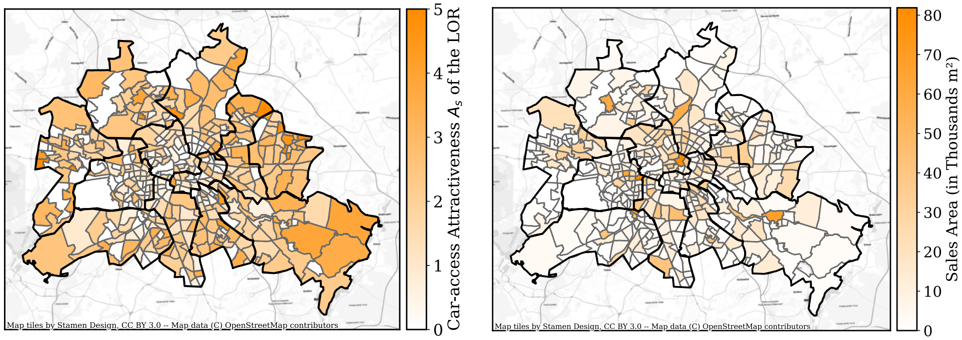

(a) Case S6.

(b) Sales area.

Figure 4.24: Attractiveness-based district rating for shopping trips (case S6) and sales area in the Berlin LORs.

4.2.3.1.2 Results on LOR Level for Shopping Trips

For case S6, the results of the parking situation analysis and the attractiveness-based building rating are shown for two Berlin LORs in Figure 4.25. Buildings displayed in grey do not contain any sales area. Buildings displayed in white have an attraction-factor x_s of 0 which means that no parking space has been assigned to these buildings. The numbers displayed on the parking spaces indicate the calculated number of parking spots. In case S6, the main weighting of car-access attractiveness is on the number of parking spots per m^2 of sales area (weighting-coefficient $w_{1s} = 0.8$). Accordingly, the buildings that have been assigned many parking spots receive a high attraction-factor. The average car-access attractiveness A_s of the LOR "Karl-August-Platz" is 1.086. The average car-access attractiveness of the LOR "Germania Straße" is 1.772. The value for the "Germania Straße" is higher because a higher percentage of the buildings have been assigned parking spaces and thus do not receive an attraction-factor of 0. In addition, in the LOR "Karl-August-Platz", several buildings often share one parking space. In contrast, in the "Germania Straße" LOR, customer parking spaces are each assigned to a single building, which then results in a higher number of parking spots per m^2 of sales area.

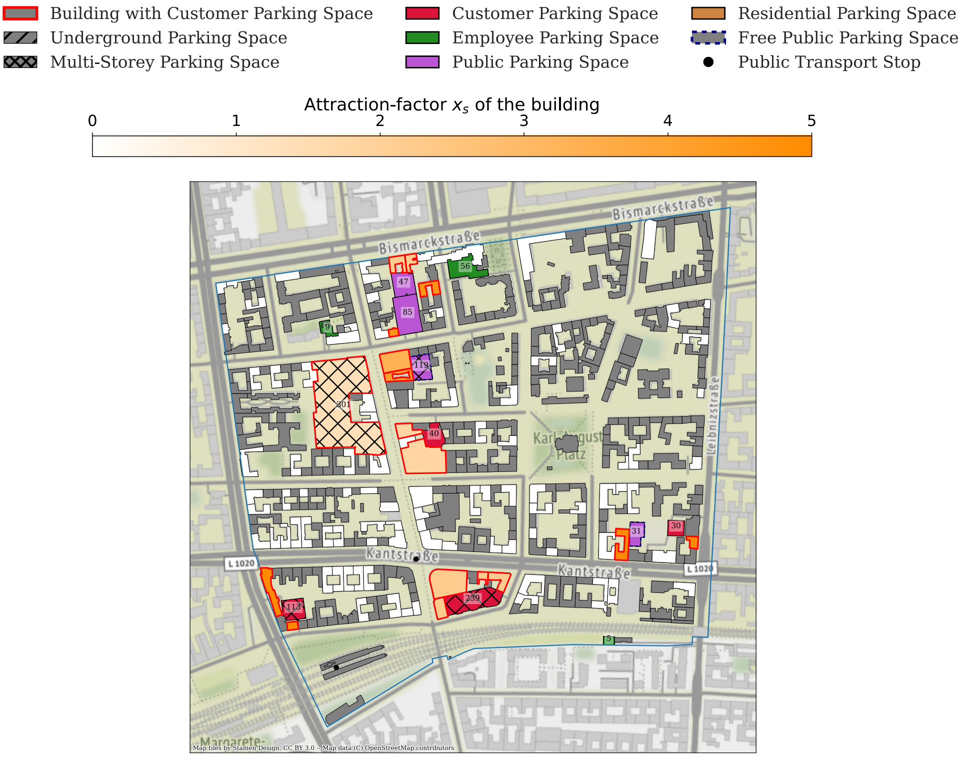

(a) “Karl-August-Platz” LOR.

(b) “Germania Straße” LOR.

Figure 4.25: Attractiveness-based building rating for shopping trips for two Berlin LORs. Case S6.

4.2.3.2 Attractiveness-Based District Rating for Working Trips

The structure of this section is identical to Section 4.2.3.1. First, the results of the district rating for working trips are presented and discussed for the entire city of Berlin. Subsequently, the results for the buildings in two LORs are analysed.

4.2.3.2.1 Results on Berlin Level for Working Trips

With the same objectives as in Section 4.2.3.1.1, a sensitivity analysis based on 15 parameter combinations is conducted in this section (see Table 4.12). For the investigation of the sensitivity of LOR attractiveness to search ranges, the cumulative distribution function of the car-access attractiveness A_w is depicted in Figure 4.26a for three different combinations of search ranges. Additionally, the sensitivity of the LOR attractiveness to the criteria y_{1w}, y_{2w} and y_{3w} is investigated for each combination. It can be observed that for each case, the cumulative frequency is non-zero for $A_s = 0$ and that smaller search ranges lead to a greater number of LORs with a car-access attractiveness $A_s = 0$. These findings have already been justified in Section 4.2.3.1.1.

The highest attractiveness ratings are obtained by cases W2, W11 and W14 (orange), where only the distance of the buildings to the parking spaces is considered. This is because a building automatically receives a high attraction-factor x_w if it is located near a parking space. However, this neglects that only a small number of parking spots may be assigned to the building. Intermediate results are obtained by cases W3, W12 and W15 (grey), where only the minimal distance of a building to the nearest public transportation stop is considered. The lowest scores are obtained by cases W1, W10 and W13 (blue), where only the number of parking spots per employee is considered.

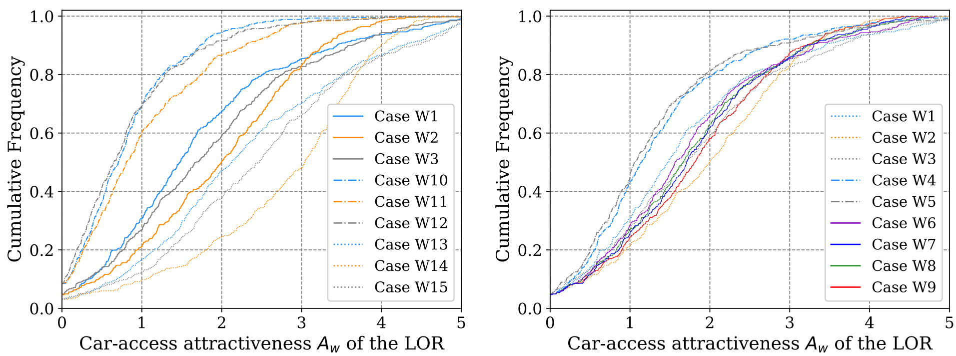

(a) Variable search range for parking spaces. **(b)** Constant search range for parking spaces.

Figure 4.26: Attractiveness-based district rating for working trips in the Berlin LORs. Cumulative distribution function.

For the investigation of the sensitivity of LOR attractiveness to different value ranges of the criteria and different weighting-coefficients, the cumulative distribution function of car-access attractiveness A_w of the LORs is depicted in Figure 4.26b for a fixed search range. The comparison of case W3 and case W5 shows that the attractiveness rating is very sensitive to a change in the criterion distance to public transportation y_{3w}, since the doubling of its threshold values leads to a significant decrease in LOR attractiveness.

Table 4.12: Investigated cases and selected parameters to compute the attractiveness of the Berlin LORs to drive to by car for working trips.

<table>
<tr><th rowspan="2">Cases</th><th colspan="3">Weighting-Factor</th><th colspan="3">Search Range Parking Space (m)</th><th colspan="2">Parking Spots per Employee y_{1w}</th><th colspan="2">Distance to Parking Space y_{2w}</th><th colspan="2">Distance to Public Transport Stop y_{3w}</th></tr>
<tr><th>w_{1w}</th><th>w_{2w}</th><th>w_{3w}</th><th>Employee</th><th>Public</th><th>Customer</th><th>Very Attractive</th><th>Very Unattractive</th><th>Very Attractive</th><th>Very Unattractive</th><th>Very Attractive</th><th>Very Unattractive</th></tr>
<tr><td>Case W1</td><td>1.0</td><td>0.0</td><td>0.0</td><td rowspan="9">50.0</td><td rowspan="9">200.0</td><td rowspan="9">10.0</td><td rowspan="3">$y_{1w} > 0.0\overline{6}$</td><td rowspan="3">$y_{1w} \leq 0.01\overline{6}$</td><td rowspan="9">$y_{2w} \leq 40.0\ m$</td><td rowspan="9">$y_{2w} > 160.0\ m$</td><td rowspan="4">$y_{3w} \geq 800.0\ m$</td><td rowspan="4">$y_{3w} < 200.0\ m$</td></tr>
<tr><td>Case W2</td><td>0.0</td><td>1.0</td><td>0.0</td></tr>
<tr><td>Case W3</td><td>0.0</td><td>0.0</td><td>1.0</td></tr>
<tr><td>Case W4</td><td>1.0</td><td>0.0</td><td>0.0</td><td>$y_{1w} > 0.1\overline{3}$</td><td>$y_{1w} \leq 0.0\overline{3}$</td></tr>
<tr><td>Case W5</td><td>0.0</td><td>0.0</td><td>1.0</td><td rowspan="11">$y_{1w} > 0.0\overline{6}$</td><td rowspan="11">$y_{1w} \leq 0.01\overline{6}$</td><td>$y_{3w} \geq 1600.0\ m$</td><td>$y_{3w} < 400.0\ m$</td></tr>
<tr><td>Case W6</td><td>0.8</td><td>0.1</td><td>0.1</td><td rowspan="10">$y_{3w} \geq 800.0\ m$</td><td rowspan="10">$y_{3w} < 200.0\ m$</td></tr>
<tr><td>Case W7</td><td>0.6</td><td>0.3</td><td>0.1</td></tr>
<tr><td>Case W8</td><td>0.6</td><td>0.1</td><td>0.3</td></tr>
<tr><td>Case W9</td><td>$0.\overline{3}$</td><td>$0.\overline{3}$</td><td>$0.\overline{3}$</td></tr>
<tr><td>Case W10</td><td>1.0</td><td>0.0</td><td>0.0</td><td rowspan="3">15.0</td><td rowspan="3">30.0</td><td rowspan="3">5.0</td><td rowspan="3">$y_{2w} \leq 6.0\ m$</td><td rowspan="3">$y_{2w} > 24.0\ m$</td></tr>
<tr><td>Case W11</td><td>0.0</td><td>1.0</td><td>0.0</td></tr>
<tr><td>Case W12</td><td>0.0</td><td>0.0</td><td>1.0</td></tr>
<tr><td>Case W13</td><td>1.0</td><td>0.0</td><td>0.0</td><td rowspan="3">150.0</td><td rowspan="3">400.0</td><td rowspan="3">10.0</td><td rowspan="3">$y_{2w} \leq 80.0\ m$</td><td rowspan="3">$y_{2w} > 320.0\ m$</td></tr>
<tr><td>Case W14</td><td>0.0</td><td>1.0</td><td>0.0</td></tr>
<tr><td>Case W15</td><td>0.0</td><td>0.0</td><td>1.0</td></tr>
</table>

This can be explained as follows: for case W5, an LOR attractiveness A_w of 5 indicates that the distance of all buildings with employees to the nearest transportation stop is at least 1600 m. In Berlin, however, the public transport network is very well developed. Therefore, LORs in which all, or most, buildings meet these requirements are rare.

As observed for the district rating for shopping trips, the comparison of cases W6, W7, W8 and W9 shows that an increased weighting of the criterion y_{1w} leads to a decreasing car-access attractiveness of the LORs, which is in accordance with the previous findings. In addition, the comparison of case W7 and case W8 shows that the influence of criteria y_{2w} and y_{3w} on the attractiveness of LORs is similar if the car-access attractiveness is determined using all three criteria.

In Figure 4.27, the spatial distribution of the car-access attractiveness A_w of the Berlin LORs is shown for case W6 and is compared to the number of employees in the LORs. The parameter combination of case W6 is chosen because it results in medium attractiveness values for the entire city of Berlin (as shown in Figure 4.26b). By comparing Figure 4.27a,b, it can be observed that LORs with a high quantity of employees are mostly located in the city centre area and do not match LORs with a high number of parking spaces per employee, which are mostly located in the outer areas of the city. The reasons for this and the implications of the results have already been discussed in the analogous study for shopping trips (see Figure 4.24).

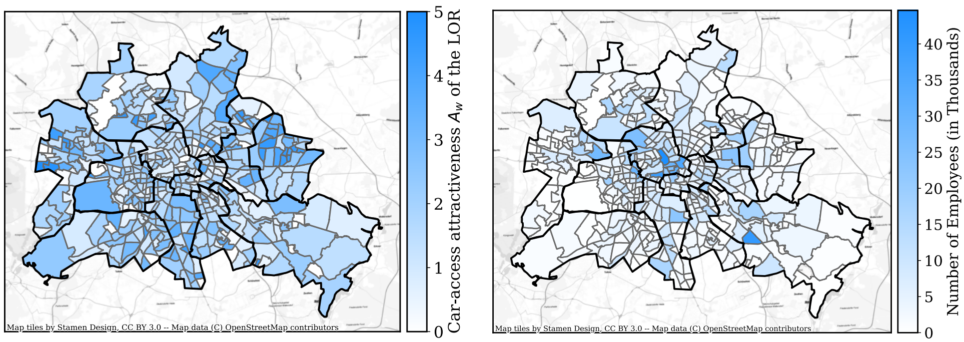

(a) Case W6. **(b)** Number of Employees.

Figure 4.27: Attractiveness-based district rating for working trips (case W6) and number of employees in the Berlin LORs.

4.2.3.2.2 Results on LOR Level for Working Trips

For case W6, the results of the parking situation analysis and the attractiveness-based building rating are shown for the LORs ”Karl-August-Platz” and ”Germania Straße” in Figure 4.28. Buildings displayed in grey do not contain any employees. Buildings displayed in white have an attraction-factor x_w of 0, which means that no parking space has been assigned to these buildings. Since the main weighting of the car-access attractiveness A_w is on the number of parking spots per employee (weighting-coefficient $w_{1w} = 0.8$), the buildings that have been assigned many parking spots receive a high attraction-factor. The average car-access attractiveness A_w of the LOR “Karl-August-Platz” is 1.263. The average car-access attractiveness of the LOR “Germania Straße” is 2.057. The low value in the

LOR “Karl-August-Platz” is due to the high percentage of buildings that have not been assigned a parking space and therefore receive an attraction-factor of 0. Additionally, in the LOR “Karl-August-Platz”, most parking spaces are customer and public parking spaces. In contrast, there are many employee parking spaces in the LOR “Germania Straße”. As a result, many buildings, especially in the south of the LOR, have a high attraction factor, resulting in a higher attractiveness A_w of the LOR.

4.2.3.3 Discussion

After presenting the results of the attractiveness-based district rating and the method for determining it, a couple of aspects concerning the proposed approach should be discussed.

- The proposed method should be validated by extensive surveys of motorists about their location choice behaviour. From the parameter combinations presented in Sections 4.2.3.1 and 4.2.3.2 for calculating the attractiveness-based district rating, the combination that most accurately describes reality can then be selected.

- The proposed computation of the building’s attraction-factors x_s and x_w is based on the combination of three different criteria, each of which should be understood as the initial point for further improvements. Due to the weighted sum approach, additional criteria can be easily added in order to further refine the results.

  1. It is conceivable to investigate the accessibility of the building by determining the distance of the building to a main road using the OpenRouteService Distance Matrix API [159].

  2. Since OSM is a community project, geographic data are collected on a voluntary basis. Therefore, not every parking space is labelled as such in the data set. Unlabelled parking spaces are mainly located on the roadside. Based on a district’s land area, road network, building density and degree of motorisation, it is possible to estimate the number of unmarked roadside parking spaces available for shopping and work activities. The density of the buildings can be derived from the results of the building usage analysis (Section 4.2.2.1). The road network can be extracted from the OSM data set. For Berlin, the degree of motorisation is given in [93].

  3. In order to evaluate the car-access attractiveness of the work locations, we consider, among other criteria, the accessibility of the locations by public transportation. The results can be further improved by considering pedestrian and bicycle accessibility. This accessibility could be evaluated, for example, by infrastructure per capita, as shown in [160].

- As described in Figure 4.16, the vehicle-based mobility profiles and the attractiveness-based district rating can be combined with an appropriate routing algorithm to determine BEV routes. To avoid assigning too many BEVs to certain districts during the routing process, each district must be assigned a maximum intake capacity for each activity. One solution is to use the total number of customer or employee parking spots per district as an upper limit.

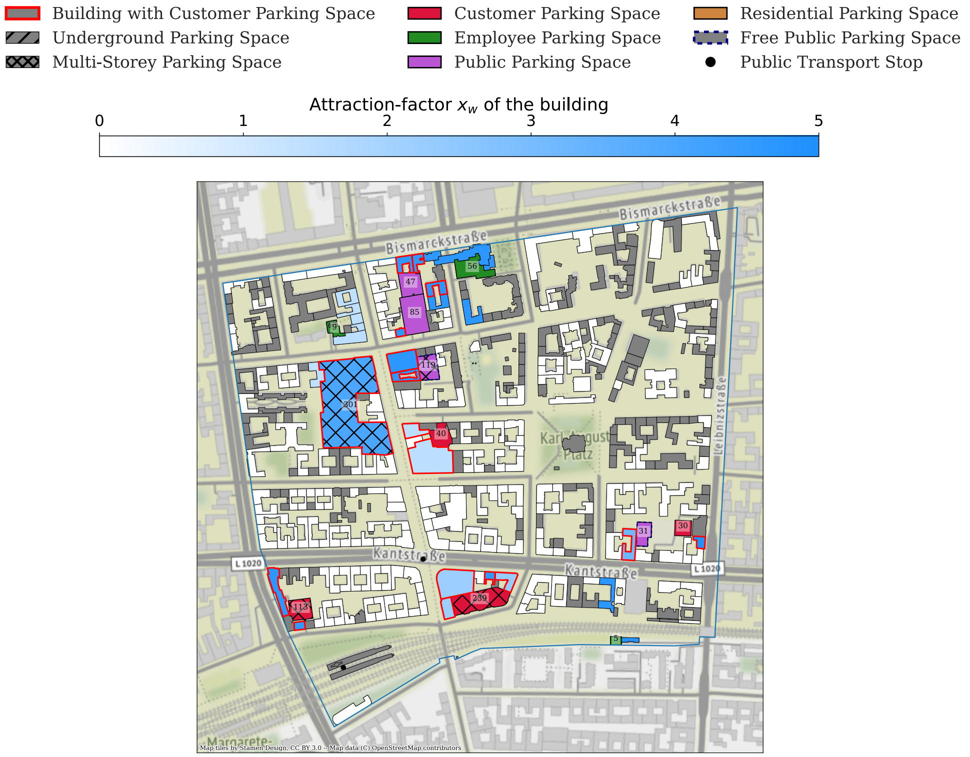

(a) "Karl-August-Platz" LOR.

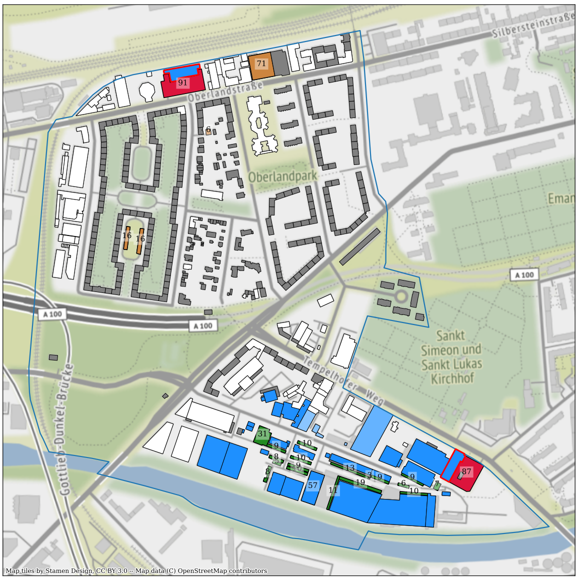

(b) "Germania Straße" LOR.

Figure 4.28: Attractiveness-based building rating for working trips for two Berlin LORs. Case W6.

4.2.4 Conclusions and Outlook

The increasing number of battery electric vehicles (BEVs) and their demand for electrical power can lead to bottlenecks in the electrical grid infrastructure if it is not strengthened [20], [21]. In order to locate those bottlenecks, the spatial distribution of the energy demand of BEVs needs to be known. For this purpose, travel schedules of individuals can be combined with an attractiveness rating of districts within an e-mobility traffic simulation to estimate traffic flows. Typically, attractiveness is represented by the "size" of locations (e.g., number of employees or sales area), assuming that larger places attract more persons than smaller ones [128], [129], [131]. Whereas this assumption can be applied when all modes of transportation are considered, it cannot be applied if cars are the only mode of transport under consideration, since the availability of parking spaces is neglected. Due to this neglect, department stores with a high amount of sales area and companies with many employees, for example, are classified as very attractive, regardless of whether sufficient parking infrastructure is available. Since the evaluation of car-access attractiveness of locations has not been addressed so far in the literature, this research gap is filled by this paper.

The car-access attractiveness of a district regarding shopping and working trips is determined in each case in a two-step process. First, we determine the car-access attractiveness of the individual buildings in the district by applying the weighted sum model and then aggregate the results on the district level. For shopping trips, the car-access attractiveness of a building is based on three criteria: the amount of parking spots per sales area of the building, the distance of the parking spaces to the building and whether there are fees for the usage of the parking spaces. For working trips, the car-access attractiveness is computed by considering the number of parking spots per employee of the building, the distance of the parking spaces to the building and the average distance of the building to the nearest public transportation stop. We have demonstrated the approach for the urban area of Berlin and its 448 sub-districts called LORs. Since the method is based on open geodata and freely available data sets, our approach is traceable and reproducible. The data sets we used to develop our method are available in a similar or identical form in many rural and urban regions in Germany. Therefore, an upscaling of our model is feasible. For Berlin, we show that LORs with a great amount of sales area or employees are mostly located in the city centre. Those LORs would obtain high attractiveness under the assumption that larger places are more attractive. However, this contradicts the fact that in Berlin, more parking spaces are available in the outer districts since the building density there is lower. In contrast, we showed that LORs with a high attractiveness according to our evaluation method are mostly located in the outer areas of the city, which matches the parking situation.

Our model provides an important building block for the complete evaluation of power demand due to the massive electrification of private urban mobility expected in upcoming years. Nevertheless, the validity of the model should be investigated in detail by surveying car drivers on their location choice behaviour in the near future.

4.2.5 Author Contributions

Florian Straub: Conceptualization, Supervision, Writing - Original Draft. **Florian Straub, Otto Maier:** Methodology, Investigation, Visualization. **Florian Straub, Dietmar Göhlich:** Writing - Review & Editing. **Dietmar Göhlich:** Project administration, Funding acquisition.

4.2.6 Appendix A. Sales Area in the Berlin Districts and Buildings

Table 4.13: Comparison of the average sales area of retail buildings and the total sales area of three department stores with computed values.

Building Usage Class	Type	Average/ Total Sales Area (m^2)	Average/ Total Computed Sales Area (m^2)	Relative Error (%)
Retail Building	Aldi Nord [139]	850	826	−2.8
	Kaufland [140]	4340	4390	−1.1
Department Store	Wima Shopping [161]	25,000	23,552	−5.8
	Spandauer Arcarden [162]	33,000	32,046	−2.9
	Bikini Berlin [163]	17,000	17,954	5.6

Table 4.14: Sales area per district; comparison of authority data with computed values.

District	Inhabitants	Sales Area per Inhabitant (m^2)	Total Sales Area (m^2)	Computed Sales Area (m^2)	Relative Error (%)
Mitte	375,500	1.79	672,145	691,234	2.8
Friedrichshain-Kreuzberg	275,400	0.86	236,844	246,543	4.1
Pankow	395,100	1.14	450,414	435,786	−3.2
Charlottenburg-Wilmersdorf	317,100	1.55	491,505	485,342	−1.3
Spandau	237,400	1.29	306,246	288,523	−5.8
Steglitz-Zehlendorf	289,600	1.16	335,936	349,876	4.1
Tempelhof-Schöneberg	340,300	1.47	500,241	451,478	−9.7
Neukölln	318,000	1.09	346,620	334,893	−3.4
Treptow-Köpenick	265,500	1.15	305,325	298,652	−2.2
Marzahl-Hellersdorf	255,800	1.24	317,192	267,639	4.6
Lichtenberg	278,900	0.91	253,799	261,757	3.1
Reinickendorf	255,700	1.02	260,814	255,739	−1.9

4.3 Publication III

Forecasting the Spatial and Temporal Charging Demand of Fully Electrified Urban Private Car Transportation based on Large-Scale Traffic Simulation

Florian Straub[1], Otto Maier[1], Dietmar Göhlich[1], Yuan Zou[2]

[1]Chair of Methods for Product Development and Mechatronics, Technische Universität Berlin, Strasse des 17.Juni 135, 10623 Berlin, Germany

[2]Beijing Collaborative Innovation Center for Electric Vehicle, National Engineering Laboratory for Electric Vehicles, School of Mechanical Engineering, Beijing Institute of Technology, Beijing 100081, China

(This article has been published on 23 October 2022 by Elsevier in "Green Energy and Intelligent Transportation", available online: https://doi.org/10.1016/j.geits.2022.100039)

Abstract: To support power grid operators to detect and evaluate potential power grid congestions due to the electrification of urban private cars, accurate models are needed to determine the charging energy and power demand of battery electric vehicles (BEVs) with high spatial and temporal resolution. Typically, e-mobility traffic simulations are used for this purpose. In particular, activity-based mobility models are used because they individually model the activity and travel patterns of each person in the considered geographical area. In addition to inaccuracies in determining the spatial distribution of BEV charging demand, one main limitation of the activity-based models proposed in the literature is that they rely on data describing traffic flow in the considered area. However, these data are not available for most places in the world. Therefore, this paper proposes a novel approach to develop an activity-based model that overcomes the spatial limitations and does not require traffic flow data as an input parameter. Instead, a route assignment procedure assigns a destination to each BEV trip based on the evaluation of all possible destinations. The basis of this evaluation is the travel distance and speed between the origin of the trip and the destination, as well as the car-access attractiveness and the availability of parking spots at the destinations.

The applicability of this model is demonstrated for the urban area of Berlin, Germany, and its 448 sub-districts. For each district in Berlin, both the required daily BEV charging energy demand and the power demand are determined. In addition, the load shifting potential is investigated for an exemplary district. The results show that peak power demand can be reduced by up to 31.7% in comparison to uncontrolled charging.

Keywords: electric vehicle; activity-based simulation; transportation electrification; spatial temporal distribution of charging demand; open data

4.3.1 Introduction

Man-made climate change can be slowed down if greenhouse gas emissions are reduced quickly and drastically. The signatories to the 2015 Paris Climate Agreement have therefore committed to reducing their greenhouse gas emissions to such an extent that the man-made temperature increase is limited to below 2 °C [1]. A key driver of this decline is the decarbonization of the transport sector. The European Union, for example, has agreed on an emission limit of 95 $g\,CO_2/km$ for passenger cars registered in 2021 [11]. As a result, private passenger cars with internal combustion engines (hereinafter referred to as internal combustion engine vehicles (ICEVs)) are being replaced by passenger cars with alternative drive systems, primarily battery electric passenger cars (hereinafter referred to as battery electric vehicles (BEVs)). Without reinforcement of the electric grid infrastructure, the resulting additional demand for electrical energy and power may cause congestion in the power supply [20], [21]. To enable electric grid operators to identify possible congestions in the grid, accurate models are needed that predict the spatial and temporal energy and power demand resulting from the electrification of private ICEVs. Typically, e-mobility traffic simulations are used for this purpose:

The authors of [24] develop a traffic simulation to forecast the spatial and temporal distribution of the charging energy demand of an urban area. In their method, they first divide the area into different functional areas (e.g., residential, work, shopping and entertainment) and assign a certain number of BEVs to each functional area. Using the known geographic origin of each BEV trip, the destinations are randomly selected. Based on the geographic location of the destinations, arrival and departure times, and travel distances, the spatial and temporal distribution of BEV charging demand is determined. However, this spatial distribution is highly inaccurate due to the random selection of destinations. Each functional area is different from the others (e.g., number of employees or number of available parking spaces) and therefore has a different probability of attracting trips which is not considered.

In [72], the authors simulate the spatial and temporal distribution of charging energy demand for an artificial city consisting of a city center, suburban areas, and connecting highways. All simulated individuals and their vehicles make a round trip that begins in a suburb and then travels to a randomly selected location in the city center and back. At each stop, the individuals decide whether to charge their vehicles, depending on their current state of charge (SOC). Based on the resulting charging demand of the vehicles at the different locations, the charging times are determined, which allows the spatial and temporal distribution of the charging demand to be determined. Due to the assumption that all vehicles make two trips per day and travel to a random location in the city, both the spatial and temporal distribution of charging demand are highly inaccurate.

For 11 districts in the city of Reykjavík, Iceland, the authors of [73] use a traffic simulation to determine the spatial and temporal distribution of BEV energy demand. The authors do not divide Reykjavík into 11 districts themselves, but use an existing classification created by official bodies. To determine the energy demand per district, the daily distances of the combustion engine vehicles and the arrival times of the vehicles at the places of residence are first extracted from a travel survey (travel surveys are obtained by surveying households in a geographic area about their activities and trips on reference days). The conventional cars are then replaced by a reference BEV with 60 kWh battery capacity and an average energy consumption of 0.2 kWh/km. All vehicles are assumed to be charged at home at the end of the day, as this charging scenario is expected to have the largest impact on the power grid. Since only arrival times at residences and the geographic locations of the residences are determined, the method can only determine the spatial and temporal distribution of charging demand, assuming that charging occurs exclusively at the residences. This does not reflect reality.

Another approach for forecasting the spatial and temporal BEV charging demand distribution is to use an activity-based mobility model [75]–[78], [164].
Activity-based models are particularly well suited for simulating the energy and power demand of BEVs because they capture the relationship between activities and mobility patterns, which can be used to determine the parking times of vehicles at different locations [84]. Energy and power demand can then be estimated by applying charging scenarios. In activity-based mobility models, individual full-day travel schedules are generated for each person in the considered area. The assumption for this generation is that a person's activity and travel patterns depend on the person's characteristics (e.g. the place of residence, income, age, household and other social structures).
The travel schedules (also referred to as mobility profiles) consist of a sequence of activities at different locations and trips between these activities. They are usually generated based on a detailed travel survey [75], [77], [78], [164]. Travel surveys are conducted by interviewing households in a geographic area about their activities and trips on reference days, which allows the determination of the daily travel patterns of the population in the studied area.

In Figure 4.29 an example of a mobility profile of a person is depicted. The person starts with its car at its "Home" location and goes shopping and works during the day, before arriving back home at 17:15. The daily distance covered is 45 km in total.

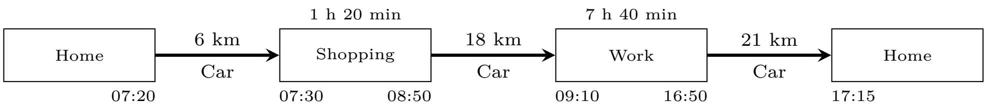

Figure 4.29: Example of a general mobility profile.

An activity-based model is used by the authors of [77] to determine the spatial and temporal BEV charging demand of electric cars in the Flemish region, Belgium. The basis of the determination is the number of vehicles in each district in the region, which are replaced by electric reference vehicles of three different vehicle size classes. The authors do not divide the Flemish region into districts themselves, but use an existing classification created by official bodies. For each vehicle, a mobility profile is generated using a detailed travel survey. Based on the average consumption of the reference BEVs, the arrival and departure times, and the travel distances of the BEVs, the spatial and temporal distribution of charging demand is determined. However, this spatial distribution is inaccurate because it is assumed that the proportions of the three vehicle size classes are the same in all districts. In general, larger and heavier vehicles have higher energy consumption than smaller and lighter vehicles. Thus, if the individual distribution of vehicle size classes in the districts is not taken into account, the charging demand will be underestimated in districts with many large vehicles and overestimated in districts with many small vehicles.

The authors of [78] determine the spatial and temporal BEV charging demand for Singapore using an activity-based model. They first determine the number of current internal combustion engine cars in each district, which are then replaced with electric reference vehicles. The authors do not divide Singapore into districts themselves, but use an existing classification created by official bodies. A mobility profile is created for each vehicle based on a detailed travel survey. These mobility profiles and a vehicle dynamics model are used to determine the temporal and spatial distribution of BEV charging demand in Singapore and its districts. Similar to the method developed in [77], the proportions of vehicle size classes are assumed to be the same in all districts. Therefore, the spatial distribution of charging demand is inaccurate, as previously justified (see study [77]).

For the Seattle metropolitan area, USA, the authors of [76] use an activity-based model to investigate how the current ICEV driving behavior of the population can be electrified. The current driving behavior of the population is derived from extensive GPS measurements in conventional vehicles. A mobility profile is created from this data for each vehicle in the area under consideration. The conventional vehicles are then replaced by a reference BEV with an average consumption of 0.186 kWh/km and a range of 161 km (100 miles). Based on the BEV consumption and mobility profiles of the BEVs, the temporal and spatial distribution of the charging demand can be determined. However, since only one reference vehicle is used, the determined spatial distribution is inaccurate. In general, larger and heavier vehicles have higher energy consumption than smaller and lighter vehicles. If vehicle size is not taken into account, the charging demand will be underestimated in districts with many large vehicles and overestimated in districts with many small vehicles.

This paper makes two important contributions to the literature. As shown, the studies proposed in the literature have limitations that lead, in particular, to inaccuracies in the identified spatial distribution of BEV charging demand. Therefore, this paper develops an activity-based mobility model that overcomes these spatial limitations.
In activity-based models, a person's destination choice is usually determined based on traffic flow data between subareas of the area under consideration. These traffic flow data can be obtained from extensive GPS measurements, as in reference [76], but are usually derived from detailed travel surveys. However, to derive traffic flows, the input data must be available at an extremely high level of detail. These detailed datasets are usually not available for most regions of the world because they are very expensive to generate. To address this problem, in this paper we develop an activity-based mobility model that does not rely on traffic flow data. In contrast, we propose a model based on open data, which ensures its traceability, reproducibility, and transferability. The developed model is applied to forecast the spatial and temporal distribution of charging energy and power demand resulting from the complete electrification of private ICEVs in an urban area. The use case of this paper is Berlin, Germany, with a total number of 1,045,000 [97] private passenger cars.

The developed model consists of three main parts which are discussed in Section 4.3.2. Two of these three parts have already been presented in previous articles [27], [28]. In this paper, we present the development of the third part in Section 4.3.3, thereby completing the model and enabling the determination of the spatial and temporal charging energy and power demand. The charging scenarios investigated are discussed in Section 4.3.4. The results are presented and analysed in Section 4.3.5. Finally, the main conclusions of this paper are presented in Section 4.3.6.

4.3.2 Three-step Model for Estimating the Charging Demand of BEVs using Open Data

The three-step model for estimating the spatial and temporal distribution of BEV charging demand is depicted in Figure 4.30. The model is applied to the urban area of Berlin, Germany, and its 448 sub-districts, which are referred to as "Lebensweltlich orientierte Räume" (Eng.: neighbourhood-oriented districts, abbr.: LORs). The LOR classification is an official classification of the Berlin administration. Within each LOR, the structure of the included buildings and the socio-economic status of the inhabitants are similar. The LORs are usually separated from each other by major roads, rivers or rails [98], [133].

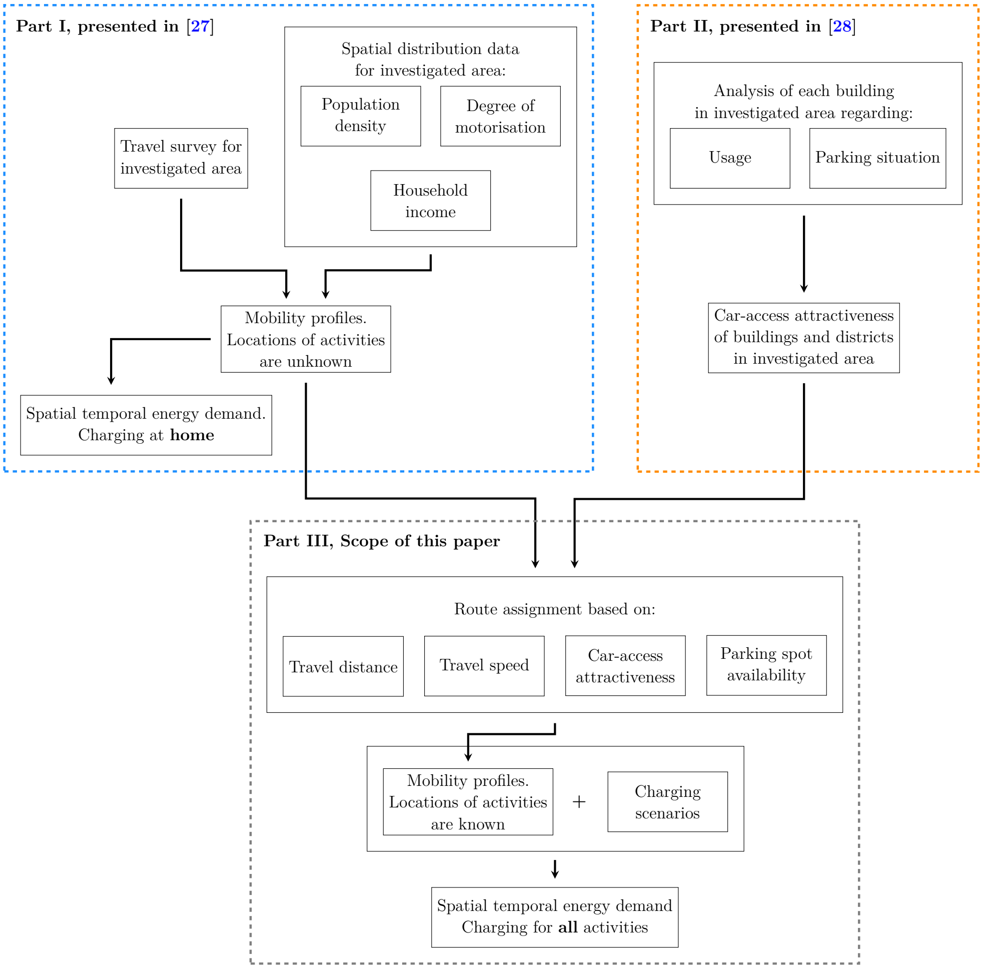

Figure 4.30: Three-step model for estimating the spatial and temporal energy and power demand from the electrification of private ICEVs.

The first part of the model was developed in [27] and is summarized below.
In [27], the current conventional vehicle fleet in the districts (in total, 1,045,000 private cars in Berlin [97]) is first completely electrified. For electrification, data on motorization levels and population density are used to determine the spatial distribution of the vehicles in the considered area. The spatial distribution of household income is then used to determine the spatial distribution of vehicle size classes in the districts. This yields the number and size of vehicles for each district, which are then replaced with reference electric vehicles.
For the replacement of the current ICEV fleet 12 electric passenger cars are used which are depicted in Table 4.16. For each reference vehicle, Table 4.16 also specifies its energy consumption per 100 km and its battery capacity. The average consumption is divided into inner-city trips, characterised by distances of less than 20 km and outer-city trips. The values of the energy consumption and battery capacity are based on test drives of the “Allgemeine Deutsche Automobil Club” (ADAC), a German motoring association, and already include charging losses [100].

Subsequently, a travel survey is used to determine vehicle-based mobility profiles. Vehicle-based mobility profiles are generated (instead of person-based ones) because they realistically represent multiple uses of the same vehicle by multiple people (e.g. families). The survey data is limited. While it is possible to determine the driving behaviour of the population from this data, it is not possible to derive activity- and time-dependent traffic flows between districts. Therefore, the vehicle-based mobility profiles generated do not contain information about the geographic location where the vehicle is parked while the BEV user is performing an activity. Unlike travel surveys, from which traffic flows can be derived, these limited travel surveys are widely available. Figure 4.31 shows example vehicle-based mobility profiles for the 1,045,000 private BEVs in Berlin. It can be seen that some vehicles are not driving on the simulated day and each vehicle is assigned an individual route.

Based on these preliminary mobility profiles, the spatial and temporal distribution of charging energy and power demand in Berlin is determined. However, there is one major limitation to the results. Since the locations of the activities are not known, the charging demand can only be determined for the assumption that charging occurs exclusively at the residences of BEV owners.

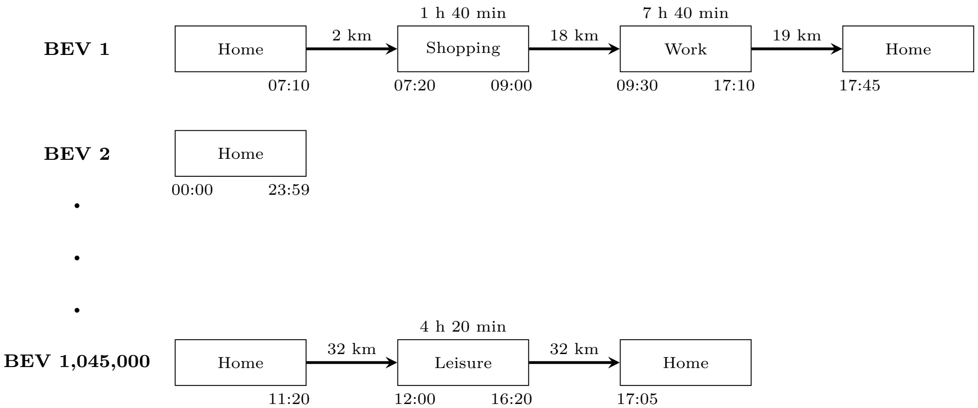

Figure 4.31: Vehicle-based mobility profiles of the population under consideration.

To overcome this limitation, the geographic location where the vehicle is parked while the BEV user is performing an activity needs to be determined. An important input variable in this determination is the car-access attractiveness of the districts. The determination of the car-access attractiveness is the second part of the model. It was developed in [28] and applied to the 448 LORs of Berlin. The car-access attractiveness is a measure of how attractive buildings and districts are to drive to by car for a particular activity. A high attractiveness indicates that a location is highly likely to be accessed by car, while a low attractiveness means that the location is more likely to be accessed by another mode of transportation. The car-access attractiveness is determined based on the number of available parking spots in the districts, the distance of the buildings in the district from the parking spots, and their distance to public transportation.

The last part of the model combines the results of Parts I and II and corresponds to the scope of this paper. A route assignment method is developed that is used to assign an appropriate route to each BEV to determine the unknown geographic destinations of BEV trips (in the following, a BEV's route is referred to as the sequence of the BEV's locations, not the route the vehicle chooses on the road to get from an origin to a destination). This allows the determination of the spatial and temporal distribution of charging energy demand of an urban region, taking into account charging for all activities.
The basis of this route assignment method is a destination choice model. In destination choice models, the most plausible destination among all possible destinations is selected for each BEV trip based on predefined criteria. The most common criteria are the attractiveness of the destination and the distance between origin and destination, which are usually combined in a gravity model [129]–[131], [165], [166]. The basic principle of the gravity model is the assumption that a traffic cell behaves like a gravitational point, i.e. the more mass (attractiveness) a cell has (e.g. number of employees or sales area), the higher its gravitational pull. As the distance increases, the cell's gravitational pull decreases [66]. Analogous to the gravity model, we also use the distance between origin and destination and the attractiveness of the destination for the destination choice model of this paper.

However, we do not use the number of employees or the sales area to describe the attractiveness of a district, but the car-access attractiveness developed in Part II. This is because the availability of parking spots is neglected. This neglect means that, for example, shopping centers with a large sales area and companies with many employees are considered very attractive, regardless of whether sufficient parking infrastructure is available. However, it is obvious that it is not possible to park at a location where there is no parking infrastructure. Additionally, to these two criteria, the travel speed between origin and destination is considered as a criterion, as it has a strong influence on the choice of the destination itself [166]–[169]. As fourth criterion the time-dependent availability of parking spots in the districts is considered. This is necessary to prevent individual districts with high car-access attractiveness from being allocated all vehicles.

We apply the route assignment method to the mobility profiles generated for BEVs in the urban area of Berlin, Germany, and its 448 sub-districts (LORs) in Part I. These mobility profiles show that in Berlin 41.5% of the trips lead to the BEV owner's residence (18.3 hours average parking time), 17.7% to work locations (7.5 hours average parking time) and 8.3% to shopping locations (50 minutes average parking time). Other activities such as leisure activities, visits to the doctor etc., each account for less than 2% of the trips [27], [91].

From these findings, we conclude that the home, workplace, and shopping locations are where most charging events will occur in the future. Therefore, the locations of shopping and work activities are determined in this paper. However, the method is designed to be extensible so that additional activities can be easily integrated.

Since Berlin cannot be considered a closed unit, commuters must be taken into account. The total number of commuters in and outbound is derived from [143], [145], [146]. Vehicle-based mobility profiles are created for inbound commuters analogous to the procedure described in [27] for Berlin; the driving behaviour of inbound commuters is described in [89], [90], [113], [146], [170].
Based on the routing results, the spatial and temporal distribution of BEV charging energy and power demand is determined for four different charging scenarios. The results are then used to investigate the load shifting potential in an exemplary LOR.

4.3.3 Methodology

The goal of the route assignment method is to determine the most likely destination for each vehicle trip. To achieve this goal, all possible destinations must be evaluated and compared. In this paper, the evaluation of each destination is based on four criteria according to the weighted sum model, which is commonly used for multicriteria decision analysis [151]. The basic concept behind the weighted sum model is the additive utility assumption. If all criteria are measurable with the same unit, the best alternative is the one with the largest cumulative value R [151], [152]. The value R of each alternative j can be computed as

$$R_j = \sum_{i=1}^{n} k_i \cdot w_i \quad \text{for } j = 1, 2, \ldots, m \tag{4.13}$$

where n is the number of criteria, k_i is the value for the criterion i and w_i is the individual weighting-coefficient of the criterion i. In general, the higher the value of w_i, the more important the criterion. Typically, the weighting-coefficients are normalized so that their sum is one [151].

As explained in the previous section, the four selected criteria for rating a destination are the distance and travel speed between districts, as well as the car-access attractiveness and the availability of parking spots in the districts. Since these criteria do not have the same unit, a dimensionless rating value k is used for each criterion, ranging from 1 to 10. The derivation of the rating values of the criteria is explained in detail in Section 4.3.3.1 – Section 4.3.3.4. Section 4.3.3.5 then presents the route assignment method. The methodological approach is applied to Berlin and its 448 sub-districts (LORs), in the following sections.

4.3.3.1 Criterion 1: Travel Distance

The mobility profiles of the BEVs are the basis for route assignment. As shown in Figure 4.31, they consist of a sequence of activities at different locations and trips between these activities. For each trip, the travel distance is known. Since the origin district of each trip is also known (as explained in Section 4.3.3.5), all possible destination districts can be determined and rated based on the distance travelled. For this evaluation, we determine the frequency distribution of travel distances for each origin-destination LOR combination (448 LORs yield 200,704 combinations).
The basis for this determination is a self-generated dataset containing 50 randomly distributed

coordinates on roads in the LOR for each LOR (highways, forest roads, etc. are excluded). This dataset is used to calculate the travel distances between the 50 origin coordinates and the 50 destination coordinates for each O-D LOR combination. Thus, a total of 2500 travel distances are determined for each combination. The calculation of the driving distance between two coordinates is done via the freely usable OpenRouteService Time-Distance Matrix API [159].

The 2500 values of each combination form the basis for the evaluation of the travel distances. We assume that the probability of traveling to a destination LOR decreases as the deviation between the travel distance and the median of the 2500 values increases. The median is used instead of the average because it is more robust to outliers.
In order to convert the 2500 values into a dimensionless rating, they are sorted in ascending order and divided into 20 equal-sized data bins, i.e. 125 values are assigned to each bin. Similar to [171], [172], each bin is then assigned a rating value k_d between 1 and 10. A rating value $k_d = 10$ means that it is very likely to travel from the known origin to the destination LOR, and correspondingly very unlikely for $k_d = 1$.

The assignment of rating values to bins is exemplified for one origin LOR and three possible destination LORs in Figure 4.32. The location of the origin LOR and the destination LORs in Berlin is shown in Figure 4.32a. In Figure 4.32b, the division of the calculated driving distances into the 20 bins and the rating value assigned to them is shown.
It can be seen that the further the driving distances are from the distance median, the lower the rating value obtained. For an example travel distance of 9.5 km, it can be determined which of the three destination LORs is the most likely destination (when starting from the origin LOR). It can be seen that destination LOR 1 is not a possible destination, because it cannot be reached from the origin LOR with a travel distance of 9.5 km. The distance median of O-D LOR combination 2 is 8.3 km which is close to 9.5 km. Therefore, the destination LOR 2 receives a medium rating value k_d of 6. For O-D LOR combination 3 the distance median is 13 km. Accordingly, at a distance of 9.5 km, destination LOR 3 receives a low rating value k_d of 2. Therefore, it is more likely to travel to destination LOR 2 than to destination LOR 3, considering the travel distance criterion.

4.3.3.2 Criterion 2: Travel Speed

The travel speed between an origin and a destination is a key criterion in destination choice models [166]–[169]. The basic assumption is that the higher the travel speed between an origin and a destination, the more likely it is to travel to the destination.
Although it would be possible to describe the travel speed for each O-D LOR combination with a mean value, we use frequency distributions to achieve greater accuracy. The basis of these frequency distributions are the 2500 travel distances computed for each O-D LOR combination in Section 4.3.3.1. Using the OpenRouteService Time-Distance Matrix API, it is possible to calculate the associated travel time and thus travel speed for each of the travel distances.

For two origin-destination LOR combinations, the 2500 data tuples obtained are shown as a scatter plot in Figure 4.33a. In particular, for the origin-destination LOR combination 2, it can be seen that higher travel distances lead to higher travel speeds. This is due to the fact that increasing travel distance increases the likelihood of using major roads or highways that allow higher travel speeds.

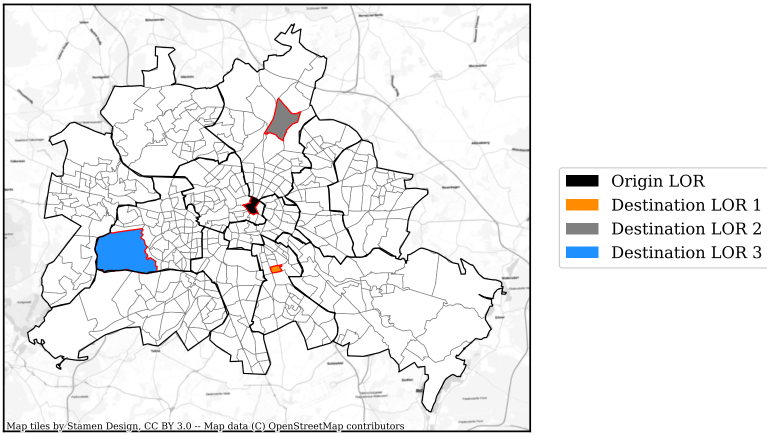

(a) Location of the origin LOR and the three destination LORs in Berlin.

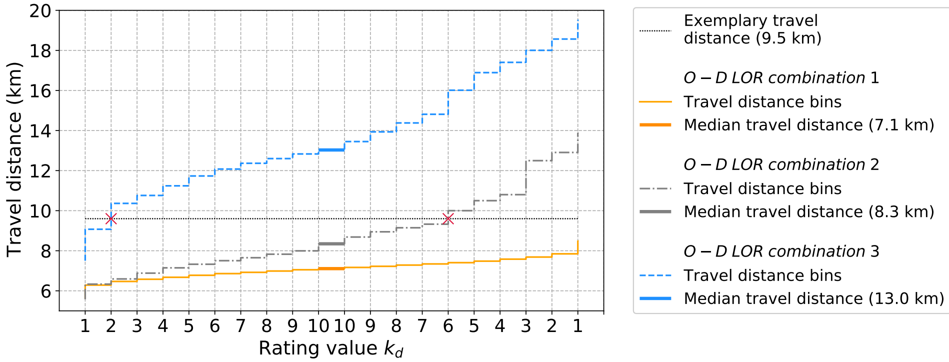

(b) Division of computed travel distances into 20 bins and corresponding rating value k_d.

Figure 4.32: Travel distance criterion.

To reflect this correlation, the evaluation of travel speed between origin and destination must be based on travel distance.
Since different travel speeds occur for the same distance, the average speed of each of the 20 travel distance ranges identified in Section 4.3.3.1 is determined for each O-D LOR combination. This average speed is shown as solid green line in Figure 4.33a.
For the 9.5 km travel distance used as an example in Section 4.3.3.1, the average travel speed for the O-D LOR combination 2 is 28 km/h, as can be seen in Figure 4.33a. To derive a dimensionless rating value for this travel speed, it is compared to the distribution of travel speeds for all of Berlin. To derive this Berlin distribution, the 2500 calculated travel speeds for all origin-destination-LOR combinations are first combined into one dataset and sorted in ascending order. Then, the values are divided into 10 equal-sized data bins, i.e. 10% of the values are assigned to each bin. Similar to [171], [172], a dimensionless rating value k_s is then assigned to each bin. As shown in Figure 4.33b, the 10% lowest speeds in Berlin are assigned a rating value k_s of 1 and the 10% highest are assigned a rating value of 10. This classification means that the higher the travel speed between an origin and a destination, the more likely it is to travel to the destination.

In Figure 4.33b it can be seen that 28 km/h is a rather low speed in Berlin. This results in a low rating value k_s of 2. Therefore, it is unlikely to travel from the origin LOR to destination LOR 2, considering the travel speed criterion.

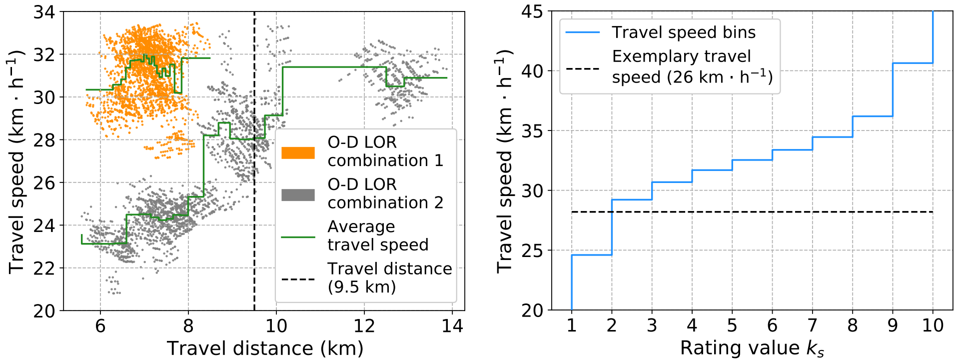

(a) **(b)**

Figure 4.33: Travel speed criterion. (a) Correlation between travel distance and travel speed for 2 origin-destination LOR combinations. (b) Division of the calculated travel speeds in Berlin into 10 bins and corresponding rating value k_s.

4.3.3.3 Criterion 3: Car-access Attractiveness

The attractiveness of locations is another key factor in destination choice models [129]–[131]. The higher the attractiveness of a location, the higher is the probability for trips to that location. In this paper we use an attractiveness description of locations, specifically developed for access by car. This car-access attractiveness provides information on how attractive it is to drive to a particular LOR to perform a particular activity. The determination of the car-access attractiveness of Berlin's LORs is described in detail in [28].

In [28] car-access attractiveness is first determined for shopping and work trips at the building level, and the results are then aggregated at the LOR level. For shopping trips, the car-access attractiveness is based on three criteria: the number of customer parking spots per sales area of the building, the distance of the parking spaces to the building, and whether there is a charge for using the parking spaces. For work trips, the car-access attractiveness is determined based on the number of employee parking spots per employee of the building, the distance of the parking spaces to the building, and the average distance of the building to the nearest public transportation stop.

Car-access attractiveness is described in [28] with a dimensionless value between 1-5, where a value of 5 indicates high attractiveness. In this paper, the scale is adjusted to the other rating values by multiplying by 2. The result is a rating value k_a between 1 and 10 for each LOR, which describes its car-access attractiveness.

4.3.3.4 Criterion 4: Availability of Parking Spots

A rating value k_c is determined to evaluate the parking availability in the LORs. Its values vary from 1 (if less than 10% of parking spots are available) to 10 (if at least 90% of the parking spots are available). The total number of customer and employee parking spots

per LOR, available for shopping or work activities, is determined along with car-access attractiveness in [28] using OpenStreetMap geodata.
In [28], roadside parking spots that are not labelled in the OpenStreetMap dataset are not considered. To determine the additional number of roadside parking spots available for shopping and work trips, we first determine the total number of roadside parking spots for each LOR, analogous to the method described in [173].
Then, roadside parking spots that are permanently occupied by commercial or private vehicles are excluded. In the city of Berlin, 40% of the population has access to private parking (e.g. garages), while the remaining 60% park their cars on roadside parking spots when they are at home [90]. 63% of commercial vehicles are parked at roadside parking spots [90]. As a result, especially in densely populated LORs, many roadside parking spots are occupied at night and in the morning and become vacant when vehicles leave. Consistent with [28] we assume that 50% of vacant roadside parking spots can be used for activities that are not considered in this paper, such as leisure activities or doctor visits. The remaining 50% are equally usable for work and shopping activities.

4.3.3.5 Route Assignment Method

The input data for the route assignment method are the mobility profiles of the Berlin vehicles and the inbound commuter vehicles. While the home locations of the vehicles (i.e., the residences of the vehicle owners) are known, the locations where the other activities are performed are unknown. Therefore, the goal of the route assignment method is to determine the most likely destination LOR for each vehicle trip.
The route assignment method distinguishes between two different types of mobility profiles, depending on whether the first trip starts at the residence of the BEV's owner. For those BEVs whose first trip begins at home, an iterative process is performed, as shown in Figure 4.34. For BEVs that do not start at home, the route assignment is described at the end of this section.

In Step (1), all possible routes are determined for each vehicle. The determination is based on the individual travel distances of the trips and the minimum and maximum travel distances of the O-D LOR combinations (determined in Section 4.3.3.1).
The selection of the most plausible route is time-driven, i.e., routes are determined trip by trip rather than vehicle by vehicle. This means that destinations are assigned chronologically based on the starting time of each trip for each vehicle. This approach allows considering the availability of parking spots as a time-dependent parameter.

When the first trip of a vehicle starts and is to be assigned to a destination LOR, it is first checked for each possible destination whether its maximum BEV intake capacity has already been reached. The maximum intake capacity of a LOR for work activities is 85% of its number of employees. The number of employees per LOR was derived in [28]. 85% is derived from the ratio of full-time and part-time employees according to [174], [175].
The maximum BEV intake capacity per LOR for shopping activities is 10% of its sales area. This number is derived from [28], where it was shown that the average Berlin supermarket provides one parking spot per 10 m^2 of sales area.
The LORs to which a vehicle can be assigned are then rated according to Equation 4.14 in step (2). For shopping and work trips, the evaluation of the single destination LOR R_{LOR} is based on the four criteria introduced in Section 4.3.3.1 – Section 4.3.3.4.

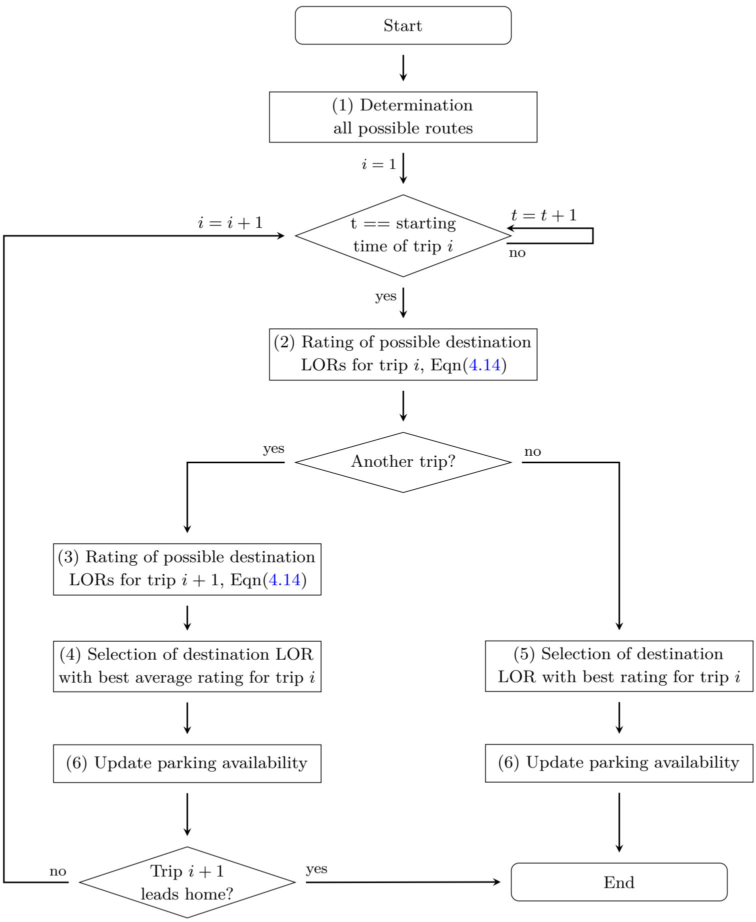

Figure 4.34: Route assignment method.

As we explained in Section 4.3.2, this paper analyzes the spatial and temporal BEV charging energy demand considering home and workplace charging, as well as opportunity charging at shopping locations. For all other activities, vehicle charging is not considered. Therefore, a reduced version of Equation 4.14 is used to rate a destination LOR for "other" activities. However, this reduced version still ensures that a plausible destination LOR is determined for the trip.

$$
\begin{aligned}
\text{Work or shopping trips:} \quad & R_{LOR} = k_d \cdot w_d + k_s \cdot w_s + k_a \cdot w_a + k_c \cdot w_c \\
& \text{with} \ \sum (w_d, w_s, w_a, w_c) = 1 \\
\text{Home or other trips:} \quad & R_{LOR} = k_d \cdot w_d + k_s \cdot w_s \\
& \text{with} \ \sum (w_d, w_s) = 1
\end{aligned}
\tag{4.14}
$$

Following the rating of all possible destination LORs for the first trip, the route assignment procedure continues depending on whether another trip takes place. If no further trip takes place, the destination LOR with the highest rating according to Equation 4.14 is selected (Step (5) in Figure 4.34). Since a parking spot in the selected LOR is now occupied, the criterion "availability of parking spots" for this LOR is updated considering the parking time of the vehicle (Step (6) in Figure 4.34).

If another trip takes place, it is also considered when determining the destination LOR for the first trip. The necessity of this consideration is illustrated in Figure 4.35a for two destinations D1 and D2. It can be seen, that both destinations can be reached with the first trip. The rating of destination D2, $R_{LOR} = 9.2$, is significantly higher than the rating of destination D1, $R_{LOR} = 4.4$. However, the subsequent possible trips from D2 to destination D4 or D5 are very unlikely, as indicated by the very low ratings R_{LOR} of 1.2 and 1.6, respectively.

Therefore, to avoid selecting a destination for the first trip that is an unsuitable origin for the second trip, the ratings of the possible second trips are also taken into account. For this purpose, first their average rating (Step (3)) is calculated as 1.4. Then, in Step (4), the average rating of the first and second trip $R_{LOR,\,a}$ is determined according to Equation 4.15.

$$R_{LOR,\,a} = \frac{R_{LOR,\,i} + R_{LOR,\,i+1}}{2} \tag{4.15}$$

In Equation 4.15, $R_{LOR,\,i}$ is the rating of the destination LOR for trip i, while $R_{LOR,\,i+1}$ is the average rating of the destination LORs for subsequent trip $i+1$. As can be seen in Figure 4.35b, the average rating $R_{LOR,\,a}$ for destination D2 is 5.3. For destination D1, $R_{LOR,\,a} = 5.7$. Consequently, destination D1 is selected as the destination of the first trip. After this selection, in Step (6), the criterion "availability of parking spots" is updated for the selected LOR, taking into account the parking time of the car. Since the second trip does not lead home, the route assignment procedure starts again and the destination of the second trip is determined.

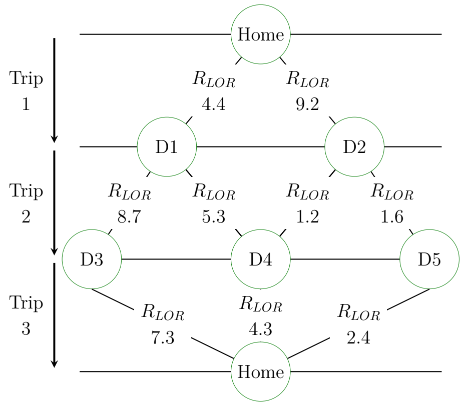

(a) Rating of the possible destinations

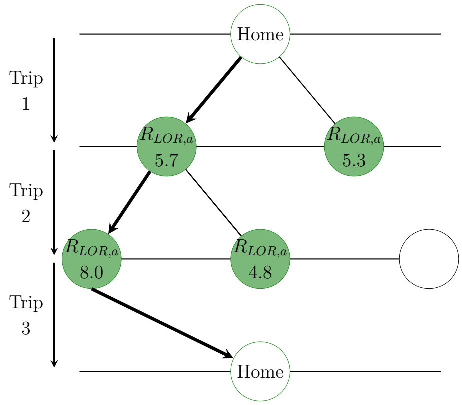

(b) Selection of the most probable route

Figure 4.35: Route assignment procedure for an example vehicle.

For vehicles whose starting location of the first trip is unknown, the described route assignment procedure cannot be performed because it requires a known starting location. Therefore, the starting location must first be determined. For this purpose, all possible routes of the vehicle are first determined. This is possible because it is known that the last trip of the vehicle ends at the home location. If the first trip is to be assigned to a destination LOR, the possible destination LORs for all possible origin LORs are rated analogously to Step (2). If the vehicle makes a second trip, the possible destination LORs for the second trip are also rated (Step (3)). Then, the origin-destination LOR combination with the highest rating is selected, which means that both the destination LOR and the origin LOR are determined for the first trip of the vehicle. Since the starting location of the vehicle's first trip is now known, the route assignment procedure described in Figure 4.34 can be applied starting from Step (6).

4.3.4 Investigated Charging Scenarios

In Berlin 41.5% of the trips lead to the BEV owner's residence (18.3 hours average parking time), 17.7% to work locations (7.5 hours average parking time) and 8.3% to shopping locations (50 minutes average parking time). Other activities such as leisure activities, visits to the doctor etc., each account for less than 2% of the trips [27], [91]. From these findings, we conclude that the home, workplace, and shopping locations are where most charging events will occur in the future and which are therefore considered in the charging scenarios. For these locations four different types of parking spots are considered (see Section 4.3.3.3 and Section 4.3.3.4):

1. Employee parking spots, used for parking while at work;
2. Customer parking spots, used for parking while shopping;
3. Private parking at the residences, used for parking while at home;
4. Roadside parking spots, that can be used for parking while at work and shopping and by BEV owners who do not have a private parking spot at their residence.

In this paper, four different charging scenarios are investigated. Three base charging scenarios which are described in Section 4.3.4.1 and one data-driven charging scenario which is described in Section 4.3.4.2.

4.3.4.1 Base Charging Scenarios

- Home-charging scenario.
  The state of charge (SOC) of each BEV is 100% before its first trip. Each BEV starts charging immediately upon arrival at home and does not end until the vehicle is fully charged or starts driving again.
  As some inbound commuters drive long distances, these vehicles cannot travel their daily distance without recharging. Therefore, these vehicles are charged at the commuter's workplace.
- Work-charging scenario.
  The SOC of each BEV is 100% before its first trip. Each BEV starts charging immediately upon arrival at its place of work and at home and does not end until the vehicle is fully charged or starts driving again.

Many vehicles are not used for a trip to work on the simulated day. In order not to neglect the energy demand of these vehicles and to allow a comparison between the home-charging and work-charging scenario, the vehicles can also be charged at home.

- Opportunity-charging at shopping locations.
  The SOC of each BEV is 100% before its first trip. Charging starts immediately upon arrival at a shopping location and at home and does not end until the vehicle is fully charged or starts driving again. As justified above, home charging is required for comparison with the other scenarios. Analogous to the Home-charging scenario, the vehicles of commuters who travel long distances are recharged at workplaces.

The maximum available charging power is set to 11 kW for private parking and roadside parking spots in accordance with [176]. For charging at employee parking spots, the maximum power is limited to 22 kW in accordance with real world applications [177], [178]. For customer parking spots, the maximum power is limited to 50 kW which is in accordance with real world applications as well [179]–[181].
The three charging scenarios presented should be understood as extreme cases. Setting the SOC to 100% before the first trip is necessary to ensure comparability between the scenarios. The maximum charging power that BEVs can use is SOC-dependent. BEVs can usually retrieve the highest charging power at a SOC between 20% and 80%. At a higher SOC, the usable charging power decreases significantly, resulting in longer charging times.
In Berlin, the average daily distance of private passenger cars is 59.5 km (parked vehicles excluded) [27]. Consequently, the SOC of the vehicles usually ranges between 80% - 100% if the above charging scenarios are applied. In order not to massively overestimate the charging times, we assume for the base charging scenarios that 95% of the maximum charging power can be retrieved constantly by the BEVs regardless of their SOC. The reduction factor of 95% is taken from [176].

4.3.4.2 Data-driven Charging Scenario

The spatial and temporal distribution of BEV charging demand resulting from the three base-charging scenarios can be used for extreme value analyses. The actual future charging behavior and thus the future distribution of BEV charging demand is unknown.
One way to model the future charging behavior is to assume that the future charging behavior corresponds to the current BEV charging behavior. Since no BEV charging data is available for Berlin, we use charging data from 41 private BEVs in Beijing, China. The data and its analysis are described in [182]. For the development of the data-driven charging scenario, the authors of this paper were provided with the raw data set. The data from Beijing are used because the driving behavior of the 41 BEVs and the driving behavior of the BEVs in Berlin are very similar. In Beijing, for example, 80% of vehicle trips are shorter than 21 km, compared to 81.1% of vehicle trips in Berlin. In addition, the average daily distance of non-parked vehicles is similar. In Berlin, this distance is 53.2 km while it is 49.8 km in Beijing. Furthermore, in Beijing 85.2% of the total daily distances are below 80 km, while 82.3% are computed for Berlin in [27]. It is important to note that charging behavior depends not only on driving behavior, but also on the available charging infrastructure (number, locations, charging power). It is unclear whether the charging infrastructure available to the 41 BEVs in Beijing is comparable to that in Berlin. To reduce the resulting uncertainty, charging behavior is not modeled by predetermined statements (e.g., 80% of charging events

occurs at home with 11 kW), but by two driving behavior-based probability distributions derived from the dataset. These distributions are depicted in Figure 4.36. Figure 4.36a shows the relative frequency distribution of SOC at the first trip of the day of Beijing BEVs. The Beijing dataset reveals, that vehicles that use a greater share of their battery capacity over the course of a day (i.e., tend to drive longer distances), have a higher SOC before their first trip of the day. To map this, one distribution is determined for vehicles that use more than 50% of their battery capacity during the day. The other for vehicles that consume less than 50% of their battery capacity during the day. For both cases it can be seen that it is most likely to start the first trip of the day with a SOC of 100%. Figure 4.36b shows the charging probability of Beijing BEVs for different rechargeable SOC differences. The rechargeable SOC difference describes the difference between an initial SOC and an end SOC up to which charging is possible during parking time. A SOC of 10% before charging and a rechargeable SOC difference of 60% would for example result in a SOC of 70% after charging. As can be seen in Figure 4.36b, 78% of BEV users charge their vehicle when the rechargeable SOC difference is 60%.

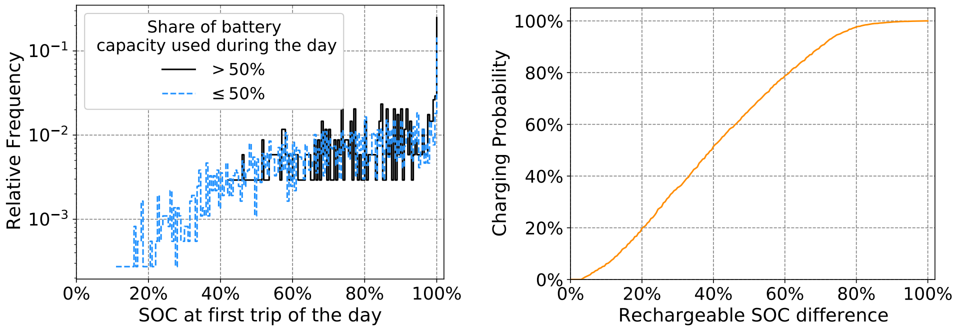

(a) SOC at the first trip of the day **(b)** Rechargeable SOC difference at charging event

Figure 4.36: Data-driven charging scenario. Charging behaviour of the BEVs, according to Beijing dataset [182].

Based on these two probability distributions, the data-driven charging scenario is developed, which is shown schematically in Figure 4.37. It is applied to each BEV individually.
In Step (1) the share of battery capacity used over the course of a day is determined. In Step (2), depending on this result, the SOC before the first trip is determined using Figure 4.36a. In Step (3) the energy consumption of the next trip is calculated. If the SOC, determined in Step (2) is not sufficient to complete the next trip, Step (2) is executed again. If the SOC is sufficient, it is examined whether charging is possible at the destination of the trip. As justified in the introduction of this section, this paper only considers charging at home, at work, and while shopping. If the vehicle travels to another destination, it is not charged. If the BEV can be charged at the destination, the rechargeable SOC difference is calculated in Step (4) based on the parking time of the vehicle. Besides the parking time, the rechargeable SOC difference depends on the available charging power at the charging station and the charging curve of the BEV. The SOC-dependent charging power of the reference vehicles is described by charging curves, which are shown in the Appendix (Figure 4.43). The charging curves were determined by experimental measurement [65], [183]. Consistent with the other charging scenarios the maximum available charging power is set to 11 kW for private parking

and roadside parking spots, to 22 kW at employee parking spots and to 50 kW at customer parking spots.
In Step (5), the rechargeable SOC difference is used to determine whether the vehicle is recharged according to the probability distribution shown in Figure 4.36b. If the vehicle makes another trip, Step (3) is executed again.

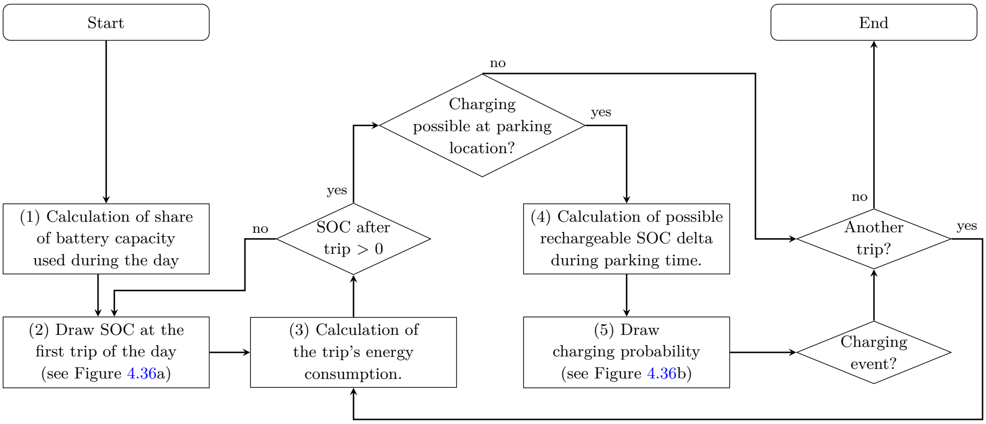

Figure 4.37: Data-driven charging scenario. Method for determining the charging behaviour of a BEV.

4.3.5 Results and Discussion

By applying the route assignment method to all vehicles, a route can be determined for each BEV. Thus, it is known which districts the BEVs travel to for their trips, as well as the parking times of the vehicles in the districts. This, in turn, enables the prediction of spatial and temporal BEV charging demand through the application of charging scenarios.
In this section, this demand is computed for the city of Berlin. For all results presented below, an identical weighting of the rating criteria is used, i.e. $w_d = w_s = w_a = w_c = 0.25$. In terms of destination choice, this means that all criteria are considered equally important.

This section is organized as follows: the total BEV charging energy demand for Berlin is discussed in Section 4.3.5.1. We present the spatial and temporal distribution of the charging energy demand in the Berlin LORs in Section 4.3.5.2 and Section 4.3.5.3, respectively. These results are the basis for intelligent load shifting methods. Therefore, in Section 4.3.5.4, we demonstrate for an example LOR how load shifting can reduce the grid impact of BEVs. Finally, the results are discussed in Section 4.3.5.5.

4.3.5.1 BEV Charging Energy Demand in Berlin

In Table 4.15, the total BEV charging energy demand for an average working day (Monday-Thursday) in Berlin is listed for each charging scenario. Energy demand is lowest for the home charging scenario at 5468 MWh. This is because most inbound commuters do not charge in Berlin.
In the work-charging scenario, 72.9% of the BEVs' total energy demand is charged at residences. This high share compared to workplaces is due to the fact that (i) not all BEVs travel to work and are therefore still charged at their owner's residence, and (ii) vehicles that

charged at work also charge each time they arrive home. The higher total demand compared to the home charging scenario is due to inbound commuters charging at their workplaces. Similar results are observed for the opportunity-charging scenario. 90.1% of the total energy demand is charged at the residences. The higher percentage compared to the work-charging scenario can be explained by the lower number of vehicles going shopping and by the fact that shopping stops are usually short and therefore the amount of energy that can be charged is limited. The higher total energy demand compared to the home-charging scenario is due to commuters shopping in Berlin.

Table 4.15: BEV charging energy demand results for an average workday in Berlin by charging scenario.

Charging scenario	BEV energy demand (MWh) at			
	Residences	Places of work	Shopping locations	Total
Home	5435.1	32.5	-	5467.6
Work	4405.1	1629.7	-	6034.8
Opportunity	5066.6	23.3	530.3	5620.2
Data-driven	3765.9	2044.8	281.8	6092.5

The highest total energy demand results from the data-driven charging scenario. It is found that the energy demand at the places of work is 25.5% higher compared to the work-charging scenario. This is due to the fact that vehicles in this scenario do not start their first trip with a SOC of 100%. Especially for BEVs that only drive to work and back to the owner's home and do not perform any other activities, this leads to a high charging demand at the workplaces. In contrast, the energy demand at shopping locations is 46.9% lower compared to the opportunity-charging scenario. This is because the amount of energy that can be charged during the stops is limited due to the short parking times. As a result, many vehicles do not to charge. In the data-driven charging scenario, 61.8% of the total charging energy demand is charged at the residences.

4.3.5.2 Spatial Distribution of the Charging Energy Demand

In Figure 4.38 the spatial distribution of the BEV charging energy demand in the Berlin LORs is shown for the data-driven charging scenario on an average working day. Separate figures are shown for the total energy demand as well as for the share of total energy demand charged at residences, workplaces, and shopping locations.

For the spatial distribution of energy demand at workplaces, the demand is relatively similar in the inner-city and outer-city LORs. This is because there are more employees in the inner-city LORs than in the outer-city LORs, but a higher proportion of employees in the outer-city LORs drive to work because of lacking public transportation and good parking possibilities (see Figure 13 in [28]). The highest energy demand at workplaces can be observed for the LOR “Motardstraße” in western Berlin. This is due to (i) the high number of employees, (ii) the high parking ratio per capita and (iii) the proximity to a highway. As a result, the car-access attractiveness and accessibility of this LOR is very high.
Except for two LORs, the spatial distribution of energy demand at shopping locations in Berlin is also relatively homogeneous. These exceptions are the LOR “Alexanderplatz” in the

center of Berlin and the LOR “Alt Tegel” in the northwest. Both districts have a significantly higher energy demand than the other LORs. The LOR “Alexanderplatz” has the largest sales area of all LORs. Several parking garages allow parking there. However, the fact that many vehicles are assigned to it in the routing process is mainly due to its central location and the very good connection via several federal highways. The LOR can therefore be reached easily and quickly from anywhere. The high demand in the LOR “Alt Tegel”, on the other hand, can be explained by the fact that the surrounding LORs have hardly any sales area as can be seen in Figure 10 in [28]. Since the LOR “Alt Tegel” is easily accessible by highway access and people tend to shop close to their residences, the LOR attracts people from the surroundings to shop there.

In Figure 4.38c, the spatial distribution of the charging energy demand at the residences in the Berlin LORs can be seen. LORs with high energy demand coincide with LORs with high population density, high motorization rate, and high household income. These results have already been discussed in Section 3.4 in [27]. The spatial distribution of total energy demand is very similar to the distribution of the demand charged at residences. This is due to the fact that 61.8% of total demand is charged at the residences, as shown in Table 4.15. LORs with near zero total charging energy are sparsely populated, as they mostly consist of forests and lakes.

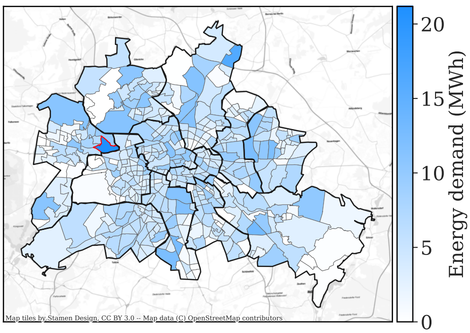

(a) Energy demand at places of work

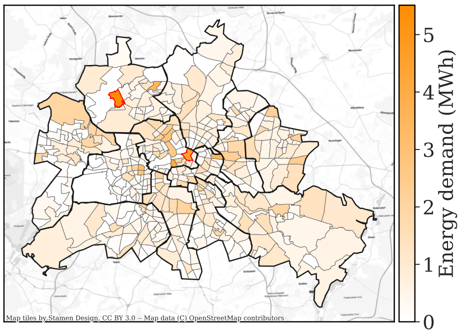

(b) Energy demand at shopping locations

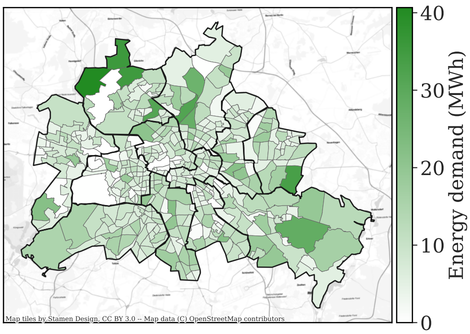

(c) Energy demand at residences

(d) Total energy demand

Figure 4.38: Spatial distribution of the BEV charging energy demand in the Berlin LORs – Data-driven charging scenario.

4.3.5.3 Temporal Distribution of the Charging Power Demand

In Figure 4.39 the temporal distribution of the BEV charging power demand in the Berlin LORs is shown for all charging scenarios on an average working day. For the work- and data-driven charging scenario, it can be seen that the power demand at the workplaces mainly occurs in the morning hours, reaching its maximum around 9:00 AM and decreases thereafter.

The decrease is significantly faster for the work-charging scenario, because all vehicles are charged immediately after arrival at their user's workplace (regardless of their SOC). Since their energy demand is therefore often low, power demand drops sharply due to decrease of arriving BEVs after the start of the work day. In contrast, fewer vehicles are charged in the data-driven charging scenario, but these vehicles have a higher energy demand. Because of this higher demand, the vehicles have a longer charging time, which means that charging power is needed over a longer period of time. The power demand curve becomes wider.

Charging power demand at shopping locations reaches its maximum around 4:30 PM, both for data-driven charging and opportunity-charging scenario. This corresponds approximately to the time when people leave work. As justified in Section 4.3.5.1, the energy demand at the shopping locations is lower for the data-driven charging scenario than for the opportunity-charging scenario, resulting in a lower peak in the power demand.

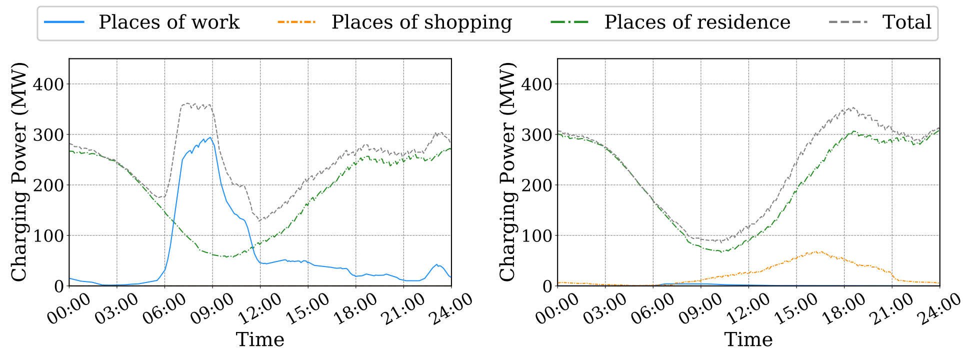

(a) Work-charging scenario **(b)** Opportunity-charging scenario

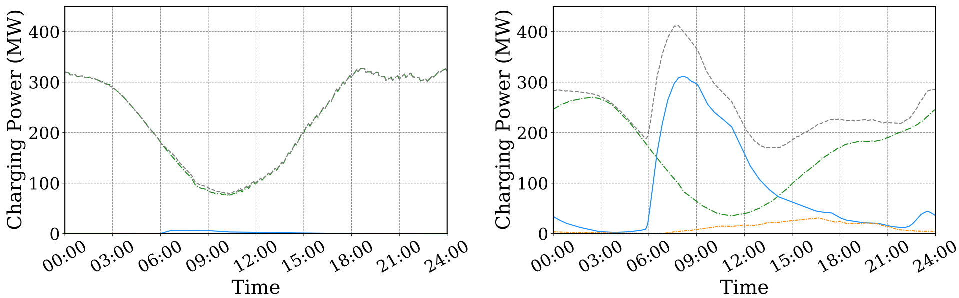

(c) Home-charging scenario **(d)** Data-driven charging scenario

Figure 4.39: Temporal distribution of the BEV charging power demand in Berlin.

The shape of the power demand curves at the residences is similar for all charging scenarios except the data-driven charging scenario and has already been discussed in Section 3.5 in [27]. In contrast to the other scenarios, it can be observed for the data-driven charging scenario that the peak power demand is reached at about 2:00 AM instead of 6:30 PM. This is due to outbound commuters driving long distances to work (>85 km). Due to the longer distances and associated longer travel times, these outbound commuters return to Berlin late in the evening. Since the BEVs have travelled long distances, their rechargeable SOC difference is high and thus the probability that the BEVs will be charged is high as well. In addition, the vehicles in the data-driven charging scenario tend to have a higher energy demand than in the other charging scenarios. Therefore, the transition point where the number of BEVs that start charging is lower than the number of BEVs that finish charging is later.

For the data-driven charging scenario, the spatial distribution of charging power demand over the course of the day is shown in the Appendix (Figure 4.44 to Figure 4.47).

4.3.5.4 Temporal Distribution of the Charging Power Demand with Load Shifting

The parking times of BEVs are usually much longer than their charging times. Therefore, it is possible to shift vehicles' charging times to times when the impact on the electric grid is minimal. These load shifting investigations require knowledge of the parking location and duration of the vehicles as well as their charging requirements, which were determined in this paper.

In Berlin, 45% of private cars are parked all day. The used vehicles are parked on average 18.3 hours per day at the owner's place of residence [27], [91]. Due to these long parking times, it is of particular interest to investigate the load shifting potential at the residences. Therefore, this section investigates how the BEV charging power demand can be shifted (depending on the residential load curve) to reduce the grid impact. For this purpose, a valley-filling method is used which is shown schematically in Figure 4.40. As can be seen, valley-filling is done vehicle by vehicle. The individual vehicle is not charged immediately after its arrival, but at times (within its parking time) when power demand in the considered area is minimal.

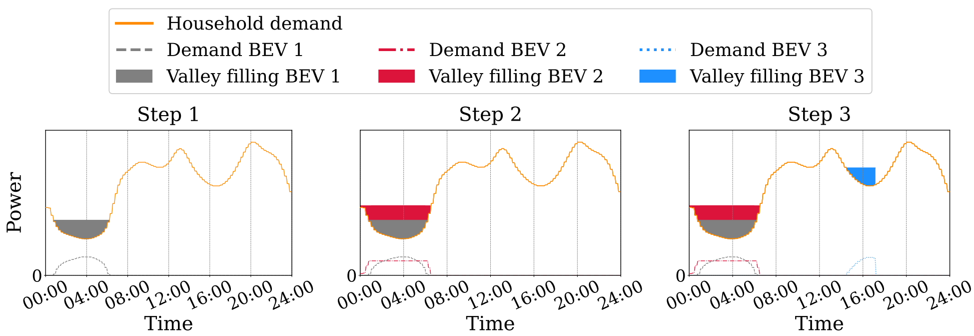

Figure 4.40: Smart charging using valley-filling approach.

The load-shifting investigation is conducted using the LOR “Heiligensee” as example, which is located on the north-western city boundary. It is selected because it has both, the highest BEV energy demand at the residences of all LORs and a very high BEV charging energy demand per resident in Berlin. The determination of the residential power demand for the LOR "Heiligensee" is described in detail in Section 3.5 in [27]. In Figure 4.41 the load shifting results for the home-charging and the data-driven charging scenario is presented. For both charging scenarios, it can be seen that in the case of uncontrolled charging (immediate charging upon arrival with maximum charging power), the BEV charging peak coincides with the residential evening power demand peak. The peak value is lower for the data-driven charging scenario because the total amount of energy charged at the residences is lower (see Table 4.15).

When load shifting is applied, the peak power demand for the home-charging scenario can be reduced by 31.7%. Due to the comparatively low charging times and the high parking times in the home-charging scenario, the BEV power demand can be distributed in such a way that the total demand in the LOR remains constant. Therefore, the peak-to-average power ratio of a LOR, which describes the ratio of peak power demand to average power demand, is 1.0. Compared to residential power demand, the maximum power demand (residential + BEV power demand) increases by 21.5% for controlled charging and by 77.9% for uncontrolled charging. In the data-driven charging scenario, the peak power demand can be reduced by 28.2%. Due to the longer charging times of BEVs compared to the home-charging scenario, the power demand of BEVs cannot be shifted to achieve a peak-to-average power ratio of 1.0. However, the total power demand is nearly constant. The peak-to-average power ratio is 1.055. Compared to residential power demand, the maximum power demand increases by only 6.6% for controlled charging and by 48.4% for uncontrolled charging.

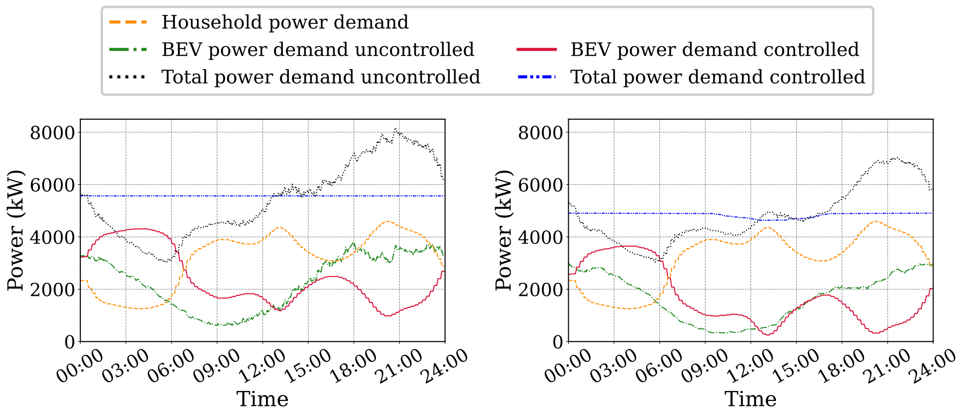

(a) Power demand. Home-charging scenario.

(b) Power demand. Data-driven charging scenario.

Figure 4.41: Load shifting results in the LOR "Heiligensee" for the home- and data-driven charging scenario.

Since the load shifting investigations are conducted for a LOR with one of the highest BEV charging demands per resident, it is expected that peak power demand in most other LORs can also be significantly reduced compared to uncontrolled charging. It should be noted, however, that the results represent a theoretical ideal case and indicate the theoretically possible optimum. In a real application, the driving and parking behavior of all considered vehicles is not exactly known in advance.

4.3.5.5 Discussion

The results show that between 5468 MWh and 6093 MWh of charging energy is required on an average working day in Berlin, depending on the charging scenario. At least 61.8% of this energy is charged at the residences.
Regarding the spatial distribution of energy demand at workplaces, demand is relatively similar in inner-city and outer-city LORs. Demand ranges from 0 kWh per day in LORs with no employees to 21.2 MWh per day in a LOR with many employees, high car-access attractiveness, and good accessibility. Charging energy demand at shopping locations ranges from 0 kWh per day in LORs without shopping facilities to 5.5 MWh per day in LORs that attract many shopping trips due to their location and parking situation. Charging energy demand at residences ranges from 0 kWh per day in uninhabited LORs to 40.7 MWh per day in LORs with high population and motorization levels. High demand is most prevalent in outer-city LORs. The temporal distribution of the charging power demand is highly dependent on the charging scenario. The peak power demand ranges from 328 MW to 412 MW. The minimum power demand is between 78 MW and 169 MW.

In 2021, the peak load in the Berlin power grid was 2119 MW [184]. Assuming that this peak load coincides with the BEV peak power demand of 412 MW, this results in a 19.4% increase in peak power demand. However, there is significant load shifting potential in the LORs. As shown in Sectio 4.3.5.4, the peak power demand at the residences can be reduced by 28.2% through load shifting for the data-driven charging scenario.
Berlin's total electric energy demand in 2021 was 13.9 TWh [184]. In this paper, we calculated a daily charging demand on an average workday (Monday-Thursday) of 5435 MWh for the Berlin BEVs. In [27], a charging demand of 4730 MWh was determined for an average Saturday. Assuming that the energy demand on Fridays and Sundays corresponds to the demand on Saturdays, an annual charging energy demand of 1.87 TWh is derived for Berlin from our results. Comparing this number with Berlin's current total energy demand shows that it increases by 13.5% due to the additional BEV charging demand.

To check the validity of the results, they can be compared with the results of other studies. Due to different assumptions, differences between the results of this dissertation and the comparative studies are to be expected. Therefore, the main focus of the comparison of results is to check whether the results are in the same order of magnitude. A summary of the comparisons is presented in Figure 4.42.

It is estimated, that complete electrification of all 45 million passenger cars in Germany would require 100 TWh of annual energy [185]. Of this, 2.32 TWh would be required for the electrification of vehicles in Berlin. As derived above, our results for Berlin yield an annual charging energy demand of 1.87 TWh. This corresponds to 80.6% of the demand determined in [185] (see Figure 4.42a). The difference is most likely due to the fact that reference [185] uses the average mileage of passenger cars in all of Germany, which is significantly higher than the mileage of passenger cars in Berlin [89], [90].

The author of [186] determines the power demand of BEVs in German urban areas. Analogous to our approach, the German household travel survey provides the data basis for simulating the driving behaviour of the BEVs. The temporal distribution of BEV charging power demand is determined for two charging scenarios assuming a constant charging power of 11 kW.

Scenario 1: all vehicles are charged exclusively at their users' residences. Due to similar assumptions, the results obtained for scenario 1 are comparable to the temporal charging power demand we determined for the residences for the home-charging scenario (see Figure 4.39c). Scenario 2: vehicles are charged at both the residences and the places of work. The results determined for scenario 2 are comparable to the total charging power demand we determined for the work-charging scenario (see Figure 4.39a).
For scenario 1, the peak power demand can be observed at 6:00 PM. Due to the high simultaneity of the charging events, the required charging power starts to decrease sharply from 7:00 PM and is close to 0 kW per vehicle during the night hours. As a result of this high simultaneity, the peak power demand of 0.5 kW per vehicle in the study is slightly higher than the 0.31 kW per vehicle we determined in this paper (see Figure 4.42b). The high simultaneity of the charging events is not discussed in the study. One reason for this could be the simulation condition that forces all BEVs to arrive back at their owners' residences on the same day they left.
For scenario 2, the study identifies a power demand curve that reaches its global maximum around 8:30 AM (0.65 kW per vehicle), then decreases until around 11:00 AM before rising again slightly and reaching a local maximum around 4:00 PM. During the night-time hours, the power demand is again close to 0 kW per vehicle. In contrast, in this paper we show that peak power demand is reached as early as 7:30 AM and then stagnates at this level until 9:00 AM, as BEVs that start charging and those that stop charging balance each other out. Although we assume a charging capacity of 22 kW at employee parking spots, we determine a lower maximum power demand per vehicle of 0.32 kW. This discrepancy is most likely also due to the high simultaneity of the charging events in the study as well.

In [187], the energy demand resulting from the electrification of passenger cars in Stuttgart, Germany and its surrounding areas is determined. Analogous to our approach, the driving behaviour of BEVs is modeled based on a travel survey. In the study, vehicles are charged as soon as their SOC value is below 50%. Charging power at private parking spots at residential buildings is assumed to be 3.7 kW and 50 kW at all other locations (roadside, workplaces, etc.). Due to similar assumptions, the results of the study can be compared to the total charging power demand we determined for the data-driven charging scenario. This comparison shows similar results for the daytime. The power demand peak is observed around 9:00 AM, which is mainly due to charging at the places of work. After this peak, power demand decreases before increasing again in the evening hours due to charging at residences. However, in contrast to our results the study identifies a power demand of nearly 0 kW per vehicle between 4:00 and 5:00 AM. This low power demand in the night is not discussed. One possible reason for this could be the simulation condition that forces all BEVs to arrive back at their owners' residences on the same day they left. Another reason could be that the charging events are terminated more quickly since the study assumes a charging power of 50 kW at roadside parking spots.
In addition, differences in peak power demand can be observed. While the peak power demand calculated in this paper is 0.37 kW per vehicle, it is 0.54 kW per vehicle in the study (see Figure 4.42c). This higher demand is most likely due to the higher car usage in Stuttgart (58% of all trips) [188] compared to Berlin (34%) [90]. As a result, peak power demand is higher. A higher peak power demand per vehicle also results from the fact that the study assumes a charging power of 50 kW, which is higher than in our work (22 kW at employee parking spots and 11 kW at roadside parking spots).

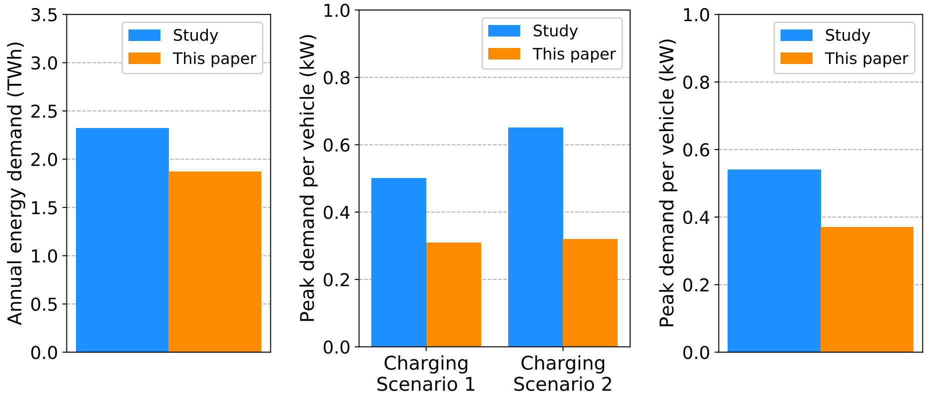

(a) Study [185] **(b)** Study [186] **(c)** Study [187]

Figure 4.42: Comparison of the results of this paper with the results of studies [185]–[187].

Reference [189] presents the results of an experimental study on BEV usage behaviour of 10 households and their 11 BEVs, conducted in Stuttgart, Germany. The BEVs in the study were charged exclusively at residences; accordingly, the results are comparable to the residential charging power demand we determined for the home-charging scenario. The temporal distribution of charging power demand in the study is similar to our results, showing highest demand at 9:00 PM and lowest demand at 9:00 AM. In the study, the minimum power demand is 43% of the peak power demand. This is higher than our results, where the minimum demand is 22.8% of the peak demand. The difference is most likely due to the overrepresentation of pensioners among the study participants. In particular, pensioners do not have the "typical" daily routine of going to work in the morning and returning in the evening. As a result, charging events are much more evenly distributed throughout the day.

Overall, it can be stated that our results show some deviations from the existing literature, but are in overall agreement with it. The deviations can be plausibly justified by methodological differences and deviating parameters. Therefore, the results of this paper can be considered valid.

4.3.6 Conclusions and Outlook

To support power grid planners in detecting and evaluating potential power grid congestions due to the electrification of urban private cars, accurate models are needed to determine BEV charging energy and power demand with high spatial and temporal resolution.
Typically, activity-based mobility models are used for this purpose, with detailed travel surveys forming the data basis. From these surveys, activity- and time-dependent traffic flows between sub-areas in the considered area can be directly determined, which in turn can be used to derive BEV charging demand. However, detailed travel surveys are typically not available for most places in the world.

To address this research gap, we developed an activity-based model for estimating the spatial and temporal distribution of BEV charging demand that does not require detailed travel surveys as input parameters. The method is based on individual, full-day travel schedules for each vehicle in the considered area, which provide information on the sequence of activities and trips between these activities [27]. Since the locations where activities are performed are not included in these travel schedules, we developed a route assignment method in this paper to determine the unknown activity locations.

We applied our approach to the urban area of Berlin and its 448 sub-districts. Assuming full electrification of the 1,045,000 private cars in Berlin, we determined both the required BEV charging energy demand and the power demand over the course of the day for each district. Since the developed method operates at the vehicle level, it can also be used to determine BEV charging energy demand for lower levels of electrification (e.g. 50%).
The method is based on open data (e.g. OpenStreetMap and publicly available statistics), therefore it is transferable to other urban regions.

On the basis of our results, load shifting potentials can be investigated. Compared to uncontrolled charging, we show for an exemplary district that it is theoretically possible to reduce peak power demand at residences by up to 31.7% through load shifting. In addition, we show that the peak-to-average power ratio can be significantly reduced. Since load shifting is often easier and cheaper to implement (e.g., via price incentives) than grid expansion, grid expansion should only take place if no further load shifting potential exists. In addition to load shifting, the results of this paper can also be used to investigate vehicle-to-grid potential in an urban area, which will be part of future work.

In Germany, only 0.64% of passenger cars were battery electric at the end of 2021 [190]. Accordingly, there is no data on the charging behavior of BEV users in Germany or Berlin. BEV charging demand was therefore determined for four different charging scenarios in this paper. As soon as data on charging behavior in Germany is available, the BEV charging demand for Berlin should be recalculated and compared with the results of the four scenarios. We have validated our results by comparing them with similar studies. However, since the results are forecasts, it is desirable to compare them with exhaustive data. This requires extensive measurement campaigns in which both the routes and the charging behaviour of BEVs are recorded.

4.3.7 Author Contributions

Florian Straub: Conceptualization, Supervision, Writing - Original Draft.
Florian Straub, Otto Maier: Methodology, Investigation, Visualization.
Florian Straub, Dietmar Göhlich, Yuan Zou: Writing - Review & Editing.
Dietmar Göhlich: Resources, Project administration, Funding acquisition.
Yuan Zou: Provision of data for development of data-driven charging scenario.

4.3.8 Appendix A. Electric Reference Vehicles and Charging Curves

Table 4.16: Electric reference vehicles.

Class	Model	Battery Capacity (kWh)	Consumption (kWh/100km)	
			Inner City	Outer City
Mini compact	Mitsubishi i-MiEV [191]	16.2	11.4	18.0
	Renault Zoe [102]	64.3	14.5	19.0
	VW e-Up! [103]	18.7	14.0	17.7
Compact	BMW i3 [104]	48.8	13.0	17.9
	Hyundai Kona E [105]	73.9	14.0	19.5
	VW e-Golf [192]	34.9	12.7	17.3
Medium	Kia e-Niro [107]	72.3	12.5	18.1
	Nissan Leaf [108]	68.4	17.2	22.7
	Tesla Model 3 [193]	60.0	17.4	19.5
Large	Audi e-tron [110]	94.3	23.5	25.8
	Mercedes EQC [111]	93.1	23.0	27.6
	Tesla Model S [194]	93.6	21.7	24.0

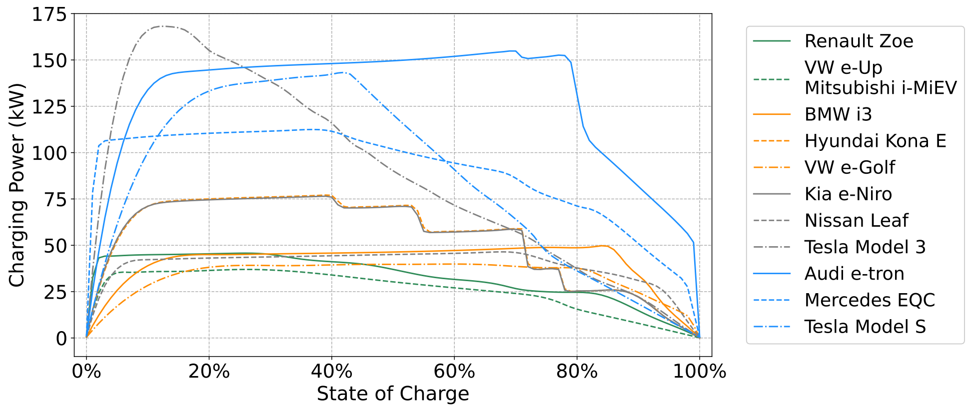

Figure 4.43: Charging curves of the reference vehicles [65], [183].

4.3.9 Appendix B. Spatial Temporal Distribution of Charging Power Demand in the Berlin LORs

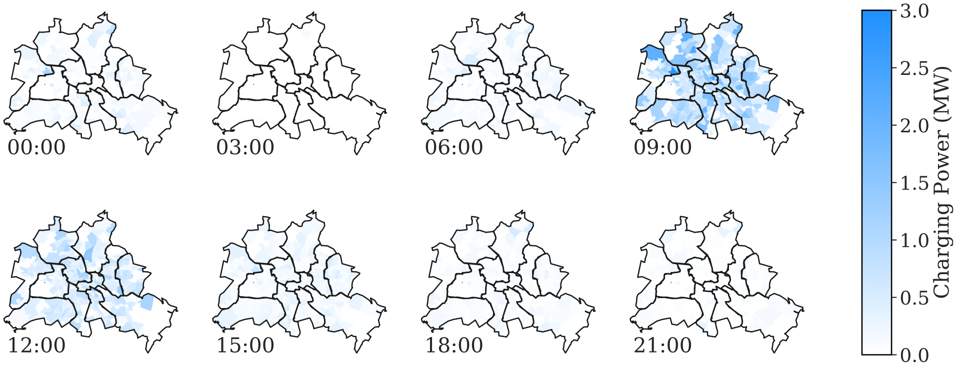

Figure 4.44: Spatial temporal distribution of charging power demand at workplaces in the Berlin LORs – Data-driven charging scenario.

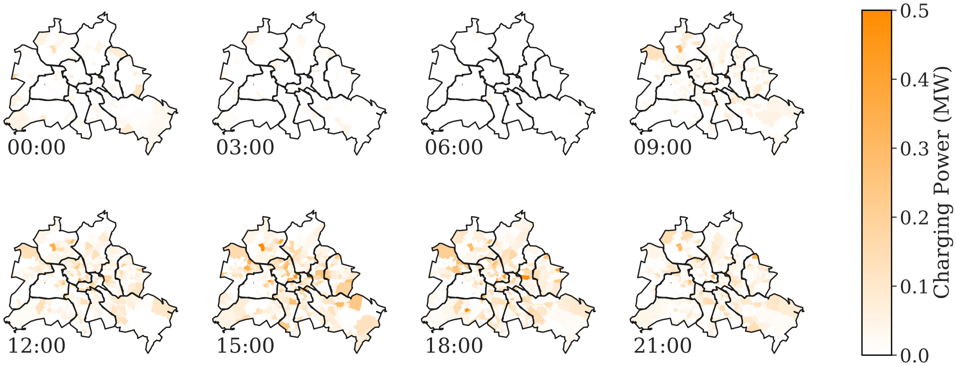

Figure 4.45: Spatial temporal distribution of charging power demand at shopping locations in the Berlin LORs – Data-driven charging scenario.

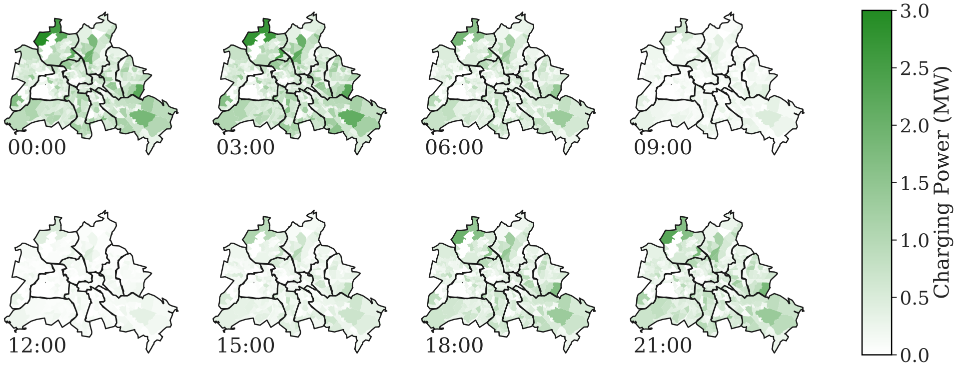

Figure 4.46: Spatial temporal distribution of charging power demand at residences in the Berlin LORs – Data-driven charging scenario.

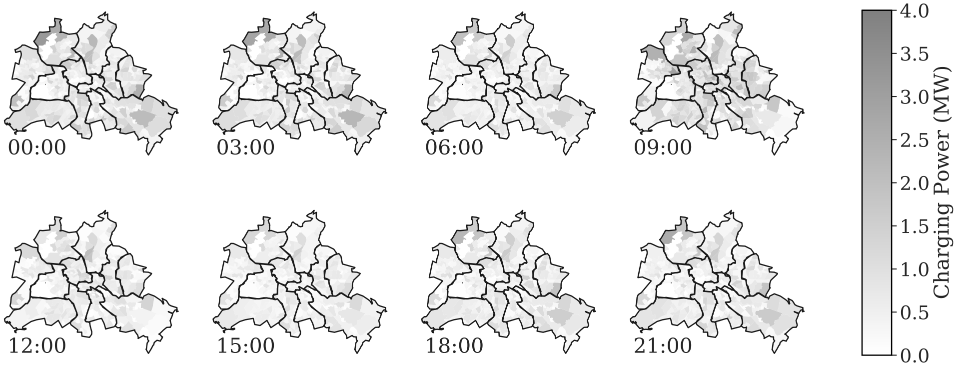

Figure 4.47: Spatial temporal distribution of the total charging power demand in the Berlin LORs – Data-driven charging scenario.

5 Further Research

In this chapter, research is conducted based on the results of the methodology developed in Chapter 4. Section 5.1 examines the Vehicle to grid (V2G) potential of fully electrified passenger cars. Section 5.2 determines the charging infrastructure demand to meet BEV charging demand.

5.1 Publication IV

Sector Coupling through Vehicle to Grid: A Case Study for Electric Vehicles and Households in Berlin, Germany

Florian Straub[1], Otto Maier[1], Dietmar Göhlich[1], Kai Strunz[2]

[1]Chair of Methods for Product Development and Mechatronics, Technische Universität Berlin, Strasse des 17.Juni 135, 10623 Berlin, Germany

[2]Chair of Sustainable Electric Networks and Sources of Energy, Technische Universiät Berlin, Einsteinufer 11, 10587 Berlin, Germany

(This article has been published on 22 March 2023 by MDPI in "World Electric Vehicle Journal", available online: https://doi.org/10.3390/wevj14030077)

Abstract: A key factor in limiting global warming is the conversion of conventional electricity generation to renewable energy sources. However, a major obstacle is that renewable energy generation and energy demand often do not coincide in time, and energy must therefore be stored temporarily. Vehicle to grid (V2G) can be used to store excess renewable energy in battery electric vehicles (BEVs) and feed it back into the electric grid when needed. For effective V2G operation, the grid may have to be expanded, as the energy needs to be transported to BEVs. However, the grid should only be strengthened where renewable energy demand exceeds current grid capacity due to high grid expansion costs. This requires a method that determines the spatial distribution of V2G potential at a high resolution. Since such a method has not yet been reported in the existing literature, and so is developed in this paper. The method is demonstrated for the city of Berlin and its 448 sub-districts. For each sub-district, the method allows determining the percentage of residential and BEV energy demand that can be met by renewables if V2G is deployed, and answers the question of whether a full renewable supply is possible. The results show that BEVs can be effectively used as intermediate storage for renewable energy. If 30% of the BEVs participate in V2G, more than 99% of the energy demand of households and BEVs in Berlin can be covered by renewables on certain days. On the other hand, V2G deployment increases the average peak load in the districts by up to 100% and results in a nearly double load on vehicle batteries. High shares of renewable energy can be observed in districts with a high degree of motorization, which are predominantly found in the outskirts of the city.

Keywords: electric vehicle; renewable energy; vehicle to grid; sector coupling; spatial resolution

5.1.1 Introduction

The worldwide reduction in greenhouse gas emissions is the main factor limiting the global temperature increase to 2 °C above pre-industrial levels, as agreed in the 2015 Paris Agreement [1]. To meet this goal, the European Commission has agreed on the “European Green Deal” which stipulates net zero greenhouse gas emissions for the entire European Union by 2050 [2]. In accordance with these guidelines, Germany plans to reduce greenhouse gas emissions by 50% by 2030 with respect to 1990 [80].
The decarbonization of the transport sector is one of the most important levers to achieve this result. Therefore, private vehicles with internal combustion engines (ICEVs) are increasingly being replaced worldwide by vehicles with decarbonized drive systems, especially battery electric vehicles (BEVs) [12]. According to the German Federal Motor Transport Authority (KBA), around 356,000 BEVs were registered in Germany in 2021, 5.6 times as many as in 2019 [19].
In addition to decarbonizing the transportation sector, replacing electricity generation by fossil fuels with renewable energy sources such as solar and wind energy is an important component to reduce emissions. Tröndle et al. [195] have shown that all European countries can cover their entire energy consumption with renewable energies if their infrastructure is expanded accordingly. However, a major limitation of renewable energies is their volatile generation. Power generation and demand do not always coincide in time [196]–[198]. To reduce this discrepancy, load shifting strategies can be employed to charge BEVs whenever a surplus of energy is available [196], [197], [199]–[201].

Load shifting cannot be fully exploited in times when the demand exceeds the power generation. This problem can be addressed by coupling the energy and transportation sectors through Vehicle to grid (V2G). Sector coupling is the connection, interaction and joint optimisation of energy sectors. The aim is to consider all sectors (e.g., electricity, transport and industry) holistically and to create synergy effects instead of developing solutions tailored to individual sectors [202]–[204].
One possibility for sector coupling is V2G, in which surplus renewable energy is stored in BEVs and fed back into the electric grid as needed. This allows other consumers, such as households, to increase their share of renewable energy in their total energy demand [205]–[207]. However, the grid may have to be expanded for effective V2G operation, as the energy needs to be transported to the BEVs unless it is generated locally.

The need to strengthen the grid is evident from Figure 5.1, which shows the energy demand of an example region and the renewable energy provided to meet that demand. The energy demand in the region is equal to the energy supply from renewable sources. However, because renewable energy is available primarily at midday (e.g., solar energy), more energy must be supplied to the region at midday than is needed. The excess energy is temporarily stored in the BEV batteries to meet the region’s demand in the evening and morning. This significantly increases the peak load in the example region. If the grid is not dimensioned for this new peak power demand, it must be reinforced.

In addition to the integration of renewable energies, BEVs can also be used for other services when connected to the grid. For example, for voltage regulation [208], frequency regulation [209]–[211] or as reactive power support operation [212].

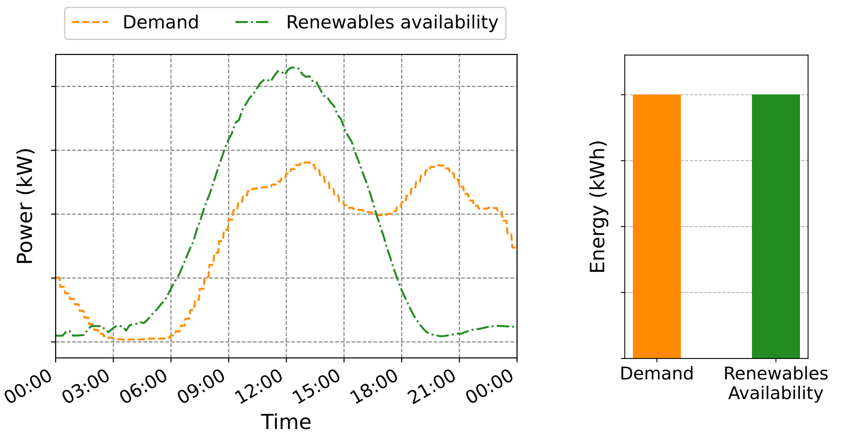

(a) Power demand and availability

(b) Energy demand and availability

Figure 5.1: Peak power increase due to V2G.

The application of V2G for renewable energy integration has been the object of extensive research both in the case of microgrids [120], [198], [213], [214] and in large geographic areas with thousands of BEVs [215]–[219].
For a reference area in northern Italy containing 200,000 BEVs, Fattori et al. [215] studied the usage of V2G to reduce the peak power demand. Assuming a photovoltaic peak power of 620 MW, they showed that a 35% reduction in the peak power demand is possible.
For four interconnected islands in Croatia, Pfeifer et al. [216] investigated what share of the total energy demand could be covered by renewable energies if 7700 BEVs were used for V2G. They showed that, for three of the four islands, a share of at least 80% can be achieved with a photovoltaic capacity of 62 MW and additional stationary batteries with a capacity of 179 MWh.
For the Croatian island of Korčula, Dorotić et al. [217] showed that the entire energy consumption can be covered by renewable energies by 2030 if 40 MW of wind and 6 MW of solar capacity were installed and V2G deployed.
Forrest et al. [218] predicted that California can meet 80% of its total energy demand by using renewables in 2050 if 80% of light-duty vehicles are BEVs and V2G is deployed. No additional energy storage systems are required for this.
Again for 2050, Nunes et al. [219] showed that, with an installed photovoltaic capacity of 16,669 MW and an electric vehicle fleet of 4.176 million, 95% of Portugal's energy demand can be met by renewable energies if V2G is deployed.

The studies discussed do not consider spatial variance in the degree of motorization, the BEV driving behaviour, and the distribution of vehicle size classes. As a result, spatial variance in available battery capacity, and consequently in energy storage, are not represented. Therefore, these results provide a good overview of a geographic area's V2G potential, but cannot be used by grid planners to adapt infrastructure for effective V2G operation. For this, the V2G potential of an area must be known with high spatial resolution, as the grid should only be strengthened where renewable energy demand exceeds current grid capacity due to high grid expansion costs.
To overcome the aforementioned limitations and fill this research gap, we develop a method to

determine the V2G potential of an entire geographic area with high spatial resolution. To ensure the ability to trace and reproduce this method, only open data were used. The method is demonstrated for the urban area of Berlin, Germany and its 448 sub-districts called “Lebensweltlich-orientierte Räume” (Eng.: neighbourhood-oriented districts, abbr.: LORs). The LOR classification is an official classification of the Berlin administration. Within each LOR, the structure of the included buildings and the socio-economic status of the inhabitants are similar. The LORs are usually separated from each other by major roads, rivers or rails [98], [133]. For each of the 448 sub-districts, the method is able to determine the percentage of residential and BEV energy demand that can be met by renewables if V2G is deployed and answer the question of whether a full renewable supply is possible.
The percentage of power demand that can be met by renewable energies if V2G is applied is highly dependent on the number of BEV owners who provide their vehicles for V2G services. Therefore, we examine a total of ten scenarios ranging from 0 to 75% participation in V2G services. The availability of renewable energies during the course of the day depends on the season. We, therefore, distinguish between a summer and a winter case.
V2G requires communication between the vehicle owner and the V2G control centre, in which the vehicle owner specifies, for example, their planned parking time. The V2G control centre collects the information and processes it. Appropriate communication between the V2G control centre and the vehicle owner is assumed in this work. An overview of the current communication standards can be found in [206], [220].

The rest of this paper is structured as follows: in Section 5.1.2, the methodology is introduced. The results are presented and analysed in Section 5.1.3. The main conclusions of this paper are derived in Section 5.1.4.

5.1.2 Methodology

This section is divided into three parts. In Section 5.1.2.1, the driving and charging behaviour of the BEVs is described. In Section 5.1.2.2, the availability of renewable energy sources depending on the time of day is discussed. Section 5.1.2.3 presents the method we used to determine the share of residential and BEV power demand that can be met by renewables if V2G is applied.

5.1.2.1 Driving and Charging Behaviour

In order to determine the V2G potential of a geographic area with high spatial resolution, the spatial distribution of BEVs in the area must be determined. In addition, to know when BEVs are available for V2G services, the daily driving behaviour of each BEV must be known, including parking times, parking locations, and parking duration.

A method for determining these input parameters is described in [27] and is demonstrated for the urban area of Berlin, Germany. In the first step of this method, the spatial distribution of conventional passenger cars (1,045,000 in Berlin in 2018 [97]) is determined using statistics on population density, motorization rate, and household income. Then, assuming full electrification of the conventional fleet, the vehicles are replaced by electric reference vehicles. The vehicle type, battery capacity, and WLTP consumption of all reference vehicles are listed in the Appendix (Table 5.2). Finally, on the basis of a travel survey, a full-day travel schedule for an average work day (Monday–Thursday) is generated for each BEV.

As can be seen in Figure 5.2, each schedule consists of a sequence of activities and trips between these activities and describes the driving behaviour of the BEVs.

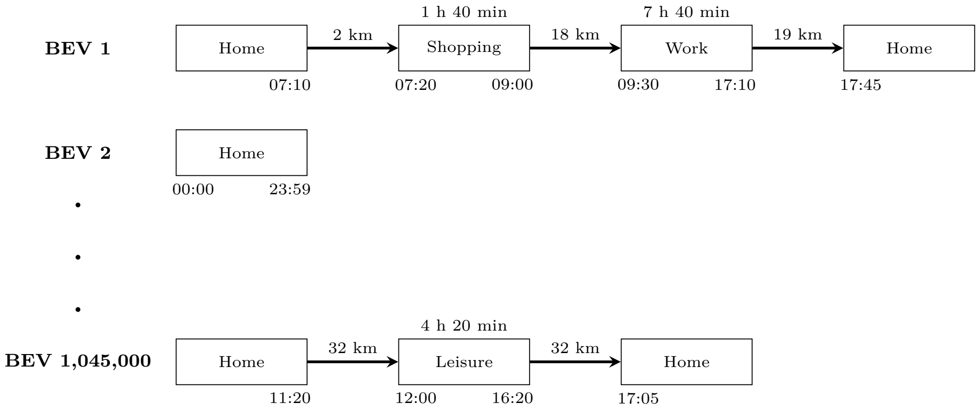

Figure 5.2: Full-day travel schedules of BEVs [29].

Based on the known driving behaviour, the charging behaviour of BEVs can be simulated by applying charging scenarios. Two different charging scenarios are applied in this paper depending on whether the owner of the BEVs has decided to participate in V2G.

Charging scenario 1: BEVs whose owners have decided to participate in V2G services are charged exclusively at the owner's place of residence, as we assume that an energy contract has been negotiated with the grid operator. This is advantageous for the grid operator since in Berlin 45% of private cars are parked all day at their owners' places of residence. The vehicles used are parked on average 18.3 h per day at their owners' places of residence [27], [91]. Such an agreement is also worthwhile for vehicle owners, as the contract includes benefits such as a lower electricity price in comparison with other locations, such as charging stations at their workplace or at public parking spots [221], [222]. The grid connection time of a BEV for scenario 1 corresponds to its parking time.

Charging scenario 2: the charging behaviour of BEVs whose owners have decided not to participate in V2G services is derived from the operational data measured for 41 private BEVs in Beijing, China in [182]. This charging scenario is described in detail in Section 4.2 in [29]. According to this scenario, BEVs are charged at locations with long parking times, namely private residences, workplaces, and shopping locations. The probability of BEV charging at these locations is determined based on the rechargeable state of charge (SOC) difference of the vehicles during their parking times. The higher the rechargeable SOC difference, the higher the probability of charging. The rechargeable SOC difference describes how much SOC can be recharged at a specific location during the parking time (a SOC of 20% before charging and a rechargeable SOC difference of 40% would, for example, result in a SOC of 60% after charging). When charging, the maximum available charging power is always used. The grid connection time of a BEV for scenario 2 corresponds to its charging time.

The maximum charging power available at the charging stations is set to 11 kW at the residences. For charging at work, the maximum power is set to 22 kW in accordance with real-world applications [177], [178]. For opportunity charging while shopping, the maximum power is set to 50 kW, which is in accordance with real-world applications [179]–[181] as well. The maximum charging power that can be used by the BEVs is SOC-dependent and is described by charging curves. For both previously described charging scenarios 1 and 2, the charging curves of the reference vehicles are shown in the Appendix (Figure 5.13). The charging curves were determined by experimental measurements [65], [183].

5.1.2.2 Energy Availability from Renewable Sources

In contrast to other renewable energy sources such as biomass or geothermal energy, the availability of wind and solar power is weather- and time-dependent. Since energy generation often does not match demand, temporary storage of surplus energy is desirable. Therefore, for intermediate energy storage in car batteries, only wind and solar energy are considered in this paper. In Figure 5.3, the daily profiles of average power generation from renewable energies (RE) in Germany are depicted. It is assumed that these profiles are also valid in Berlin. The profiles are derived from reference [223], which lists historical data on energy generation in Germany.
To compensate for fluctuations in power generation (e.g., summer day with zero hours of sunshine), the average values from two weeks are used to generate the profiles. Accordingly, the results that will be derived show the V2G potential for such an average day. On a particular day, the amount of renewable energy that can be integrated into the electricity mix depends on the actual daily profile.

Since the availability of solar and wind energy is highly dependent on the season, a distinction is made between a day in summer and a day in winter. The comparison between Figure 5.3a,b shows that power generation from renewable sources is dominated by solar energy in summer, while it is dominated by wind energy in winter. The peak power in summer is 64% higher than in winter. However, the electrical energy generated is almost the same in summer and winter. 4% less energy is available on the summer day than on the winter day.

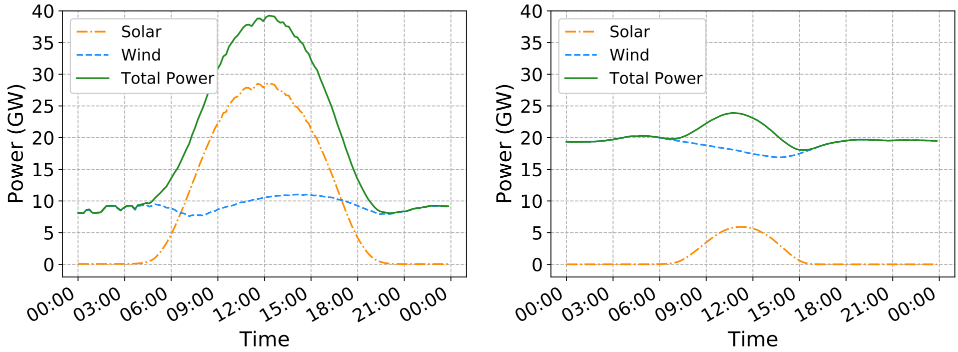

(a) Average summer day **(b)** Average winter day

Figure 5.3: Average energy generation from renewables in Germany, determined from data for two weeks in summer and winter 2021 [223].

5.1.2.3 Vehicle to Grid Approach

The iterative V2G approach developed in this paper is schematically shown in Figure 5.4 and is applied to each LOR in Berlin individually. The goal is to determine for each LOR whether V2G can be used to store and release renewable energy in such a way that the residential and BEV power demand is met exclusively with RE sources. To reach this goal, BEVs are employed to store energy when the available RE exceeds the demand (surplus) and to release it back to the electric grid when the demand exceeds the available RE (deficit). The availability of renewable energy in the LORs is described by the RE profiles defined in Section 5.1.2.2. It is assumed that the required amount of renewable energy in the LOR can be provided. To avoid RE losses, the amount of RE available is adjusted by fitting the RE profile to each LOR. In districts where energy demand cannot be met with renewable energy without loss, the method determines how much additional energy is needed from non-renewable sources.

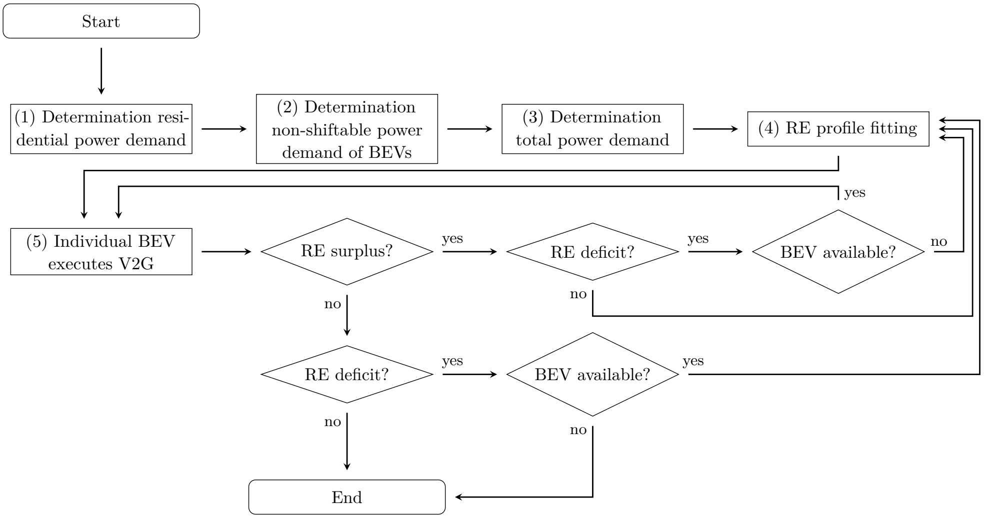

Figure 5.4: Method for determining the share of residential and BEV power demand coverable by renewables if V2G is deployed.

In step (1), the residential power demand of the LOR is determined by scaling the standard load profile for Berlin households. This is performed based on the household numbers and sizes in the LOR. The scaling process is described in detail in Section 3.5 in [27]. In step (2) the non-shiftable power demand (at the residences) of the BEVs whose owners have decided not to participate in V2G is determined (see charging scenario 2 in Section 5.1.2.1). The charging efficiency (grid to battery) is considered with a constant factor of 0.88 according to [32]. In step (3) the total, non-shiftable power demand of the LOR is determined as the sum of the residential power demand and the non-shiftable BEV power demand, as can be seen in Figure 5.5a. Then in step (4) the base RE profile is fitted to the energy demand of the LOR. This is performed by fitting the RE profile defined in Section 5.1.2.2 in such a way that the amount of renewable energy available is equal to the energy demand in the LOR. The base RE curve is depicted for the summer case as a green dotted line in Figure 5.5a as well. Subtracting the total power demand from this base RE curve yields the initial curve for the V2G process. This initial curve is depicted in Figure 5.5b. During the day, there is both a surplus (+area in Figure 5.5b) and a deficit (−area) of RE power, which is to be balanced by applying V2G.

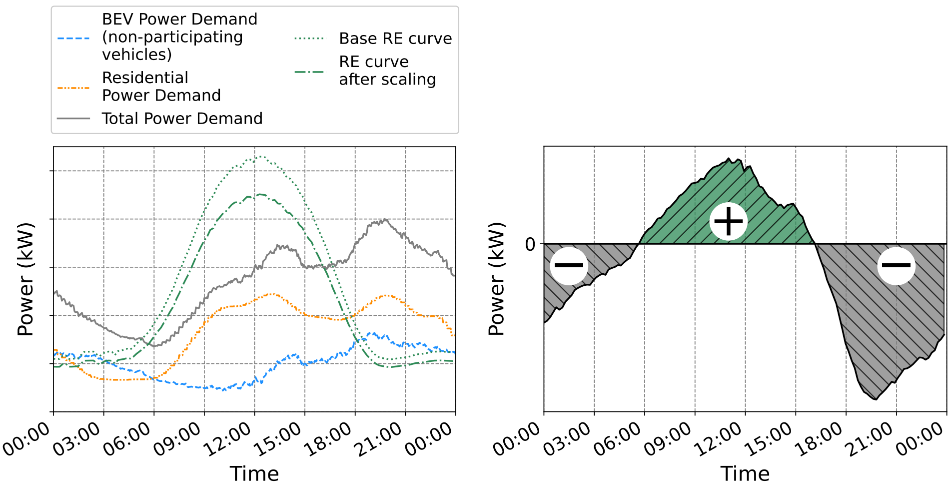

(a) Power demand and RE profile for a LOR **(b)** Initial curve for V2G

Figure 5.5: Exemplary power demand and RE profile for a LOR and resulting initial curve for V2G.

The V2G process is a combination of peak-shaving and valley-filling and is performed in step (5) for one BEV at a time. Peak-shaving is used for charging the vehicle. This means that the vehicle is charged at times when the surplus of renewable energy is greatest.
Valley-filling is used for discharging the vehicle. This means that the vehicles feed energy back into the grid when the renewable energy deficit is greatest. Thus, the combination of peak shaving and valley filling reduces both the surplus and deficit of renewable energy. All parking events at the BEV owner's residence are considered grid connection events. Therefore, the vehicle can only participate in V2G at home and can only be discharged at home. While the vehicle is connected to the electric grid, it is allowed to charge and discharge several times.

The charging and discharging efficiencies are both considered to be 88% according to [32]. The factors are similar, but slightly more conservative compared to [31], [33], which consider a charging and discharging efficiency of 90%. High discharge rates lead to accelerated battery ageing [224], [225]. Therefore, discharge during V2G is limited to a SOC of 20%, which is consistent with literature data and real V2G applications [226], [227]. The charge target value is set to a SOC of 90% in accordance with [227] and must be reached before the vehicle leaves for its next trip.

If the vehicle requires more than 90% capacity for its trips between two grid connection times, the charge target value is adjusted accordingly. This is necessary to ensure that the vehicle has sufficient energy to complete the trip.
After V2G is executed for the individual BEV in step (5), the following conditions are checked, and the iterative process continues accordingly:

- If there remains a RE surplus but no RE deficit (see Figure 5.6a), the process continues with step (4) and the RE profile is scaled down, which is exemplarily shown in Figure 5.5a. This is necessary to prevent RE losses in the LOR.

- If both, a RE surplus and a RE deficit remain (see Figure 5.6b) and another BEV is available for V2G, step (5) is executed again for the next BEV. If no other BEV is available, the process continues with step (4) and the RE profile is scaled down to prevent RE losses.
- If no RE surplus but a RE deficit remains (see Figure 5.6c) and another BEV is available for V2G, the RE profile is scaled up in step (4) to try to further reduce the RE deficit. If no other BEV is available, the process is terminated and the additional energy which is required from non-renewable sources is determined for the LOR.
- If neither a RE surplus nor a RE deficit remain (surplus deficit balance achieved, see Figure 5.6d), the process is terminated. Residential and BEV energy demand is met exclusively with RE sources.

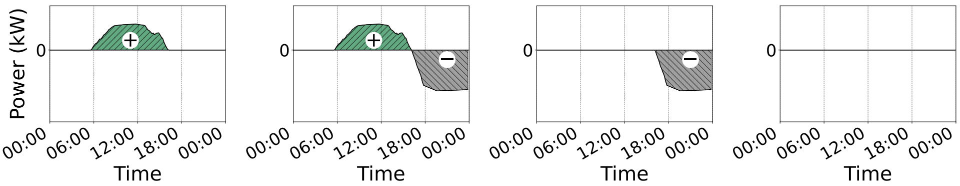

Figure 5.6: Distribution possibilities of renewable energy surplus and deficit after V2G application. (a) RE surplus, (b) RE surplus and deficit, (c) RE deficit, (d) Surplus deficit balance.

5.1.3 Results and Discussion

This section is organized as follows: Section 5.1.3.1 presents the power demand and supply for an example LOR as a function of time. Section 5.1.3.2 discusses the share of renewable energy in the total energy demand that can be provided through V2G application. Section 5.1.3.3 analyses the increase in peak power demand in the Berlin LORs due to V2G application. In Section 5.1.3.4, the battery load increase due to V2G is investigated. The results are discussed in Section 5.1.3.5.

5.1.3.1 Power Demand and Supply over the Course of the Day

This section presents the results of applying the method described in Section 5.1.2.3 to the LOR “Invalidenstraße”, which is located in the centre of Berlin. The LOR has 17,950 inhabitants and a motorization rate of 173 vehicles/1000 inhabitants. Figure 5.7 shows the power demand and supply over the course of the day in the LOR “Invalidenstraße” for the summer and winter case and different V2G participation scenarios.

For the summer case and 0% vehicle participation in V2G, Figure 5.7a shows that significant non-renewable energy must be provided to meet energy demand, especially in the evening hours (peaking between 6:00 PM and 9:00 PM). This is due to (i) the high residential demand in the evening hours, (ii) the high BEV charging energy demand in the evening (vehicles start charging immediately when they arrive home), and (iii) the low availability of renewable energy in the evening compared to midday hours. In total, 52.4% of the total energy demand is covered by renewables. If the share of vehicles participating in V2G is increased to 20% in summer (participating vehicles are randomly selected), the share of renewable energy in the total energy demand can be increased to 89.9%, as shown in Figure 5.7b. This is because BEVs store renewable energy during midday hours and feed it back into the grid during evening hours.

As shown in Figure 5.7d, with a V2G share of 20%, 100% of the districts' energy demand can be met by renewables in winter, although residential energy demand is significantly higher than in summer. This is due to the fact that renewable energy is available more evenly throughout the day in winter compared to summer (see Section 5.1.2.2). In particular, availability during midday is not significantly higher than at other times in winter. Midday is generally the time when the least amount of renewable energy can be temporarily stored by BEVs, as this is the time when the fewest vehicles are parked at their homes.

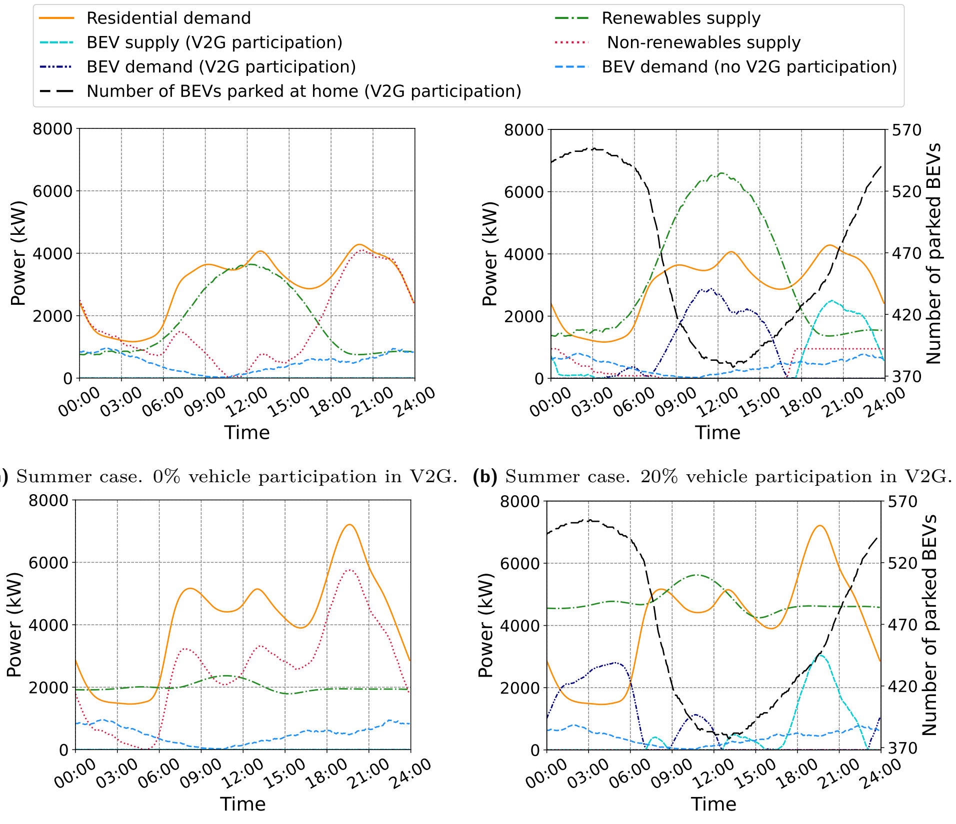

(a) Summer case. 0% vehicle participation in V2G. **(b)** Summer case. 20% vehicle participation in V2G.

(c) Winter case. 0% vehicle participation in V2G. **(d)** Winter case. 20% vehicle participation in V2G.

Figure 5.7: Power demand and supply for the LOR "Invalidenstraße" as a function of time.

5.1.3.2 Share of Renewable Energies in the LORs

Table 5.1 shows, for the ten V2G participation scenarios studied, the number of LORs whose energy demand can be met entirely by renewable energy if V2G is deployed. It can be seen that in winter, already at a V2G share of 15% (participating vehicles are randomly selected for each LOR individually), more than 50% of the LORs can fully cover their energy demand with renewables, compared to only 6.7% in summer.

Table 5.1: Number of LORs whose energy demand is met entirely by renewables and share of renewable energy in Berlin for the ten V2G participation scenarios investigated.

Case		**V2G participation scenario**									
		0%	**5%**	**10%**	**15%**	**20%**	**25%**	**30%**	**40%**	**50%**	**75%**
LORs that use 100% RE (x/448)	Summer	0	0	2	30	213	383	408	445	446	448
	Winter	0	4	113	260	430	445	446	446	448	448
Renewables share in Berlin (%)	Summer	49.5	66.2	80.4	90.0	96.1	98.0	99.1	99.93	99.98	100
	Winter	46.3	83.0	95.2	98.4	99.5	99.8	99.95	99.99	100	100

The reason that more LORs are able to cover their energy demand entirely from renewables in the winter than in the summer is due to the near-constant availability of renewables throughout the day in the winter. Therefore, as described in Section 5.1.3.1, more renewable energy can be temporarily stored by BEVs than in summer. With 75% vehicle participation in V2G, the energy demand of Berlin's households and BEVs can be met entirely by renewable energy in winter and summer. Table 5.1 also shows the share of renewables in total energy demand (i.e., household and BEV demand) in Berlin for the ten participation scenarios. With 10% vehicle participation in V2G, 80.4% of the energy demand in summer and 95.2% in winter can be covered by renewable energies. From a V2G share of 30%, more than 99% of the energy demand of Berlin's households and BEVs can be covered by renewable energy.

The share of renewable energy in the total energy demand of each LOR is shown in Figure 5.8 as boxplots. The blue square indicates the mean error. The outliers are shown as circles. It can be seen that the average share in the LORs is very similar to the average share in Berlin shown in Table 5.1. In summer, the average share is 49.2% at 0% vehicle participation in V2G and then increases to 66.3% at 5% participation. With a V2G participation of 25%, the average renewable energy share in the LORs is 98.2%. Therefore, the renewables share has almost doubled compared to the 0% V2G participation scenario.
In winter, this doubling is already achieved with a V2G share of 10%. At 0% vehicle participation in V2G, the average renewable energy share in the LORs is 46.1%, and at 10% participation, it is 95.8%. The reason why doubling the renewables share in winter is possible with lower V2G participation is that renewables are available more evenly throughout the day in winter compared to summer.

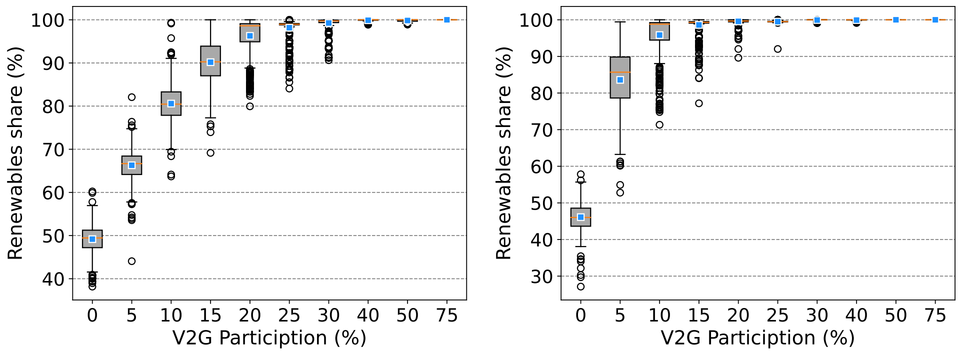

(a) Summer case **(b)** Winter case

Figure 5.8: Share of renewables in the Berlin LORs with V2G application.

Figure 5.9 shows the spatial distribution of the share of energy demand that can be met by renewables in summer, both at 0 and 15% vehicle participation in V2G. With 0% vehicle participation in V2G, higher shares are achieved in the inner-city LORs. This is due to the fact that inner-city LORs have low levels of motorization, correspondingly few BEVs, and thus a low BEV charging energy demand. The share of renewable energy in the residential area and BEV energy demand is therefore the highest.
In contrast, as the number of BEVs participating in V2G increases, high shares of renewables are observed, especially in outer-city LORs. Due to the high level of motorization and the

resulting higher number of BEVs, more renewable energy can be temporarily stored during the midday hours (and fed back into the grid in the evening) than in the inner-city districts. Accordingly, the share of renewable energy in the energy demand of households and BEVs is higher.

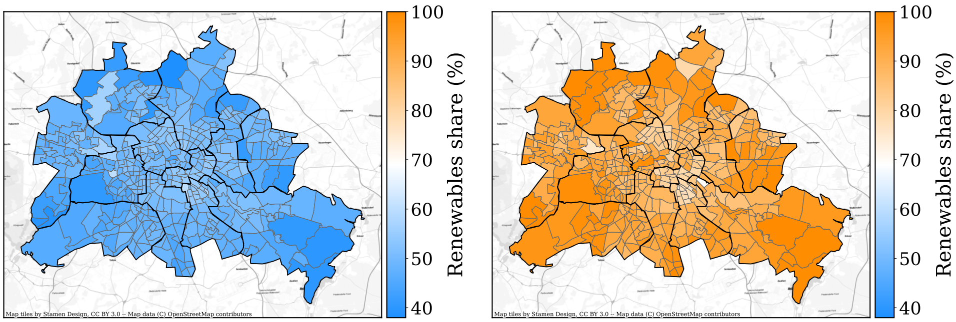

(a) 0% vehicle participation in V2G. **(b)** 15% vehicle participation in V2G.

Figure 5.9: Spatial distribution of the share of energy demand met by renewables in Berlin LORs. Summer case.

5.1.3.3 Peak Power Demand Increase in the LORs

This section examines the increase in peak load in the LORs resulting from the application of V2G. The peak power demand increase PDI always refers to the residential peak load and is calculated as follows:

$$PDI = \frac{max(LOR\ demand) - max(Residential\ demand)}{max(Residential\ demand)} \tag{5.1}$$

where $LOR\ demand$ is obtained by adding the curves of renewable energy supply, non-renewable energy supply, and BEV supply (see Figure 5.7).

The distribution of the peak power demand increase in the LORs can be seen in Figure 5.10 as boxplots. The blue square depicts the average increase in the LORs. The outliers are shown as circles. For the summer case shown in Figure 5.10a, it can be seen that the average increase is 28% when no BEVs are participating in V2G and therefore uncontrolled charging occurs. This increase is due to the fact that the residential peak power demand in the evening coincides with the BEV peak charging demand (as shown in Figure 5.7a). With 5% vehicle participation in V2G (participating vehicles are randomly selected for each LOR individually), the increase in peak power demand decreases to 22% because 5% of BEVs are charged in a controlled manner and therefore BEV power demand is reduced in the evening hours.

From a V2G participation of 10%, the peak power demand increases sharply compared to the 0% V2G participation scenario; at a participation of 20%, the average increase in peak power demand is 86%. At 75% participation, the average increase is 102%. This increase is due to the fact that, as V2G participation increases, more renewable energy can be temporarily stored and the renewable energy curve rises accordingly (see Figure 5.7a,b). As can be seen in Figure 5.7b, the renewable peak load then exceeds the residential peak load. Accordingly, the peak load in the LOR increases. Other findings can be observed for the winter case in Figure 5.10b. With 0% vehicle participation in V2G, the average peak power demand increase is 16%, which is lower than in summer. The lower increase is due to the fact that the residential peak power demand is significantly higher in winter (see Figure 5.7). From 5% participation, the average peak power demand increase is close to 0%. This is due to the fact that, in contrast to summer, renewable energy is available more evenly throughout the day and the residential peak power demand is higher. As a result, the renewable energy peak load is lower than the residential peak load (see Figure 5.7d). Accordingly, the peak power demand in the LOR does not increase.

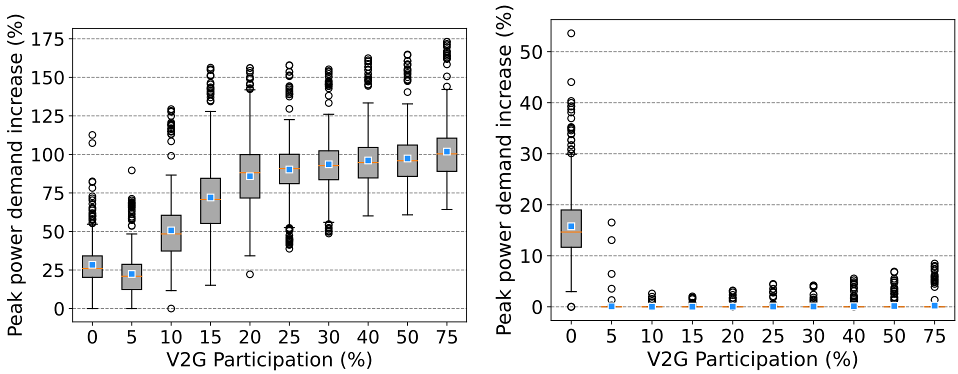

(a) Summer case

(b) Winter case

Figure 5.10: Peak power demand increase in the Berlin LORs with V2G application.

Figure 5.11 shows the spatial distribution of the peak power demand increase in Berlin LORs in summer, both at 0 and 15% vehicle participation in V2G. As explained above, it can be seen that as the number of BEVs participating in V2G increases, the peak power demand in the LORs increases.

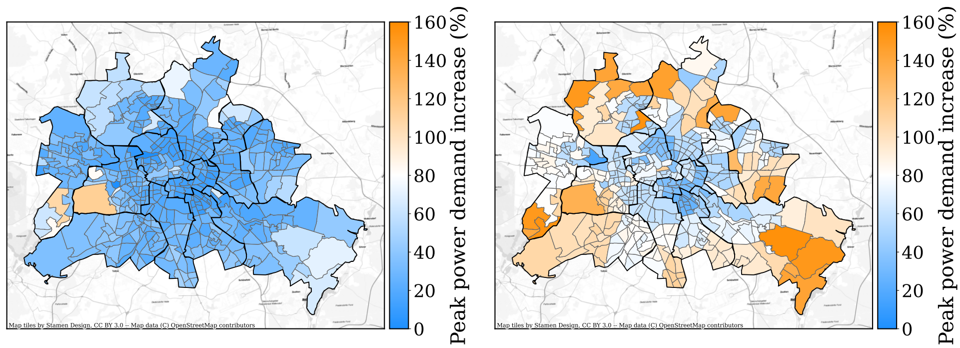

(a) 0% vehicle participation in V2G.

(b) 15% vehicle participation in V2G.

Figure 5.11: Spatial distribution of the peak power demand increase in Berlin LORs. Summer case.

In addition, it can be seen that the increase in peak power demand is higher in the outer-city LORs than in the inner-city LORs. This is due to the fact that, with a higher level of motorization and a correspondingly higher number of BEVs in the LOR, more renewable energy can be temporarily stored. As discussed in the previous paragraph, the renewable peak load then exceeds the residential peak load. Accordingly, the peak power demand in the LOR increases.

5.1.3.4 Battery Load Increase due to Vehicle to Grid

This section examines the increase in battery load due to V2G. The battery load increase (BLI) is calculated for each LOR as follows:

$$BLI = \frac{E_c - E_d}{E_d} \tag{5.2}$$

where E_c is the amount of energy charged by the vehicles which participate in V2G and E_d is the amount of energy consumed by the participating vehicles during their trips.

The distribution of the battery load increase in the LORs is shown in Figure 5.12 as boxplots. The blue square depicts the average battery load increase in the LORs.
In the summer case shown in Figure 5.12a, the average increase in battery load in the LORs is 134% at 5% vehicle participation in V2G and 173% at 10% vehicle participation. At higher participation rates, the average battery load continues to decrease and is 54% at 75% vehicle participation in V2G. The reason for this decrease is the increasing number of LORs whose energy demand is fully met by renewable energy. The amount of energy charged therefore remains almost constant, while the number of vehicles to which this amount of energy is distributed increases. Accordingly, the battery load decreases. The reason that the average increase in battery load is lower when 5% of vehicles participate in V2G than when 10% participate is because, when 5% of vehicles participate, the absolute number of participating vehicles is very small in some LORs (<10 vehicles). Due to the small number of vehicles, it is possible that all vehicles are on the road during the midday hours. In summer, however, midday is the time when renewable energy is mainly available. From 10% participation, it becomes increasingly unlikely that all vehicles are on the road during midday due to the larger absolute number of participating vehicles. Therefore, more renewable energy can be temporarily stored and the average battery load increases.

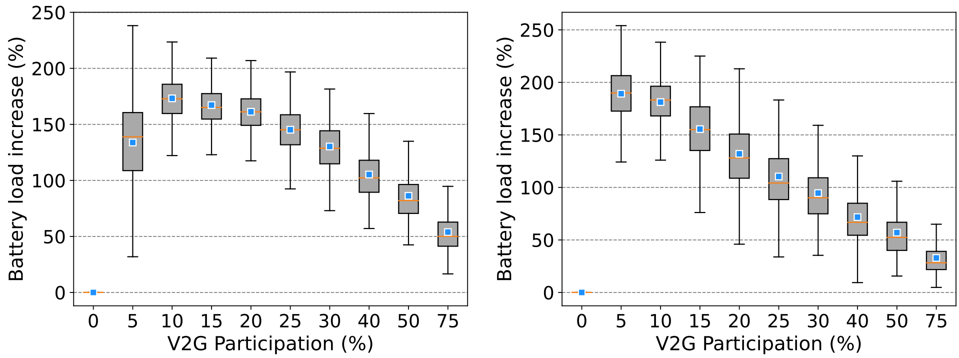

(a) Summer case **(b)** Winter case

Figure 5.12: Battery load increase in the Berlin LORs due to V2G application.

For the winter case shown in Figure 5.12b, this effect cannot be observed because renewable energy is more evenly available throughout the day. The highest average increase in battery load is observed for 5% vehicle participation in V2G and is 189%. As explained previously, the average battery load decreases at higher participation rates and is 33% at 75% vehicle participation in V2G. The reason that the average battery load is lower in winter than in summer when 75% of vehicles participate in V2G, is due to the nearly constant availability of renewable energy. As a result, more renewable energy can be used directly and does not have to be stored temporarily in the BEVs.

5.1.3.5 Discussion

The results show that, already at 10% vehicle participation in V2G, a significant share of the energy demand of households and BEVs in Berlin can be covered by renewable energy (80.4% in summer and 95.2% in winter). High shares of renewables are observed mainly in the outer-city LORs, as the motorization rate is higher than in the inner-city. With 30% vehicle participation in V2G, more than 99% of household and BEV energy demand can be met by renewables in summer and winter. A renewables share of 100% can be obtained with 75% vehicle participation in V2G.
Uncontrolled charging (0% V2G participation) increases the average peak power demand in summer by 28% compared to residential power demand. V2G deployment increases the average peak power demand in the LORs by up to 102% in summer compared to residential power demand. In winter, peak power demand in the LORs hardly increases due to V2G (close to 0% increase) and can even be reduced compared to uncontrolled charging.
V2G deployment leads to an additional load on the vehicle batteries. The average battery load increase is up to 189% in winter and 173% in summer.

Concerning these results and the proposed approach, a couple of aspects should be discussed:

- In this work, the V2G potential in Berlin was determined for two specific days, one in summer and one in winter. An average profile for available renewable energy was used for each of these two days. However, the availability of renewable energy fluctuates and can deviate significantly from this average. Accordingly, the generated results indicate the V2G potential in Berlin. On a particular day, the amount of renewable energy that can be integrated into the electricity mix depends on the actual daily profile (see Outlook).

- The vehicles participating in V2G are randomly selected in the LORs for each V2G participation scenario. Depending on the selected vehicles, the results may vary from the calculated value, which has not been investigated. However, due to the large number of vehicles in Berlin (1,045,000), we expect a rather small fluctuation.

- The power grid was not modelled. Therefore, network congestion as well as losses of transmission and distribution of electric power were disregarded. If grid conditions are also considered in the model, a lower V2G potential is expected. A possibility of modelling grid conditions is described in [228].

- V2G requires communication between the vehicle owner and the V2G control centre, in which the vehicle owner specifies, for example, their planned parking time. The V2G control centre collects the information and processes it. Appropriate communication between the V2G control centre and the vehicle owner was assumed in this work. An overview of the current communication standards can be found in [206], [220].

- Battery ageing is not considered for the V2G investigations. However, due to the increase in battery load battery life is expected to be shortened. The V2G investigations should therefore be extended by a battery ageing model with the aim to find a good trade-off between renewable energy integration and battery degradation. In addition, BEV owners should receive financial compensation for the loss in value of their vehicle due to battery ageing.
- In our case study, we assume that the driving and parking behaviour of all considered vehicles is known in advance. In reality, however, these factors are subject to considerable uncertainty. Therefore, our study clearly shows the potential benefits of V2G integration but the results must be seen as an upper bound and further work is necessary to include uncertainty in our model. One possibility is to use stochastic approaches, as shown in [229].
- With 30% vehicle participation in V2G, more than 99% of the residential energy demand and BEV charging demand in Berlin can be met by renewable energy. Accordingly, there is further untapped V2G potential that could be used to increase the share of renewable energy in commercial or industrial energy consumption.
- In addition to passenger cars, other vehicles such as commercial vehicles or buses are currently being electrified. These vehicles can contribute significantly to the integration of renewable energies into the electricity mix through V2G, as shown in [230]. For a holistic view, these vehicles should therefore be included in our model.

5.1.4 Conclusions and Outlook

In this paper, a method is developed that determines the V2G potential of BEVs in a considered area with high spatial resolution. The method is applied to the urban area of Berlin and its 448 sub-districts, assuming full electrification of the 1,045,000 private cars in Berlin. For each sub-district, the method allows determining the percentage of residential and BEV energy demand that can be met by renewables if V2G is deployed, and answers the question of whether a full renewable supply is possible. We investigated the V2G potential for each district considering ten V2G participation scenarios (0–75% participation). Since the availability of renewable energy during the day depends on the season, we distinguish between a summer and a winter case. For each case, the availability of renewable energy is described by an availability profile. The profiles correspond to the average availability of renewable energy in Germany for two weeks each in the summer and winter of 2021. Accordingly, the results obtained refer to a single day in summer or winter with the two-week-average renewable power availability.

The results show that with 5% vehicle participation in V2G, more than 60% of the energy demand of households and BEVs in Berlin can be met by renewable energy in summer and more than 80% in winter. High shares of renewables are mainly observed in the outer-city districts, as they have a higher motorization rate than the inner-city districts. With 30% vehicle participation in V2G, more than 99% of household and BEV energy demand in summer and winter can be met with renewable energy. A share of 100% renewable energy can be achieved with 75% vehicle participation in V2G.

However, V2G deployment increases the average peak power demand in the LORs by up to 100% in summer compared to residential power load. This may require reinforcement of the electric grid. In winter, peak load in the LORs hardly increases due to V2G (close to 0% increase). In addition, the deployment of V2G leads to an additional load on the vehicle batteries. The average battery load increase is up to 190% in winter and 170% in summer. This increase in battery load leads to increased battery ageing. BEV owners must therefore receive financial compensation for the loss in value of their vehicle.

Based on the proposed methodology, we plan to conduct further research in the future: It was assumed that vehicles only participate in V2G if they are parked at their owner's residence. The method also allows for investigation of the V2G potential for other parking locations such as workplaces.
In this work, full electrification of Berlin's private vehicles was assumed. Since the developed method operates at the vehicle level, it can also be used to determine V2G potential in the districts for lower levels of electrification (e.g., 50%).
An average profile for available renewable energy was used for one day in summer and one day in winter. To account for the fluctuation of renewables, simulations should be conducted on a daily basis with the actual daily availability profile over several weeks and across different seasons. In addition, the local resolution of renewable energy availability should be increased by using the profile of the geographic region around Berlin instead of the profile of Germany. Furthermore, it is desirable to consider the modelling of the power grid in order to account for the effects of network congestion as well as losses of transmission and the distribution of electric power.
Finally, the electricity demand side has to be expanded beyond private households by including commercial and industrial electricity demand.

5.1.5 Author Contributions

Florian Straub: Conceptualization, Supervision, Writing - Original Draft.
Florian Straub, Otto Maier: Methodology, Investigation, Visualization.
Florian Straub, Dietmar Göhlich, Kai Strunz: Writing - Review & Editing.
Dietmar Göhlich, Kai Strunz: Resources, Project administration, Funding acquisition.

5.1.6 Appendix A. Electric Reference Vehicles and Charging Curves

Table 5.2: Electric reference vehicles. The vehicle data are obtained from databases of the ADAC (Allgemeiner Deutscher Automobil Club), a German motoring association [231].

Class	Model	Battery Capacity (kWh)	WLTP Consumption (kWh/100km)
Mini compact	Mitsubishi i-MiEV	14.5	13.5*
	Renault Zoe	52.0	17.7
	VW e-Up!	16.0	14.3
Compact	BMW i3	37.9	15.3
	Hyundai Kona E	64.0	14.7
	VW e-Golf	32.0	15.8
Medium	Kia e-Niro	64.0	15.9
	Nissan Leaf	60.0	18.5
	Tesla Model 3	53.0	14.3
Large	Audi e-tron	83.6	23.0
	Mercedes EQC	80.0	22.6
	Tesla Model S	85.8	18.9

*New European Driving Cycle (NEDC) consumption. WLTP consumption is not available.

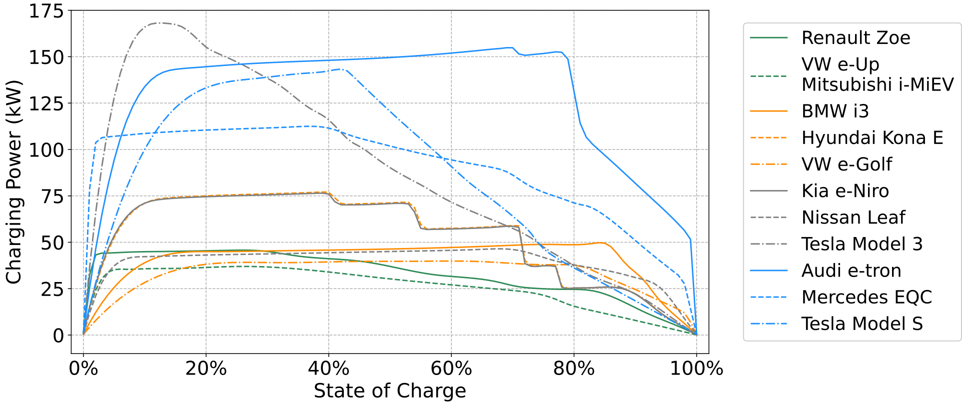

Figure 5.13: Charging curves of the reference vehicles [65], [183].

5.2 Charging Infrastructure Demand in Berlin

Installing and operating charging infrastructure for BEVs is costly. Installing private charging stations cost up to €2500, fast charging stations can cost more than €50000 [232], [233]. The operating costs for charging stations (e.g maintenance costs) are up to €2500 per year [233], [234]. Due to these high costs, charging stations should only be installed at locations where they are sufficiently utilized and can therefore be operated economically.
In order to determine the optimal number and location of charging stations, research is being conducted worldwide [75], [76], [235]–[237]. A comprehensive overview can be found in [238]. For Germany, there are numerous studies that determine the number of charging stations required for the electrification of passenger cars [25], [239]–[243]. However, these studies have limited spatial resolution and only identify demand at the county or state level or for Germany as a whole.

In contrast, based on the spatial and temporal distribution of energy and power demand in Berlin identified in Chapter 4, the number of charging stations required to meet demand can be determined with high spatial resolution. The methodology used for this determination is presented in Section 5.2.1. The results are discussed in Section 5.2.2.

5.2.1 Methodology

This section presents the method used to determine the demand for charging infrastructure in Berlin on the average working day simulated in this dissertation. The developed method determines the number of required charging stations per LOR for each of the four parking spot types distinguished in this dissertation.

These parking spot types are:

1. Private parking spots at the residences. Charging power 11 kW.
2. Employee parking spots, used for parking while at work. Charging power 22 kW.
3. Customer parking spots, used for parking while shopping. Charging power 50 kW
4. Public parking spots and public roadside parking spots, that can be used for parking while at work and while shopping and by BEV owners who do not have a private parking spot at their residence. Charging power 11 kW.

The determination of the number and spatial distribution of private charging stations is explained in Section 5.2.1.1. The determination of the number and spatial distribution of employee, customer, and public charging stations is explained in Section 5.2.1.2.

5.2.1.1 Determination of the Number of Private Charging Stations per LOR

In Berlin, 1,045,000 private cars were registered in 2018 [97], 54.8% of which are used on an average working day [89], [91]. 40% of these passenger car owners have a private parking spot for their vehicle [89], [90]. Since this dissertation examines full electrification of private passenger cars, this equates to 418,000 BEVs with a private parking spot. In the following, it is assumed that vehicle owners install a separate charging station for each of these vehicles for reasons of convenience. For Berlin, this results in a total number of 418,000 private charging stations. To determine their spatial distribution, the number of private parking spots per LOR has to be determined. In Berlin, there are two different types of private parking.

On the one hand, there are private parking spots that belong to small residential buildings. These are for example garages or carports on the property of one- or two-family houses. On the other hand, there are residential parking spaces, for residents of larger residential buildings (e.g apartment buildings). Since residential parking spaces are usually larger contiguous areas, these parking spaces are usually marked in the OSM dataset. The number and capacity of residential parking spaces in the LORs was therefore determined using OSM data, as described in Section 4.2.2.4.
The private parking spots belonging to small residential buildings are not marked in the OSM dataset. To determine their number for each LOR, the gross living space of each residential building in each LOR is first determined. The gross living space is equal to the gross floor area of the building multiplied by the number of floors of the building. The determination of these two variables is described in Section 4.2.2.1 and is based on OSM data.
Then the BEVs in the LOR are assigned to the residential buildings. For this purpose, BEVs are allocated according to the percentage of the total living space of the respective residential building. For example, if the total number of BEVs in the LOR is 100 and the residential building's living space is 2% of the total living space in the LOR, two BEVs are assigned to that building. If a building is assigned three or fewer BEVs, it is assumed to be a small residential building with private parking spots for the BEVs. If more than three vehicles are allocated to a building, it is assumed that either a designated residential parking space is provided to the building's residents[4] or the residents park their vehicles on public roadside parking spots.

The preliminary number of private parking spots per LOR is then determined by summing the capacity of residential parking spaces in the LOR and the number of private parking spots belonging to small residential buildings. In total, this approach can be used to determine the spatial distribution of 345,000 private parking spots.
In order to distribute the remaining 73,000 private parking spots among Berlin, the sum of the preliminary number of private parking spots and public roadside parking spots is determined for each LOR. The determination of the number of public roadside parking spots per LOR is described in Section 4.3.3.4. If the number of BEVs per district exceeds this sum, the remaining BEVs are assigned a private parking spot. Finally, the remaining unallocated private parking spots are randomly distributed among the LORs[5].
As a result of the process described, the number of private parking spots and therefore the number of private charging stations for each LOR is known.

5.2.1.2 Determination of the Number of Employee-, Customer-, and Public Charging Stations per LOR

While private parking spots belong to a specific vehicle and therefore a direct correlation can be made between the number of private charging stations required and the number of private parking spots, customer-, employee-, and public parking spots can be used by different vehicles, consequently there is no direct correlation.
The determination of the number of charging stations for these parking spot types is based on the results of the route assignment method developed in Section 4.3. During route assignment,

[4] The determination of the capacity of such residential parking spaces has been discussed previously in this section.
[5] The maximum number of private parking spots allowed per LOR is equal to the number of BEVs per LOR.

each vehicle was assigned not only a destination LOR for each trip but also a parking spot type where it parks. Accordingly, for each district, it is known at any time how many parking spots of a certain type are occupied. The charging infrastructure demand can therefore be determined from the maximum number of parking spots occupied at the same time.
For this determination, a table is generated separately for each LOR and each parking spot type, in which the charging station connection times of the BEVs are listed. This is exemplarily illustrated in Table 5.3 for four BEVs. A "1" indicates that the vehicle is connected to a charging station, and a "0" indicates that it is not connected. The entries are then summed up. The maximum value (4 in the example) corresponds to the number of vehicles that are connected to a charging station simultaneously. This maximum number of simultaneously charging BEVs per LOR corresponds to the number of required charging stations per LOR.

Table 5.3: Determination of the demand for charging infrastructure to meet the charging demand. Legend: "1" BEV connected to charging station; "0" BEV not connected.

	Time									
	00:00 – 00:01	00:01 – 00:02	—	13:01 – 13:02	13:02 – 13:03	—	18:20 – 18:21	18:21 – 18:22	—	23:59 – 00:00
BEV 1	1	1		0	1		1	1		1
BEV 2	0	0		1	1		0	0		0
BEV 3	1	1		1	1		1	1		1
BEV 4	0	0		1	1		0	0		0
Sum	2	2		3	4		2	2		2

BEV users often block a charging station for longer than the time it takes their vehicle to fully charge. This behavior is referred to as "charging station hogging". In order to investigate the impact of charging station hogging on the charging infrastructure demand, three different charging station connection time cases are examined:

1. Case A:
   Each vehicle is connected to the charging station for the duration of the charging process. The charging station can be used by another vehicle as soon as the previous vehicle has finished charging.

2. Case B:
   The connection time is equal to the parking time of the vehicle.

3. Case C for public charging stations:
   Especially in the case of public charging stations, it can be assumed that operators will charge a blocking fee in order to increase utilization. This fee must be paid if the vehicle continues to block the charging station after the charging process has been completed. The fee is already charged by individual operators in Germany [244]. To estimate the number of public charging stations required for case C, it is assumed that the connection time is twice as long as the charging time. This 50% blocking time corresponds to the findings for Berlin [74].

For each of the three charging station connection time cases, three different levels of satisfaction are examined (100%, 99%, and 95%). A satisfaction level of 95% means that 95% of the time the demand for infrastructure is satisfied. 5% of the day, or 72 minutes, the demand for charging infrastructure is higher than the available infrastructure, which means that more BEVs want to charge than infrastructure is available. By introducing different levels of satisfaction, it is possible to investigate what proportion of charging stations are needed to cover short-term peaks in demand and are therefore often only used for a few minutes per day.
The introduction of satisfaction levels may lead to a situation where BEVs that need to be charged in order to complete their next trip cannot find a free charging station. This is a realistic scenario, as there is no guarantee from policymakers that sufficient charging infrastructure will be available at all times. The affected drivers must search for free infrastructure again at a later time (e.g., during a break from work). An alternative is the introduction of an intelligent and automated system that connects such vehicles to a charging station as soon as one is available.

5.2.2 Results and Discussion

In Section 5.2.2.1, the necessary charging infrastructure for the full electrification of private cars in Berlin is discussed. In Section 5.2.2.2, the spatial distribution of the infrastructure demand is analyzed.

5.2.2.1 Charging Infrastructure Demand in Berlin

In Table 5.4 – Table 5.6, the determined charging infrastructure demand is shown for the three charging station connection time cases and satisfaction levels, as well as for all charging scenarios described in Section 4.3.4. For private charging stations, the tables distinguish between the total number and the used number of charging stations on the simulated day. The number "used" corresponds to the number of charging stations actually used by BEVs on the simulated day.
Tables 5.7 – 5.9 show the number of charging events at the charging stations.
The results are discussed in the following based on Figure 5.14 – Figure 5.18.

Table 5.4: Required number of charging stations on the simulated average working day. 100% satisfaction level.

Charging scenario	private		Case A			Case B			Case C
	total	used	employee	customer	public	employee	customer	public	public
Home	418,000	221,774	665	0	22,823	1216	0	294,699	38,391
Work		221,774	15,147	0	36,178	114,436	0	377,287	68,724
Opportunity		221,774	515	2276	21,515	866	16,350	294,711	36,177
Data-driven		42,692	15,022	1565	29,985	26,563	2592	76,251	46,357

Table 5.5: Required number of charging stations on the simulated average working day. 99% satisfaction level.

Charging scenario	private		Case A			Case B			Case C
	total	used	employee	customer	public	employee	customer	public	public
Home	418,000	221,774	615	0	21,666	1202	0	294,002	37,129
Work		221,774	14,241	0	34,008	113,942	0	375,754	66,954
Opportunity		221,774	470	2072	20,041	860	15,884	294,010	34,906
Data-driven		42,692	14,312	1479	28,560	26,364	2497	75,684	45,609

Table 5.6: Required number of charging stations on the simulated average working day. 95% satisfaction level.

Charging scenario	private		Case A			Case B			Case C
	total	used	employee	customer	public	employee	customer	public	public
Home	418,000	221,774	545	0	20,136	1169	0	292,407	35,292
Work		221,774	12,703	0	31,545	112,448	0	372,601	63,454
Opportunity		221,774	416	1835	18,302	837	15,051	292,410	33,174
Data-driven		42,692	13,534	1306	26,749	25,880	2355	74,403	43,660

Table 5.7: Number of charging events at the different charging station types on the simulated average working day. 100% satisfaction level.

Charging scenario	private	employee	customer	public
Home	266,661	1504	0	403,499
Work	266,661	202,316	0	581,848
Opportunity	266,661	1030	163,603	404,917
Data-driven	44,380	42,803	15,257	108,670

Table 5.8: Number of charging events at the different charging station types on the simulated average working day. 99% satisfaction level.

Charging scenario		Case A			Case B			Case C
	private	employee	customer	public	employee	customer	public	public
Home	266,661	1393	0	385,347	1487	0	402,557	391,313
Work	266,661	195,063	0	557,109	201,255	0	578,598	570,723
Opportunity	266,661	958	150,515	384,076	1022	159,077	403,971	392,717
Data-driven	44,380	41,597	14,534	104,807	42,553	14,707	107,866	106,972

Table 5.9: Number of charging events at the different charging station types on the simulated average working day. 95% satisfaction level.

Charging scenario		Case A			Case B			Case C
	private	employee	customer	public	employee	customer	public	public
Home	266,661	1235	0	363,141	1445	0	400,381	372,720
Work	266,661	178,975	0	524,009	198,884	0	573,821	545,469
Opportunity	266,661	894	136,123	362,646	994	150,689	401,794	380,022
Data-driven	44,380	40,906	13,013	100,466	41,833	13,882	106,046	104,368

In Figure 5.14 the relative deviation of the required number of charging stations between 100% and 99% satisfaction level and between 100% and 95% satisfaction level is shown for the charging station connection time case A and for all charging scenarios.
As expected, the required number of charging stations decreases as the satisfaction level decreases. The reduction in charging stations is higher for employee and customer charging stations than for public charging stations. This is because there is a high simultaneity of charging events at the employee charging stations during the morning hours (see Section 4.3.5.3). At 99% and 95% satisfaction levels, not all BEVs are provided with a charging station during this peak period, and the number of charging stations decreases accordingly. Charging events at customer parking spots do not overlap at any particular time of day. Rather, there is a short-term, simultaneous demand for charging stations in the LORs at different times of the day.
Public charging stations can be used by BEVs while at work while shopping or at home. As a result, there are fewer short-term peaks in demand compared to employee and customer charging stations. Accordingly, a decrease in the satisfaction level leads to a smaller decrease in the number of charging stations.
Of all the charging scenarios studied, the effect that the required number of charging stations decreases as the satisfaction level decreases is the smallest for the data-driven charging scenario. This is because the charging time is longer compared to the other charging scenarios, thus short-term peaks are unlikely.

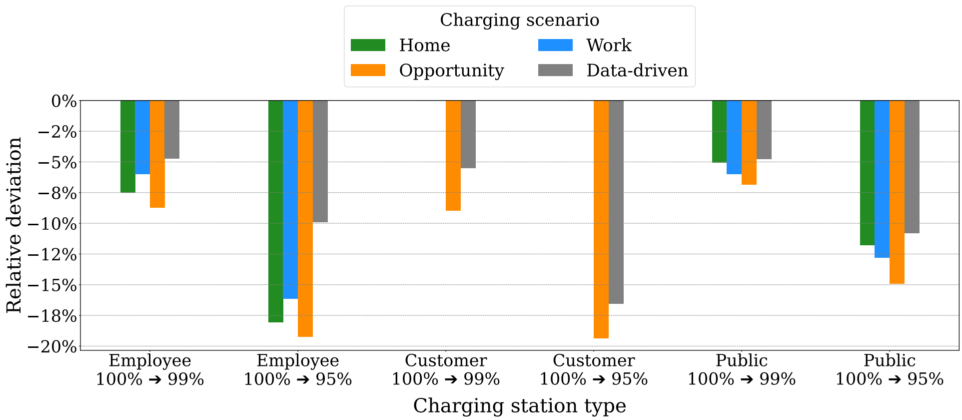

Figure 5.14: Relative deviation of the required number of charging stations for the charging station connection time case A. Comparison between 100% and 99% satisfaction level and between 100% and 95% satisfaction level for all charging scenarios.

In Figure 5.15 the relative deviation of the required number of charging stations between 100% and 99% satisfaction level and between 100% and 95% satisfaction level is shown for the charging station connection time case B and for all charging scenarios.
Compared to the charging station connection time case A in Figure 5.14, it can be seen that a decrease in the satisfaction level leads to a smaller decrease in the number of charging stations. This can be explained by the fact that the vehicles are connected to the charging stations for their entire parking time. Accordingly, there are fewer short-term peaks in charging station demand.
In comparison to the employee and public charging stations, the relative deviation for

customer charging stations is high. This is because there are short-term peaks in charging station demand due to the shorter parking times.
In contrast to the results in Figure 5.14, it can be seen that for the data-driven charging scenario, most charging infrastructure can be reduced at low satisfaction levels. This is due to the lower total number of vehicles charging compared to the other charging scenarios. Accordingly, short-term peaks in demand for charging stations are more likely.

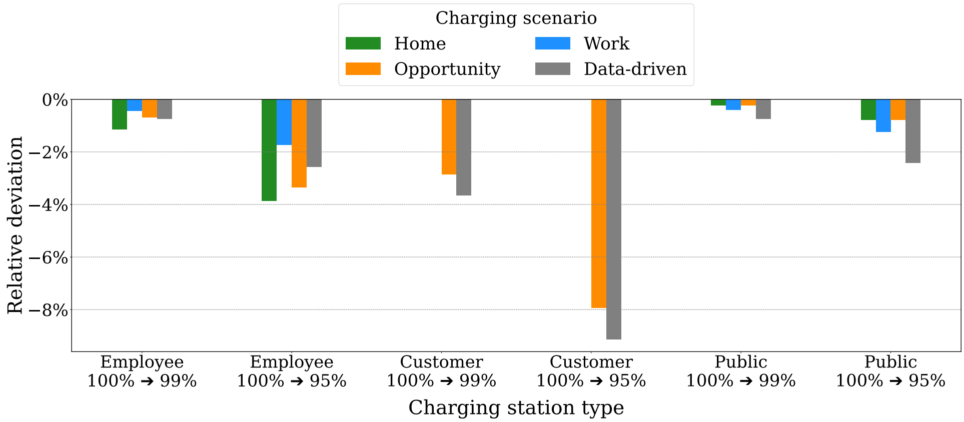

Figure 5.15: Relative deviation of the required number of charging stations for the charging station connection time case B. Comparison between 100% and 99% satisfaction level and between 100% and 95% satisfaction level for all charging scenarios.

In Figure 5.16 the relative deviation of the required number of charging stations between the charging station connection time cases A and B is depicted for all charging scenarios and a satisfaction level of 99%.
A significant charging station demand reduction of more than 35% can be observed for employee-, customer-, and public charging stations. This is because of the higher utilization rate in the charging station connection time case A which is due to the fact that each vehicle is only connected to the charging station as long as it is being charged. The charging station demand reduction is the smallest for the data-driven charging scenario since the charging times are higher compared to the other scenarios. Thus the difference between charging time and parking time is lower.
For the home-, work- and opportunity-charging scenario, slightly more than half of the private charging stations are used on the simulated day. This is partly due to vehicles not driving on the simulated day and partly due to a small number of vehicles not returning to their home location. The lowest number of private charging stations used, results from the data-driven charging scenario. This is because, unlike the other charging scenarios, the BEVs are not charged every time they arrive at home.
From these results, it can be concluded that the effective control of charging, e.g. through blocking fees, leads to a significant reduction in the number of charging stations required. This applies not only to public charging stations but also to employee and customer charging stations.

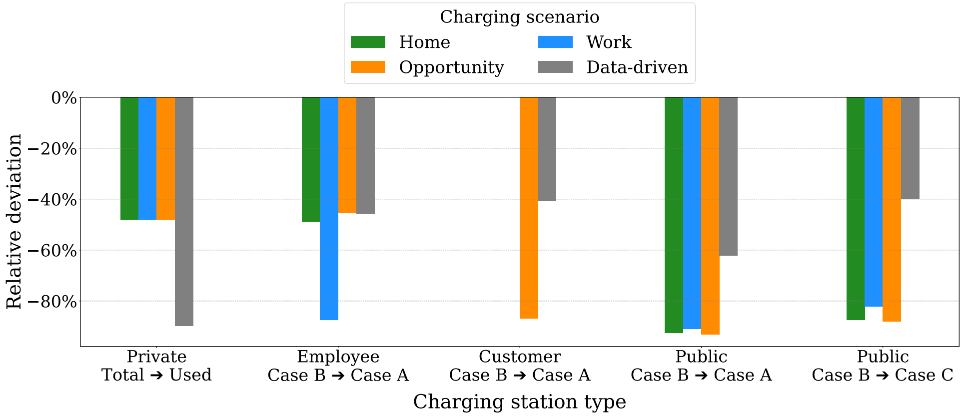

Figure 5.16: Relative deviation of the required number of charging stations at a satisfaction level of 99%. Comparison between the charging station connection time cases A and B for all charging scenarios.

In Figure 5.17, the number of charging events per charging station (hereinafter also referred to as utilization) is shown for the home-charging scenario and charging station connection time cases A and B. Since private charging stations are only used by a single vehicle, the number of charging events per charging station is the same for all satisfaction levels and both charging station connection time cases.

For public charging stations, utilization increases significantly in the charging station connection time case A compared to case B. This is due to the fact that in the home-charging scenario, vehicles are charged regardless of their charging demand (see Section 4.3.4 for a detailed description of the charging scenario). As the average daily distance of Berlin's vehicles is 29.2 km, their charging demand is low and the charging time is therefore short. Since in charging station connection time case A it is assumed that vehicles are only connected to a charging station as long as they are charging, the very short charging times lead to significantly higher utilization of charging stations than in case B, where vehicles are connected as long as they are parked.

This effect is less distinct at the employee charging stations, since in the home-charging scenario only those vehicles are charged at the employee charging stations that cannot cover their daily distance without recharging. Accordingly, these vehicles have a high charging demand. Therefore, the difference between parking and charging time is smaller than for public charging stations, which means that the difference in utilization between cases A and B is also smaller.

In addition, it can be seen in Figure 5.17 that in charging station connection time case A the utilization of charging stations increases with lower satisfaction levels, while this is not observed in case B. This is due to the fact that there are more short-term peaks in infrastructure demand in case A, as the charging station connection times are shorter. The infrastructure required to meet these short-term peaks in demand is often not needed for the rest of the day. As the amount of infrastructure provided is reduced during these peak demand periods with lower satisfaction levels, the utilization of charging stations increases. However, it should be noted that at lower satisfaction levels, fewer charging events take place.

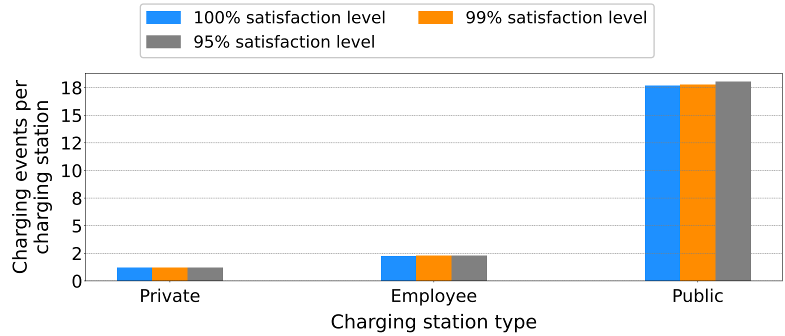

(a) Charging station connection time case A

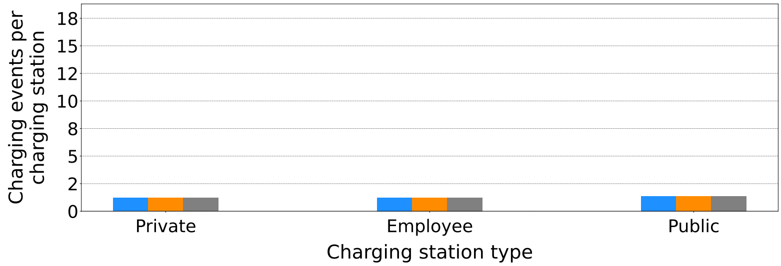

(b) Charging station connection time case B

Figure 5.17: Charging events per charging station type. Home-charging scenario.

In Figure 5.18, the number of charging events per charging station is shown for the data-driven charging scenario and charging station connection time cases A and B.
As already discussed for the home-charging scenario, it can be observed that the utilization of the charging stations in case A increases at lower satisfaction levels, while this is not observed in case B.
Furthermore, it can be seen that the utilization rates of the charging stations in case A are higher than in case B, which has also been discussed for the home-charging scenario.
The highest utilization in both connection time cases is observed at customer charging stations. This is due to the fact that customer charging stations have the shortest charging and parking times.

In summary, the analysis of Figure 5.17 and Figure 5.18 shows that a reduced satisfaction level increases the utilization of charging stations in the connection time case A. However, a lower satisfaction level also means that fewer charging events take place.
In comparison to reducing satisfaction levels, charging station utilization can be more effectively increased by reducing vehicle connection times, i.e., by preventing vehicles from continuing to block charging stations when they are fully charged.
It is therefore advisable to control vehicle charging and motivate BEV users to leave the charging stations after charging, rather than increasing the utilization of charging stations through artificial scarcity.

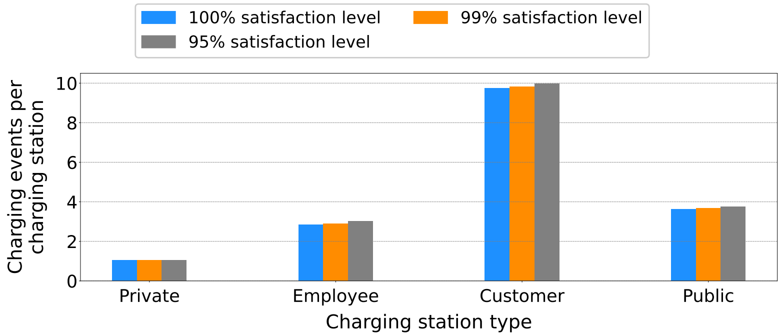

(a) Charging station connection time case A

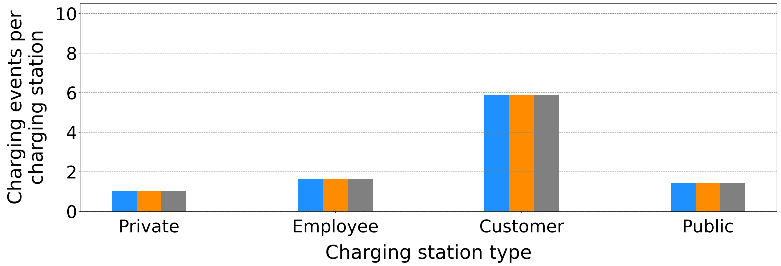

(b) Charging station connection time case B

Figure 5.18: Charging events per charging station type. Data-driven charging scenario.

5.2.2.2 Spatial Distribution of Charging Infrastructure Demand in Berlin

In Figure 5.19 the spatial distribution of the required number of charging stations in the Berlin LORs is depicted for the data-driven charging scenario, the charging station connection time case B and a satisfaction level of 99%. The number of required charging stations is shown for (a) employee, (b) customer, (c) private, and (d) public parking spots. The spatial distribution of the required number of charging stations is not shown for the other charging scenarios, charging station connection time cases, and satisfaction levels since similar distributions are obtained.

It can be seen, that the spatial distribution of customer and employee charging stations is consistent with the observations on the spatial distribution of energy demand discussed in detail in Section 4.3.5.2.
For private charging stations, it can be observed that most of them are located in the outer-city LORs. This is mainly due to the fact that there are more single- and two-family houses in the outer-city LORs than in the densely populated inner-city LORs.
In the case of public charging stations, it can be seen that demand is relatively evenly distributed across Berlin. This is because public charging infrastructure usually compensates for a lack of private charging infrastructure. In inner-city LORs, this compensation is necessary because there is limited private parking due to the lack of space. In outer-city LORs the share of BEVs with private infrastructure is much higher than in inner-city LORs. However, since there are more BEVs in the outer-city LORs due to high population density and high motorization rate (see Figure 4.1 and Figure 4.2), the number of BEVs without

private charging infrastructure is also high. This results in a similar need for public charging infrastructure as in inner-city LORs.

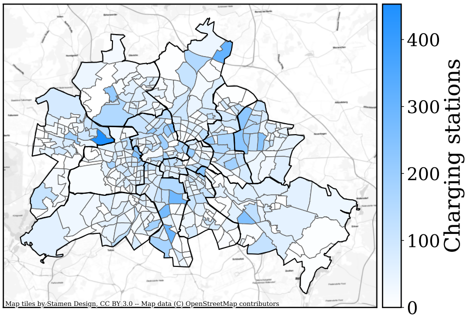

(a) At employee parking spots

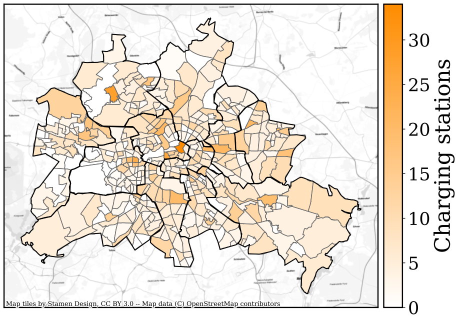

(b) At customer parking spots

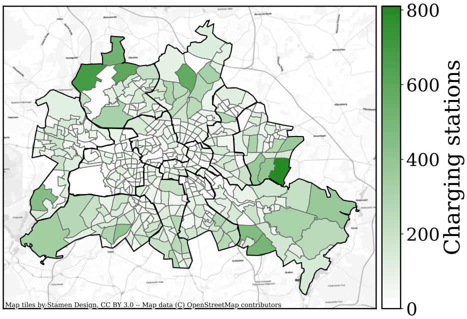

(c) At private parking spots

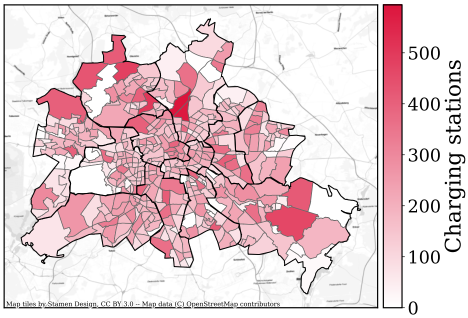

(d) At public parking spots

Figure 5.19: Required number of charging stations in the Berlin LORs. Charging station connection time case B, data-driven charging scenario, 99% satisfaction level.

6 Discussion

In order to check the plausibility of the results of this dissertation, they are compared with the results of similar studies in Section 6.1. In Section 6.2 the charging infrastructure demand results are compared with policy guidelines. Finally, the limitations of the methodology developed in this dissertation are discussed in Section 6.3.

6.1 Comparison of the Results with Literature

In this dissertation, a methodology was developed to determine the spatial and temporal charging demand resulting from the electrification of large ICEV fleets. The methodology was applied to Berlin, Germany, with its 1,045,000 private passenger cars, and a future scenario of full electrification of these vehicles was studied. Since hardly any passenger cars are fully electrified today (in Germany, 1.4% of all passenger cars were BEVs in April 2022 [245]), the empirical data required to validate the generated results cannot be collected.
Therefore, in order to check the plausibility of the results, they are compared with the results of other studies. Due to different assumptions, differences between the results of this dissertation and the comparative studies have been found.

In Section 6.1.1 the temporal distribution of BEV charging power demand identified in this dissertation is compared to other studies. In Section 6.1.2 the spatial distribution of the charging energy demand. Section 6.1.3 compares the charging infrastructure demand identified in this dissertation with another Berlin study.

6.1.1 Temporal Distribution of Power Demand

The dissertation results on the temporal distribution of charging power demand have already been extensively compared with other studies in Publication III (Section 4.3.5.5). However, a comparison with the results of [74], a study that was commissioned by the Berlin government, has not been conducted in Publication III. This study also estimates the spatial and temporal distribution of charging demand resulting from the electrification of Berlin's passenger vehicles. Hereafter, reference [74] is referred to as “RLI-study” because it was conducted at the Reiner Lemoine Institute.

A comparison between the methodologies employed in the RLI-study and this dissertation can be found in Table 6.1. In the RLI-study, the German household travel survey 2017 and expert interviews serve as the major data basis. In this dissertation, the travel survey is also used, but the second main source of information is OpenStreetMap geodata.
In the RLI-study, mobility profiles are generated for 5 different person groups (residents, commuters, day visitors, overnight visitors, commercial traffic), providing information on the traveled distances, activities, and parking times of BEVs. A total of 1,768,000 cars are considered, with 79.2% of their mileage being battery-electric. In contrast, only the passenger cars of residents and commuters are considered in this work. It is assumed that 100% of these cars are electrified.
In the RLI study, a total of 7 different charging locations (so-called “charging use cases”) with different maximum charging power are considered[6]. BEVs are assumed to be charged

[6] In Table 6.1 the charging locations “small residential buildings” (one or two family houses) and “larger residential buildings” (e.g. apartment buildings) are already grouped into “private parking spots”.

Table 6.1: Comparison between the methodology of the RLI-study and the methodology of this dissertation.

Feature	RLI-study	Dissertation
Major data basis	German household travel survey 2017, expert interviews	German household travel survey 2017, OpenStreetMap geodata
Groups of people whose cars are included in the simulation	Residents, commuters, day and overnight visitors, commercial traffic	Residents and commuters
Degree of electrification	79.2% of total mileage	100% of total mileage
Charging locations	Private-, customer-, employee-, and public parking spots, inner-city- and motorway charging hubs	Private-, customer-, employee-, and public parking spots
Max. charging power at charging locations	11 kW at private-, 22 kW at employee-, 50 kW at customer- and 22 kW at public parking spots, 150 kW at inner-city- and 350 kW at motorway charging hubs[a]	11 kW at private-, 22 kW at employee-, 50 kW at customer- and 11 kW at public parking spots
Temporal resolution of charging demand	Minute-level	Minute-level
Spatial resolution of charging demand	448 LORs in Berlin	448 LORs in Berlin
Approach for determining the spatial and temporal distribution of charging demand	Generation of mobility profiles without information on the geographic locations of activities → Application of charging scenarios → Temporal distribution of total charging demand per charging location → Application of spatial-distribution keys → Charging demand per LOR and charging location (same charging demand profile per LOR and charging location)	Generation of mobility profiles without information on the geographic locations of activities → Vehicle-routing to determine the locations of the activities → Application of charging scenarios → Spatial and temporal charging demand per LOR

[a] The charging process in the RLI-study is carried out at each charging location with the lowest possible charging power with which the vehicle can be fully charged during its parking time. If the vehicle cannot be fully charged, it is charged with the maximum charging power.

throughout the time they are parked. The charging process is carried out with the lowest possible charging power with which the vehicle can be fully charged during its parking time. If the vehicle cannot be fully charged, it is charged with the maximum charging power. This means, for example, if the vehicle has a charging demand of 10 kWh, and the parking time is 10 hours, the vehicle is charged for 10 hours with a charging power of 1 kW (independent of the available max. charging power). In this dissertation, 4 different charging locations are considered. The maximum charging power available at the respective location is always used for charging.

The temporal resolution of the charging demand is determined at minute-level in both the RLI-study and this dissertation. The spatial resolution corresponds to the 448 Berlin LORs in both works.

In order to determine the spatial and temporal distribution of charging demand, the RLI-study first generates mobility profiles for the various groups of people. The data basis for this generation is the German household travel survey 2017. The mobility profiles created do not contain any information on activity locations. Subsequently, a charging scenario is applied to determine the total charging demand and the temporal distribution of the total charging demand per charging location. This charging scenario specifies (among other constraints) that a vehicle is charged only (i) when the vehicle's SOC is below a SOC threshold and (ii) the parking time is sufficient to charge, for example, at least 2 kWh at private parking spots or 11 kWh at employee- or customer parking spots. In addition, parking constraints are defined, e.g. if the vehicle has a private parking spot, it is only 68% likely that it will also be charged at a workplace.

These constraints are most comparable to the "data-driven charging scenario" used in this dissertation. Therefore, the "data-driven charging scenario" is used as the comparative charging scenario in the following.

In the final step of determining the spatial and temporal distribution of charging demand in the RLI-study, the total charging demand is distributed among the 448 LORs using charging-location-dependent spatial distribution keys. These distribution keys are described in detail in Section 6.1.2. As a result of this distribution, the temporal distribution of the charging demand per charging location is obtained per district. However, it should be noted that the temporal profiles of the charging demand are the same in each district, only the scaling of the profiles is different per district.

In Figure 6.1 the charging power demand curves determined in the RLI-study and in this dissertation are shown. A comparison of the results shows that the total energy demand determined in the RLI-study is lower than in this dissertation and the power demand is more evenly distributed throughout the day. The more even power demand curve can be explained by the fact that in the RLI-study BEVs are assumed to be charged for the entire time they are parked. As explained above, the charging process is carried out with the lowest possible charging power with which the vehicle can be fully charged during its parking time.

The fact that the RLI-study identifies a lower energy demand even though more vehicles are considered can be explained by several reasons. First, in the RLI-study, only 79.2% of the mileage is battery-electric, while this dissertation assumes 100%. In addition, the RLI-study assumes that inbound commuters and day visitors charge primarily at their residences. In contrast, commuters charge a significant fraction of their energy demand in Berlin if the "data-driven charging scenario" of this dissertation is applied. Finally, a daily average distance of 22.2 km is assumed for the 1,045,000 private cars in Berlin in the RLI-study, which corresponds to the average distance for the entire week [89], [90]. This dissertation uses a daily average distance of 29.2 km, which corresponds to the average of a working day (Monday-Thursday) [89], [90].

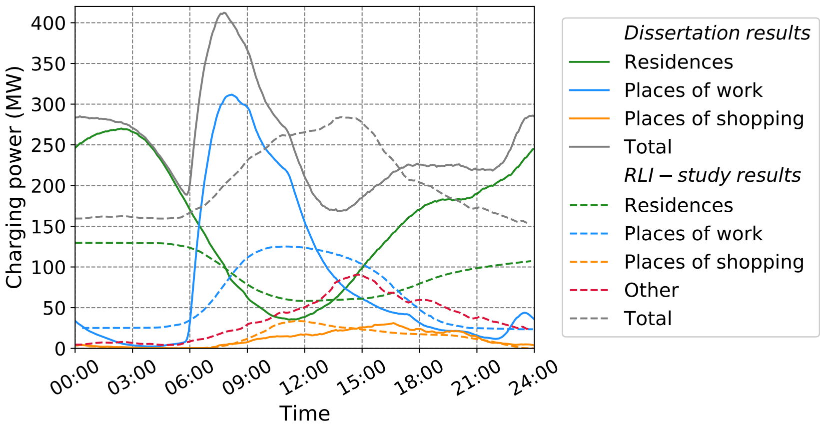

Figure 6.1: Temporal distribution of the BEV charging power demand in Berlin. Comparison between the results of this dissertation and the RLI-study. (*The "Senatsverwaltung für Umwelt, Mobilität, Verbraucher- und Klimaschutz" kindly granted permission to republish the results of the RLI-study in this dissertation.*)

For the power demand at workplaces, the RLI-study determines a high power demand between 9:30 AM and 2:30 PM. The peak value of about 125 MW is reached around 11:00 AM. The minimum power demand of about 25 MW is required between 10:00 PM and 04:00 AM. These results differ from the results of this dissertation. A maximum charging power of about 310 MW is determined, which occurs around 8:00 AM; at night, demand is close to 0 kW. The difference in peak load is most likely due to the fact that the entire parking time is assumed to be the charging time in the RLI-study. In contrast, this dissertation assumes that arriving vehicles are immediately charged at maximum charging power, which leads to the distinct peak power demand.

For the power demand at customer parking spots, the RLI-study determines a peak power demand of 35 MW around 11:30 AM. In this dissertation, peak power demand is determined around 4:30 PM, which is about the time people leave their workplaces. The earlier peak in the RLI-study is most likely due to the fact that not only shopping activities are taken into account in the RLI-study, but also customers of office buildings, banks, etc. charge their vehicles at customer parking spots. Nevertheless, the peak power demand in the RLI-study and this dissertation is similar. The larger number of simultaneously charging vehicles in the RLI-study compensates for the fact that the peak power demand per vehicle is lower since the total parking time is used as charging time.

For charging power demand at residences, the RLI-study identifies a peak power demand of about 130 MW at night and a minimum power demand of about 60 MW. In contrast, this dissertation determines a peak power demand of 270 MW and a minimum power demand of 35 MW. The lower peak demand and higher minimum demand in the RLI-study are most likely due to the fact that the RLI-study uses the total parking time as the charging time. Especially at the residences, parking times are very high, which allows for a significant reduction of charging power. Consequently, the peak-to-average power ratio (ratio of peak power demand to average power demand) in the RLI-study is also significantly lower at 1.39 than in this dissertation at 1.74. Furthermore, it can be seen that the total energy demand at the residences determined in this dissertation is higher than in the RLI-study. This is most likely due to the lower daily average distance of 22.2 km for Berlin cars assumed in the RLI-study.

6.1.2 Spatial Distribution of Energy Demand

The dissertation results on the spatial distribution of charging energy demand are not comparable to most other studies discussed in the literature review (see Section 2.3). This is due to the fact that the studies do not include sufficient information about the selected districts to allow a comprehensive comparison of the results (e.g., no information on population, number of vehicles, number of employees, sales area, etc.) [25], [71]–[73], [77], [78], [246]. In contrast, as described in Section 6.1.1, reference [74] (RLI-study) estimates the spatial and temporal charging demand resulting from the electrification of Berlin's passenger cars. Therefore, a comparison of the results can be conducted.

In the RLI-study, the total charging energy demand is first determined and then distributed to the 448 Berlin LORs using a charging-location-dependent spatial distribution key. For the energy demand charged at residences, this distribution key is mainly based on the number of inhabitants and the degree of motorization in the LORs, which is similar to the assumptions used in this dissertation (see Section 4.1). Therefore, the distributions obtained in the RLI-study and this dissertation are very similar (see Figure 4.38c).

Energy demand at workplaces is distributed in the RLI study according to the number of employees per LOR. Other criteria are not considered. This means that if, for example, a district accounts for 5% of the total number of employees in Berlin, it is allocated 5% of BEV charging demand at workplaces. As can be seen in Figure 6.2a, this leads to high energy demand in inner-city LORs due to their high number of employees[7].
This concentration of energy demand in inner-city LORs is not found in this dissertation (see Figure 6.2b). The difference is mainly due to the fact that this dissertation considers not only the number of employees but also the availability of parking spots in the LORs, which is low in the inner-city LORs.

Energy demand at customer parking spots is distributed in the RLI-study according to the number of customers per LOR. These numbers are determined by dividing employees into different sectors and then multiplying them by a specific factor that indicates how many customers an employee generates. For example, an employee in the retail sector generates 25.1 customers, while an employee in the manufacturing sector generates 0.51 customers. As can be seen in Figure 6.3a, this results in the spatial distribution of energy demand at shopping locations being very similar to that determined for workplaces. The energy demand is especially high in the inner-city LORs[8]. In contrast, this dissertation identified a more homogeneous distribution of energy demand at customer parking spots as shown in Figure 6.3b.

[7] It should be noted that the energy demand is not quantified in the RLI study, but is stated as "high" or "low".
[8] See Footnote 7

One possible reason for this deviation could be, that in this dissertation only shopping activities are considered, while in the RLI-study also customers of office buildings, banks, etc. charge their vehicles at customer parking spots. However, this is most likely not the reason, as this dissertation has found that inner-city LORs have more sales area and thus more employees than outer-city LORs. Thus, if the distribution key of the RLI-study would be applied, this dissertation would also show a concentration of charging demand in the inner-city LORs. Therefore, similar to the spatial distribution of charging demand at workplaces, the difference is most likely due to the consideration of parking availability.

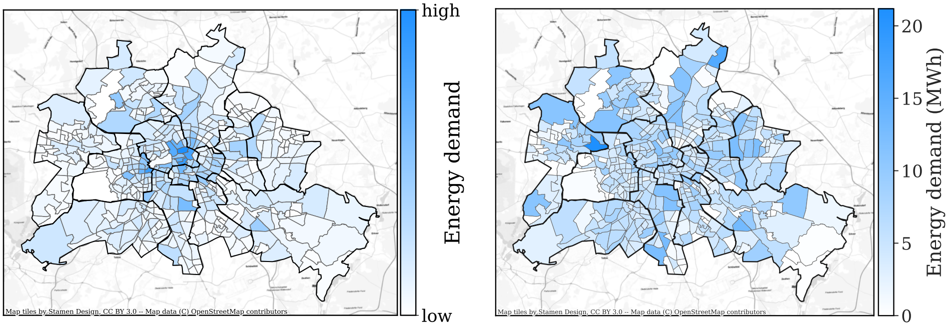

(a) RLI-study **(b)** Dissertation result

Figure 6.2: Spatial distribution of BEV charging energy demand in Berlin at places of work. (*The "Senatsverwaltung für Umwelt, Mobilität, Verbraucher- und Klimaschutz" kindly granted permission to republish the result of the RLI-study in this dissertation.*)

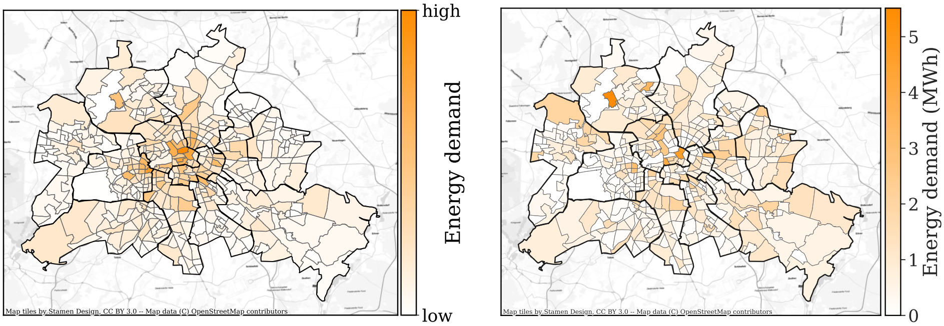

(a) RLI-study **(b)** Dissertation result

Figure 6.3: Spatial distribution of BEV charging energy demand in Berlin at shopping locations. (*The "Senatsverwaltung für Umwelt, Mobilität, Verbraucher- und Klimaschutz" kindly granted permission to republish the result of the RLI-study in this dissertation.*)

6.1.3 Charging Infrastructure Demand

In this section, the results of this dissertation on charging infrastructure demand are compared with reference [74] (RLI-study), which also determined the future charging station demand in Berlin. For this comparison, it is necessary to estimate the number of charging stations needed by vehicles which were not considered in this dissertation.

For this purpose, their energy demand is first estimated:

- Free-floating carsharing BEVs:
  According to [247], 5300 free-floating BEVs are registered in Berlin in 2019 (without a fixed rental station). In 2013, an average daily mileage of 51 km was measured for these vehicles [248]. More recent data is not available, thus it is not known if the daily mileage of vehicles has increased in recent years. To compensate for this uncertainty, a high energy consumption of 0.2 kWh/km is assumed for the BEVs. Accordingly, their daily energy demand is 54 MWh. It is assumed that this energy demand is fully charged at public charging stations.

- Day visitors and overnight visitors:
  Their energy demand is determined using data from the RLI-study. According to the RLI-study, there are 219,937 BEVs of day visitors in Berlin, with an average daily mileage of 37.1 km. Assuming a consumption of 0.18 kWh/km, this results in an energy demand of 1469 MWh. For overnight visitors, 20,245 BEVs and a daily average distance of 22.5 km result in an energy demand of 82 MWh. It is also assumed that these vehicles are exclusively charged at public charging stations.

- Commercial vehicles:
  There are 158,000 registered commercial vehicles in Berlin [97], with a average daily mileage of 54.2 km [74]. This results in an additional energy demand of 1541 MWh at 0.18 kWh/km. According to [89], [90], 63% of commercial vehicles park at public parking spots and the rest at private parking spots. Accordingly, 972 MWh are charged at public charging stations and 570 MWh at employee charging stations.

Among the different combinations for which charging infrastructure demand was determined in this dissertation, the results obtained for the charging station connection time case A, the "data-driven charging scenario", and a 99% satisfaction level are most comparable to the results of the RLI-study.
To determine the charging station demand of the above-mentioned vehicles for this combination, it is assumed that the infrastructure demand increases linearly to the energy demand. From the charging station and energy demand results (see Section 5.2 and Section 4.3), a specific demand of 9.23 public charging stations per MWh is calculated. This means that 9.23 charging stations are needed to charge one megawatt-hour in public parking spots. Therefore, additional demand of 2576 MWh leads to an additional demand for 23,776 public charging stations. For employee charging stations, the specific demand is 14.67 charging stations per MWh. Accordingly, 570 MWh results in 8362 additional employee charging stations.
In Table 6.2 the required number of charging stations determined in this dissertation and in the RLI-study are given. It can be observed that although the RLI-study identified a total energy demand of 5530 MWh and this dissertation identifies 9238.5 MWh (including additional vehicles)[9], the total amount of charging infrastructure required is almost identical which can be explained by several reasons. In the RLI-study, it is assumed that 82% of commercial vehicles are charged at employee parking spots, while this dissertation assumes 37%. Since the specific demand for employee charging stations is higher than for public charging stations, more charging stations are needed in the RLI-study to charge the same amount of energy.

[9] The large difference in energy demand was discussed in Section 6.1.1.

Furthermore, the RLI-study assumes that 8.4% of vehicles can only charge with a maximum charging power of 3.7 kW at private- and 90.8% can only charge with 11 kW at employee parking spots. Due to the lower charging power, the vehicles charge longer, therefore the charging events overlap more often and more infrastructure is needed.

Table 6.2: Required charging infrastructure in Berlin. Comparison between the results of this dissertation and the RLI-study.

	Number of charging stations				
	private	employee	customer	public	total
Dissertation[a]	418,000	22,674	1479	52,336	494,489
RLI-study	342,000	92,000	2,000	52,000	488,000

[a] Results are obtained for the charging station connection time case A, the "data-driven charging scenario", and a 99% satisfaction level (see Table 5.5 in Section 5.2). Number of employee and public charging stations is scaled up as previously described.

Overall, for both the spatial and temporal distribution of BEV charging demand and charging infrastructure demand, it can be observed that the results show deviations from the existing literature. However, the deviations can be plausibly justified by methodological differences and deviating parameters. The results of this work can therefore be considered plausible. Due to the more detailed methodology used in this dissertation, the results obtained are likely to be more accurate than the literature results.

6.2 Comparison of the Charging Infrastructure Demand with Policy Guidelines

In the following, the dissertation results on public charging infrastructure demand are compared with policy guidelines.

The Berlin government has set a goal of providing one public charging station for every 10 registered BEVs [240]. This goal is in line with EU requirements [249]. To evaluate this ratio, it is compared to the maximum charging station demand determined for the charging station connection time case C, a satisfaction level of 100%, and the "data-driven charging scenario". The "data-driven charging scenario" is chosen because it is the most realistic among the charging scenarios used in this dissertation. The charging station connection time case C is chosen since it is likely that charging station operators will charge blocking fees for their public charging stations to increase their utilization rate [244].

Analogous to Section 6.1.3, the charging station demand of vehicles not considered in this dissertation is determined first to enable a comparison. Using the specific demand of 14.45 public charging stations per MWh, the additional energy demand of 2576 MWh at public charging stations results in an additional demand of 37,223 public charging stations. For Berlin, this results in a total demand of 83,580 public charging stations, which corresponds to a ratio of 14.4:1 for 1,203,000 BEVs. This result is higher than the government's target ratio but is in line with the findings of reference [239], which determined a ratio of 14:1 for urban areas in Germany.

A ratio of 14.4:1 can still be considered conservative (i.e., more charging stations are provided than necessary) since the assumption that the energy demand of car-sharing BEVs and visitors is fully charged at public charging stations is rather unlikely. Therefore, from the results of this dissertation, it can be concluded that the 10:1 target ratio of the government can be considered oversized.

In addition to the number of public charging stations, the Berlin government has defined locations where the charging stations should be installed [250]. These areas are predominantly located in inner-city LORs.
In Figure 6.4a the registered public charging stations in Berlin are depicted. It can be seen that, in line with the government's target, public charging infrastructure is mainly available in inner-city LORs. The dataset on registered charging stations is provided by the "Federal Network Agency" and also includes the number and spatial distribution of semi-public charging stations[10] (supermarkets, furniture stores, etc.) [251]. Contrary to the government's target, the results identified in this dissertation show that there is no increased need for public charging stations in inner-city LORs compared to outer-city LORs (see Figure 6.4b).
The reasons for this have already been discussed in Section 5.2.2.2. Consequently, based on the results of this dissertation, a balanced expansion of the public charging infrastructure in Berlin's LORs is recommended.

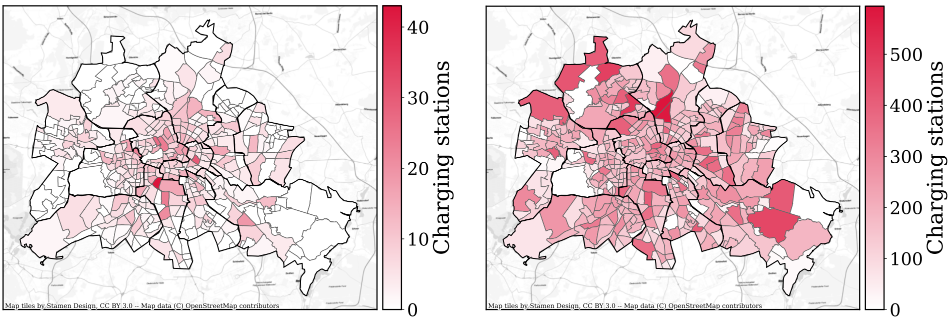

(a) Registered charging stations in November 2022 **(b)** Demand identified in this dissertation

Figure 6.4: Spatial distribution of public charging stations in Berlin.

6.3 Limitations of the Methodology

The methodology developed in this work enables high-resolution determination of the spatial and temporal charging energy and power demand in an urban area, resulting from the electrification of private vehicles with internal combustion engines. Since the SOC, BEV user activities and geographic location of activities are tracked for each BEV, the results can be used for further investigation, such as determining the demand for charging stations or the V2G potential of the considered area. Being based on open data, the methodology is transferable to other urban areas.
The proposed methodology overcomes the limitations of the methods proposed in the literature (see Section 2.4). However, due to the resulting complexity of the methodology, a compromise had to be found between the level of detail and the implementation effort for certain subcomponents. Accordingly, the methodology has some limitations, which are discussed in the following:

[10] Semi-public charging stations are not shown in Figure 6.4a.

The spatial and temporal distribution of charging demand is determined for Berlin's private passenger cars and inbound commuters. The energy demand of other vehicles such as cars of day and overnight visitors, commercial passenger cars, or car-sharing vehicles is not determined. Therefore, the total energy demand is underestimated.

It is assumed that the current conventional vehicle fleet is fully electrified while its driving behavior remains unchanged. Potential future developments in urban mobility (e.g., more carsharing) or changes in vehicle numbers are not considered. This can lead to an inaccurate estimate of future energy demand.

When determining energy demand, it is assumed that charging occurs at residences, workplaces, and shopping locations. This may result in an inaccurate estimate of the spatial distribution of charging energy demand, since charging may also be performed for other activities.

The energy consumption of BEVs is based on average values, assuming different consumption for distances of more than 20 km than for distances of less than 20 km. Depending on the route, the actual consumption can deviate considerably from the average consumption. This simplification may result in an inaccurate estimate of the charging energy demand.

The accuracy of the results is dependent on the completeness of the employed OSM geodataset. For example, if parking spaces are not labeled in the OSM geodataset, they are not considered in the investigations. Therefore, an incomplete data set may cause an inaccurate spatial distribution of BEV charging demand.

How to overcome these limitations is discussed in the Outlook (Section 7.2).

7 Summary and Outlook

7.1 Summary

In this dissertation a method was developed which enables high-resolution determination of the spatial and temporal charging energy and power demand in an urban area, resulting from the electrification of private vehicles with internal combustion engines. The method consists of three main parts:
In the first part (see Section 4.1), the urban area is divided into districts, and the current conventional vehicle fleet in the districts is completely electrified. For electrification, data on motorization levels and population density are used to determine the spatial distribution of the vehicles in the considered area. The spatial distribution of household income is then used to determine the spatial distribution of vehicle size classes in the districts. This yields the number and sizes of vehicles for each district, which are then replaced with reference electric vehicles. Subsequently, a travel survey is used to determine vehicle-based mobility profiles. The survey data is limited. While it is possible to determine the driving behaviour of the population from this data, it is not possible to derive activity- and time-dependent traffic flows between districts. Therefore, the vehicle-based mobility profiles generated do not contain information about the geographic location where the vehicle is parked while the battery electric vehicle (BEV) user is performing an activity. Based on these preliminary mobility profiles, the spatial and temporal distribution of charging energy and power demand in the urban area is determined. However, there is one major limitation to the results. Since the locations of the activities are not known, the charging demand can only be determined by assuming that BEVs are exclusively charged at or near the residences of BEV owners.

To overcome this limitation, the geographic location where the vehicle is parked while the BEV user is performing an activity needs to be determined. An important input variable in this determination is the car-access attractiveness of the districts. The determination of the car-access attractiveness is the second part of the model which is described in Section 4.2. The car-access attractiveness is a measure of how attractive buildings and districts are to drive to by car for a particular activity. A high attractiveness indicates that a location is highly likely to be accessed by car, while a low attractiveness means that the location is more likely to be accessed by another mode of transportation. The car-access attractiveness is determined based on the number of available parking spots in the districts, the distance of the buildings in the district from the parking spots, and their distance to public transportation.

Thirdly, the unknown geographical locations of the activities are determined (see Section 4.3). For this purpose, a route assignment approach is developed that assigns a destination district to each vehicle trip based on a destination choice model. In addition to the car-access attractiveness determined in the second part of the method, the distance and travel speed between districts, as well as the availability of parking spots in the districts are considered for destination choice. By determining the destinations of BEV trips, a complete mobility profile is now available for each BEV. This allows determining the spatial and temporal BEV charging energy and power demand in the urban area by applying charging scenarios.

The developed method is demonstrated for Berlin, Germany, and its 448 sub-districts called “Lebensweltlich orientierte Räume” (neighbourhood oriented districts) (LORs), assuming full electrification of Berlin’s 1,045,000 private cars. However, because the method is based

on open data, it is reproducible and transferable to other urban areas. Since the developed method operates at the vehicle level, it can also be used to determine BEV charging demand for lower levels of electrification (e.g. 50%).
The results show that between 5468 MWh and 6093 MWh of charging energy is required on an average working day in Berlin, depending on the charging scenario. At least 61.8% of this energy is charged at the residences.
Regarding the spatial distribution of energy demand at workplaces, demand is relatively similar in inner-city and outer-city LORs. Demand ranges from 0 kWh per day in LORs with no employees to 21.2 MWh per day in a LOR with many employees, high car-access attractiveness, and good accessibility. Charging energy demand at shopping locations ranges from 0 kWh per day in LORs without shopping facilities to 5.5 MWh per day in LORs which attract many shopping trips due to their location and parking situation. Charging energy demand at residences ranges from 0 kWh per day in uninhabited LORs to 40.7 MWh per day in LORs with high population and motorization levels.
The temporal distribution of the charging power demand in Berlin is highly dependent on the charging scenario as well. The peak power demand ranges from 328 MW to 412 MW. The minimum power demand is between 78 MW and 169 MW. In 2021, the peak load in the Berlin power grid was 2119 MW [184]. Assuming that this peak load coincides with the BEV peak power demand of 412 MW, this results in a 19.4% increase in peak power demand.
Berlin's total electric energy demand in 2021 was 13.9 TWh [184]. In this dissertation, an annual BEV charging energy demand of 1.87 TWh was calculated (see Section 4.3.5.5). The additional BEV charging demand would therefore increase Berlin's energy demand by 13.5%.

The determined temporal distribution of charging power demand shows some deviations from the existing literature but is in overall agreement with it. The deviations are caused by methodological differences and deviating parameters such as different assumptions on driving and charging behavior (see Section 6.1.1).
The identified spatial distribution of BEV charging demand in the LORs shows differences from the results of another Berlin study. The differences are primarily due to the fact that the study makes oversimplified assumptions to spatially distribute the charging demand (e.g., based on the number of employees per LOR). Different parking availability in the LORs is not considered (see Section 6.1.2). Due to the more detailed methodology used in this dissertation, the results obtained are likely to be more accurate than the study results.

Based on the complete mobility profiles of BEVs and the charging demand of BEVs determined for Berlin, further investigations were conducted:
(i) It was investigated whether vehicle charging times can be shifted to times when the impact on the electric grid is minimal. In Section 4.3.5.4 it was shown for an example LOR that it is possible to reduce peak power demand by up to 31.7% through load shifting, compared to uncontrolled charging. In addition, the peak-to-average power ratio can be significantly reduced. Since the load shifting investigations were conducted for a LOR with one of the highest BEV charging demands per resident, it is likely that peak power demand in most other LORs can also be significantly reduced through load shifting.
Load shifting is often easier and less expensive to implement (e.g., through price incentives) than grid expansion and, as shown, can contribute significantly to reducing grid load. Therefore, grid expansion should only take place if no further load shifting potential exists.

(ii) Section 5.1 examined for each of Berlin's LORs the percentage of household and BEV energy demand that can be met by renewable energy if Vehicle to grid (V2G) is deployed. Ten different V2G participation scenarios were investigated (0% – 75% participation, 75% participation means that 75% of the Berlin BEVs participate in V2G), and for each scenario a distinction was made between one day in winter and one day in summer since the availability of renewable energies differs between the seasons.
Results show, that already at 10% vehicle participation in V2G, a significant share of the energy demand of households and BEVs in Berlin can be covered by renewable energy (80.4% in summer and 95.2% in winter). With 30% vehicle participation in V2G, more than 99% of household and BEV energy demand can be met with renewables in summer and winter. 100% renewables share can be obtained with 75% vehicle participation in V2G.
V2G deployment increases the average peak power demand in the LORs by up to 102% in summer compared to residential power demand. In winter, peak power demand in the LORs hardly increases due to V2G (close to 0% increase). In addition, the deployment of V2G leads to an additional load on the vehicle batteries. The average battery load increase is up to 189% in winter and 173% in summer.
In summary, the results show that BEVs can be effectively used as electricity storage units and can contribute to increasing the share of renewable energy in the electricity mix. However, grid reinforcement may be required as the peak load increases significantly. Furthermore, the increase in battery load leads to increased battery aging. BEV owners must therefore receive financial compensation for the loss in value of their vehicle.

(iii) In Section 5.2, the number and spatial distribution of charging stations required to meet the BEV charging demand were determined for Berlin. For public charging stations, a BEV to charging station ratio of 14.4:1 was determined, which is significantly lower than the Berlin government's target ratio of 10:1. Therefore, based on the results of this dissertation, the target ratio of 10:1 can be considered oversized.
In addition, the Berlin government has identified areas where charging stations should be installed as a priority. These areas are predominantly located in inner-city areas. Contrary to the government's target, the results identified in this dissertation show a similar need for public charging infrastructure in inner-city and outer-city LORs. Consequently, based on the results of this dissertation, a balanced expansion of the public charging infrastructure in Berlin's LORs is recommended.

7.2 Outlook

The route assignment method generates district-level results. Improved accuracy could be achieved by increasing the resolution of the model, such as building-level results. Some of the data required for this are already available, for example, both the car-access attractiveness and the number of parking spots have already been determined at the building level in this dissertation.

Average energy consumption values are used to determine the energy demand of BEVs. Depending on the route, the actual consumption can deviate considerably from the average consumption. By using the OpenRouteService Directions API [252] a route could be determined for each BEV and energy consumption could be estimated based on a vehicle dynamics model. In addition, seasonal consumption could be considered to account for heating or cooling.

When determining energy demand, it is assumed that charging occurs at residences, workplaces, and shopping locations. This may result in an inaccurate estimate of the spatial distribution of charging energy demand, since charging may also be performed for other activities. Further activities were defined when the mobility profiles were created. For these, charging events can also be considered.

Battery aging is not considered for the V2G investigations. However, due to the higher number of charge cycles when V2G is employed, battery life is expected to be reduced. The V2G investigations should therefore be extended by a battery aging model with the aim to find a good trade-off between grid support and battery degradation. In addition, a financial compensation system needs to be developed to compensate BEV owners for the loss in value of their vehicle due to battery aging.

It is assumed that the current conventional vehicle fleet is fully electrified while its driving behavior remains unchanged. Potential future developments in urban mobility (e.g., more carsharing) or changes in vehicle numbers are not considered. Since the methodology is based on the mobility profiles of individual vehicles, changes in BEV numbers and modal share can be easily considered by adjusting the mobility profiles.

The spatial and temporal distribution of charging demand in Berlin is determined assuming electrification of private car transport and inbound commuter vehicles. To increase the accuracy, the model should be expanded to include other types of passenger cars, such as cars owned by day and overnight visitors, commercial passenger cars, or car-sharing vehicles. The charging demand of these vehicles can be estimated by generating mobility profiles for these vehicles, which could be easily integrated into the simulation.
In addition, the developed method should be extended to include other vehicle types such as buses or trucks for a holistic determination of the energy demand. The electrification of buses and trucks has already been studied, e.g. in [81]–[83].
Since future electrification of conventional vehicles is not limited to urban areas, the model should be extended to larger areas (e.g., state-level/Germany).

Although it is shown that the dissertation results are plausible by comparing them with similar studies, the validity of the results remains to be verified. One possibility would be to compare the results with extensive measurement campaigns on vehicles in Berlin (which are currently unavailable). Due to the variability of the methodology, it can be adjusted to the results of the measurements. Both the car-access attractiveness and the route assignment model can be extended to include additional criteria. In addition, the weighting of the criteria can be changed.

References

[1] United Nations, *Paris Agreement*, New York, NY, USA, 2015. URL: `https://unfccc.int/sites/default/files/english_paris_agreement.pdf` (visited on Feb. 19, 2022).

[2] European Comission, *The European Green Deal*, Brussels, 2019. URL: `https://eur-lex.europa.eu/legal-content/EN/TXT/?qid=1588580774040&uri=CELEX:52019DC0640` (visited on Jan. 30, 2021).

[3] Bundesministerium für Umwelt, Naturschutz und nukleare Sicherheit, *Klimaschutzplan 2050: Klimaschutzpolitische Grundsätze und Ziele der Bundesregierung*, Berlin, 2016. URL: `https://www.bmuv.de/fileadmin/Daten_BMU/Download_PDF/Klimaschutz/klimaschutzplan_2050_bf.pdf` (visited on Feb. 14, 2022).

[4] Deutsche Bundesregierung, *Gesetz zur Einführung eines Bundes-Klimaschutzgesetzes und zur Änderung weiterer Vorschriften*, 2019. URL: `https://dip.bundestag.de/vorgang/gesetz-zur-einf%C3%BChrung-eines-bundes-klimaschutzgesetzes-und-zur-%C3%A4nderung-weiterer-vorschriften/254400` (visited on Feb. 14, 2022).

[5] Bundesministerium für Umwelt, Naturschutz und nukleare Sicherheit, *Nationales Luftreinhalteprogramm der Bundesrepublik Deutschland*, 2019. URL: `https://www.bmuv.de/fileadmin/Daten_BMU/Download_PDF/Luft/luftreinhalteprogramm_bericht_bf.pdf` (visited on Feb. 14, 2022).

[6] Umweltbundesamt and Bundesministerium für Umwelt, Naturschutz und nukleare Sicherheit, *Treibhausgasemissionen gingen 2019 um 6,3 Prozent zurück: Große Minderungen im Energiesektor, Anstieg im Gebäudesektor und Verkehr*, Dessau-Roßlau, 2020. URL: `https://www.umweltbundesamt.de/presse/pressemitteilungen/treibhausgasemissionen-gingen-2019-um-63-prozent` (visited on Feb. 14, 2022).

[7] Umweltbundesamt, *Emissionen von Luftschadstoffen*, 2020. URL: `https://www.umweltbundesamt.de/themen/luft/emissionen-von-luftschadstoffen` (visited on Feb. 14, 2022).

[8] Umweltbundesamt, *Emissionsquellen*, 2021. URL: `https://www.umweltbundesamt.de/themen/klima-energie/treibhausgas-emissionen/emissionsquellen` (visited on Feb. 14, 2022).

[9] European Parliament, *CO2 emissions from cars: facts and figures*, 2019. URL: `https://www.europarl.europa.eu/news/en/headlines/society/20190313STO31218/co2-emissions-from-cars-facts-and-figures-infographics` (visited on Feb. 16, 2022).

[10] Bundesministerium für Umwelt, Naturschutz und nukleare Sicherheit, *Klimaschutz in Zahlen: Fakten, Trends und Impulse deutscher Klimapolitik Ausgabe 2019*, Berlin, 2019. URL: `https://www.klimakompakt.de/fileadmin/redaktion/Datei-downloads/Bund_Land/klimaschutz_zahlen_2019_broschuere_BMU.pdf` (visited on Sep. 20, 2022).

[11] European Union, "Regulation No 443/2009 of the European Parliament and of the Council," *Official Journal of the European Union*, no. 140, pp. 1–15, 2009.

[12] J. A. Sanguesa, V. Torres-Sanz, P. Garrido, F. J. Martinez, and J. M. Marquez-Barja, "A Review on Electric Vehicles: Technologies and Challenges," *Smart Cities*, vol. 4, no. 1, pp. 372–404, 2021. DOI: `10.3390/smartcities4010022`.

[13] Kraftfahrt Bundesamt, *Umwelt 2021: Neuzulassungen von Kraftfahrzeugen mit alternativem Antrieb im Dezember 2021 (FZ 28)*, Flensburg, 2022. URL: `https://www.kba.de/DE/Statistik/Fahrzeuge/Neuzulassungen/Umwelt/n_umwelt_node.html` (visited on Feb. 16, 2022).

[14] A. Ajanovic and R. Haas, "Prospects and impediments for hydrogen and fuel cell vehicles in the transport sector," *International Journal of Hydrogen Energy*, vol. 46, no. 16, pp. 10 049–10 058, 2021. DOI: `10.1016/j.ijhydene.2020.03.122`.

[15] Y. Manoharan, S. E. Hosseini, B. Butler, H. Alzhahrani, B. T. F. Senior, T. Ashuri, and J. Krohn, "Hydrogen Fuel Cell Vehicles; Current Status and Future Prospect," *Applied Sciences*, vol. 9, no. 11, p. 2296, 2019. DOI: `10.3390/app9112296`.

[16] Umweltbundesamt, *Erneuerbare Energien in Zahlen*, 2022. URL: `https://www.umweltbundesamt.de/themen/klima-energie/erneuerbare-energien/erneuerbare-energien-in-zahlen#uberblick` (visited on Nov. 18, 2022).

[17] Enerdata, *Share of renewables in electricity production*, 2022. URL: `https://yearbook.enerdata.net/renewables/renewable-in-electricity-production-share.html` (visited on Nov. 18, 2022).

[18] S. Bigerna, C. A. Bollino, and P. Polinori, "Convergence in renewable energy sources diffusion worldwide," *Journal of environmental management*, vol. 292, p. 112 784, 2021. DOI: `10.1016/j.jenvman.2021.112784`.

[19] Kraftfahrt Bundesamt, *Fahrzeugzulassungen (FZ): Neuzulassungen von Kraftfahrzeugen nach Umwelt-Merkmalen Jahr 2021*, Flensburg, 2022. URL: `https://www.kba.de/SharedDocs/Downloads/DE/Statistik/Fahrzeuge/FZ14/fz14_2021_pdf.pdf;jsessionid=D512D10C416439BC18113838C94355D6.live21324?__blob=publicationFile&v=7` (visited on Jun. 29, 2022).

[20] J. A. P. Lopes, F. J. Soares, and P. M. R. Almeida, "Integration of Electric Vehicles in the Electric Power System," *Proceedings of the IEEE*, vol. 99, no. 1, pp. 168–183, 2011. DOI: `10.1109/JPROC.2010.2066250`.

[21] G. A. Putrus, P. Suwanapingkarl, D. Johnston, E. C. Bentley, and M. Narayana, "Impact of electric vehicles on power distribution networks," in *VPPC '09*, [Piscataway, NJ]: IEEE, 2009, pp. 827–831. DOI: 10.1109/VPPC.2009.5289760.

[22] R. C. Green, L. Wang, and M. Alam, "The impact of plug-in hybrid electric vehicles on distribution networks: A review and outlook," *Renewable and Sustainable Energy Reviews*, vol. 15, no. 1, pp. 544–553, 2011. DOI: 10.1016/j.rser.2010.08.015.

[23] J. Y. Yong, V. K. Ramachandaramurthy, K. M. Tan, and N. Mithulananthan, "A review on the state-of-the-art technologies of electric vehicle, its impacts and prospects," *Renewable and Sustainable Energy Reviews*, vol. 49, pp. 365–385, 2015. DOI: 10.1016/j.rser.2015.04.130.

[24] T. Yi, C. Zhang, T. Lin, and J. Liu, "Research on the spatial-temporal distribution of electric vehicle charging load demand: A case study in China," *Journal of Cleaner Production*, vol. 242, p. 118 457, 2020. DOI: 10.1016/j.jclepro.2019.118457.

[25] R. Pagany, A. Marquardt, and R. Zink, "Electric Charging Demand Location Model—A User- and Destination-Based Locating Approach for Electric Vehicle Charging Stations," *Sustainability*, vol. 11, no. 8, p. 2301, 2019. DOI: 10.3390/su11082301.

[26] Kraftfahrt Bundesamt, *Bestand nach Haltern: Bestand an Personenkraftwagen am 1. Januar 2020 nach Bundesländern sowie privaten und gewerblichen Haltern absolut*, Flensburg, 2020. URL: https://www.kba.de/DE/Statistik/Fahrzeuge/Bestand/Halter/2020/2020_b_halter_tabellen.html?nn=3524774&fromStatistic=3524774&yearFilter=2020&fromStatistic=3524774&yearFilter=2020 (visited on Feb. 16, 2022).

[27] F. Straub, S. Streppel, and D. Göhlich, "Methodology for Estimating the Spatial and Temporal Power Demand of Private Electric Vehicles for an Entire Urban Region Using Open Data," *Energies*, vol. 14, no. 8, p. 2081, 2021. DOI: 10.3390/en14082081.

[28] F. Straub, O. Maier, and D. Göhlich, "Car-Access Attractiveness of Urban Districts Regarding Shopping and Working Trips for Usage in E-Mobility Traffic Simulations," *Sustainability*, vol. 13, no. 20, p. 11 345, 2021. DOI: 10.3390/su132011345.

[29] F. Straub, O. Maier, D. Göhlich, and Y. Zou, "Forecasting the spatial and temporal charging demand of fully electrified urban private car transportation based on large-scale traffic simulation," *Green Energy and Intelligent Transportation*, vol. 2, no. 1, p. 100 039, 2023. DOI: 10.1016/j.geits.2022.100039.

[30] F. Straub, O. Maier, D. Göhlich, and K. Strunz, "Sector Coupling through Vehicle to Grid: A Case Study for Electric Vehicles and Households in Berlin, Germany," *World Electric Vehicle Journal*, vol. 14, no. 3, p. 77, 2023. DOI: 10.3390/wevj14030077.

[31] H. Lund and W. Kempton, “Integration of renewable energy into the transport and electricity sectors through V2G,” *Energy Policy*, vol. 36, no. 9, pp. 3578–3587, 2008. DOI: `10.1016/j.enpol.2008.06.007`.

[32] E. Apostolaki-Iosifidou, P. Codani, and W. Kempton, “Measurement of power loss during electric vehicle charging and discharging,” *Energy*, vol. 127, pp. 730–742, 2017. DOI: `10.1016/j.energy.2017.03.015`.

[33] U. Datta, N. Saiprasad, A. Kalam, J. Shi, and A. Zayegh, “A price-regulated electric vehicle charge-discharge strategy for G2V, V2H, and V2G,” *International Journal of Energy Research*, vol. 43, no. 2, pp. 1032–1042, 2019. DOI: `10.1002/er.4330`.

[34] J. Wieler, *Elektroautos im Test: So hoch ist der Stromverbrauch*, ADAC e.V., Ed., 2022. URL: `https://www.adac.de/rund-ums-fahrzeug/tests/elektromobilitaet/stromverbrauch-elektroautos-adac-test/` (visited on Jan. 31, 2022).

[35] S. A. Birrell, D. Wilson, C. P. Yang, G. Dhadyalla, and P. Jennings, “How driver behaviour and parking alignment affects inductive charging systems for electric vehicles,” *Transportation Research Part C: Emerging Technologies*, vol. 58, pp. 721–731, 2015. DOI: `10.1016/j.trc.2015.04.011`.

[36] R. Bosshard and J. W. Kolar, “Inductive power transfer for electric vehicle charging: Technical challenges and tradeoffs,” *IEEE Power Electronics Magazine*, vol. 3, no. 3, pp. 22–30, 2016. DOI: `10.1109/MPEL.2016.2583839`.

[37] H. H. Wu, A. Gilchrist, K. Sealy, P. Israelsen, and J. Muhs, “A review on inductive charging for electric vehicles,” in *2011 IEEE International Electric Machines & Drives Conference (IEMDC)*, IEEE, 2011, pp. 143–147. DOI: `10.1109/IEMDC.2011.5994820`.

[38] M. Zucca, O. Bottauscio, S. Harmon, R. Guilizzoni, F. Schilling, M. Schmidt, P. Ankarson, T. Bergsten, K. Tammi, P. Sainio, J. B. Romero, E. L. Puyal, L. Pichon, F. Freschi, V. Cirimele, P. Bauer, J. Dong, A. Maffucci, S. Ventre, N. Femia, G. Di Capua, N. Kuster, and I. Liorni, “Metrology for Inductive Charging of Electric Vehicles (MICEV),” in *2019 AEIT International Conference of Electrical and Electronic Technologies for Automotive (AEIT AUTOMOTIVE)*, IEEE, 2019, pp. 1–6. DOI: `10.23919/EETA.2019.8804498`.

[39] E. Aydin, M. T. Aydemir, A. Aksoz, M. El Baghdadi, and O. Hegazy, “Inductive Power Transfer for Electric Vehicle Charging Applications: A Comprehensive Review,” *Energies*, vol. 15, no. 14, p. 4962, 2022. DOI: `10.3390/en15144962`.

[40] N. Mohamed, F. Aymen, M. Alqarni, R. A. Turky, B. Alamri, Z. M. Ali, and S. H. Abdel Aleem, “A new wireless charging system for electric vehicles using two receiver coils,” *Ain Shams Engineering Journal*, vol. 13, no. 2, p. 101 569, 2022. DOI: `10.1016/j.asej.2021.08.012`.

[41] Plugless Power Inc., *The World is Going Electric: Wireless Technology*, 2022. URL: `https://www.pluglesspower.com/learn-about-plugless-2/` (visited on Nov. 21, 2022).

[42] Volvo Cars Media Relations, *Volvo Cars tests new wireless charging technology*, 2022. URL: `https://www.media.volvocars.com/global/en-gb/media/pressreleases/295720/volvo-cars-tests-new-wireless-charging-technology` (visited on Nov. 21, 2022).

[43] A. M. Vallera, P. M. Nunes, and M. C. Brito, "Why we need battery swapping technology," *Energy Policy*, vol. 157, p. 112 481, 2021. DOI: `10.1016/j.enpol.2021.112481`.

[44] H.-Y. Mak, Y. Rong, and Z.-J. M. Shen, "Infrastructure Planning for Electric Vehicles with Battery Swapping," *Management Science*, vol. 59, no. 7, pp. 1557–1575, 2013. DOI: `10.1287/mnsc.1120.1672`.

[45] F. Ahmad, M. Saad Alam, I. Saad Alsaidan, and S. M. Shariff, "Battery swapping station for electric vehicles: opportunities and challenges," *IET Smart Grid*, vol. 3, no. 3, pp. 280–286, 2020. DOI: `10.1049/iet-stg.2019.0059`.

[46] F. Adegbohun, A. von Jouanne, and K. Lee, "Autonomous Battery Swapping System and Methodologies of Electric Vehicles," *Energies*, vol. 12, no. 4, p. 667, 2019. DOI: `10.3390/en12040667`.

[47] Z. Yang, Q. Lei, J. Sun, X. Hu, and Y. Zhang, "Strategizing battery swap service: Self-operation or authorization?" *Transportation Research Part D: Transport and Environment*, vol. 110, p. 103 411, 2022. DOI: `10.1016/j.trd.2022.103411`.

[48] NIO Deutschland GmbH, *Erste Power-Swap-Station (PSS) von NIO in Deutschland geht ans Netz*, 2022. URL: `https://www.nio.com/de_DE/news/202209280001` (visited on Nov. 19, 2022).

[49] M. Knez, G. K. Zevnik, and M. Obrecht, "A review of available chargers for electric vehicles: United States of America, European Union, and Asia," *Renewable and Sustainable Energy Reviews*, vol. 109, pp. 284–293, 2019. DOI: `10.1016/j.rser.2019.04.013`.

[50] D. Hall and N. Lutsey, *Whitepaper: Emerging best practices for electric vehicle charging infrastructure*, 2017. URL: `https://www.researchgate.net/publication/320211098_Emerging_best_practices_for_electric_vehicle_charging_infrastructure` (visited on Jan. 29, 2022).

[51] P. Boev, E. Lauth, and D. Göhlich, *Whitepaper: Betriebshöfe der Zukunft: Hauptaspekte bei der Umstellung auf Elektrofahrzeuge*, 2020. URL: `https://new.siemens.com/global/en/products/energy/medium-voltage/solutions/emobility/smartdepot.html` (visited on Jan. 29, 2022).

[52] Tesla Inc., *Supercharger*, 2022. URL: `https://www.tesla.com/supercharger` (visited on Jan. 29, 2022).

[53] CHAdeMO Association, *CHAdeMO releases the latest version of the protocol enabling up to 400KW*, 2021. URL: `https://www.chademo.com/chademo-releases-the-latest-version-of-the-protocol-enabling-up-to-400kw/` (visited on Jan. 29, 2022).

[54] CHAdeMO Association, *High Power: High Power roadmap*, 2021. URL: `https://www.chademo.com/technology/high-power/` (visited on Jan. 29, 2022).

[55] G. R. C. Mouli, P. Venugopal, and P. Bauer, "Future of electric vehicle charging," in *2017 International Symposium on Power Electronics (Ee)*, IEEE, 2017. DOI: `10.1109/pee.2017.8171657`.

[56] M. C. Falvo, D. Sbordone, I. S. Bayram, and M. Devetsikiotis, "EV charging stations and modes: International standards," in *2014 International Symposium on Power Electronics, Electrical Drives, Automation and Motion*, IEEE, 2014. DOI: `10.1109/speedam.2014.6872107`.

[57] Q. Lin, J. Wang, R. Xiong, W. Shen, and H. He, "Towards a smarter battery management system: A critical review on optimal charging methods of lithium ion batteries," *Energy*, vol. 183, pp. 220–234, 2019. DOI: `10.1016/j.energy.2019.06.128`.

[58] P. Keil and A. Jossen, "Charging protocols for lithium-ion batteries and their impact on cycle life—An experimental study with different 18650 high-power cells," *Journal of Energy Storage*, vol. 6, pp. 125–141, 2016. DOI: `10.1016/j.est.2016.02.005`.

[59] M. Sterner and I. Stadler, *Energiespeicher - Bedarf, Technologien, Integration*. Berlin, Heidelberg: Springer Berlin Heidelberg, 2017. DOI: `10.1007/978-3-662-48893-5`.

[60] Y. Miao, P. Hynan, A. von Jouanne, and A. Yokochi, "Current Li-Ion Battery Technologies in Electric Vehicles and Opportunities for Advancements," *Energies*, vol. 12, no. 6, p. 1074, 2019. DOI: `10.3390/en12061074`.

[61] W. Shen, T. T. Vo, and A. Kapoor, "Charging algorithms of lithium-ion batteries: An overview," in *2012 7th IEEE Conference on Industrial Electronics and Applications (ICIEA)*, IEEE, 2012, pp. 1567–1572. DOI: `10.1109/ICIEA.2012.6360973`.

[62] D. Fasthuber, "Integration der Ladeinfrastruktur in das elektrische Energiesystem," *e & i Elektrotechnik und Informationstechnik*, vol. 137, no. 4-5, pp. 156–160, 2020. DOI: `10.1007/s00502-020-00806-9`.

[63] K. Liu, K. Li, Q. Peng, and C. Zhang, "A brief review on key technologies in the battery management system of electric vehicles," *Frontiers of Mechanical Engineering*, vol. 14, no. 1, pp. 47–64, 2019. DOI: `10.1007/s11465-018-0516-8`.

[64] H. Liu, I. H. Naqvi, F. Li, C. Liu, N. Shafiei, Y. Li, and M. Pecht, “An analytical model for the CC-CV charge of Li-ion batteries with application to degradation analysis,” *Journal of Energy Storage*, vol. 29, p. 101 342, 2020. DOI: `10.1016/j.est.2020.101342`.

[65] Fastned B.V., *Fast charging*, 2021. URL: `https://support.fastned.nl/hc/en-gb/sections/4409800889105-Fast-charging` (visited on Feb. 15, 2022).

[66] J. d. D. Ortúzar and L. G. Willumsen, *Modelling transport*, 4 ed. Chichester: Wiley, 2014.

[67] M. G. McNally, “The Four-Step Model,” in *Handbook of Logistics and Supply-Chain Management*, ser. Handbooks in Transport, A. M. Brewer, K. J. Button, and D. A. Hensher, Eds., vol. 1, Emerald Group Publishing Limited, 2008, pp. 35–53. DOI: `10.1108/9780857245670-003`.

[68] M. G. McNally and C. R. Rindt, “The Activity-Based Approach,” in *Handbook of Logistics and Supply-Chain Management*, ser. Handbooks in Transport, A. M. Brewer, K. J. Button, and D. A. Hensher, Eds., vol. 1, Emerald Group Publishing Limited, 2008, pp. 55–73. DOI: `10.1108/9780857245670-004`.

[69] J. Su, T. T. Lie, and R. Zamora, “Modelling of large-scale electric vehicles charging demand: A New Zealand case study,” *Electric Power Systems Research*, vol. 167, pp. 171–182, 2019. DOI: `10.1016/j.epsr.2018.10.030`.

[70] N. Andrenacci, R. Ragona, and G. Valenti, “A demand-side approach to the optimal deployment of electric vehicle charging stations in metropolitan areas,” *Applied Energy*, vol. 182, pp. 39–46, 2016. DOI: `10.1016/j.apenergy.2016.07.137`.

[71] F. Heymann, C. Pereira, V. Miranda, and F. J. Soares, “Spatial load forecasting of electric vehicle charging using GIS and diffusion theory,” in *2017 IEEE PES Innovative Smart Grid Technologies Conference Europe (ISGT-Europe)*, Piscataway, NJ: IEEE, 2017, pp. 1–6. DOI: `10.1109/ISGTEurope.2017.8260172`.

[72] Z. Yi and P. H. Bauer, “Spatiotemporal Energy Demand Models for Electric Vehicles,” *IEEE Transactions on Vehicular Technology*, vol. 65, no. 3, pp. 1030–1042, 2016. DOI: `10.1109/TVT.2015.2502249`.

[73] K. J. Dillman, R. Fazeli, E. Shafiei, J. Ö. G. Jónsson, H. V. Haraldsson, and B. Davidsdóttir, “Spatiotemporal analysis of the impact of electric vehicle integration on Reykjavik’s electrical system at the city and distribution system level,” *Utilities Policy*, vol. 68, p. 101 145, 2021. DOI: `10.1016/j.jup.2020.101145`.

[74] O. Arnhold, C. Daam, R. Hirschberg, J. Hofmann, B. Teschner, and F. Gscheidlinger, *Studie Elektromobilität Berlin 2025+*, Reiner Lemoine Institut, Ed., Berlin, 2021.

[75] L. Pan, E. Yao, Y. Yang, and R. Zhang, “A location model for electric vehicle (EV) public charging stations based on drivers’ existing activities,” *Sustainable Cities and Society*, vol. 59, p. 102 192, 2020. DOI: `10.1016/j.scs.2020.102192`.

[76] J. Dong, C. Liu, and Z. Lin, "Charging infrastructure planning for promoting battery electric vehicles: An activity-based approach using multiday travel data," *Transportation Research Part C: Emerging Technologies*, vol. 38, pp. 44–55, 2014. DOI: 10.1016/j.trc.2013.11.001.

[77] L. Knapen, B. Kochan, T. Bellemans, D. Janssens, and G. Wets, "Activity based models for countrywide electric vehicle power demand calculation," in *2011 IEEE First International Workshop on Smart Grid Modeling and Simulation*, IEEE, 2011, pp. 13–18. DOI: 10.1109/SGMS.2011.6089019.

[78] P. Hidalgo, A. E. Trippe, M. Lienkamp, and T. Hamacher, "Mobility Model for the Estimation of the Spatiotemporal Energy Demand of Battery Electric Vehicles in Singapore," in *2015 IEEE 18th International Conference on Intelligent Transportation Systems (ITSC)*, Piscataway, NJ: IEEE, 2015, pp. 578–583. DOI: 10.1109/ITSC.2015.101.

[79] European Union EU, Ed., *Energy Roadmap 2050*, Luxembourg, 2012. DOI: 10.2833/10759. URL: https://data.europa.eu/doi/10.2833/10759 (visited on Dec. 2, 2020).

[80] Presse- und Informationsamt der Bundesregierung, *Ziele der Bundesregierung: Bis 2030 die Treibhausgase halbieren*, Berlin, 2019. URL: https://www.bundesregierung.de/breg-de/themen/klimaschutz/klimaziele-und-sektoren-1669268 (visited on Dec. 2, 2020).

[81] E. Lauth, P. Mundt, and D. Gohlich, "Simulation-based Planning of Depots for Electric Bus Fleets Considering Operations and Charging Management," in *The 4th International Conference on Intelligent Transportation Engineering*, Piscataway, NJ: IEEE, 2019, pp. 327–333. DOI: 10.1109/ICITE.2019.8880250.

[82] D. Jefferies and D. Göhlich, "A Comprehensive TCO Evaluation Method for Electric Bus Systems Based on Discrete-Event Simulation Including Bus Scheduling and Charging Infrastructure Optimisation," *World Electric Vehicle Journal*, vol. 11, no. 3, p. 56, 2020. DOI: 10.3390/wevj11030056.

[83] K. Martins-Turner, A. Grahle, K. Nagel, and D. Göhlich, "Electrification of Urban Freight Transport - a Case Study of the Food Retailing Industry," *Procedia Computer Science*, vol. 170, pp. 757–763, 2020. DOI: 10.1016/j.procs.2020.03.159.

[84] N. Daina, A. Sivakumar, and J. W. Polak, "Modelling electric vehicles use: a survey on the methods," *Renewable and Sustainable Energy Reviews*, vol. 68, pp. 447–460, 2017. DOI: 10.1016/j.rser.2016.10.005.

[85] T. Bellemans, B. Kochan, D. Janssens, G. Wets, T. Arentze, and H. Timmermans, "Implementation Framework and Development Trajectory of FEATHERS Activity-Based Simulation Platform," *Transportation Research Record: Journal of the Transportation Research Board*, vol. 2175, no. 1, pp. 111–119, 2010. DOI: 10.3141/2175-13.

[86] D. Göhlich, K. Nagel, A. M. Syré, A. Grahle, K. Martins-Turner, R. Ewert, R. Miranda Jahn, and D. Jefferies, "Integrated Approach for the Assessment of Strategies for the Decarbonization of Urban Traffic," *Sustainability*, vol. 13, no. 2, p. 839, 2021. DOI: `10.3390/su13020839`.

[87] A. Horni, K. Nagel, and K. Axhausen, *The Multi-Agent Transport Simulation MATSim*. London: Ubiquity Press, 2016. DOI: `10.5334/baw`.

[88] D. Ziemke, I. Kaddoura, and K. Nagel, "The MATSim Open Berlin Scenario: A multimodal agent-based transport simulation scenario based on synthetic demand modeling and open data," *Procedia Computer Science*, vol. 151, pp. 870–877, 2019. DOI: `10.1016/j.procs.2019.04.120`.

[89] C. Nobis and T. Kuhnimhof, *Mobilität in Deutschland – MiD Ergebnisbericht.* Bundesministerium für Verkehr und digitale Infrastruktur, Ed., Bonn, 2019. URL: `http://www.mobilitaet-in-deutschland.de/pdf/MiD2017_Ergebnisbericht.pdf` (visited on Dec. 2, 2020).

[90] infas Institut für angewandte Sozialwissenschaft GmbH and Deutsches Zentrum für Luft- und Raumfahrt e.V., *Mobilität in Tabellen (MiT 2017)*, Bundesministerium für Verkehr und digitale Infrastruktur, Ed., 2019. URL: `https://mobilitaet-in-tabellen.dlr.de/mit/` (visited on Dec. 2, 2020).

[91] Deutsches Zentrum für Luft- und Raumfahrt e.V., *Mobilität in Deutschland 2017 / Zeitreihendatensatz: B3: Lokal-Datensatzpaket – Datensätze mit Angabe von kleinräumigen Gitterzellen*, 2018. URL: `https://daten.clearingstelle-verkehr.de/279/` (visited on Dec. 2, 2020).

[92] Amt für Statistik Berlin-Brandenburg, Ed., *Einwohnerinnen und Einwohner im Land Berlin am 31. Dezember 2018: LOR-Planungsräume*, Berlin, 2019. URL: `https://www.statistik-berlin-brandenburg.de/archiv/a-i-16-hj` (visited on Sep. 1, 2021).

[93] Senatsverwaltung für Umwelt, Verkehr und Klimaschutz, *Mobilität der Stadt: Berliner Verkehr in Zahlen 2017*, 2017. URL: `https://www.berlin.de/sen/uvk/verkehr/verkehrsdaten/zahlen-und-fakten/mobilitaet-der-stadt-berliner-verkehr-in-zahlen-2017/` (visited on Sep. 2, 2021).

[94] Amt für Statistik Berlin-Brandenburg, *Ergebnisse des Mikrozensus im Land Berlin 2018: Haushalte,Familien und Lebensformen*, 2019. URL: `https://www.statistik-berlin-brandenburg.de/publikationen/stat_berichte/2019/SB_A01-11-00_2018j01_BE.pdf` (visited on May 29, 2020).

[95] Senatsverwaltung für Wirtschaft, Energie und Betriebe, Ed., *Wohnlagenkarte nach Adressen zum Berliner Mietspiegel 2019*, Berlin, 2019. URL: `https://daten.berlin.de/datensaetze/wohnlagenkarte-nach-adressen-zum-berliner-mietspiegel-2019-wms-1` (visited on Dec. 2, 2020).

[96] BDEW Bundesverband der Energie- und Wasserwirtschaft e.V., *Meinungsbild E-Mobilität: Meinungsbild der Bevölkerung zur Elektromobilität*, Berlin, 2019. URL: `https://www.bdew.de/media/documents/Awh_20190527_Fakten-und-Argumente-Meinungsbild-E-Mobilitaet.pdf` (visited on Jan. 9, 2021).

[97] Kraftfahrt Bundesamt, *Bestand an Personenkraftwagen am 1. Januar 2018 nach Bundesländern sowie privaten und gewerblichen Haltern absolut*, Flensburg, 2018. URL: `https://www.kba.de/DE/Statistik/Fahrzeuge/Bestand/Halter/2018/2018_b_halter_tabellen.html?nn=3524774&fromStatistic=3524774&yearFilter=2018&fromStatistic=3524774&yearFilter=2018` (visited on Dec. 2, 2020).

[98] H. Bömermann, "Stadtgebiet und Gliederungen," *Zeitschrift für amtliche Statistik Berlin und Brandenburg*, no. 1+2, pp. 76–87, 2012. URL: `https://www.statistik-berlin-brandenburg.de/publikationen/aufsaetze/2012/HZ_201201-06.pdf` (visited on Dec. 2, 2020).

[99] G. Meinlschmidt, *Handlungsorientierter Sozialstrukturatlas Berlin 2013*, Senatsverwaltung für Gesundheit und Soziales, Ed., Berlin, 2014. URL: `https://www.gesundheitliche-chancengleichheit.de/handlungsorientierter-sozialstrukturatlas-berlin-2013/` (visited on Jan. 10, 2021).

[100] ADAC e.V., Ed., *Ecotest: Test-und Bewertungskriterien(ab 2/2019)*, München, 2020. URL: `https://www.adac.de/_mmm/pdf/Methodik_EcoTest_2020_292234.pdf` (visited on Dec. 2, 2020).

[101] ADAC e.V., *Mitsubishi i-MiEV*, 2011. URL: `https://www.adac.de/_ext/itr/tests/Autotest/AT4517_Mitsubishi_i_MiEV/Mitsubishi_i_MiEV.pdf` (visited on Dec. 2, 2020).

[102] ADAC e.V., *Renault Zoe R135 Z.E. 50 (52 kWh) Intens*, 2020. URL: `https://assets.adac.de/image/upload/Autodatenbank/Autotest/AT5969_Renault_Zoe_R135_Z_E_50_52_kWh_Intens_mit_Batteriemiete/Renault_Zoe_R135_Z_E_50_52_kWh_Intens_mit_Batteriemiete.pdf` (visited on Jun. 6, 2022).

[103] ADAC e.V., *VW e-up!* 2018. URL: `https://assets.adac.de/image/upload/Autodatenbank/Autotest/AT5776_VW_e_up/VW_e_up.pdf` (visited on Jun. 6, 2022).

[104] ADAC e.V., *BMW i3 (120 Ah)*, 2019. URL: `https://assets.adac.de/image/upload/Autodatenbank/Autotest/AT5861_BMW_i3_120_Ah/BMW_i3_120_Ah.pdf` (visited on Jun. 6, 2022).

[105] ADAC e.V., *Hyundai Kona Elektro (64 kWh) Premium*, 2018. URL: `https://assets.adac.de/image/upload/Autodatenbank/Autotest/AT5773_Hyundai_Kona_Elektro_64_kWh_Premium/Hyundai_Kona_Elektro_64_kWh_Premium.pdf` (visited on Jun. 6, 2022).

[106] ADAC e.V., *VW e-Golf*, 2018. URL: `https://www.adac.de/_ext/itr/tests/Autotest/AT5678_VW_e-Golf/VW_e-Golf.pdf` (visited on Dec. 2, 2020).

[107] ADAC e.V., *KIA e-Niro (64 kWh) Spirit*, 2019. URL: https://assets.adac.de/image/upload/Autodatenbank/Autotest/AT5866_KIA_e_Niro_64_kWh_Spirit/KIA_e_Niro_64_kWh_Spirit.pdf (visited on Jun. 6, 2022).

[108] ADAC e.V., *Nissan Leaf (62 kWh) e+ Tekna*, 2020. URL: https://assets.adac.de/image/upload/Autodatenbank/Autotest/AT5962_Nissan_Leaf_62_kWh_ePlus_Tekna/Nissan_Leaf_62_kWh_ePlus_Tekna.pdf (visited on Jun. 6, 2022).

[109] ADAC e.V., *Tesla Model 3 Standard Range Plus*, 2019. URL: https://www.adac.de/_ext/itr/tests/Autotest/AT5933_Tesla_Model_3_Standard_Range_Plus/Tesla_Model_3_Standard_Range_Plus.pdf (visited on Dec. 2, 2020).

[110] ADAC e.V., *Audi e-tron 55 quattro*, 2019. URL: https://assets.adac.de/image/upload/Autodatenbank/Autotest/AT5926_Audi_e_tron_55_quattro/Audi_e_tron_55_quattro.pdf (visited on Jun. 6, 2022).

[111] ADAC e.V., *Mercedes EQC 400 AMG Line 4MATIC*, 2020. URL: https://assets.adac.de/image/upload/Autodatenbank/Autotest/AT5973_Mercedes_EQC_400_AMG_Line_4MATIC/Mercedes_EQC_400_AMG_Line_4MATIC.pdf (visited on Jun. 6, 2022).

[112] ADAC e.V., *Tesla Model S P90D*, 2017. URL: https://www.adac.de/_ext/itr/tests/Autotest/AT5531_Tesla_Model_S_P90D/Tesla_Model_S_P90D.pdf (visited on Dec. 2, 2020).

[113] Statistisches Bundesamt, *Zeitverwendungserhebung: Aktivitäten in Stunden und Minuten für ausgewählte Personengruppen*, Wiesbaden, 2015. URL: https://www.destatis.de/DE/Themen/Gesellschaft-Umwelt/Einkommen-Konsum-Lebensbedingungen/Zeitverwendung/Publikationen/Downloads-Zeitverwendung/zeitverwendung-5639102139004.pdf?__blob=publicationFile (visited on Dec. 2, 2020).

[114] Stromnetz Berlin GmbH, Ed., *Netznutzer: Standartlastprofile für 2009-2021*, Berlin, 2023. URL: https://www.stromnetz.berlin/en/grid-use/grid-user/ (visited on Mar. 9, 2023).

[115] C. Fünfgeld and R. Tiedemann, *Anwendung der Repräsentativen VDEW-Lastprofile: step - by - step*, BDEW Bundesverband der Energie- und Wasserwirtschaft e.V., Ed., 2000. URL: https://www.bdew.de/media/documents/2000131_Anwendung-repraesentativen_Lastprofile-Step-by-step.pdf (visited on Nov. 4, 2020).

[116] M. Frondel, N. Ritter, and S. Sommer, "Stromverbrauch privater Haushalte in Deutschland – Eine ökonometrische Analyse," *Zeitschrift für Energiewirtschaft*, vol. 39, no. 3, pp. 221–232, 2015. DOI: 10.1007/s12398-015-0157-0.

[117] M. Muratori, "Impact of uncoordinated plug-in electric vehicle charging on residential power demand," *Nature Energy*, vol. 3, no. 3, pp. 193–201, 2018. DOI: 10.1038/s41560-017-0074-z.

[118] S. Mal, A. Chattopadhyay, A. Yang, and R. Gadh, “Electric vehicle smart charging and vehicle-to-grid operation,” *International Journal of Parallel, Emergent and Distributed Systems*, vol. 28, no. 3, pp. 249–265, 2013. DOI: 10.1080/17445760.2012.663757.

[119] E. Veldman and R. A. Verzijlbergh, “Distribution Grid Impacts of Smart Electric Vehicle Charging From Different Perspectives,” *IEEE Transactions on Smart Grid*, vol. 6, no. 1, pp. 333–342, 2015. DOI: 10.1109/TSG.2014.2355494.

[120] D. Göhlich and A. F. Raab, Eds., *Mobility2Grid - Sektorenübergreifende Energie- und Verkehrswende*. Berlin, Heidelberg: Springer Berlin Heidelberg, 2021. DOI: 10.1007/978-3-662-62629-0.

[121] H. J. van Zuylen and L. G. Willumsen, “The most likely trip matrix estimated from traffic counts,” *Transportation Research Part B: Methodological*, vol. 14, no. 3, pp. 281–293, 1980. DOI: 10.1016/0191-2615(80)90008-9.

[122] M. J. Maher, “Inferences on trip matrices from observations on link volumes: A Bayesian statistical approach,” *Transportation Research Part B: Methodological*, vol. 17, no. 6, pp. 435–447, 1983. DOI: 10.1016/0191-2615(83)90030-9.

[123] M. Savrasovs and I. Pticina, “Methodology of OD Matrix Estimation Based on Video Recordings and Traffic Counts,” *Procedia Engineering*, vol. 178, pp. 289–297, 2017. DOI: 10.1016/j.proeng.2017.01.116.

[124] D. Bauer, G. Richter, J. Asamer, B. Heilmann, G. Lenz, and R. Kolbl, “Quasi-Dynamic Estimation of OD Flows From Traffic Counts Without Prior OD Matrix,” *IEEE Transactions on Intelligent Transportation Systems*, vol. 19, no. 6, pp. 2025–2034, 2018. DOI: 10.1109/TITS.2017.2741528.

[125] L. Alexander, S. Jiang, M. Murga, and M. C. González, “Origin–destination trips by purpose and time of day inferred from mobile phone data,” *Transportation Research Part C: Emerging Technologies*, vol. 58, pp. 240–250, 2015. DOI: 10.1016/j.trc.2015.02.018.

[126] M. S. Iqbal, C. F. Choudhury, P. Wang, and M. C. González, “Development of origin–destination matrices using mobile phone call data,” *Transportation Research Part C: Emerging Technologies*, vol. 40, pp. 63–74, 2014. DOI: 10.1016/j.trc.2014.01.002.

[127] D. Bachir, G. Khodabandelou, V. Gauthier, M. El Yacoubi, and J. Puchinger, “Inferring dynamic origin-destination flows by transport mode using mobile phone data,” *Transportation Research Part C: Emerging Technologies*, vol. 101, pp. 254–275, 2019. DOI: 10.1016/j.trc.2019.02.013.

[128] A. Horni, D. M. Scott, M. Balmer, and K. W. Axhausen, “Location Choice Modeling for Shopping and Leisure Activities with MATSim,” *Transportation Research Record: Journal of the Transportation Research Board*, vol. 2135, no. 1, pp. 87–95, 2009. DOI: 10.3141/2135-11.

[129] A. Kubis and M. Hartmann, “Analysis of Location of Large-area Shopping Centres. A Probabilistic Gravity Model for the Halle–Leipzig Area,” *Jahrbuch für Regionalwissenschaft*, vol. 27, no. 1, pp. 43–57, 2007. DOI: 10.1007/s10037-006-0010-3.

[130] J. Gonzalez-Feliu and C. Peris-Pla, “Impacts of retailing attractiveness on freight and shopping trip attraction rates,” *Research in Transportation Business & Management*, vol. 24, pp. 49–58, 2017. DOI: 10.1016/j.rtbm.2017.07.004.

[131] N. Caceres, L. M. Romero, and F. G. Benitez, “Estimating Traffic Flow Profiles According to a Relative Attractiveness Factor,” *Procedia - Social and Behavioral Sciences*, vol. 54, pp. 1115–1124, 2012. DOI: 10.1016/j.sbspro.2012.09.826.

[132] T. Drezner and Z. Drezner, “Validating the Gravity-Based Competitive Location Model Using Inferred Attractiveness,” *Annals of Operations Research*, vol. 111, no. 1/4, pp. 227–237, 2002. DOI: 10.1023/A:1020910021280.

[133] Senatsverwaltung für Stadtentwicklung und Wohnen, *Lebensweltlich orientierte Räume (LOR) in Berlin*, Berlin, 2023. URL: https://www.berlin.de/sen/sbw/stadtdaten/stadtwissen/sozialraumorientierte-planungsgrundlagen/lebensweltlich-orientierte-raeume/ (visited on Mar. 1, 2023).

[134] OpenStreetMap contributors, *OpenStreetMap*, 2021. URL: https://www.openstreetmap.org (visited on Feb. 4, 2021).

[135] Geofabrik GmbH, *OpenStreetMap*, Karlsruhe, 2021. URL: https://www.geofabrik.de/en/geofabrik/ (visited on Feb. 4, 2021).

[136] Open Knowledge Foundation, *Open Data Commons: Open Data Commons Open Database License (ODbL)*, 2021. URL: https://opendatacommons.org/licenses/odbl/ (visited on Feb. 4, 2021).

[137] OpenStreetMap Wiki contributors, *Elements*, OpenStreetMap Wiki, Ed., 2021. URL: https://wiki.openstreetmap.org/w/index.php?title=Elements&oldid=2056268 (visited on Feb. 4, 2021).

[138] H.-G. Tillmann, W. Kleiber, and W. Seitz, *Tabellenhandbuch zur Ermittlung des Verkehrswerts und des Beleihungswerts von Grundstücken: Tabellen, Indizes, Formeln und Normen für die Praxis*, 2nd ed. Köln: Bundesanzeiger Verlag, 2017. URL: https://ebookcentral.proquest.com/lib/gbv/detail.action?docID=5091491.

[139] EHI Retail Institute GmbH, *Entwicklung der durchschnittlichen Verkaufsfläche der Lebensmittel-Discountmärkte Aldi Nord in Deutschland in den Jahren 2009 bis 2019 (in Quadratmetern)*, Köln, 2020. URL: `https://www.handelsdaten.de/lebensmittelhandel/durchschnittliche-verkaufsflaeche-discountmaerkte-aldi-nord-deutschland-zeitreihe` (visited on Feb. 7, 2021).

[140] EHI Retail Institute GmbH, *Durchschnittliche Verkaufsfläche der Verkaufsstellen ausgewählter Lebensmittelhändler in Deutschland in den Jahren 2013 bis 2018 (in Quadratmetern)*, Köln, 2019. URL: `https://www.handelsdaten.de/lebensmittelhandel/durchschnittliche-verkaufsflaeche-der-standorte-ausgewaehlter` (visited on Feb. 7, 2021).

[141] Landesamt für Bauen und Verkehr, *Einzelhandelsstruktur und Verkaufsflächen in der Hauptstadtregion Berlin-Brandenburg 2015/2016*, Gemeinsame Landesplanungsabteilung Berlin-Brandenburg, Ed., 2017. URL: `https://lbv.brandenburg.de/dateien/stadt_wohnen/einzelhandelsstruktur_und_verkaufsraumfl_chen_in_der_hauptstadtregion_berlin-brandenburg_2015_2016.pdf` (visited on Jun. 27, 2021).

[142] Amt für Statistik Berlin-Brandenburg, *Ergebnisse des Mikrozensus im Land Berlin 2016: Bevölkerung und Erwerbstätigkeit*, 2017. URL: `https://www.statistik-berlin-brandenburg.de/publikationen/stat_berichte/2017/SB_A01-10-00_2016j01_BE.pdf` (visited on Feb. 7, 2021).

[143] Amt für Statistik Berlin-Brandenburg, *Ergebnisse des Mikrozensus im Land Berlin 2019: Bevölkerung und Erwerbstätigkeit*, 2020. URL: `https://www.statistik-berlin-brandenburg.de/publikationen/stat_berichte/2020/SB_A01-10-00_2019j01_BE.pdf` (visited on Feb. 7, 2021).

[144] Fraunhofer-Institut für System- und Innovationsforschung, *Energieverbrauch des Sektors Gewerbe, Handel, Dienstleistungen (GHD) in Deutschland für die Jahre 2011 bis 2013: Schlussbericht an das Bundesministerium für Wirtschaft und Energie (BMWi)*, 2015. URL: `https://www.bmwk.de/Redaktion/DE/Publikationen/Studien/sondererhebung-zur-nutzung-erneuerbarer-energien-im-gdh-sektor-2011-2013.pdf?__blob=publicationFile&v=6` (visited on Jun. 27, 2021).

[145] Amt für Statistik Berlin-Brandenburg, *Sozialversicherungspflichtig Beschäftigte im Land Berlin 30. Juni 2019*, Berlin, 2020. URL: `https://www.statistik-berlin-brandenburg.de/publikationen/Stat_Berichte/2020/SB_A06-20-00_2019j01_BE.pdf` (visited on Feb. 7, 2021).

[146] Bundesagentur für Arbeit, *Pendlerverflechtungen der sozialversicherungspflichtig Beschäftigten nach Kreisen: Berlin, Stichtag 30. Juni 2019*, 2020. URL: `https://statistik.arbeitsagentur.de/SiteGlobals/Forms/Suche/Einzelheftsuche_Formular.html?nn=20934&topic_f=beschaeftigung-sozbe-krpend` (visited on Feb. 8, 2021).

[147] P. van der waerden, H. Timmermans, and M. de Bruin-Verhoeven, "Car drivers' characteristics and the maximum walking distance between parking facility and final destination," *Journal of Transport and Land Use*, 2013. DOI: 10.5198/jtlu.2015.568.

[148] W. Zhang, F. Gao, S. Sun, Q. Yu, J. Tang, and B. Liu, "A Distribution Model for Shared Parking in Residential Zones that Considers the Utilization Rate and the Walking Distance," *Journal of Advanced Transportation*, vol. 2020, pp. 1–11, 2020. DOI: 10.1155/2020/6147974.

[149] K. Hymel, "Do parking fees affect retail sales? Evidence from Starbucks," *Economics of Transportation*, vol. 3, no. 3, pp. 221–233, 2014. DOI: 10.1016/j.ecotra.2014.08.001.

[150] P. van der Waerden, A. Borgers, and H. Timmermans, "Consumer Response to Introduction of Paid Parking at a Regional Shopping Center," *Transportation Research Record: Journal of the Transportation Research Board*, vol. 2118, no. 1, pp. 16–23, 2009. DOI: 10.3141/2118-03.

[151] E. Triantaphyllou and K. Baig, "The Impact of Aggregating Benefit and Cost Criteria in Four MCDA Methods," *IEEE Transactions on Engineering Management*, vol. 52, no. 2, pp. 213–226, 2005. DOI: 10.1109/tem.2005.845221.

[152] P. C. Fishburn, "Additive Utilities with Incomplete Product Sets: Application to Priorities and Assignments," *Operations Research*, vol. 15, no. 3, pp. 537–542, 1967. DOI: 10.1287/opre.15.3.537.

[153] C. Boulange, L. Gunn, B. Giles-Corti, S. Mavoa, C. Pettit, and H. Badland, "Examining associations between urban design attributes and transport mode choice for walking, cycling, public transport and private motor vehicle trips," *Journal of Transport & Health*, vol. 6, pp. 155–166, 2017. DOI: 10.1016/j.jth.2017.07.007.

[154] N. Limtanakool, M. Dijst, and T. Schwanen, "The influence of socioeconomic characteristics, land use and travel time considerations on mode choice for medium- and longer-distance trips," *Journal of Transport Geography*, vol. 14, no. 5, pp. 327–341, 2006. DOI: 10.1016/j.jtrangeo.2005.06.004.

[155] S. S. Wibowo and P. Olszewski, "Modeling walking accessibility to public transport terminals: Case study of Singapore mass rapid transit," *Journal of the Eastern Asia Society for Transportation Studies*, vol. 6, pp. 147–156, 2005. DOI: 10.11175/easts.6.147.

[156] U. Schäffeler, "Netzgestaltungsgrundsätze für den öffentlichen Personennahverkehr in Verdichtungsräumen," Dissertation, ETH Zurich, 2005. DOI: 10.3929/ETHZ-A-004882967.

[157] Transport for London, *Assessing transport connectivity in London*, London, 2015. URL: `https://content.tfl.gov.uk/connectivity-assessment-guide.pdf` (visited on Feb. 23, 2021).

[158] R. Daniels and C. Mulley, "Explaining walking distance to public transport: The dominance of public transport supply," *Journal of Transport and Land Use*, vol. 6, no. 2, p. 5, 2013. DOI: `10.5198/jtlu.v6i2.308`.

[159] HeiGIT gGmbH, *OpenRouteService: Services, Time-Distance Matrix*, 2020. URL: `https://openrouteservice.org/services/` (visited on Feb. 25, 2021).

[160] A. E. Dingil, J. Schweizer, F. Rupi, and Z. Stasiskiene, "Transport indicator analysis and comparison of 151 urban areas, based on open source data," *European Transport Research Review*, vol. 10, no. 2, 2018. DOI: `10.1186/s12544-018-0334-4`.

[161] Verlag Der Tagesspiegel GmbH, *Lückenschluss in der Fußgängerzone: Heute eröffnen die Wilmersdorfer Arcaden als 57. Shoppingcenter Berlins*, Berlin, 2007. URL: `https://www.tagesspiegel.de/berlin/lueckenschluss-in-der-fussgaengerzone/1052184.html` (visited on Mar. 20, 2021).

[162] IZ Immobilien Zeitung Verlagsgesellschaft mbH, *Spandau Arcaden vor der Eröffnung*, Wiesbaden, 2001. URL: `https://www.immobilien-zeitung.de/20401/spandau-arcaden-vor-eroeffnung` (visited on Mar. 20, 2021).

[163] BerlinOnline Stadtportal GmbH & Co. KG, *Bikini Berlin*, Berlin, 2020. URL: `https://www.berlin.de/special/shopping/einkaufscenter/3305576-1724954-bikini-berlin.html` (visited on Mar. 20, 2021).

[164] J. E. Kang and W. W. Recker, "An activity-based assessment of the potential impacts of plug-in hybrid electric vehicles on energy and emissions using 1-day travel data," *Transportation Research Part D: Transport and Environment*, vol. 14, no. 8, pp. 541–556, 2009. DOI: `10.1016/j.trd.2009.07.012`.

[165] V. L. Bernardin, F. Koppelman, and D. Boyce, "Enhanced Destination Choice Models Incorporating Agglomeration Related to Trip Chaining While Controlling for Spatial Competition," *Transportation Research Record: Journal of the Transportation Research Board*, vol. 2132, no. 1, pp. 143–151, 2009. DOI: `10.3141/2132-16`.

[166] L.-F. Chow, F. Zhao, M.-T. Li, and S.-C. Li, "Development and Evaluation of Aggregate Destination Choice Models for Trip Distribution in Florida," *Transportation Research Record: Journal of the Transportation Research Board*, vol. 1931, pp. 18–27, 2005. DOI: `10.3141/1931-03`.

[167] B. Mei, "Destination Choice Model for Commercial Vehicle Movements in Metropolitan Area," *Transportation Research Record: Journal of the Transportation Research Board*, vol. 2344, no. 1, pp. 126–134, 2013. DOI: `10.3141/2344-14`.

[168] N. Jonnalagadda, J. Freedman, W. A. Davidson, and J. D. Hunt, "Development of Microsimulation Activity-Based Model for San Francisco: Destination and Mode Choice Models," *Transportation Research Record: Journal of the Transportation Research Board*, vol. 1777, no. 1, pp. 25–35, 2001. DOI: `10.3141/1777-03`.

[169] C. Bhat, A. Govindarajan, and V. Pulugurta, "Disaggregate Attraction-End Choice Modeling: Formulation and Empirical Analysis," *Transportation Research Record: Journal of the Transportation Research Board*, vol. 1645, no. 1, pp. 60–68, 1998. DOI: `10.3141/1645-08`.

[170] V. Kutzki, "Pendlerverflechtungen sozialversicherungspflichtig Beschäftigter in der Metropolregion Berlin-Brandenburg," *Zeitschrift für amtliche Statistik*, no. 3, pp. 32–39, 2015. URL: `https://download.statistik-berlin-brandenburg.de/c9211799b5b546e4/df4b2ae3fafd/hz_201503-04.pdf` (visited on Jan. 20, 2022).

[171] V. Klingspor, "Berechnung populärer Routen Calculating Popular Routes," *AGIT Journal für Angewandte Geoinformatik*, no. 4, pp. 189–198, 2018. DOI: `10.14627/537647024`.

[172] L. Bornmann, H. Schier, W. Marx, and H.-D. Daniel, "Is interactive open access publishing able to identify high-impact submissions? A study on the predictive validity of Atmospheric Chemistry and Physics by using percentile rank classes," *Journal of the American Society for Information Science and Technology*, vol. 62, no. 1, pp. 61–71, 2011. DOI: `10.1002/asi.21418`.

[173] A. Seidel, *Parkplatzzählung und Parkraumanalysen auf OSM-Basis*, 2021. URL: `https://supaplexosm.github.io/strassenraumkarte-neukoelln/parkraumkarte/report` (visited on Dec. 10, 2021).

[174] Statistisches Bundesamt, *Strukturdaten über sozialversicherungspflichtige Beschäftigte am Arbeitsort*, Wiesbaden, 2021. URL: `https://www.destatis.de/DE/Themen/Arbeit/Arbeitsmarkt/Erwerbstaetigkeit/Tabellen/strukturdaten.html` (visited on Dec. 17, 2021).

[175] Statistisches Bundesamt, *Wöchentliche Arbeitszeit*, Wiesbaden, 2021. URL: `https://www.destatis.de/DE/Themen/Arbeit/Arbeitsmarkt/Qualitaet-Arbeit/Dimension-3/woechentliche-arbeitszeitl.html` (visited on Dec. 17, 2021).

[176] F. Hacker, R. Blanck, F. Hülsmann, P. Kasten, C. Loreck, S. Ludig, M. Mottschall, and W. Zimmer, *eMobil 2050: Szenarien zum möglichen Beitrag des Szenarien zum möglichen Beitrag des elektrischen Verkehrs zum langfristigen Klimaschutz*, Berlin, 2014. URL: `https://www.bmuv.de/fileadmin/Daten_BMU/Pools/Forschungsdatenbank/fkz_um_11_96_106_elektromobilitaet_bf.pdf` (visited on Jan. 12, 2022).

[177] BMW Group, Ed., *BMW Group baut Ladeinfrastruktur weiter aus*, 2019. URL: `https://www.press.bmwgroup.com/deutschland/article/detail/T0303719DE/bmw-group-baut-ladeinfrastruktur-weiter-aus?language=de` (visited on Sep. 1, 2021).

[178] Audi AG, Ed., *Audi investiert rund 100 Millionen Euro in Ladeinfrastruktur an eigenen Standorten*, Ingolstadt, 2020. URL: https://www.audi-mediacenter.com/de/pressemitteilungen/audi-investiert-rund-100-millionen-euro-in-ladeinfrastruktur-an-eigenen-standorten-12480 (visited on Sep. 1, 2021).

[179] ALDI SÜD Dienstleistungs-GmbH & Co. oHG, Ed., *ALDI elektrisiert: E-Ladestationen an weiteren ALDI SÜD Filialen*, Mülheim an der Ruhr, 2021. URL: https://www.aldi-sued.de/de/nachhaltigkeit/neuigkeiten/e-ladestationen.html (visited on Sep. 1, 2021).

[180] Lidl Digital International GmbH & Co. KG, Ed., *Volle Ladung E-Mobilität*, Neckarsulm, 2021. URL: https://www.lidl.de/c/echarge-app/s10007751 (visited on Sep. 1, 2021).

[181] Handelsgesellschaft für Baustoffe mbH & Co. KG and Energie Baden-Württemberg AG, Eds., *Schnelles Laden kommt zum Kunden*, Dorsten, Soltau, and Karlsruhe, 2019. URL: https://www.hagebau.com/unternehmen/hagebau-unternehmensgruppe/aktuelles/presse/schnelles-laden-kommt-zum-kunden.html (visited on Sep. 1, 2021).

[182] X. Zhang, Y. Zou, J. Fan, and H. Guo, "Usage pattern analysis of Beijing private electric vehicles based on real-world data," *Energy*, vol. 167, pp. 1074–1085, 2019. DOI: 10.1016/j.energy.2018.11.005.

[183] W. Rudschies, *Elektroautos auf der Langstrecke: Wie kann das funktionieren?* 2020. URL: https://www.adac.de/rund-ums-fahrzeug/tests/elektromobilitaet/schnellladen-langstrecke-ladekurven/ (visited on Jun. 11, 2020).

[184] Stromnetz Berlin GmbH, *Faktenblatt, Stromnetz Berlin GmbH*, Berlin, 2022. URL: https://www.stromnetz.berlin/globalassets/dokumente/presse/faktenblatt-stromnetz-berlin.pdf (visited on Jun. 2, 2022).

[185] Bundesministerium für Umwelt, Naturschutz, nukleare Sicherheit und Verbraucherschutz, *Strombedarf und Netze: Ist das Stromnetz fit für die Elektromobilität?* 2020. URL: https://www.bmuv.de/themen/luft-laerm-mobilitaet/verkehr/elektromobilitaet/strombedarf-und-netze (visited on Mar. 18, 2022).

[186] L. Liu, "Einfluss der privaten Elektrofahrzeuge auf Mittel- und Niederspannungsnetze," Dissertation, Technische Universität Darmstadt, Darmstadt, 2017. URL: https://tuprints.ulb.tu-darmstadt.de/7171/1/Liu_Diss_2018e.pdf (visited on Jun. 17, 2020).

[187] R. Wörner, P. Bauer, D. Schneider, M. Oncken, I. Morozova, M. Kagerbauer, N. Kostorz, P. Jochem, A. Märtz, M. Blesl, M. Wiesmeth, D. Mayer, C. Körner, and J. Schmalen, *Elektromobilität im urbanen Raum - Analysen und Prognosen im Spannungsfeld von Elektromobilität und Energieversorgung am Fallbeispiel Stuttgart*, 2019. URL: `https://pudi.lubw.de/detailseite/-/publication/10118-elektromobilit%c3%a4t_im_urbanen_raum_-_analysen_und_prognosen_im_spannungsfeld_von_elektromobilit%c3%a4t_und_.pdf` (visited on Mar. 18, 2022).

[188] R. Follmer, D. Gruschwitz, J. Eggs, C. Nobis, M. Bäumer, and M. Herter, "Mobilität in der Europäischen Metropolregion Stuttgart," in *Mobilitätskongress der Europäischen Metropolregion Stuttgart*, 2019, pp. 1–23. URL: `https://nachhaltige-mobilitaet.region-stuttgart.de/wp-content/uploads/2020/04/infas_Pr%C3%A4sentation_Mobilit%C3%A4tskongress-2019.pdf` (visited on Mar. 19, 2022).

[189] Netze BW GmbH, *Die E-Mobility-Allee: Das Stromnetz-Reallabor zur Erforschung des zukünftigen E-Mobility-Alltags*, 2019. URL: `https://assets.ctfassets.net/xytfb1vrn7of/6gXs8wiRSF0E2SqkwSq406/fc1c9430ba88b81c31e399242b09b17e/20191217_BroschuereE-Mobility_210x275mm_100Ansicht.pdf` (visited on Mar. 18, 2022).

[190] Kraftfahrt Bundesamt, *Bestand an Personenkraftwagen in den Jahren 2012 bis 2021 nach ausgewählten Kraftstoffarten*, 2022. URL: `https://www.kba.de/DE/Statistik/Fahrzeuge/Bestand/Umwelt/2021/2021_b_umwelt_zeitreihen.html?nn=3525028&fromStatistic=3525028&yearFilter=2021&fromStatistic=3525028&yearFilter=2021` (visited on Feb. 15, 2022).

[191] ADAC e.V., *Mitsubishi i-MiEV*, 2013. URL: `https://assets.adac.de/image/upload/Autodatenbank/Autotest/AT5051_Mitsubishi_i_MiEV/Mitsubishi_i_MiEV.pdf` (visited on Jun. 4, 2022).

[192] ADAC e.V., *VW e-Golf*, 2018. URL: `https://assets.adac.de/image/upload/Autodatenbank/Autotest/AT5678_VW_e-Golf/VW_e-Golf.pdf` (visited on Jun. 6, 2022).

[193] ADAC e.V., *Tesla Model 3 Standard Range Plus*, 2019. URL: `https://assets.adac.de/image/upload/Autodatenbank/Autotest/AT5933_Tesla_Model_3_Standard_Range_Plus/Tesla_Model_3_Standard_Range_Plus.pdf` (visited on Jun. 6, 2022).

[194] ADAC e.V., *Tesla Model S P90D*, 2017. URL: `https://assets.adac.de/image/upload/Autodatenbank/Autotest/AT5531_Tesla_Model_S_P90D/Tesla_Model_S_P90D.pdf` (visited on Jun. 6, 2022).

[195] T. Tröndle, S. Pfenninger, and J. Lilliestam, "Home-made or imported: On the possibility for renewable electricity autarky on all scales in Europe," *Energy Strategy Reviews*, vol. 26, p. 100 388, 2019. DOI: `10.1016/j.esr.2019.100388`.

[196] João Peças Lopes, Pedro Miguel Rocha Almeida, Antero Miguel Silva, and Filipe Joel Soares, "Smart Charging Strategies for Electric Vehicles: Enhancing Grid Performance and Maximizing the Use of Variable Renewable Energy Resources," *Proc. EVS24 Int. Battery, Hybrid and Fuel Cell EV Symp*, 2009. URL: `https://repositorio.inesctec.pt/handle/123456789/3091`.

[197] P. Mesarić and S. Krajcar, "Home demand side management integrated with electric vehicles and renewable energy sources," *Energy and Buildings*, vol. 108, pp. 1–9, 2015. DOI: `10.1016/j.enbuild.2015.09.001`.

[198] M. Aziz, T. Oda, T. Mitani, Y. Watanabe, and T. Kashiwagi, "Utilization of Electric Vehicles and Their Used Batteries for Peak-Load Shifting," *Energies*, vol. 8, no. 5, pp. 3720–3738, 2015. DOI: `10.3390/en8053720`.

[199] V. Heinisch, L. Göransson, R. Erlandsson, H. Hodel, F. Johnsson, and M. Odenberger, "Smart electric vehicle charging strategies for sectoral coupling in a city energy system," *Applied Energy*, vol. 288, p. 116 640, 2021. DOI: `10.1016/j.apenergy.2021.116640`.

[200] F. Lo Franco, M. Ricco, R. Mandrioli, and G. Grandi, "Electric Vehicle Aggregate Power Flow Prediction and Smart Charging System for Distributed Renewable Energy Self-Consumption Optimization," *Energies*, vol. 13, no. 19, p. 5003, 2020. DOI: `10.3390/en13195003`.

[201] K. Seddig, P. Jochem, and W. Fichtner, "Integrating renewable energy sources by electric vehicle fleets under uncertainty," *Energy*, vol. 141, pp. 2145–2153, 2017. DOI: `10.1016/j.energy.2017.11.140`.

[202] G. Fridgen, R. Keller, M.-F. Körner, and M. Schöpf, "A holistic view on sector coupling," *Energy Policy*, vol. 147, p. 111 913, 2020. DOI: `10.1016/j.enpol.2020.111913`.

[203] J. Ramsebner, R. Haas, A. Ajanovic, and M. Wietschel, "The sector coupling concept: A critical review," *WIREs Energy and Environment*, vol. 10, no. 4, 2021. DOI: `10.1002/wene.396`.

[204] M. Robinius, A. Otto, P. Heuser, L. Welder, K. Syranidis, D. Ryberg, T. Grube, P. Markewitz, R. Peters, and D. Stolten, "Linking the Power and Transport Sectors—Part 1: The Principle of Sector Coupling," *Energies*, vol. 10, no. 7, p. 956, 2017. DOI: `10.3390/en10070956`.

[205] W. Kempton and J. Tomić, "Vehicle-to-grid power implementation: From stabilizing the grid to supporting large-scale renewable energy," *Journal of Power Sources*, vol. 144, no. 1, pp. 280–294, 2005. DOI: `10.1016/j.jpowsour.2004.12.022`.

[206] F. Mwasilu, J. J. Justo, E.-K. Kim, T. D. Do, and J.-W. Jung, “Electric vehicles and smart grid interaction: A review on vehicle to grid and renewable energy sources integration,” *Renewable and Sustainable Energy Reviews*, vol. 34, pp. 501–516, 2014. DOI: `10.1016/j.rser.2014.03.031`.

[207] K. M. Tan, V. K. Ramachandaramurthy, and J. Y. Yong, “Integration of electric vehicles in smart grid: A review on vehicle to grid technologies and optimization techniques,” *Renewable and Sustainable Energy Reviews*, vol. 53, pp. 720–732, 2016. DOI: `10.1016/j.rser.2015.09.012`.

[208] S.-A. Amamra and J. Marco, “Vehicle-to-Grid Aggregator to Support Power Grid and Reduce Electric Vehicle Charging Cost,” *IEEE Access*, vol. 7, pp. 178 528–178 538, 2019. DOI: `10.1109/ACCESS.2019.2958664`.

[209] J. Tomić and W. Kempton, “Using fleets of electric-drive vehicles for grid support,” *Journal of Power Sources*, vol. 168, no. 2, pp. 459–468, 2007. DOI: `10.1016/j.jpowsour.2007.03.010`.

[210] J. C. Hernández, F. Sanchez-Sutil, P. G. Vidal, and C. Rus-Casas, “Primary frequency control and dynamic grid support for vehicle-to-grid in transmission systems,” *International Journal of Electrical Power & Energy Systems*, vol. 100, pp. 152–166, 2018. DOI: `10.1016/j.ijepes.2018.02.019`.

[211] N. DeForest, J. S. MacDonald, and D. R. Black, “Day ahead optimization of an electric vehicle fleet providing ancillary services in the Los Angeles Air Force Base vehicle-to-grid demonstration,” *Applied Energy*, vol. 210, pp. 987–1001, 2018. DOI: `10.1016/j.apenergy.2017.07.069`.

[212] M. Kesler, M. C. Kisacikoglu, and L. M. Tolbert, “Vehicle-to-Grid Reactive Power Operation Using Plug-In Electric Vehicle Bidirectional Offboard Charger,” *IEEE Transactions on Industrial Electronics*, vol. 61, no. 12, pp. 6778–6784, 2014. DOI: `10.1109/TIE.2014.2314065`.

[213] M. van der Kam and W. van Sark, “Smart charging of electric vehicles with photovoltaic power and vehicle-to-grid technology in a microgrid; a case study,” *Applied Energy*, vol. 152, pp. 20–30, 2015. DOI: `10.1016/j.apenergy.2015.04.092`.

[214] M. Khemir, M. Rojas, R. Popova, T. Feizi, J. F. Heinekamp, and K. Strunz, “Real-World Application of Sustainable Mobility in Urban Microgrids,” *IEEE Transactions on Industry Applications*, vol. 58, no. 2, pp. 1396–1405, 2022. DOI: `10.1109/TIA.2021.3132847`.

[215] F. Fattori, N. Anglani, and G. Muliere, “Combining photovoltaic energy with electric vehicles, smart charging and vehicle-to-grid,” *Solar Energy*, vol. 110, pp. 438–451, 2014. DOI: `10.1016/j.solener.2014.09.034`.

[216] A. Pfeifer, V. Dobravec, L. Pavlinek, G. Krajačić, and N. Duić, “Integration of renewable energy and demand response technologies in interconnected energy systems,” *Energy*, vol. 161, pp. 447–455, 2018. DOI: 10.1016/j.energy.2018.07.134.

[217] H. Dorotić, B. Doračić, V. Dobravec, T. Pukšec, G. Krajačić, and N. Duić, “Integration of transport and energy sectors in island communities with 100% intermittent renewable energy sources,” *Renewable and Sustainable Energy Reviews*, vol. 99, pp. 109–124, 2019. DOI: 10.1016/j.rser.2018.09.033.

[218] K. E. Forrest, B. Tarroja, L. Zhang, B. Shaffer, and S. Samuelsen, “Charging a renewable future: The impact of electric vehicle charging intelligence on energy storage requirements to meet renewable portfolio standards,” *Journal of Power Sources*, vol. 336, pp. 63–74, 2016. DOI: 10.1016/j.jpowsour.2016.10.048.

[219] P. Nunes, T. Farias, and M. C. Brito, “Enabling solar electricity with electric vehicles smart charging,” *Energy*, vol. 87, pp. 10–20, 2015. DOI: 10.1016/j.energy.2015.04.044.

[220] Vadi, Bayindir, Colak, and Hossain, “A Review on Communication Standards and Charging Topologies of V2G and V2H Operation Strategies,” *Energies*, vol. 12, no. 19, p. 3748, 2019. DOI: 10.3390/en12193748.

[221] J. Geske and D. Schumann, “Willing to participate in vehicle-to-grid (V2G)? Why not!” *Energy Policy*, vol. 120, pp. 392–401, 2018. DOI: 10.1016/j.enpol.2018.05.004.

[222] K. van Heuveln, R. Ghotge, J. A. Annema, E. van Bergen, B. van Wee, and U. Pesch, “Factors influencing consumer acceptance of vehicle-to-grid by electric vehicle drivers in the Netherlands,” *Travel Behaviour and Society*, vol. 24, pp. 34–45, 2021. DOI: 10.1016/j.tbs.2020.12.008.

[223] Fraunhofer Institute for Solar Energy Systems ISE, *Energy Charts: Net electricity generation in Germany*, 2021. URL: https://energy-charts.info/charts/power/chart.htm?l=en&c=DE&stacking=stacked_absolute_area (visited on Sep. 2, 2021).

[224] J. Schmalstieg, S. Käbitz, M. Ecker, and D. U. Sauer, “A holistic aging model for Li(NiMnCo)O2 based 18650 lithium-ion batteries,” *Journal of Power Sources*, vol. 257, pp. 325–334, 2014. DOI: 10.1016/j.jpowsour.2014.02.012.

[225] A. Marongiu, M. Roscher, and D. U. Sauer, “Influence of the vehicle-to-grid strategy on the aging behavior of lithium battery electric vehicles,” *Applied Energy*, vol. 137, pp. 899–912, 2015. DOI: 10.1016/j.apenergy.2014.06.063.

[226] K. Clement-Nyns, E. Haesen, and J. Driesen, “The impact of vehicle-to-grid on the distribution grid,” *Electric Power Systems Research*, vol. 81, no. 1, pp. 185–192, 2011. DOI: 10.1016/j.epsr.2010.08.007.

[227] F. Oldfield, K. Kumpavat, R. Corbett, A. Price, M. Aunedi, G. Strbac, C. O'Malley, D. Gardner, D. Pfeiffer, and J.-T. Kamphus, *The Drive towards a Low-Carbon Grid: Unlocking the value of vehicle-to-grid fleets in Great Britain*, 2021. URL: https://www.eonenergy.com/content/dam/eon-energy-com/Files/vehicle-to-grid/The%20Drive%20Towards%20A%20Low-Carbon%20Grid%20Whitepaper.pdf (visited on May 16, 2021).

[228] A. Flores-Quiroz and K. Strunz, "A distributed computing framework for multi-stage stochastic planning of renewable power systems with energy storage as flexibility option," *Applied Energy*, vol. 291, p. 116 736, 2021. DOI: 10.1016/j.apenergy.2021.116736.

[229] D. Goehlich, F. Spangenberg, and A. Kunith, "Stochastic total cost of ownership forecasting for innovative urban transport systems," in *2013 IEEE International Conference on Industrial Engineering and Engineering Management (IEEM 2013)*, Piscataway, NJ: IEEE, 2013, pp. 838–842. DOI: 10.1109/IEEM.2013.6962529.

[230] A. Raab, E. Lauth, K. Strunz, and D. Göhlich, "Implementation Schemes for Electric Bus Fleets at Depots with Optimized Energy Procurements in Virtual Power Plant Operations," *World Electric Vehicle Journal*, vol. 10, no. 1, p. 5, 2019. DOI: 10.3390/wevj10010005.

[231] Allgemeiner Deutscher Automobil-Club e.V., *ADAC*, 2022. URL: https://www.adac.de/ (visited on Nov. 16, 2022).

[232] Wissenschaftlicher Dienst des Deutschen Bundestags, *Kosten und Fördermöglichkeiten von Ladestationen für Elektrofahrzeuge: WD 5 - 3000 - 111/19*, Berlin, 2019. URL: https://www.bundestag.de/resource/blob/675848/91eb74a2dbaafe8607cf73ee9e46331f/WD-5-111-19-pdf-data.pdf (visited on Jun. 1, 2022).

[233] B. J. Mortimer, A. D. Bach, C. Hecht, D. U. Sauer, and R. W. de Doncker, "Public Charging Infrastructure in Germany—A Utilization and Profitability Analysis," *Journal of Modern Power Systems and Clean Energy*, pp. 1–10, 2021. DOI: 10.35833/MPCE.2021.000181.

[234] M. Pagani, W. Korosec, N. Chokani, and R. S. Abhari, "User behaviour and electric vehicle charging infrastructure: An agent-based model assessment," *Applied Energy*, vol. 254, p. 113 680, 2019. DOI: 10.1016/j.apenergy.2019.113680.

[235] J. He, H. Yang, T.-Q. Tang, and H.-J. Huang, "An optimal charging station location model with the consideration of electric vehicle's driving range," *Transportation Research Part C: Emerging Technologies*, vol. 86, pp. 641–654, 2018. DOI: 10.1016/j.trc.2017.11.026.

[236] Y. He, K. M. Kockelman, and K. A. Perrine, "Optimal locations of U.S. fast charging stations for long-distance trip completion by battery electric vehicles," *Journal of Cleaner Production*, vol. 214, pp. 452–461, 2019. DOI: 10.1016/j.jclepro.2018.12.188.

[237] S. Hosseini and M. D. Sarder, "Development of a Bayesian network model for optimal site selection of electric vehicle charging station," *International Journal of Electrical Power & Energy Systems*, vol. 105, pp. 110–122, 2019. DOI: 10.1016/j.ijepes.2018.08.011.

[238] S. Á. Funke, F. Sprei, T. Gnann, and P. Plötz, "How much charging infrastructure do electric vehicles need? A review of the evidence and international comparison," *Transportation Research Part D: Transport and Environment*, vol. 77, pp. 224–242, 2019. DOI: 10.1016/j.trd.2019.10.024.

[239] Nationale Leitstelle Ladeinfrastruktur, Ed., *Ladeinfrastruktur nach 2025/2030: Szenarien für den Markthochlauf*, Berlin, 2020. URL: https://www.now-gmbh.de/wp-content/uploads/2020/11/Studie_Ladeinfrastruktur-nach-2025-2.pdf (visited on Feb. 5, 2022).

[240] Abgeordnetenhaus von Berlin, *Berliner Klimaschutz- und Energiewendegesetz: EWG Bln*, 2021. URL: https://gesetze.berlin.de/perma?d=jlr-EWendGBEV2IVZ (visited on Apr. 1, 2022).

[241] M. Nicholas and S. Wappelhorst, *Regional Charging Infrastructure Requirements in Germany through 2030*, 2020. URL: https://theicct.org/sites/default/files/publications/germany-charging-infrastructure-20201021.pdf (visited on Jun. 1, 2022).

[242] T. Soylu, J. E. Anderson, N. Böttcher, C. Weiß, B. Chlond, and T. Kuhnimhof, "Building Up Demand-Oriented Charging Infrastructure for Electric Vehicles in Germany," *Transportation Research Procedia*, vol. 19, pp. 187–198, 2016. DOI: 10.1016/j.trpro.2016.12.079.

[243] J. E. Anderson, N. Böttcher, and T. Kuhnimhof, "An approach to determine charging infrastructure for one million electric vehicles in Germany," in *CONFERENCE PROCEEDINGS 1: TRANSPORTATION RESEARCH BOARD*, 2016. URL: https://elib.dlr.de/104222/.

[244] EnBW Energie Baden-Württemberg AG, *Damit Ladepunkte für alle verfügbar sind: Blockiergebühr für EnBW mobility+*, Karlsruhe, 2020. URL: https://www.enbw.com/blog/elektromobilitaet/enbw-news/damit-ladepunkte-fuer-alle-verfuegbar-sind-blockiergebuehr-fuer-enbw-mobility/ (visited on Mar. 13, 2022).

[245] Kraftfahrt Bundesamt, *Bestand an Kraftfahrzeugen und Kraftfahrzeuganhängern nach Bundesländern, Fahrzeugklassen und ausgewählten Merkmalen, 1. April 2022 (FZ 27)*, Flensburg, 2022. URL: https://www.kba.de/DE/Statistik/Fahrzeuge/Bestand/Umwelt/umwelt_node.html;jsessionid=E0FAE7E9EB309F2B8492DD7FE222318C.live21323 (visited on May 24, 2022).

[246] Deutsche Energie-Agentur GmbH and Prognos AG, *Privates Ladeinfrastrukturpotenzial in Deutschland*, 2020. (visited on Feb. 5, 2022).

[247] G. Nehrke, *Stationsbasiertes CarSharing in Berlin wirkt deutlich verkehrsentlastend*, Bundesverband CarSharing e. V., Ed., Berlin, 2019. URL: `https://carsharing.de/presse/pressemitteilungen/stationsbasiertes-carsharing-berlin-wirkt-deutlich-verkehrsentlastend` (visited on Apr. 1, 2022).

[248] J. Kopp, "GPS-gestützte Evaluation des Mobilitätsverhaltens von free-floating CarSharing-Nutzern," Dissertation, Eidgenössische Technische Hochschule Zürich, Zürich, 2015. URL: `https://www.research-collection.ethz.ch/bitstream/handle/20.500.11850/101659/eth-47780-02.pdf`.

[249] European Parliament, *Directive 2014/94/EU of the European Parliament and of the Council of 22 October 2014 on the deployment of alternative fuels infrastructure*, 2014. URL: `http://data.europa.eu/eli/dir/2014/94/oj` (visited on Apr. 1, 2022).

[250] BerlinOnline Stadtportal GmbH & Co. KG, Ed., *Suchräume zur Erweiterung der Ladeinfrastruktur für Elektroautos*, Berlin, 2014. URL: `https://daten.berlin.de/datensaetze/suchr%C3%A4ume-zur-erweiterung-der-ladeinfrastruktur-f%C3%BCr-elektroautos-wms` (visited on Apr. 1, 2022).

[251] Bundesnetzagentur für Elektrizität, Gas, Telekommunikation, Post und Eisenbahnen, *Elektromobilität: Öffentliche Ladeinfrastruktur*, 2022. URL: `https://www.bundesnetzagentur.de/DE/Sachgebiete/ElektrizitaetundGas/Unternehmen_Institutionen/E-Mobilitaet/Ladesaeulenkarte/start.html` (visited on Dec. 22, 2022).

[252] HeiGIT gGmbH, *OpenRouteService: Services, Directions*, 2020. URL: `https://openrouteservice.org/services/` (visited on May 5, 2022).